Anaerobic *n*-alkane degradation coupled to nitrate respiration in Gammaproteobacterium strain HdN1

DISSERTATION

zur Erlangung des Grades eines

Doktors der Naturwissenschaften

— Dr. rer. nat. —

dem Fachbereich Biologie/Chemie der

Universität Bremen vorgelegt von

Johannes Zedelius

aus Karlsruhe

Bremen 2012

Diese Arbeit wurde von Januar 2008 bis Dezember 2012 am Max-Planck-Institut für Marine Mikrobiologie in Bremen angefertigt

Erster Gutachter:	Prof. Dr. Friedrich Widdel, Universität Bremen
Zweiter Gutachter:	Prof. Dr. Ralf Rabus, Universität Oldenburg
Tag des Promotionskolloquiums:	07.12.2012

Table of contents

Zusammenfassung

Untersuchungen zum anaeroben Abbau von Kohlenwasserstoffen durch Mikroorganismen bieten Potential zur Entdeckung neuartiger biochemischer Reaktionswege, da hier Mechanismen zum Angriff auf die reaktionsträgen C–H-Bindungen vorhanden sein müssen, die auch in Abwesenheit von Luftsauerstoff ablaufen können.

In der vorliegenden Arbeit wurde die besondere Physiologie eines fakultativ anaeroben Gammaproteobakteriums untersucht, das möglicherweise Stickstoffmonoxid (NO) aus der Nitratreduktion direkt oder indirekt für die Alkanaktivierung nutzt. Stamm HdN1 wächst aerob und anaerob mit *n*-Alkanen. Der Stamm erwies sich insofern als ungewöhnlich, als dass er für den anaeroben Abbau nicht die Aktivierungsreaktion mit Hilfe der weit verbreiteten Fumarat-Addition, sondern einen bisher unbekannten Mechanismus verwendet. Eine weitere faszinierende Eigenschaft dieses Stammes ist sein großes *n*-Alkan-Substratspektrum (C_6-C_{30}); üblicherweise weisen nur aerobe Alkanabbauer ein vergleichbar großes Spektrum auf.

Die Intermediate der Denitrifikation Nitrit (NO_2^-), Stickstoffmonoxid (NO) und Distickstoffoxid (N_2O, Lachgas) weisen ein stark positives Redox-Potential auf. Es ist vorstellbar, dass sie bisher unbekannte Reaktionsmechanismen zur Funktionalisierung reaktionsträger Verbindungen ermöglichen. Während langkettige Fettsäuren oder Alkohole von Stamm HdN1 mit Nitrat (NO_3^-), NO_2^- oder N_2O metabolisiert werden konnten, wurden Alkane nur beim Wachstum mit NO_3^- oder NO_2^- abgebaut. Interessanterweise können andere denitrifizierende Alkanabbauer, welche Fumarat-Addition nutzen, mit Alkanen und N_2O wachsen, während dies für Stamm HdN1 nicht möglich war. Es wurde angenommen, dass der Schritt im Abbauweg, der nicht möglich ist, wenn nur N_2O vorhanden ist, die anaerobe Alkan-Aktivierungsreaktion ist.

HdN1 Kulturen mit Alkanen und N_2O, zu denen kleine Mengen NO gegeben wurde, bildeten mehr Stickstoff (N_2) als bei der Veratmung des NO alleine stöchiometrisch entstehen könnte. Die Funktionalisierung der Alkane mittels NO und anschließende Oxidation per N_2O-Reduktion (unter Entstehung von N_2) stellen eine plausible Erklärung für diesen Vorgang dar.

Bei Analysen von gelösten Gasen mittels Membran-Einlass Massenspektrometrie (MIMS) in einer aktiv mit Alkanen wachsenden HdN1 Kultur stieg nach Zugabe von ^{15}N-markiertem Nitrit überraschend die Sauerstoff-Konzentration an. Außerdem bildete sich markiertes N_2, obwohl durch zugegebenes Acetylen die N_2O-Reduktase gehemmt wurde. Die Dismutation von NO zu N_2 und O_2, die bei der anaerob methanotrophen Art, *Candidatus* Me-

thylomirabilis oxyfera' gefunden wurde, böte eine elegante Erklärung für diese erstaunlichen Befunde. Demnach würde in HdN1-Zellen ein kleiner Anteil des NO nicht als Elektronenakzeptor in der Denitrifikation verwendet, sondern dismutiert. Das entstehende O_2 könnte für die Alkan-Aktivierung mit Monooxygenasen genutzt werden. Weitere Erklärungsmodelle, die nicht auf Dismutation und Oxygenasen beruhen sind jedoch ebenfalls denkbar.

Bei Etherextraktionen zur Untersuchung von Metaboliten der Alkanoxidation wurden ausschließlich in aerob, nicht aber in anaerob gewachsenen HdN1 Zellen die primären Alkohole der langkettigen Alkane (als Primärprodukte der aeroben Alkan Oxidation mittels Monooxygenasen) gefunden. Allerdings waren bei früheren Arbeiten mit Stamm HdN1 auch in anaerober Kulturen solche Alkohole detektiert worden. Dieser vermeintliche Widerspruch konnte im Verlauf dieser Arbeit aufgeklärt werden, als die Bildung langkettiger Wachsester in HdN1 Zellen detektiert wurde. Diese waren anscheinend bei der damals verwendeten Präparation hydrolysiert und hatten so die primären Alkohole und Fettsäuren freigesetzt. Solche langkettigen Ester werden oft von Bakterien bei aerobem Wachstum auf Alkanen gebildet. Dies deutet wiederum auf einen anaeroben Abbauweg hin, der dem aeroben ähnlich ist.

Vergleichende Genomik mit den unverwandten Arten HdN1 und *Ca.* M. oxyfera erlaubte die Identifizierung von Proteinen mit überraschend großer Ähnlichkeit und einer phylogenetischen Sonderstellung, was auf eine gemeinsame, spezialisierte Funktion dieser Proteine in beiden Organismen hindeuten könnten. Die NO-Reduktasen (Nor) von HdN1 (Gen-Locus HdN1F_02620) und *Ca.* M. oxyfera (Gen-Locus DAMO_2434, DAMO_2437) weisen dieselben Modifikationen bei konservierten Aminosäuren im aktiven Zentrum, an der möglichen Ubiquinol-Bindestelle und im Protonenkanal auf, die als Anpassungen an eine mögliche (bei HdN1 zusätzliche) Funktion als NO-Dismutase interpretiert werden können. Die Gene waren in *Ca.* M. oxyfera sehr hoch exprimiert und wurden beim anaeroben Wachstum von Stamm HdN1 mit Alkanen mittels Proteomik identifiziert. In den Genomen fand sich benachbart zu den putativen Dismutasen jeweils die Sequenz eines Regulators. Dieser wies strukturelle Ähnlichkeit mit einem Sauerstoffsensor auf, was auf eine mögliche Regulation dieser Enzyme abhängig von der Sauerstoff-Konzentration hindeuten könnte. Die proteomische Detektion von Monooxygenasen in anaerob mit Alkanen gewachsenen Zellen war im Einklang mit einem möglichen neuartigen anaeroben Alkanaktivierungweg mittels NO-Dismutation.

In der vorliegenden Arbeit wurde das Wissen über die einzigartige Physiologie von Stamm HdN1 vertieft und die Grundlage zur möglichen Aufklärung des neuartigen anaeroben Abbauweges für *n*-Alkane gelegt.

Summary

Investigations on anaerobic hydrocarbon degradation by microorganisms exhibit the potential for discovery of novel biochemical reaction pathways, since mechanisms to attack the inert C–H bonds must exist here that can be performed without oxygen from air.

In the present work the special physiology of a facultative anaerobe Gammaproteobacterium, which possibly employs nitric oxide (NO) from nitrate reduction directly or indirectly for the anaerobic activation of alkanes was investigated. Strain HdN1 grows aerobically and anaerobically with *n*-alkanes. The strain was found to be unusual in that it did not utilize the prevalent activation reaction for *n*-alkanes by addition to fumarate during anaerobic growth, but instead a so far uncharted mechanism. Another intriguing characteristic of this strain is the rather broad *n*-alkane substrate spectrum (C_6–C_{30}); usually only aerobic *n*-alkane degrading microorganisms exhibit comparably broad spectra of utilized *n*-alkanes.

The denitrification intermediates nitrite (NO_2^-), nitric oxide (NO) and nitrous oxide (N_2O, laughing gas) have a highly positive redox potential. It is conceivable, that they enable so far unknown reaction mechanisms for the functionalization of inert compounds. While strain HdN1 is able to metabolize long chain fatty acids and alcohols using nitrate (NO_3^-), NO_2^- and N_2O as electron acceptors, *n*-alkanes are only degraded during growth with NO_3^- and NO_2^- but not with N_2O. Interestingly, other denitrifying alkane degrading strains, which employ fumarate addition, are able to utilize *n*-alkanes during growth via N_2O-respiration. It was assumed that the step in the degradation pathway which is impossible if only N_2O is present is the anaerobic alkane activation reaction.

When small amounts of NO were added to HdN1 cultures with alkanes and N_2O, more nitrogen gas (N_2) was produced than could be accounted for by the stoichiometric respiration of NO alone. Functionalization of the alkanes with NO and subsequent oxidation via N_2O-reduction (producing additional N_2) could explain this observation.

During membrane inlet mass spectrometric (MIMS) analysis of dissolved gases in an actively growing, *n*-alkane degrading HdN1 culture, the oxygen concentration increased surprisingly after injection of ^{15}N-labelled nitrite. In addition labeled N_2 was produced, although the N_2O reductase was inhibited by acetylene. The dismutation of NO into N_2 and O_2, has recently been shown to be employed by the anaerobic methanotroph '*Candidatus* Methylomirabilis oxyfera' and would offer an elegant explanation for these astonishing results. Thus, instead of serving as electron acceptor during denitrification, a small fraction of the NO

would be dismutated. The produced oxygen could be used for alkane activation with monooxygenases. However, explanatory models not involving on NO-dismutation and oxygenases are also conceivable.

During ether extractions for analysis of metabolites from alkane oxidation, alcohols of long-chain alkanes (as primary products of aerobic oxidation of alkanes by monooxygenases) were only detected in cells grown aerobically but not anaerobically. However, in earlier investigations with strain HdN1 such alcohols had been detected in alkane- as well as in fatty acid-grown cells from anaerobic cultures. This reputed contradiction could be explained during the course of this stuy, when unknown GC peaks were identified as long-chain wax esters. These apparently hydrolyzed during the first step of the preparation applied at that time, which must have released the primary alcohols and fatty acids. Such long-chain esters are often formed by bacteria during aerobic growth with alkanes. This in turn hints on an anaerobic degradation pathway which is somewhat similar to the aerobic one.

Comparative genomics with the two unrelated bacterial species HdN1 and *Ca.* M. oxyfera enabled the identification of proteins with a surprisingly high degree of similarity and a distinct phylogenetic affiliation suggesting a shared specialized function of these proteins in both organisms. The NO-reductases (Nor) in strain HdN1 (gene locus tag HdN1F_02620) and *Ca.* M. Oxyfera (gene locus tags DAMO_2424, DAMO_2437) exhibit the same modifications in conserved amino acids of the active center, the possible ubiquinole-binding site and the proton channel, which could be interpreted as adaptations to a possible (in HdN1 additional) function as NO-dismutase. These genes were very highly expressed in *Ca.* M. oxyfera and were also identified via proteomic analysis in strain HdN1 during anaerobic growth with alkanes. The gene sequence of a regulatory protein was identified in close proximity to the putative dismutases in both genomes. This regulator showed structural similarities with a oxygen-sensor protein and thus provides a first hint towards a possible regulation of these enzymes dependent on oxygen concentrations. The proteomic detection of monooxygenases in cells of HdN1 grown anaerobically with alkanes was in accordance with a possible novel pathway for alkane activation via NO-dismutation.

In the present thesis, knowledge on the unique physiology of strain HdN1 was widened and the foundations for a possible elucidation of the novel anaerobic pathway for degradation of *n*-alkanes were laid.

List of abbreviations

BLAST	Basic local alignment search tool
DAPI	4′,6-Diamidin-2-phenylindol
e^-	Electron
FAME	Fatty acid methyl ester
FID	Flame ionization detector
FISH	Fluorescence *in situ* hybridization
GC	Gas chromatography
GCMS	Gas chromatography mass spectrometry
[H]	Reduction equivalent
HMN	2,2,4,4,6,8,8-Heptamethylnonane
HPLC	High performance liquid chromatography
MAS	(1-Methylalkyl)succinate synthase
MIMS	Membrane inlet mass spectrometry
NM	Nitrate reducer medium
NOC-18	3,3-Bis(aminoethyl)-1-hydroxy-2-oxo-1-triazene
OD	Optical density
PCR	Polymerase chain reaction
PNM	Phosphate buffered nitrate reducer medium
red.	Reduced
SRB	Sulfate reducing bacteria
TCA	Tricarboxylic acid (cycle)
TCD	Thermal conductivity detector
UPLC	Ultra performance liquid chromatography
v/v	Volume per volume

A Introduction

A.1 Introduction: Alkanes in chemistry and biology

A.1.1 Significance of alkanes and alkane degrading microorganisms

Alkanes are the simplest organic compounds, prevalent throughout the world. Global interest in alkanes is due to their chemical potential as compact energy source e.g. for combustion engines and as fundamental raw material for the synthesis of a vast array of industrial products. Both roles assign a high total economic value to alkanes as trading commodities.

Methane (CH_4) – the smallest alkane – from natural gas (and biogas) is mainly used for heating and cooking purposes but also for production of electricity via gas turbines and increasingly as fuel for transportation. The short chain alkanes propane (C_3H_8) and butane (C_4H_{10}) can be used e.g. in gas stoves or as propellant gas in aerosol sprays. Short- to medium-chain alkanes in the range of pentane (C_5H_{12}) to octane (C_8H_{18}) are mainly used as gasoline fuels, but also as organic solvents. Medium- to long-chain alkanes from nonane (C_9H_{20}) to hexadecane ($C_{16}H_{34}$) are contents of diesel and aviation fuel (kerosene). *n*-Alkanes with carbon-chains longer than heptadecane ($C_{17}H_{36}$) are solid at 25°C and can be utilized as candle wax (paraffin) and lubricating oil. Longer alkanes can be used as bitumen for road construction (Vollhardt, 1990).

Scientific interest in microorganisms that degrade all kinds of hydrocarbons is in general focused on their metabolic capabilities and consequences of their activities. In the last decades scientific spotlight was not only on their major significance in bioremediation (Atlas, 1981; Prince, 1993) as a desired process, but also on their role in deterioration of transported and stored petroleum derivatives (Yemashova *et al*., 2007) as an unwanted process causing considerable financial damage. Especially sulfate reducing bacteria (SRB) which degrade petroleum hydrocarbons (especially the less inert alkanes) are troublesome for the oil industry, since they increase corrosion of pipelines and other equipment and reduce the petroleum quality due to the formation of hydrogen sulfide. In contrast, methanogenic synthrophic communities degrading crude oil can be utilized for microbial enhanced oil recovery (Banat, 1995). Furthermore, the abundance of hydrocarbon utilizing microorganisms in marine environments can hint on natural petroleum seepage as a geographical indicator for potentially accessible oil reservoirs (Hubert and Judd, 2010). Of all hydrocarbon degraders, especially alkane degrading bacteria are studied due to their abilities for directed specific alkane functionalization re-

actions with enzymes that might be applicable in biotechnological production of value-added fine and bulk chemicals (López-Cortéz *et al*., 2010). Some species even release metabolites like surfactants (as surface active compounds) with potential industrial applications into the growth medium (Ochsner *et al*., 1996).

A.1.2 Physicochemical properties of alkanes, alkenes and alkynes

Alkanes are either aliphatic (linear with a substituted or nonsubstituted chain) or naphthenic (non-aromatic ring) compounds and as all hydrocarbons made up only of carbon and hydrogen. *n*-Alkanes are linear (*n* = normal) and not branched and have the sum-formula C_nH_{2n+2}. The range of carbon chains in this homologous series starts with one C in methane (CH_4) as the simplest alkane and has in principle no upper limit. Synthetic molecules like polyethylene which essentially represent extremely long alkanes can have several hundred thousand C-atoms in one molecule (Whiteley *et al*., 2005; Wilkes and Schwarzbauer, 2010). *n*-Alkanes are gaseous from CH_4 (methane) to C_4H_{10} (butane), liquid from C_5H_{12} (pentane) to $C_{17}H_{36}$ (heptadecane) and solid ≥ $C_{18}H_{38}$ (octadecane) at 25°C and ambient pressure (101.325 kPa). The difference in the electronegativities (Pauling's) of hydrogen (2.10) and carbon (2.55) is small; thus the C–C and the C–H bonds are non-polar leading to a hydrophobic molecule. Accordingly, solubility in water is low (e.g. 1.42 mmol l^{-1} for methane) and decreasing rapidly with increasing chain length (e.g. ~0.6 µmol l^{-1} for *n*-tetradecane; Lide, 1998-1999). In the energetically most favorable conformation of *n*-alkanes, the carbon backbone is shaped like a zig-zag line (Fig. 1).

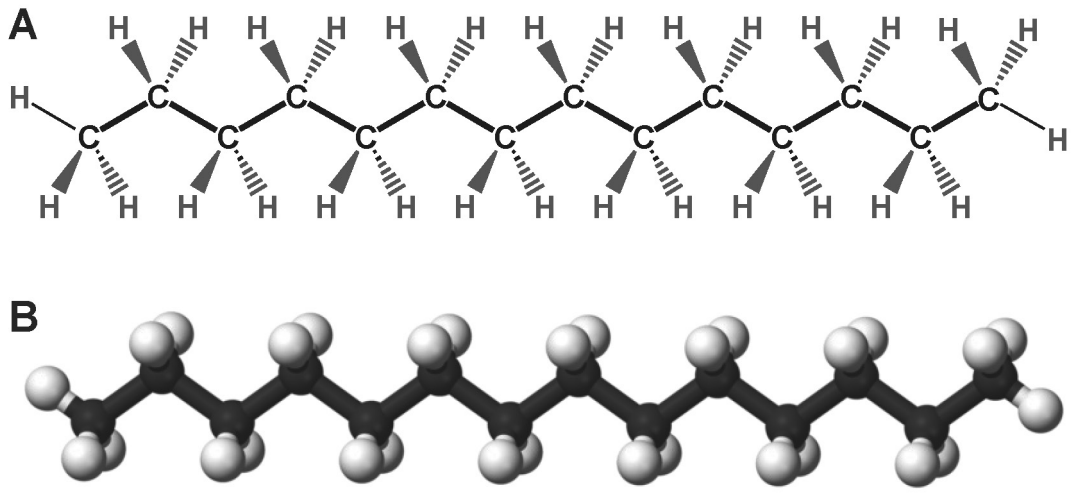

Fig. 1. Structure of *n*-tetradecane ($C_{14}H_{30}$) consisting of carbon (black) and hydrogen (grey/white) atoms. (A) Natta projection with emphasized carbon chain. (B) Ball and stick model (source: www.wikipedia.org).

Alkanes feature only covalent bonds, in which a pair of electrons is shared by both atoms. In saturated alkanes only σ-bonds exist, which are formed of overlapping sp^3 hybridized atom orbitals. The sp^3 hybridization of carbon atoms results in four single bonds with the typical tetrahedral architecture and a uniform length of about 110 pm (for structures of simple saturated and unsaturated alkanes see Fig. 2). Rotation is relatively unrestricted around these sigma bonds, leading to an infinite number of alkane rotamers. Double and triple bonds of alkenes and alkynes do not allow free rotation. They are formed of overlapping nonhybridized *p* orbitals and thus termed π-bonds. Electrons are delocalized in π-bonds. The simplest alkenes and alkynes are ethene and ethyne, respectively. The length of their C–C double and triple bonds is 134 pm and 120 pm. In general, the angle at the sp^2 hybridized C atoms of double bonds is 120° and the angle at the *sp* hybridized C atoms of triple bonds is 180°.

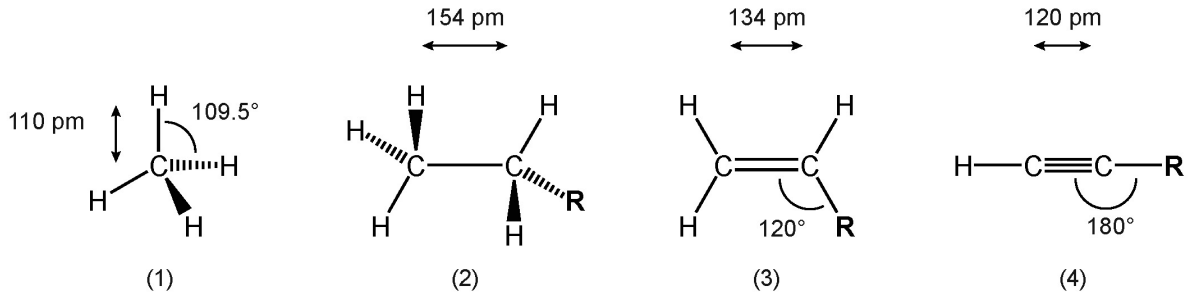

Fig. 2. Structures of saturated and unsaturated aliphatic hydrocarbons; (1) methane CH_4, exhibiting the well-known tetrahedron architecture; (2) ethane C_2H_6 or a longer chain alkane; (3) ethene (= ethylene) C_2H_4 or a longer chain terminal alkene; (4) ethyne (= acetylene) C_2H_2 or a longer chain terminal alkyne. Lengths and angles of covalent bonds for R = H are indicated. Adapted from Wilkes and Schwarzbauer (2010). R = H or alkyl residue.

The chemical reactivity of organic molecules is dictated by the nature of the intramolecular bonds. The bond strength is dependent on the distance between the C atoms and expressed as bond dissociation energy ($\Delta H°$). The small difference in electronegativities (see above) makes C–H and saturated C–C bonds quite unreactive or inert. The $\Delta H°$ is higher in C–H than in C–C bonds. For example a C–H bond at a terminal carbon in propane (C_3H_8) exhibits a $\Delta H°$ of 410 kJ mol^{-1} while a C–C bond in this compound has a $\Delta H°$ of only 364 kJ mol^{-1} (Vollhardt, 1990). The reason, why C–H bonds and not C–C bonds are attacked for activation of alkanes is probably due to steric hindrance (Beyer and Walter, 1988). The hydrogen atoms attached to the central carbon chain (compare Fig. 1 B) sterically prevent an attack. In the dark, at room temperatures alkanes are practically inert against oxygen, acids, alkali metals or halogens (apart from fluor). Only super acids are able to react with hydrocarbons. The strongest known super acid $FSO_3H{\cdot}SbF_5$ was named “magic acid”, since it can dissolve

paraffins. (Christen and Vögtle, 1985). In general only (free) radical species (atoms or molecules with single, unpaired electrons) can overcome the sluggishness of the C–H bonds of hydrocarbons. Such radical-reactions enable homolytic cleavage, thus leaving one electron with each of the two separated atoms. The required energy for homolytic bond dissociation is related to the stability of the resulting alky radical. The stability of the radical increases with the order of the carbon atom at which it is located. Thus, since they require less activation energy, radical catalyzed addition reactions in alkanes are more likely to occur at a subterminal ($\Delta H° \approx 395$ kJ mol^{-1}) than at a terminal ($\Delta H° \approx 410$ kJ mol^{-1}) carbon (Wilkes and Schwarzbauer, 2010). Still, under aerobic conditions with oxygen as a high-energy co-substrate, oxidation by most monooxygenases takes place at the terminal carbon (in the case of *terminal* monooxygenases). The agent in monooxygenases responsible for the directed activation of a C–H bond is a transition metal complex. Such complexes are especially suitable for this task, because the energy level of their outermost atomic orbitals is similar to the one found in the σ-orbitals of the C–H bonds. Although the alkane σ-orbitals are difficult to access, overlap is possible due to the extensive hybrid orbitals of the transition metal complexes (Saillard, 1990).

Alkenes and alkynes exhibit a higher reactivity than saturated compounds (structures see Fig. 2). This is due to characteristics of the σ-bonds and not due to the strength of the double or triple C–C bond ($\Delta H° \approx 724$ kJ mol^{-1} in alkenes and $\Delta H° \approx 837$ kJ mol^{-1} in alkynes), which is quite high, since the combination of σ- and π-bonds in these molecules make them more stable than the σ-bond alone. The weaker of the two is the π-bond (Vollhardt, 1990). The overlapping π-orbitals represent areas of elevated electron density and thus are prone to act as nucleophiles in chemical reactions (i.e. in electrophilic additions). The availability of the loosely held π-electrons makes alkenes so reactive. Partial oxidation of alkenes by catalytic addition of oxygen yields epoxides. The substituted ring structure can be opened via acid-catalyzed hydrolysis leading to *trans*-diols. Other possible reactions of alkenes include hydratation and hydrogenation as well as polymerization reactions. The triple bond of alkynes is less reactive than the double bond of alkenes towards electrophilic agents. Appart from addition reactions, alkynes also act as H^+ donors. This acidic property is due to the fact that electrons from the broken covalent bond can be retained at the ethylenyl radical.

A.1.3 Abundance of alkanes

The largest occurrences of alkanes on earth are deposits of petroleum and methane. Petroleum is made up mainly (> 50%) of alkanes (*n*-alkanes, branched alkanes and cyclic alkanes), the residual fraction consists mainly of aromatics (Tissot and Welte, 1984). Natural gas consists mainly of methane, but also of ethane and other short-chain alkanes. Conservative estimations of reserves of crude oil and natural gas amount to 230×10^9 t and 210×10^{12} m^3 (BP statistical review of world energy, June 2012). However, the largest amount of hydrocarbons is actually not located in geological formations, but instead in terrestrial and marine sediments in the form of bound methane as gas hydrates – crystalline structures where one molecule of gas is surrounded by a 'cage' of H_2O molecules. Twice as much methane carbon is estimated to be located in such hydrates (or 'clathrates') compared to all known carbon deposits in fossil fuels (i.e. coal, natural gas and oil; Kvenvolden, 1988). Methane and other simple alkanes including ethane have even been detected (in undetermined amounts) on other planets and their moons in our solar system (Niemann *et al*., 2005) and even on comets (Mumma *et al*., 1996).

A.1.4 Formation of alkanes

Formation of crude oil and gas from buried organic matter progresses over 5 to 100 million years especially in marine sediments (Tissot and Welte, 1984). The maturation process consists of two stages: diagenesis and catagenesis. During diagenesis (at < 50–60°C) buried organic matter is degraded mostly due to microbial catabolism coupled to denitrification, sulfate reduction or methanogenesis. From this degradation and concomitant geological transformations a complex organic mixture called *kerogen* is produced. Over time, this heterogeneous material is buried deeper and reaches zones of elevated temperatures (60–160°C) where catagenesis occurs. Under these conditions bitumen (petroleum and asphalt) and later oil and natural gas are formed due to reduction of double bonds, cracking and condensation reactions. Especially radical catalyzed reactions are the reason, why petroleum contains hardly any alkenes or alkynes – the biogenic compounds with double or triple bonds are too reactive to survive the diagenetic and catagenetic transformations (Wilkes and Schwarzbauer, 2010). If temperature and pressure are sufficiently high, the organic matter is sterilized. It was suggested, that such paleopasteurization (at > 80°C; Adams *et al*., 2006) is the reason why some oil reservoirs are not biodegraded – even though they might have been lifted to zones of lower temperature by now. At very high temperatures (>160°C) and pressures (deeper in the sedi-

ment) formation of oil and gas is unlikely since the conversion of organic matter into CO_2, CH_4 and graphite are favored under these conditions (Tissot and Welte, 1984). The transformations occurring at these depths are termed metagenesis and are considered to be a very low-grade metamorphism (Wilkes and Schwarzbauer, 2010).

Oil and gas, containing alkanes, are formed from organic matter particularly in sediment basins (Tissot and Welte, 1984). Alkanes have existed on earth since geological times. In pasteurized deposits in the subsurface, petroleum and natural gas can be stable for millions of years. The composition of hydrocarbons in such sterile reservoirs remains unaltered until they are entered by microorganisms. However it is unclear, whether prokaryotes living in reservoirs are only introduced during oil exploration or also by natural processes without anthropogenic involvement (Ollivier and Alazard, 2010). Deposits are explored and oil and gas is 'produced' (transferred to the surface) as energy sources for anthropogenic utilization.

During accidental spills like the notorious accidents of the *Deepwater Horizon* platform in 2010 or the *Exxon Valdez* tanker in 1989 vast amounts of crude oil have entered the environment (Fig. 3 A,B; Atlas and Hazen, 2011). Both events were entailed by very serious consequences for the affected ecosystems as well as health and livelihood of the local human population. Aerobic hydrocarbon degrading microorganisms discussed below are the key players during bioremediation of such oil polluted environments (Prince, 1993; Swannel and McDonagh, 1996).

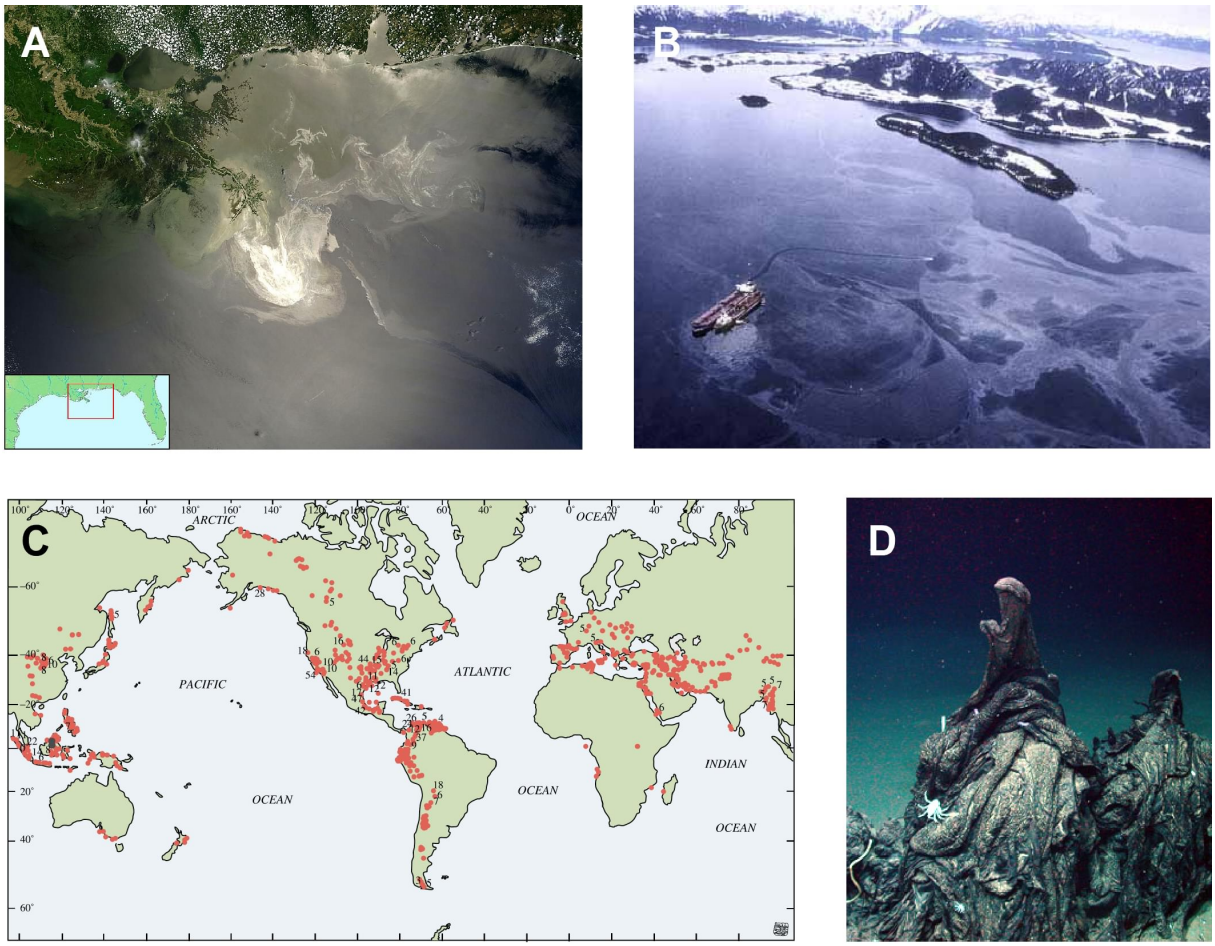

Fig. 3. Anthropogenic and natural input of hydrocarbons into the biosphere. (A) Satellite image of the Gulf of Mexico during the Deepwater Horizon oil spill in May 2010, the inlet depicts the geographical location (source: www.NASA.gov). (B) Aerial photograph of the Exxon Valdez tanker oil spill in the Prince William Sound of Alaska (source: www.NOAA.gov). (C) Global distribution of natural seeps of crude oil (onshore and offshore) which also may emit natural gas (source: Kvenvolden and Rogers, 2005). (D) Asphalt volcanoe in the Gulf of Mexico (source: MARUM, Bremen).

However, crude oil from reservoirs on land (e.g. via mud-volcanoes) and in the sea (via 'cold' gas seeps and asphalt volcanoes, Fig. 3 C,D) is assumed to have entered the biosphere by natural seepage ever since it was formed hundreds of million years ago (Wilson *et al.* 1974; Prince, 2002). Although anthropogenic activity involving oil and gas exploration, conversion to fuels and transportation has significantly increased global influx (especially at sites of accidents), the main source of hydrocarbons in the environment is synthesis by living organisms (Bragg *et al.*, 1992).

Biological formation of the most abundant hydrocarbon methane is accomplished by methanogenic archaea in anoxic environments, where more positive electronacceptors are absent. It is estimated, that 1×10^9 t of biogenic methane is formed globally per year (Thauer, 1998). This could account for 70% of the total methane production (biotic and abiotic; McIn-

erney *et al*., 2010). Appropriate conditions for methanogenesis can be found in peat bogs and marshlands, but also in the digestive tract of cellulose degrading ruminants and termites as well as in anaerobic digesters of wastewater treatment plants. Alkanes with longer carbon chains have been reported to be synthesized by various organisms including algae (Dennis and Kolattukudy, 1992), higher plants (Tissot and Welte, 1984, Samuels *et al*., 2008), insects (Tillman *et al*., 1999) and microorganisms (Birch and Bachofen, 1988; Hinrichs *et al*., 2006; Wackett, 2010). Carbon numbers in biogenic alkanes exhibit a significant odd- over even predominance. This is due to decarbonylation (resulting in loss of a C_1-unit) during the biosynthetic pathway based on fatty aldehydes, which feature a natural predominance of even numbered carbon chains (e.g. Cheesbrough and Kolattukudy, 1984).

A.1.5 Why alkanes don’t accumulate in nature

The inert nature of crude oil and natural gas led to accumulation of alkane hydrocarbons in geological formations over millions of years. In addition, biogenic formation adds up to the amount of globally occurring alkanes. Only a small fraction of these alkanes are affected by (abiotic) physicochemical attack leading to remineralization. In the absence of another sink for alkanes (and other hydrocarbons), they would accumulate constantly adjacent to the sites of production. The absence of ever-increasing amounts of alkanes is thus an obvious indicator for biological degradation. This is supported by the postulate of 'microbial infallibility' which states that for every naturally occurring organic substance at least one type of microorganism must exist with an enzyme system able to degrade it. A non-degradable biogenic substance would have accumulated in the course of earth’s history (Alexander, 1965). While this postulate should encourage microbiologists trying to find and enrich microorganisms for the degradation of natural compounds, it is a warning against release of inert non-biogenic (especially xeonobiotic and toxic) compounds. The severe accumulation of plastic from anthropogenic waste in the world oceans (UNEP, 2005) suggests that no microorganisms have yet evolved which are able to degrade all the different kinds of polymeric substances discharged by the civilized world.

Abiotic degradation of alkanes can be initiated by radicals produced from energy rich radiation (e.g. Kaplan and Kelleher, 1971) or during combustion. In case of complete oxidation, the only products are CO_2 and H_2O. Microbial alkane degradation pathways are initiated by functionalization reactions that involve breakage of the C–H bond either via radical species or

activated enzyme centers. The employed mechanisms (and principles) of alkane activation reactions in the presence and absence of oxygen (from air) will be discussed in the following section.

A.2 Degradation of *n*-alkanes under oxic and anoxic conditions

A.2.1 Introduction to aerobic *n*-alkane degradation

As described above, alkanes are ubiquitous hydrocarbons from natural and anthropogenic sources that are degradable by microorganisms. Investigations on biological alkane degradation began already a century ago (Söhngen, 1913). The ability to degrade alkanes is found in a number of bacterial and yeast (unicellular fungus) species. Examples from often investigated genera are bacterial species of *Pseudomonas*, *Acinetobacter* and *Mycobacterium* and yeast species of *Candida* (Britton, 1984; Bühler and Schindler, 1984). From these studies it was evident, that microorganisms can utilize alkanes (and other hydrocarbons) as energy rich sources of carbon and electrons. For example, the energy content ($\Delta G°$) per molecule (theoretically available by complete oxidation with O_2) of methane (viz. natural gas) is ~820 kJ mol^{-1}, that of *n*-heptane (comparable to gasoline) is ~4760 kJ mol^{-1}, and that of *n*-tetradecane (comparable to diesel) is ~9310 kJ mol^{-1}.

In general, transport of alkanes into the cell is assumed to be a passive process. Gaseous *n*-alkanes are less hydrophobic than longer-chain *n*-alkanes and dissolve in water to a higher content. They are assumed to pass the cell membranes by diffusion and can thus be activated and further degraded within the lumen of the cell (Widdel and Grundmann, 2010). Liquid and solid alkanes (with longer C–chains) are less diffusible in the aqueous phase, since their solubility decreases rapidly with increasing chain length. They are assumed to partition in the cell membrane and apparently also other hydrophobic compartments like neutral lipid inclusions (Scott and Finnerty, 1976). From there they may diffuse to the active sites of activating enzymes.

Aerobic alkane degrading bacteria have found several strategies to increase the availability of their non-polar growth substrates. With insoluble alkane substrates some species were found to live attached to the organic phase overlaying the aqueous medium (Grimaud, 2010; Abbasnezhad *et al.,* 2011). This can be facilitated by the production of hydrophobic cell surface structures (Wick *et al*., 2002). Other strains produce amphiphilic substances (surfac-

tants) to increase solubility of the organic substrates (van Hamme *et al*., 2003; Perfumo, 2010). Anaerobic bacteria have so far only been described to live attached to the alkane phase, but not to produce surfactants (Widdel and Grundmann, 2010).

A.2.2 Aerobic *n*-alkane activation reaction

The key step in *n*-alkane degradation pathways is the activation reaction. During activation an inert C–H bond is broken and a polar group is added, so that the product can be further metabolized. In general this process is accomplished by oxygenases. Several types of oxygenases have been described (e.g. methane monooxygenases or alkane hydroxylases; for a review see Ayala and Torres, 2004). The enzymatic strategy for aerobic alkane degrading microorganisms for cleavage of a C–H bond always involves O_2 as a co-substrate. Dioxygen has a high electronegativity (3.44) and consequentially a strong tendency to acquire electrons. Mostly due to this trait, the half-reaction O_2/H_2O has a very positive redox potential and thus O_2 is a strong chemical and biochemical oxidant. Due to the distribution of its two unpaired electrons into two antibonding atomic orbitals, triplet oxygen (the 'normal' ground state) does not react at room temperature with the majority of organic compounds at a timescale of years (Widdel and Musat, 2010). A configuration of electrons as in singlet oxygen would be incompatible with the existence of life and organic compounds on our oxic earth (Ingraham and Meyer, 1985; Davies, 2003).

Oxygenases usually contain metals (iron, copper) and introduce one or two oxygen atoms into their substrates (Fig. 4). The primary step is the reduction of metal-bound O_2 to the peroxide level. For this process, two electrons need to be shuffled to the O_2 (in one electron steps) from an electron donor like NADH. By a disproportionation-like electronic rearrangement the metal bound O_2 is converted into a single metal bound oxygen atom, which attacks the C–H bond of the alkane, finally yielding a hydroxyl-group (Widdel and Musat, 2010). The second oxygen atom is reduced to water. The product of the activation reaction, the alkyl-alcohol is further oxidized to an aldehyde and subsequently to a fatty acid (Fig. 4).

A dioxygenase, introducing a hydroperoxide into *n*-alkanes during the initial activation reaction has also been suggested by Maeng and coworkers (1996) but results were questioned later (Mehboob *et al*., 2009). The described initial aerobic *n*-alkane activation reaction results in functionalization at a terminal or subterminal carbon (Britton, 1984). Activation at a different position has not been described in the literatue.

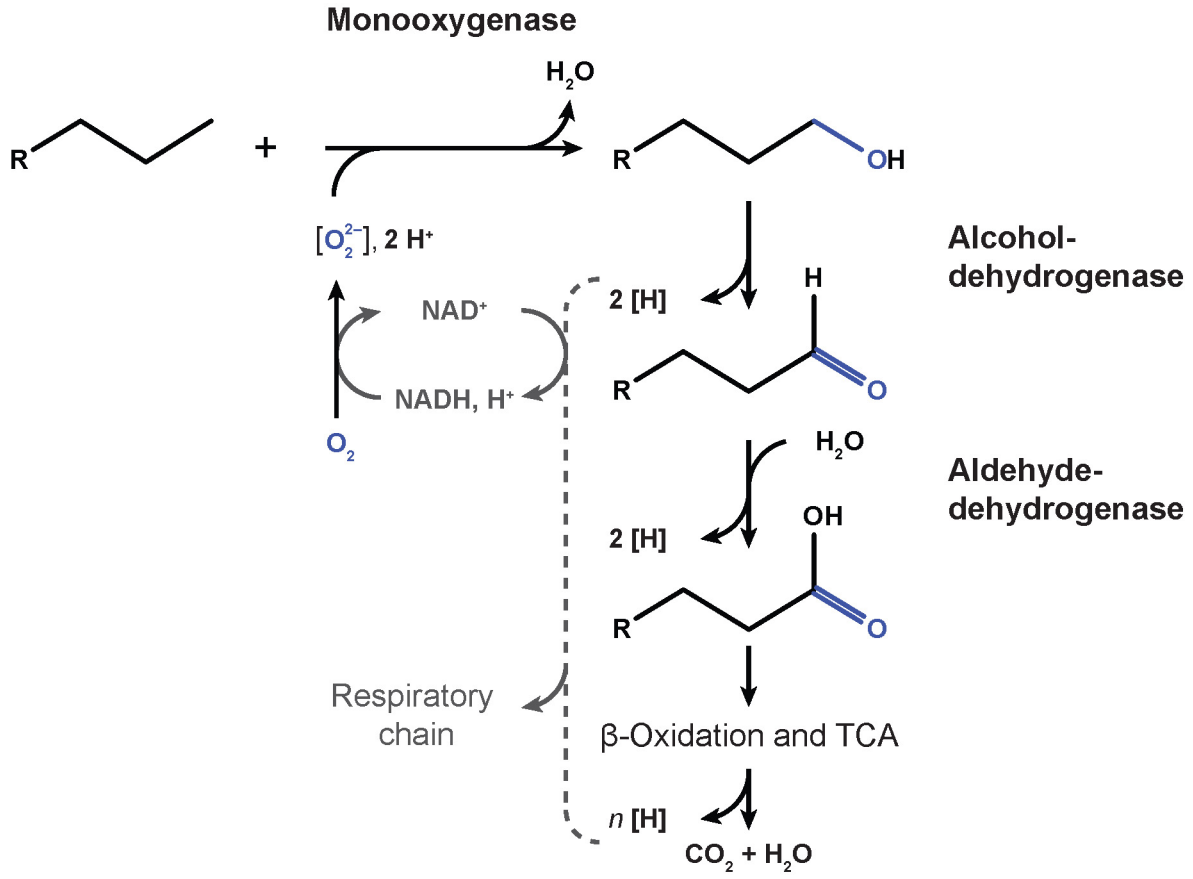

Fig. 4. Pathway for terminal oxidation of *n*-alkanes via monooxygenases and further degradation. The alkyl-alcohol formed in the initial activation reaction is further oxidized by an alcohol and an aldehyde dehydrogenase. The formed fatty acid can be completely oxidized via β-oxidation and the tricarboxylic acid cycle (TCA) to CO_2 and H_2O. Adapted from Widdel and Musat (2010).

The only available crystal structure of a long-chain alkane monooxygenase (Fig. 5; Li *et al*., 2008) suggests that the substrate is coordinated transiently to a defined position at the catalytic site of the enzyme to be oxidized after diffusing in through channels or cavities lined by hydrophobic amino acids (compare Whittington *et al*., 2001).

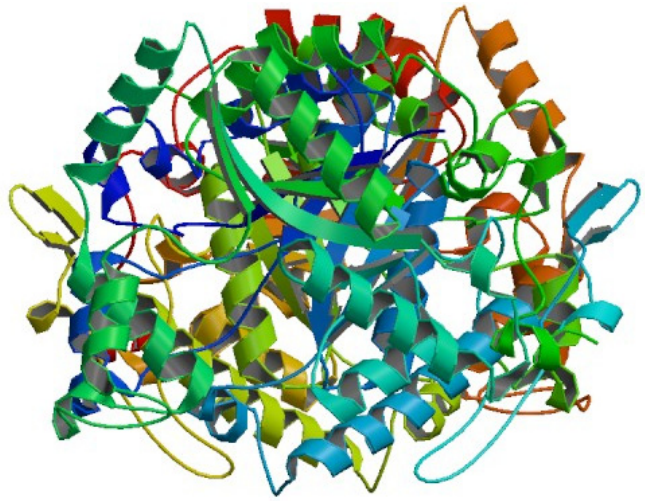

Fig. 5. Structure of long-chain alkane monooxygenase LadA from *Geobacillus thermodenitrificans* NG80-2. The enzyme was shown to hydroxylate *n*-alkanes from $C_{15}H_{32}$ to $C_{36}H_{74}$ at the terminal carbon in the presence of oxygen. Electrons are shuffled to the active site of the enzyme by its coenzyme flavin mononucleotide (FMN). Source: Li *et al*., 2008.

A.2.3 Introduction to anaerobic *n*-alkane degradation

In the course of the 20th century, the existence of anaerobic hydrocarbon degradation was discussed controversially. It was a general belief that the activation of the inert C–H bond is impossible in the absence of melcular oxygen (McKenna and Kallio, 1965, Atlas, 1981). Already in the 1940s, several microbiological laboratories had claimed, that they had observed anaerobic degradation of hydrocarbons by bacteria (e.g. Novelli and ZoBell, 1944; Rosenfeld, 1947). However, in some occasions these claims were doubted later (Atlas, 1981) or the responsible strains were not conserved, rendering verification impossible.

Microbial growth with *n*-alkanes is engergetically favorable coupled to reduction of the most common terminal electron acceptors employed by microorganisms. For illustration, the ΔG-values for oxidation of *n*-hexadecane as a model compound for long-chain alkanes are depicted in Table 1. Thus, from a thermodynamic point of view, the anaerobic degradation of *n*-alkanes was in principle expectable.

Table 1. Gibbs free energies for *n*-hexadecane ($C_{16}H_{34}$) oxidation coupled to selected electron acceptors at standard conditions (298.15 K) at pH = 7. Adapted from Mbadinga *et al*. (2011).

Electron acceptor (ox/red)	Overall energetic equation	$\Delta G°$ (kJ/mol of $C_{16}H_{34}$)[a]	$\Delta G°'$ (kJ/mol of $C_{16}H_{34}$)[b]
O_2/H_2O[c]	$C_{16}H_{34} + 24.5\ O_2 \rightarrow 16\ HCO_3^- + H_2O + 16\ H^+$	–9677.07	–10316.27
NO_2^-/N_2	$C_{16}H_{34} + 32.66\ NO_2^- + 16.66\ H^+ \rightarrow 16\ HCO_3^- + 16.33\ N_2 + 17.33\ H_2O$	–12498.24	–11832.41
ClO_3^-/Cl^-	$C_{16}H_{34} + 16.33\ ClO_3^- \rightarrow 16\ HCO_3^- + 16.33\ Cl^- + H_2O + 16\ H^+$	–11764.86	–12404.06
NO_3^-/N_2	$C_{16}H_{34} + 19.6\ NO_3^- + 3.6\ H^+ \rightarrow 16\ HCO_3^- + 9.8\ N_2 + 10.8\ H_2O$	–9819.37	–9675.55
Fe_3^+/Fe_2^+	$C_{16}H_{34} + 98\ Fe^{3+} + 48\ H_2O \rightarrow 16\ HCO_3^- + 98\ Fe^{2+} + 114\ H^+$	–5335.67	–9891.78
SO_4^{2-}/H_2S	$C_{16}H_{34} + 12.25\ SO_4^{2-} + 8.5\ H^+ \rightarrow 16\ HCO_3^- + 12.25\ H_2S + H_2O$	–897.13	–557.55
HCO_3^-/CH_4	$C_{16}H_{34} + 11.25\ H_2O \rightarrow 3.75\ HCO_3^- + 12.25\ CH_4 + 3.75\ H^+$	–204.15	–353.96

a $\Delta G°$: standard Gibbs free energy: reactants and products at 1 M concentration and gases at a partial pressure of 1 atm. Hexadecane ($C_{16}H_{34}$) was chosen as the model substrate for free energies calculations. Gibbs free energy of formation for *n*-hexadecane in the liquid state was taken from Helgeson *et al.* (1998). For all other compounds the data were taken from Thauer *et al*. (1977) and Hanselmann (1991). Methane, hydrogen, nitrogen and oxygen are in the gaseous phase at partial pressures of 1 atm. All other compounds are in the aqueous phase.
b $\Delta G°' = \Delta G° + m \times 2.303\ RT \log 10^{-7}$ (m is the net number of protons formed in the equation).
c The reaction with oxygen is shown for comparison.

In 1985, compelling but indirect evidence was presented of hydrocarbon degradation by methanogenic enrichments (Schink, 1985). The first pure bacterial strain shown to degrade hydrocarbons under strictly anoxic conditions was strain GS-15 which grew with toluene during reduction of Fe^{III} (Loveley *et al*., 1989). As recently as 1991, anaerobic degradation of *n*-alkanes was unambiguously shown for the first time with the mesophilic strain *Desulfococcus*

oleovorans Hxd3, a sulfate-reducing Deltaproteobacterium which was isolated with *n*-hexadecane (Aeckersberg, 1991). This strain coupled the reduction of sulfate to the complete oxidation of the alkane (see section A.3.1). To date, a number of bacterial species and enrichments have been described with the capacity for anaerobic *n*-alkane degradation via reduction of sulfate, nitrate or chlorate (comprehensive lists can be found in Widdel *et al*., 2010 and Mbadinga *et al*., 2011). Together with the isolation of strain HdN1 (the focus of this thesis), the isolation of two other denitrifying, alkane-degrading species affiliated with the *Betaproteobacteria* was accomplished (Ehrenreich, 2000). The two strains, named HxN1 and OcN1 were shown to degrade *n*-alkanes of a chain length of C_6–C_8 and C_8–C_{12} respectively.

Apart from pure cultures, also anaerobic enrichments with alkanes were investigated. Degradation of *n*-hexadecane coupled to methanogenesis by a syntrophic culture was described (Zengler *et al*., 1999) shortly before the organisms responsible for anaerobic oxidation of methane (AOM) coupled to sulfate reduction were identified (Boetius *et al*., 2000). Only recently, the denitrification-coupled anaerobic oxidation of methane (DAMO) was described (Raghoebarsing *et al*., 2006; Ettwig *et al*., 2010).

A.2.4 Anaerobic *n*-alkane activation reactions

In the absence of molecular oxygen, terminal oxidation via oxygenase enzymes (Fig. 6 A) is impossible. Thus, anaerobic *n*-alkane degrading microorganisms have to employ alternative biochemical reactions for cleavage of the inert C–H bonds of *n*-alkanes to achieve functionalization. The first investigated *n*-alkane degrading physiology was that of *Desulfococcus oleovorans* strain Hxd3 (Aeckersberg et al., 1991, 1998). Although carboxylation has been proposed (Fig. 6 E), the nature of the employed anaerobic activation mechanism is still in discussion (see section A.3.1.). The best understood and apparently wide-spread initial reaction involves the addition to fumarate (Kropp *et al*., 2000; Rabus *et al*, 2001, Callaghan *et al*, 2006). The subterminal carbon of an *n*-alkane is added to fumarate in a reaction catalyzed by a glycyl-radical-enzyme termed (1-Methylalkyl)succinate synthase (Mas or Ass; Fig. 6 D). The assays for enzyme activity had been conducted with *n*-hexane degrading cultures of strain HxN1 (Wilkes *et al*., 2003). The corresponding genes were detected in a gene cluster and the enzyme was found to be a heterotetramer (Grundmann et al., 2008, Webner, 2012).

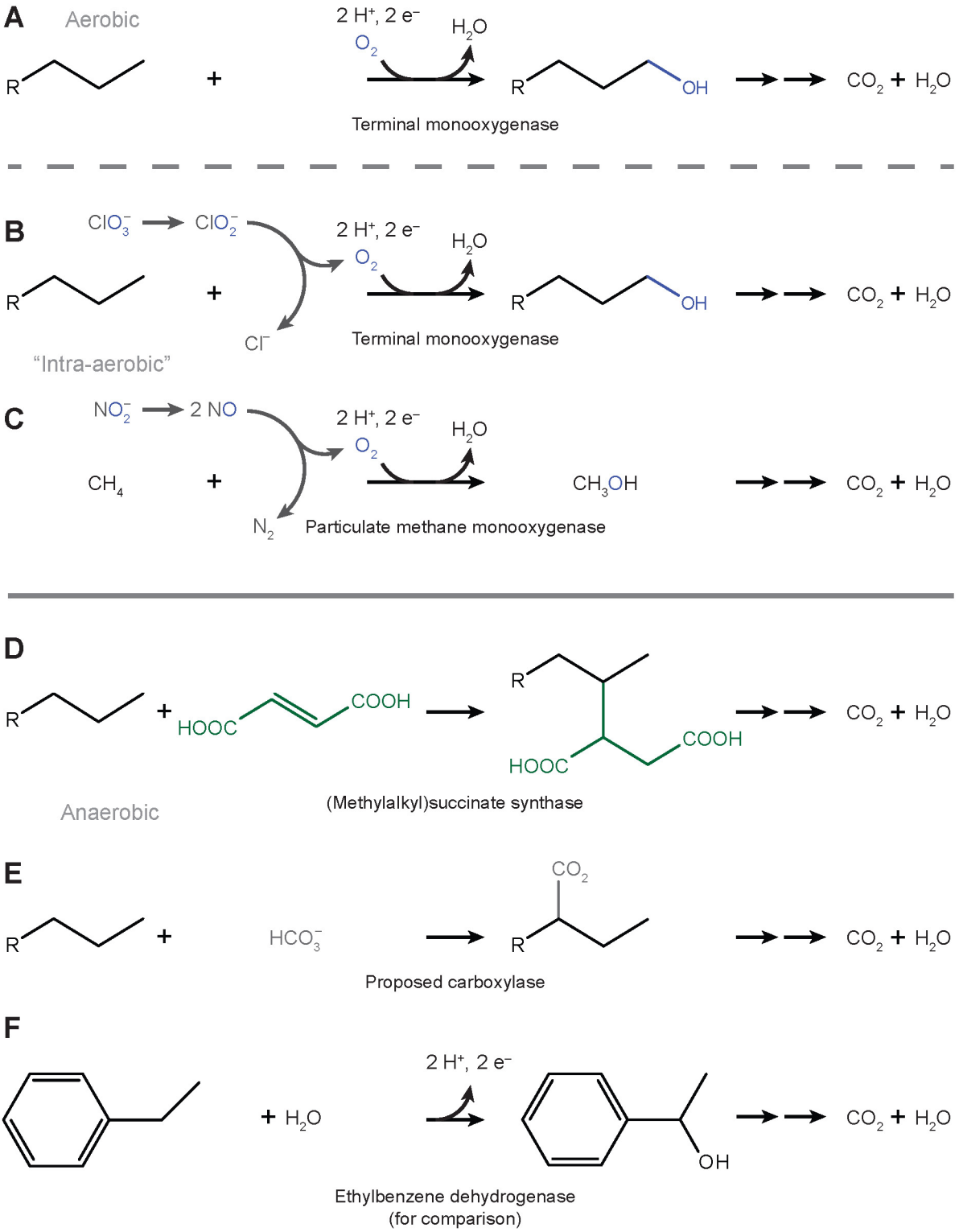

Fig. 6. Initial reactions for activation of alkanes employed by bacteria under aerobic and anaerobic conditions. Proposed responsible enzymes are indicated. Complete oxidation leads to CO_2 and H_2O. 'Classical' aerobic oxidation by a terminal monooxygenase (A). An anaerobic pathway employing intracellular formation of oxygen for 'aerobic' oxidation of alkanes has been called "intra-aerobic" (Ettwig *et al.*, 2010). Oxygen from chlorite dismutation utilized for *n*-alkane oxidation (B; Mehboob *et al.*, 2009). Oxygenic NO dismutation for methane oxidation (C; Ettwig *et al.*, 2010). *n*-Alkane activation via fumarate addition by (Methylalkyl)succinate synthase (D). Proposed *n*-alkane carboxylation by an unknown enzyme (E; So and Young, 2003; section A.3.1). Anaerobic hydroxylation of ethylbenzene added for comparison (F; Kniemeyer and Heider, 2001). R = alkyl residue.

Further degradation proceeds most likely by ligation to Coenzyme A, C-skeleton rearrangement and decarboxylation to form 4-octanoyl-CoA. The resulting fatty acid can then be channeled into β-oxidation and the central metabolism, ultimately yielding CO_2.

In addition to the above described anaerobic mechanisms, 2 pathways have been described which are proposed to employ intracellularly produced chemogenic oxygen. Monooxygenases are suggested to utilize this oxygen for activation of alkanes under these "intraaerobic" conditions (viz. in the absence of oxygen from air). The first of the two pathways was proposed for strain *Pseudomonas chloritidismutans* to enable anaerobic growth with *n*-decane (Fig. 6 B; Mehboob et al., 2009). Physiological details of this organism are discussed in section A.3.2. The second pathway was proposed for '*Ca*. Methylomirabilis oxyfera', the dominant bacterium in an enrichment which couples the anaerobic methane oxidation to nitrite reduction. Oxygen for the monooxygenase-catalyzed oxidation of methane was proposed to be formed via NO dismutation (Fig. 6 C; Ettwig *et al,* 2010).

In the denitrifying strain *Aromatoleum aromaticum* EbN1 a mechanism for the anaerobic hydroxylation of ethylbenzene has been detected (Fig. 6 F; Kniemeyer and Heider, 2001). Sulfate reducing strains degrade this compound via fumarate addition (Elshahed *et al*., 2001, Kniemeyer et al., 2003). Ethylbenzene is an aromatic compound, but the principle activation reaction has possible implications for anaerobic *n*-alkane activation and therefore is discussed here. The responsible enzyme, the ethylbenzene dehydrogenase belongs to the dimthylsulfoxide reductase family of molybdoenzymes. The molybdate in the active site withdraws a hydride from the hydrocarbon. The transiently present carbenium ion is stabilized by the π-electron system of the aromatic compound. This system functions independently of fumarate and of molecular oxygen. Still, an electron acceptor with a high redox potential is apparently necessary for this kind or activation reaction. Although it is conceivable, anaerobic hydroxylation of *n*-alkanes has never been observed to date.

A highly reactive compound able to activate alkanes is peroxynitrite as shown in abiotic experiments (Lobachev and Rudakow, 2005). However, its occurrence in anaerobically grown cells and thus a possible involvement in anaerobic alkane oxidation is highly unlikely, since hydrogenperoxide had to be added for formation of pyroxynitrite. Another highly reactive nitrogen-compound is NO_2 (nitrogen dioxide). It was proposed to be an oxidizing compound alternative to O_2 for anaerobic oxidation of ammonia in *Nitrosomonas eutropha* (Schmidt and Bock, 1997, Schmidt *et al*., 2001). In contrast, recent results indicate, that anaerobic growth

with ammonia could not be supported with NO_2 as an oxidant (Kartal *et al*., 2012). Endergonic nitrogen-oxygen compounds are potentially highly reactive and might enable unique biochemical reactions. For visualization, the nitrogen-oxygen intermediates of the canonical denitrification pathway with high redox potential present in strain HdN1 and N_2 as its endproduct are depicted (Fig. 7).

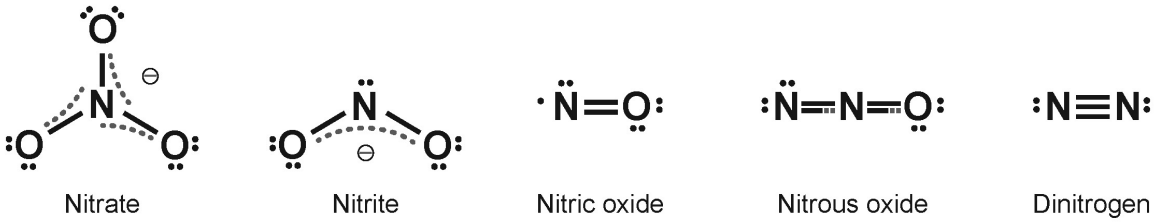

Fig. 7. Approximated chemical structures of N-compounds in the order of the canonical denitrification pathway. Nitrate, nitrite and nitrous oxide exhibit mesomeric bond structures with delocalized electrons indicated by dotted lines (grey) which cannot be correctly visualized by single Lewis formulas. Paired electrons in atomic orbitals are depicted as two dots, the unpaired electron of nitric oxide as a single dot.

A.2.5 Potential significance of overlooked metabolic pathways

Thermodynamic calculations are a powerful tool to predict the feasibility and thus the potential occurrence of metabolic pathways in nature. In a well-known paper, E. Broda (1977) predicted the possible existence of two kinds of microorganisms with lithotrophic lifestyles involved in ammonium oxidation from energetic considerations. Both metabolic processes had not been detected in nature at that time. Eighteen years later, one of them, the anaerobic ammonium oxidation (anammox) coupled to nitrite reduction was discovered (Mulder *et al*., 1995) to be performed by bacteria affiliated with the *Planctomycetes*. Another eleven years later, the anammox process was exploited for economic removal of fixed nitrogen in a first full sized wastewater treatment plant (Kuenen, 2008). Nowadays computational models have been developed to asses the possibility for biodegradation of xenobiotics (e.g. Finley *et al*., 2009).

Most of our current knowledge on metabolic pathways in prokaryotes is based on the study of model organisms. When the function of the involved metabolic enzymes is established by physiological experiments, the occurrence of the corresponding functional genes in the environment can be studied by molecular methods independent of cultivation. In contrast, no method is available to check for the occurrence of unknown pathways in nature. Such pathways might involve the same substrates or metabolic intermediates as the established

ones, but rely on alternative transformation reactions with a set of unknown enzymes. Accordingly, even metabolic routes responsible for massive turnovers in global geochemical cycles can be overlooked, when involved microorganisms are not cultivated and studied so that their metabolic activity is not recognized. An example for such a scenario is the marine anammox process: Loss of organic nitrogen in the world oceans had been assigned exclusively to the activity of denitrifiers in the past. Since the detection of the anammox process in the black sea, almost a decade ago (Kuypers *et al*., 2003) the picture has changed completely. Current experimental data suggest that marine anammox organisms of the *Planctomycetes* are responsible for a substantial part of global marine N-loss which takes place particularly in oxygen minimum zones of upwelling areas (Dalsgaard *et al*., 2003; Lam and Kuypers, 2011). The general tendency to overlook underlying causes during observation of macroscopic phenomena can be extended to the medical sciences in the 19th century. The role of pathogenic bacteria as the causative agent of disease was not recognized until they were cultivated and studied by scientists like Robert Koch and other founding fathers of today's microbiology. Overall, the successful cultivation and examination of novel unusual microorganisms can help to establish a more complete and accurate picture of the transformation reactions shaping the world we live in. The detection of a huge number of unknown genes in all prokaryotic genomes that have been sequenced and annotated today, show the vast potential for future discoveries of unrecognized metabolic pathways that have been overlooked in the environment so far.

A.3 'Unusual' hydrocarbon degrading anaerobes

A.3.1 *Desulfococcus oleovorans* Hxd3

Strain *Desulfococcus* (formerly *Desulfobacterium*) *oleovorans* Hxd3 is able to degrade $C_{12}H_{26}$ to $C_{20}H_{42}$ alkanes as well as 1-hexadecene coupled to sulfate respiration. The genome sequence was completely assembled by the Joint Genome Institute (JGI) in 2007 and is accessible (accession number CP000859.1) but not analyzed and discussed in a publication to date. Complete oxidation of alkanes to CO_2 (and H_2O) was shown by determination of degraded alkane and reduced sulfate in cultures of strain *D. oleovorans* that matched the proposed stoichiometry according to eq. 1.

$$C_{16}H_{34} + 12.15\ SO_4^{2-} \rightarrow 16\ HCO_3^- + 12.15\ H_2S + H_2O \quad (1)$$

The anaerobic alkane activation reaction employed by *D. oleovorans* was suggested to be either a (endergonic) terminal carbonylation (addition of a C_1 unit) or fumarate addition at the C3 position (Aeckersberg, 1998). However, the expected alkyl-succinate metabolites were not detected in cultures of *D. oleovorans*. A presently discussed mechanism is initiated by a carboxylation at the C3 position followed by removal of two carbon atoms from the alkane chain, based on ^{13}C-CO_2 incorporation into intermediates (So *et al*., 2003; Callaghan *et al*., 2006). However, a fatty acid with an ethyl residue at the C2 position (2-ethyl-alkanoate) should arise from the suggested activation reaction which has never been detected. Also, the carboxylation of alkanes is not thermodynamically feasible under standard conditions unless the product from the activation reaction is kept at extremely low concentrations (Thauer and Shima, 2008). Thus, the hypothetical anaerobic alkane activation via carboxylation is still challenged and awaits further experimental substantiation.

A.3.2 *Pseudomonas chloritidismutans* AW-1^T

Strain *Pseudomonas chloritidismutans* belongs to the *Gammaproteobacteria* and was isolated from a chlorate reducing bioreactor (Wolterink *et al*., 2002). The strain was able to reduce chlorate, but not nitrate initially. However it could be adapted to growth with nitrate by repeated subcultivation and decreasing oxygen concentrations according to Cladera *et al*. (2006). Bacteria able to reduce perchlorate (ClO_4^-) and/or chlorate (ClO_3^-) have been found to utilize both compounds not only as terminal electron acceptors, but also as sources of oxygen as the terminal product of the reduction sequence ($ClO_4^- \rightarrow ClO_3^- \rightarrow ClO_2^- \rightarrow Cl^- + O_2$).

Strain *P. chloritidismutans* grew with *n*-alkanes ranging from C_7H_{16} to $C_{12}H_{26}$ and oxygen (from air) or chlorate as electron acceptor (Mehboob *et al*., 2009). The proposed pathway is as follows: Chlorite (ClO_2^-) is dismutated into chloride and molecular oxygen according to $ClO_2^- \rightarrow Cl^- + O_2$ ($\Delta G° = -148.4$ kJ mol^{-1}; Rikken *et al*., 1996; Wolterink *et al*., 2002). The formed oxygen enables the activity of the aerobic pathway initiated by terminal oxidation of *n*-decane with help of a monooxygenase (Fig. 8). The produced alcohol is oxidized subsequently to the aldehyde and fatty acid, which is then channeled into β-oxidation. The study by Mehboob *et al*. (2009) was the first description of the utilization of chemogenic, intracellular oxygen for the ‘anaerobic’ activation of *n*-alkanes.

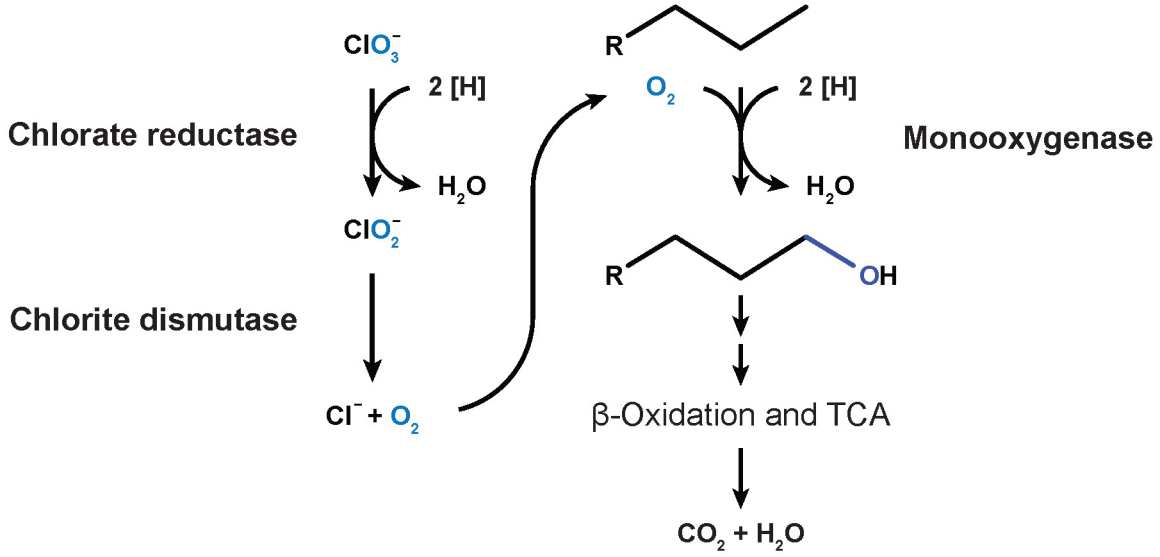

Fig. 8. Degradation of *n*-alkanes coupled to chlorate respiration in strain *Pseudomonas chloritidismutans* AW-1 with monooxygenases utilizing oxygen from chlorite dismutation for terminal oxidation (adapted from Mehboob *et al*., 2009).

A.3.3 *Candidatus* Methylomirabilis oxyfera

The first described microorganism able to degrade methane coupled to nitrite respiration was '*Candidatus* Methylomirabilis oxyfera' (Raghoebarsing *et al*., 2006) affiliated with the NC10 phylum. The genus and species name can not be officially assigned to it yet, since the examined culture is still in the state of an enrichment and not a pure strain.

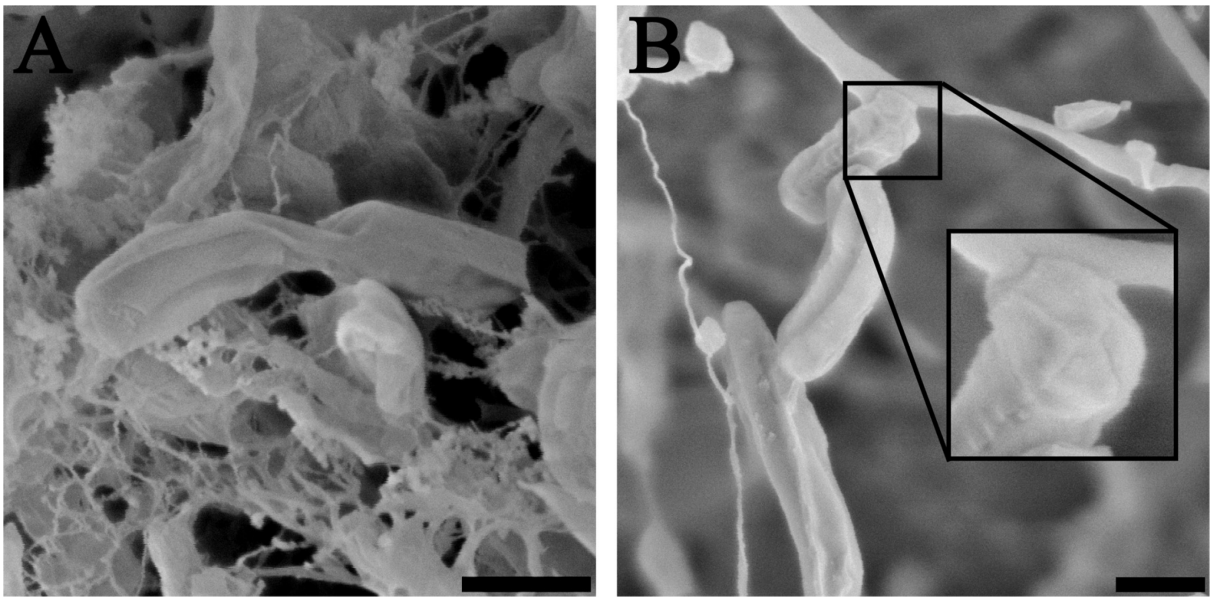

Fig. 9. Cryoscanning electron micrographs of '*Ca*. Methylomirabilis oxyfera' cells showing longitudinal ridges along the cell length. (A) Plunge-frozen '*Ca*. Methylomirabilis oxyfera' cells undergoing cell division. (B) Plunge-frozen '*Ca*. Methylomirabilis oxyfera' cells showing cap-like structure (inset) at the cell poles. Scale bars, 500 nm. Source: Wu *et al*., 2012

Cells of *M. oxyfera* exhibited an unusual polygonal shape (Fig. 9) and an additional outermost sheath, which might represent a (glyco)protein surface layer. Electron microscopy also revealed the lack of intracytoplasmic membranes, known from classical proteobacterial methanotrophs (Wu *et.al*., 2012). All of the observed distinctive morphological features might be due to adaptations to its unique lifestyle described below.

Metagenomic analysis of DNA samples extracted from the culture and bioinformatic reconstruction enabled the assembly of the whole genome sequence. The genome was assigned to a single species, even though the enrichment was not clonal and thus the genome data revealed some degree of microvariability (Ettwig *et al*., 2010). Transcriptomic and proteomic information from this culture was acquired in addition shaping a puzzling picture of *M. oxyfera*'s methane metabolism. The complete aerobic pathway for methane degradation was present in the genome and apparently operative in the anaerobically grown cells, evident from the obtained mRNA and protein data, although the culture was kept anoxic and nitrite was constantly reduced. Furthermore, N_2 was the endproduct of nitrite reduction even though the enzyme for N_2O reduction to N_2 (the last step of complete denitrification catalyzed by the N_2O reductase) was absent from the genome.

This riddle was resolved, when indications for the dismutation of NO into N_2 and O_2 enabling an 'intra-aerobic' pathway were found via physiological experiments. During methane inlet mass spectrometry (MIMS) supported by additional microsensor measurements with *M. oxyfera*, methane was reduced when nitrite or NO was added. This led to the formation of N_2 in the absence of an N_2O reductase. Only minor amounts of N_2O were produced that were assumed to be produced by the activity of accompanying species. Also, when N_2O and/or nitrate was present at high concentrations, methane was not reduced until nitrite was added. In assays with acetylene, propylene and ^{18}O-labeled H_2O, increasing amounts of $^{16,18}O_2$ and $^{18,18}O_2$ were detected in the gas phase over *M. oxyfera* cultures upon addition of unlabeled NO_2^-. This was explained by the exchange of oxygen atoms between H_2O and NO_2^- due to the activitiy of the nitrite reductase (Friedman *et al*., 1986). The path of the ^{18}O oxygen would thus have led from $N^{18}O_2^-$ via reduction to $N^{18}O$ and via dismutation to $^{16,18}O_2$ and $^{18,18}O_2$. Such oxygenic NO dismutation had not been observed before and has not been measured in cell extracts or in enzyme assays thus far.

Since oxygen was shown to be produced by these cells, presumably from NO dismutation, the question arose, whether *M. oxyfera* was able to grow with oxygen. However, addi-

tions of 2% or 8% oxygen to the cultures resulted in an instant decrease of methane and nitrite consumption and seemed to harm the cells (Luesken *et al.*, 2012). Apparently the applied oxygen concentrations had been too high. Thus the question remains whether *M. oxyfera* is able to grow under microaerophilic conditions.

The identity of the putative NO dismutating enzyme has not been resolved unambiguously. The particulate methane monooxygenase (pMMO) had been handled as a potential candidate, but also two multicopper oxidases as well as the NO reductases (Ettwig *et al*., 2010). Recent analysis of protein sequence data shifted the focus to the two closely related NO reductases (gene locus tags DAMO_2434 and DAMO_2437) related to the canonical qNORs encoded in the genome of *M. oxyfera* (Ettwig *et al*., 2012). Both were among the most abundant gene products as detected via transcriptomic and proteomic analysis, while a third Nor-gene (DAMO_1889) was expressed only in low amounts (Ettwig *et al*., 2010). The protein sequences of the two similar Nors exhibit remarkable modifications to key amino acids and a divergent phylogeny in comparison with canonical NO reductases. Due to the accumulated indications, the NO reductases of strain *M. oxyfera* were suggested to function as an NO dismutase (Ettwig *et al*., 2012). Purification and characterization of enzyme activity was suggested to test this hypothesis (Ettwig *et al*., 2012) The striking similarities and phylogenetic affiliation of their protein sequences with the protein sequence of an HdN1 Nor will be discussed in section B.2.3.

A.3.4 *Dechloromonas aromatica* RCB

The strain *Dechloromonas aromatica* which affiliates with the *Betaproteobacteria* was isolated with chlorate and BTEX compounds (benzene, toluene, ethylbenzene and xylene) from river sludge (Coates *et al*., 2001). It is the first isolated species able to completely degrade benzene to CO_2 under anaerobic conditions. The strain is able to couple growth with benzene to reduction of oxygen (aerobic) or nitrate to dinitrogen or chlorate and perchlorate to chloride (Chakraborty and Coates, 2005). The complete genome was sequenced and several mono- and dioxygenases for the aerobic degradation pathway were detected. In contrast, signature genes for the described glycyl-radical enzymes for activation mechanisms based on fumarate-addition (e.g. *bss*, *mas* (or *ass*) or *nms*; Widdel and Grundmann, 2010 and references therein) were found to be absent (Salinero *et al*., 2009). During growth of *D. aromatica* on benzene with nitrate initial hydroxylation of benzene to phenol and subsequent carboxylation to *p*-

hydroxybenzoate, and loss of the hydroxyl group to form benzoate (or benzoyl-CoA) was found (Chakraborty and Coates, 2005). Both phenol and benzoate were detected as transient metabolites via GCMS. In contrast, during aerobic growth of strain *D. aromatica* on benzene, no phenol could be detected. The hydroxylated derivative may have possibly escaped detection due to fast removal by subsequent metabolic reactions. Addition of the chemical reductant sodium dithionite (0.5 mM) did not affect phenol formation in nitrate reducing cultures, but retarded it in aerobic cultures. Higher concentrations (> 1 mM) completely inhibited aerobic growth with benzene while phenol sustained growth at the same concentrations of ditionite. Thus, it was suggested that the hydroxylation of benzene had been inhibited by the reductant (Chakraborty and Coates, 2005). In the absence of oxygen (from air), chlorite- or NO-dismutation could provide chemogenic oxygen for the oxidation of benzene via mono- or dioxygenases (Weelink *et al*., 2010). It is conceivable, that the dithionite (as an ionic compound) did not reduce intracellular oxygen. Thus a common pathway for aerobic and anaerobic activation of benzene with oxygen as a co-substrate in strain *D. aromatica* RCB can not be excluded.

The identity of the enzyme potentially responsible for oxygen generation from denitrification intermediates is unclear. The chlorite dismutase (Cld) of *Nitrospira defluvii* has been negatively tested for the dismutation of NO. In contrast, chlorite dismutating activity was found to be inhibited by addition of NO (Maixner and Ettwig unpublished data in Ettwig *et al*., 2012). An enzyme similar to the qNors of strain *M. oxyfera* (and HdN1) was absent in the genome of strain *D. aromatica* (Ettwig *et al*., 2012). Hence, either the strain features an unknown enzyme for the oxygenic dismutation of NO (or another denitrification intermediate), or growth with benzene is initiated by an alternative uncharted activation mechanism independent of O_2. Such a mechanism, not dependent on electron acceptors with a highly positive redox potential could also be employed by sulfate reducing bacteria for the anaerobic activation of benzene.

A.4 Goals of the present work

While the existence and significance of anaerobic alkane degrading bacteria in hydrocarbon remineralization had been widely neglected in the past (McKenna and Kallio, 1965, Atlas, 1981), it is commonly accepted nowadays (Rojo, 2009). Anaerobic hydrocarbon degradation is known to occur via a number of different biochemical activation mechanisms, the applicability of which is mostly dictated by the chemical properties of the substrates (Heider, 2007). One mechanism for the anaerobic degradation of alkanes based on the addition of fumarate has been recognized and studied since more than ten years and is thus quite well understood by now (Kropp *et al.,* 2000; Rabus *et al.,* 2001; Grundmann *et al.,* 2008, Callaghan *et al.,* 2008, Rabus *et al.,* 2011). Alternative pathways may exist, for which some indications are available (Aeckersberg *et al.,* 1998, So *et al.,* 2003). However, hitherto the significance of these alternative activation pathways remains largely unknown and thus awaits investigation.

The general aim of this study was to investigate the anaerobic degradation of *n*-alkanes by strain HdN1, which was suspected to employ a novel activation reaction since described pathways were found to be absent. The first objectives were to describe strain HdN1 in more detail in terms of its phylogeny, cell morphology and substrate spectrum as well as to develop and apply thorough purity controls. Such controls were necessary to resolve doubts mostly caused by strain HdN1s' obvious pleomorphism (Section B.1). Since the unique anaerobic alkane metabolism of strain HdN1 was the main topic of my thesis, experiments to investigate several physiological traits were to be conducted. When indications for a surprising functional coupling of the alkane catabolism with intermediates from denitrification became apparent, the metabolic significance of the energy rich N–O compounds was to be scrutinized (Section B.2). Furthermore, detection of trace oxygen concentrations within the HdN1 culture was to be attempted with a number of different techniques, to explore one hypothesis for anaerobic activation of alkanes by strain HdN1 that would imply the production and utilization of dioxygen, (Section B.3). The catabolic transformations of alkanes, alkenes and phenylalkanes that could reveal or hint on the nature of the potentially novel anaerobic activation reaction were to be investigated (Section B.4).

B Results and Discussion

This part provides a discussion of selected results from the original research articles and subsidiary unpublished findings. Further details may be found in Chapter D.2 and D.3.

B.1 Phylogeny and physiology of strain HdN1

B.1.1 Phylogeny

Strain HdN1 affiliates with the *Gammaproteobacteria* (Fig. 10). The three closest relatives of the strain, found by comparison with the most current ribosomal 16S rRNA sequence data available in the ARB-Silva-database (SSU Ref NR 111, July 2012; Ludwig *et al.,* 2004; Pruesse *et al.,* 2007), are *Ectothiorhodospira shaposhnikovii* (88.0% seq. identity), *Thiorhodococcus minor* (87.8% seq. identity) and *Methylococcus capsulatus* strain Bath (88.9% seq. identity).

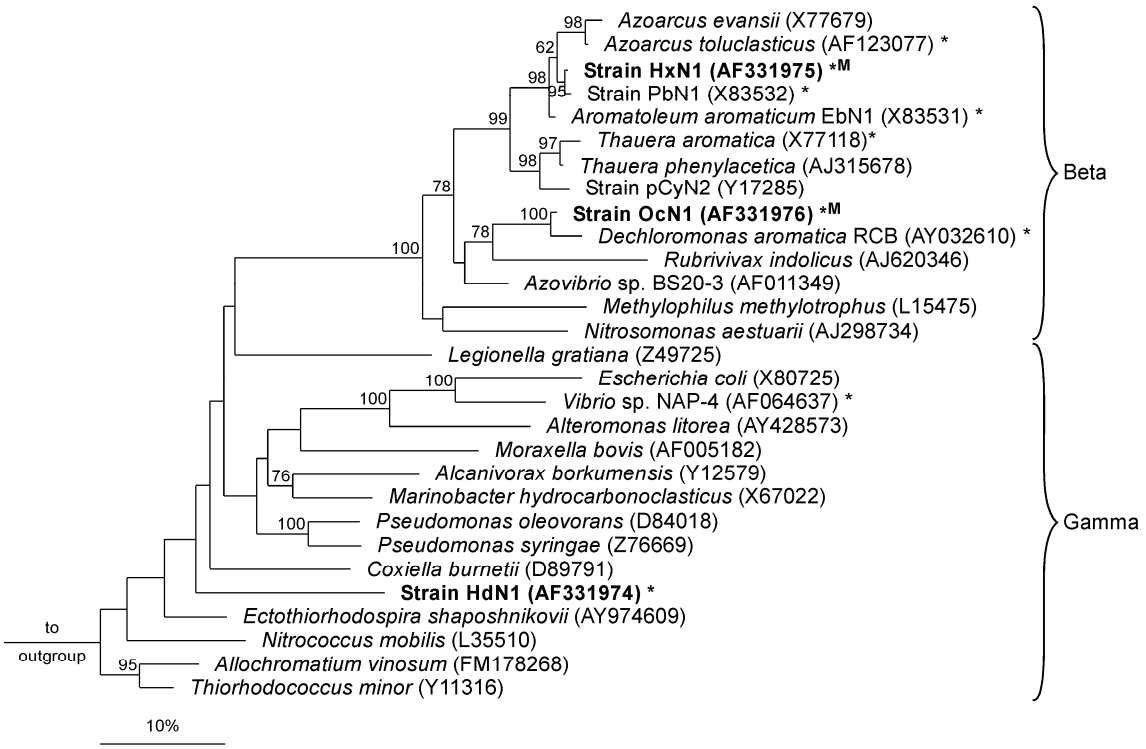

Fig. 10. Phylogenetic (16S rRNA based) affiliation of strain HdN1 with selected *Beta-* and *Gammaproteobacteria* including other strains able to degrade aromatic or saturated petroleum hydrocarbons with NO_3^- (*). Strains able to anaerobically degrade *n*-alkanes are highlighted in bold; occurrence of (1-methylalkyl)succinate formation for alkane activation is also indicated (M). Tree-reconstruction was via neighbor joining method. Bootstrap values (%; only > 60% shown) were obtained after 1000 resamplings. Scale bar, 10% estimated seq. divergence. Zedelius *et al*., 2011.

Since its 16S rRNA sequence has a similarity of less than 95% compared with the closest described genus, strain HdN1 will once be assigned a novel species of a novel genus (Yarza *et al*., 2008; Tindall *et al.,* 2010). The species name '*Oleomonas alkani*' suggested by P. Ehrenreich, who purified the strain during her PhD-thesis (1996), can not be used since the genus name '*Oleomonas*' has already been assigned to a different phylum in the meantime (Kanamori *et al.,* 2002). As her successor, I would suggest the name *Paraffinoleum pronitroxum* (Par.affin'o.le.um L. *parum affinis* lacking affinity (inert), paraffin; L. n. *oleum* oil; pro.ni.trox.um L. n. *pro* for, *nitr* nitrogen, *ox* oxygen).

B.1.2 Cell morphology

The cell morphology of strain HdN1 has been characterized before (Ehrenreich, 1996, 2000) and shall just be mentioned here briefly for the sake of completeness. The cell shape of strain HdN1 depends on its growth substrate. With fatty acids (e.g. myristate), cells were short rods, 1.5 -2.5 µm in length and with a diameter of 0.5 µm (Fig. 11 B). With alkanes, alkenes and long chain alcohols, the cells exhibited a certain pleomorphism. In such cultures, a large fraction of the cells took on a larger, more oval shape with a high variability in sizes and a strong refraction, while some cells remained small and rod-shaped, some were also motile (Fig. 11 A). The increase in size was due to the formation of internal storage inclusions likely containing the pure growth substrate and wax esters and possibly some other hydrophobic metabolites (for more details see section B.4). The cells apparently produced these neutral lipids when supply of an energy rich growth substrate was ample to provide for potential future shortages. Earlier assumptions on the formation of polyhydroxy-alkanoates (PHA) as storage compounds were refuted (A. Steinbüchel, personal communication). Nile red is known to stain cellular inclusions containing lipids or hydrocarbons (Spiekermann *et al*., 1999; Pinzon *et al*., 2011). The dye only becomes fluorescent within a hydrophobic environment (Greenspan *et al*., 1985). Staining of cells for specific detection of stored *n*-alkanes or wax esters was not possible, since not all cells with such inclusions were stained by Nile red (Fig. 11 C), and also cells grown with pentanoate shown not to produce wax esters (see section B.4.4) gave a weak signal (not shown).

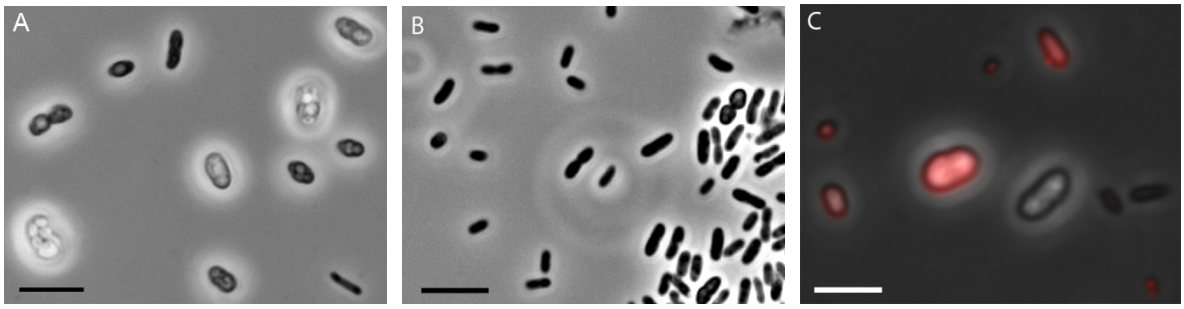

Fig. 11. Phase contrast micrographs of HdN1 cells grown anaerobically with *n*-tetradecane (A) or valerate (B) and overlay of phase contrast and fluorescence micrograph of alkane grown cells stained with Nile red (C). Excitation wavelength was 515-560 nm; emission was > 590 nm. Scale bar represents 5 µm. Zedelius *et al*., 2011.

While short-chain fatty acids (preferred: pentanoate) used for cultivation allowed measurements of optical density (OD_{660}), flocks of long-chain fatty acid substrates had to be removed beforehand. In cultures with aliphatic hydrocarbon substrates, cell aggregates that formed at a certain density and high refraction from the internal inclusions (Fig. 11 A) led to incomparable results that could only be used to roughly estimate the state of growth.

B.1.3 Key genome features

The complete genome of strain HdN1 was sequenced by a shotgun approach in cooperation with Richard Reinhardt (MPI for Plant Breeding Research) and Michael Kube (MPI for Molecular Genetics). The sequence (accession number FP929140; NCBI reference NC_014366.1) consists of 4,587,455 base pairs with a G+C content of 53.26 [mol%] and contained 3762 predicted coding sequences. More information on the genome can be found in Tables S1 (general genome features), S3 (detected genes of denitrification enzymes), S4 (detected alkane monooxygenase genes), S5 (detected terminal oxidase genes) in the appendix of Chapter D.2. Details on the methods used during genomic analysis are described in Appendix S1 of Chapter D.2. Strain HdN1 possessed no plasmids.

B.1.4 Purity

For purification, dilution techniques are useful since accompanying organisms present in minor fractions can be out-diluted, leaving only the most abundant species. The best way to check for a contamination in a culture of strain HdN1 is to use (aerobic) agar plates or liquid medium with yeast extract and glucose, since strain HdN1 does not grow with them, while they enable fast growth (and thus detection) of typical contaminant strains. Such commensals might be present in very low numbers during cultivation of the dominant strain, when they

live of lysed cells and excreted metabolites. PCR-based techniques are most useful for the detection of known organisms, since specific primers can retrieve a signal even from a few contaminating cells. With unspecific primers (e.g. for the 16S rRNA gene) low amounts of contaminating cells might escape detection. Methods based on whole cell 'fluorescence *in situ* hybridization' (FISH; Amann and Fuchs, 2008) can detect all kinds of accompanying species present in microscopically detectable numbers with help of fluorescent oligonucleotide probes specific for the dominant species. To ensure that the variation in cell shapes in the HdN1 cultures did not mask a contamination, thorough purity tests were conducted. First, liquid dilution series of strain HdN1, according to the 'most probable number' approach, with tetradecane or valerate were prepared. Cells from the highest positive dilutions were microscopically indistinguishable and always able to grow with both, tetradecane and valerate (pentanoate), showing that they were really strain HdN1. Second, agar plates with valerate and yeast extract were incubated under air with addition of CO_2 (3-6%). All colonies and cells had the same appearance and were able to grow anaerobically with NO_3^- and tetradecane, thus indicating their identity as strain HdN1. Third, a specific fluorescent oligonucleotide-probe (HdN1_112) was designed with ARB and used for whole cell hybridizations (FISH) as described before (Musat and Widdel, 2008, for details see Appendix E.4.1). While all cells in HdN1 cultures hybridized with the HdN1_112-probe and were labeled with DAPI (4′,6-Diamidin-2-phenylindol; Fig. 12 A), added cells of strain OcN1 (chosen due to the similar lifestyle of this strain) did not hybridize with this specific probe and were only visualized by their DAPI-signal. Hence, accompanying cells would be distinguishable and thus detectable via FISH (Fig. 12 B).

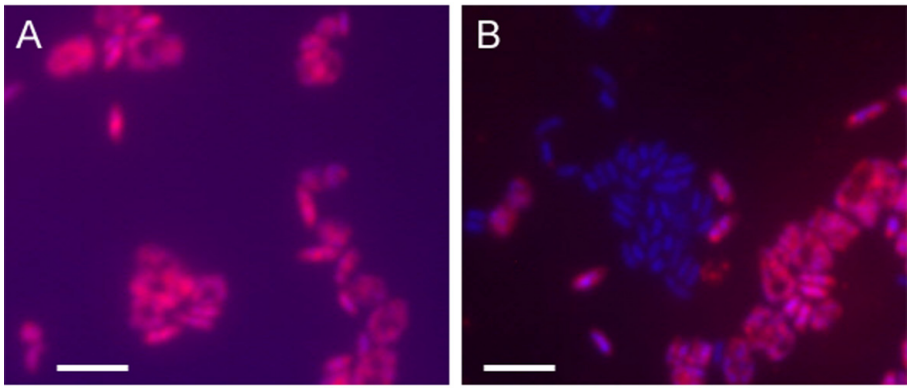

Fig. 12. Fluorescence microscope images, overlays of the specific HdN1_112 probe and DAPI signals. Cells of strain HdN1 are visualized by the specific probe (red) and DAPI (blue) signals (A). In mixtures the added OcN1 cells are only visualized by the DAPI (blue) signal (B). Bar represents 5 µm. Zedelius *et al*., 2011.

B.1.5 Cultivation

Strain HdN1 was anaerobically cultivated in bicarbonate-buffered 'nitrate reducer medium' (NM) saturated with N_2/CO_2 (9:1, v/v) with NO_3^- and ascorbate (as a reducing agent that was not metabolized) according to Widdel and Bak (1992). With fatty acids it had a doubling time of 11-13 hours. Aerobic cultivation was performed in phosphate-buffered medium (PNM; see Appendix E.2). The pH in anaerobic cultures increased from 6.8 to over 8.0, due to proton consumption during denitrification. Although the highest tolerated salinity was not determined, unrestricted growth in brackish medium (Appendix E.2) and tests with diluted freshwater medium showed that the strain could endure some osmotic variation (not shown). Aerobic or anaerobic growth on agar-plates necessitated a minimal medium (Appendix E.2) and CO_2 added to the headspace (3-5%). If a small amount of liquid alkane (preferentially tetradecane due to its relatively high vapor pressure) was added to a piece of filter-paper and placed in the lid of the petri-dish, colony formation was surprisingly fast. In liquid cultures, shaking accelerated growth only with fatty acids, while it hampered alkane cultures (as observed before with strain Hxd3, Aeckersberg *et al*., 1998). In freshly inoculated alkane-cultures, the first indication of growth was formation of small gas bubbles, and then a sheath of cells right below the organic phase. Such sheaths of cells have been considered as 'biofilms' before (Grimaud, 2010) despite the lack of a solid support. Attachment is a prevalent phenomenon for hydrocarbon degraders that facilitates uptake of highly insoluble substrates (Abbasnezhad *et al.,* 2011) and apparently is also employed by strain HdN1.

B.1.6 Exclusion of trace oxygen leakage

For anaerobic cultivation butyl-rubber stoppered glass bottles were used. Since these stoppers are pierced by steel needles often for sample acquisition or feeding of nutrients, trace amounts of oxygen could theoretically enter the bottles via micro-leakages. For "aerobic" terminal activation of alkanes by monooxygenases only one molecule of oxygen is needed per alkane molecule. In the case of *n*-hexadecane, the resulting hexadecyl-alcohol still retains most reduction equivalents (96 of 98 [H]) which could be transferred to both kinds of respiration – either coupled to oxygen- or to nitrate-reduction. In a scenario where just one mole of external oxygen per mole of degraded alkane could pass the stopper, any bacterial strain with alkane monooxygenases and the ability to denitrify could grow "*anaerobically*" with alkanes. Such a scenario is highly unlikely though, since anaerobic cultivation techniques are well established

(Bryant, 1972; Hungate 1969; Widdel, 2010) and diffusion would strongly limit such growth dependent on leaked oxygen, incompatible with fast growth rates. Besides, 4 mM ascorbate was always present in the medium acting as an oxygen sink (such medium stored in rubber-stoppered flasks remained anoxic, obvious from the reduced state of the ascorbate which was not oxidized to the orange-colored dehydroascorbate, even after months of storage). Also strain HdN1 grew well on agar plates with alkane vapors in anoxic jars, with a strong iron-based reductant (Anaerocult A, Merck, Darmstadt) and the use of tests strips that indicated anaerobiosis (Anaerotest, Merck, Darmstadt). Furthermore, the formation of N_2 due to denitrification leads to the build-up of considerable overpressure in the cultures that would only allow an efflux of gas via hypothetical leaks counteracting O_2 influx. Finally, an experimental result can be cited here to resolve any doubts: When cultures of strain HdN1 were incubated with a large surplus of hexadecane and N_2O (red. of 250 µmol N_2O [accepts 500 µmol e^-] yields max. 250 µmol N_2) in glass bottles with the same kind of rubber stoppers, leakage of O_2 for alkane activation would have lead to more N_2-production than with nitrate (red. of 100 µmol NO_3^- [accepts also 500 µmol e^-] yields max. 50 µmol N_2) since all N_2O would have been reduced with electrons from the activated alkanes. However, the contrary was observed – less N_2 is formed with N_2O, thus disproving oxygen leakage as visualized in Fig. 15 A,B.

B.1.7 Substrate spectrum

The substrate spectrum of strain HdN1 had been determined to some degree in the past (Ehrenreich, 1996) and was further investigated during this work (a table with a detailed substrate spectrum can be found in Appendix E.1.1). Under aerobic conditions a slightly narrower *n*-alkane-spectrum (C_7–C_{30}; organic substrates indicated by C-chain while other constituents are omitted) could be degraded than under anaerobic conditions (C_6–C_{30}). The reason for this discrepancy is unclear and could best be explained by different sets of enzymes involved in degradation expressed at different redox conditions. Fastest growth was observed in the range from C_{14} (tetradecane) to C_{18} (octadecane). Growth with *n*-alkanes of shorter or longer chains was slower or was preceded by a longer lag-phase. A possible explanation for these observations could be lower enzyme specificities for these chain lengths or even toxic effects (Hasinger *et al.*, 2012). The range of utilizable 1-alkenes (C_{10}, C_{14}, C_{16}, C_{17} tested positively), fatty acids (C_2–C_{18}) and 1-alkanols (C_8, C_{10}, C_{14}, C_{16} tested positively) was the same under aerobic or anaerobic conditions. Aromatics were in principle not utilized as substrates. Phenyl-

tridecane and phenyltetradecane supported growth, but only the side chains were degraded producing benzyl-substituted carboxylic acids (see also section B.4.5). Long-chain *n*-alkanes with more than 18 carbon atoms are highly insoluble and crystalline (viz. solid) at room temperature. Still, strain HdN1 and other (mostly aerobic) bacteria are known to degrade these paraffins with surprisingly large chain lengths. According to some reports the degradation of extremely long alkanes (e.g. C_{44}) was only possible when they were dissolved in a liquid organic phase (Sakai *et al.,* 1994). However, strain HdN1 was not able to degrade *n*-tetracontane (C_{40}) dissolved in HMN. While the solubility of short- to medium-chain alkanes decreases enormously with increasing chain length (still the fraction of a liquid alkane dissolved in water has the same activity as the pure alkane phase; Widdel and Musat, 2010), these substrates are in general thought to cross cell membranes by diffusion. The dissolution and uptake of solid alkanes possibly necessitates surfactants (Perfumo *et al*., 2010) and active transport into the cells by so far unknown enzymes. Due to the structural similarities of long-chain alkanes and the side-chains of low-density polyethylene (LD PE, Aldrich, St. Luis, USA), the potential for plastic-degradation was also tested with strain HdN1. Incubations with pure PE or PE and HMN did not show any growth. To test whether alkyl-residues coupled to a solid phase (irregular silica gel particles) could be degraded, octa-decyl-silan ($C_{18}H_{37}SiH_2$-R; Agilent, Santa Clara, USA) was also tested in incubations, but proved to be non-degradable by this strain.

B.2 Nitrate metabolism and the role of intermediate N–O-compounds

B.2.1 Reduction of nitrate and other electron acceptors

Denitrification is the reduction of nitrate (NO_3^-) or nitrite (NO_2^-) via nitric oxide (nitrogen monoxide, NO) to nitrous oxide (dinitrogen oxide, N_2O) and often to dinitrogen (Zumft, 1997; Fig. 13).

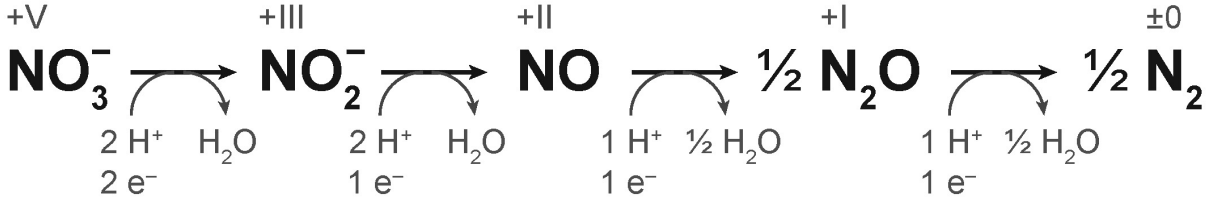

Fig. 13. Simplified canonical denitrification pathway with the complete reduction of nitrate to dinitrogen. The redox state of nitrogen is indicated by latin numbers above.

Genes for the enzymes of the canonical denitrification pathway were detected in the genome of strain HdN1 (for details see Table S3 in the appendix of Chapter D.2): A nitrate reductase (*narGHJI*), a nitrite reductase (*nirS*), a nitrous oxide reductase (*nosZ*) and three different nitric oxide reductases (*norBC* and two different *norZ*) the potential role of which will be discussed in section B.2.3. During fast growth NO_2^- and N_2O (but not NO) sometimes accumulated transiently at low concentrations (≤ 1.5 mM and ≤ 2.5 mM respectively), but were later completely reduced to N_2 in the presence of appropriate electron donors. This behavior is known to be more or less pronounced for both intermediates in other denitrifying bacteria. In heterotrophic bacteria, only a small fraction of the electron donors (C source) is transformed into biomass, while the major fraction is dissimilated to CO_2, depending on the terminal electron acceptor (Widdel and Musat, 2010). The accumulation of N_2 and CO_2 can thus be quantified as indicators of metabolic activity. For this technique cultivation needs to be conducted below a headspace of a N_2-free inert gas like argon or helium so that produced N_2 is not obscured by background N_2 and the same gas needs to be employed as carrier during gas chromatography. This approach is particularly useful for strain HdN1 since the measurement of optical density (OD) for the quantification of growth (also an indicator of metabolic activity) is skewed with alkane grown cells due to droplet-like inclusions with a high refraction (compare section B.1.2 and Fig. 11).

To examine their capability to support efficient growth, different electron acceptors were added. Build-up of cell mass of strain HdN1 was fastest with O_2, tested at concentrations of ambient air. While NO_3^- added at 100 mM slightly slowed down growth, lower concentrations (≤ 40 mM) sustained fast growth. With NO_2^-, cultures sometimes had a longer lag-phase or grew slower if more than 5 mM were added. Interestingly, no growth occurred with N_2O and alkanes as substrate. This unexpected finding demanded further examination (see following section). Other electron acceptors tested incluced (conc. in mM) sulfate (15), thiosulfate (5), sulfur (added as slurry), fumarate (10) and perchlorate (10) but none of them supported growth. Toxic effects of these compounds were excluded, since controls with additional NO_3^- exhibited fast growth. In contrast, added chlorate proved to be toxic for this strain.

B.2.2 Gas measurements for physiological analysis

For comparison, strain HdN1 and two other alkane degraders, strains HxN1 and strain OcN1 were cultivated with N_2O and either an *n*-alkane or a fatty acid in cultures with an argon at-

mosphere. When the positive controls were fully grown, headspace samples from all cultures were analyzed via gas chromatography. Strains HxN1 and OcN1 (both belong to the *Betaproteobacteria* and use fumarate addition for alkane activation) grew well on *n*-alkanes (hexane and octane, respectively) or fatty acids (hexanoate) with N_2O, and accordingly reduced it to N_2 (Fig. 14). Strain HdN1 was found to also metabolize fatty acids or primary alcohols (not shown) with this electron acceptor. Furthermore, the combination of N_2O and a long-chain alkane (*n*-hexadecane) did not inhibit growth of strain HdN1, since N_2-production was enabled with N_2O if NO_3^- was injected additionally (visualized also in Fig. 14). However, no growth occurred and only some residual N_2 was produced by strain HdN1 incubated with hexadecane and N_2O (Fig. 14).

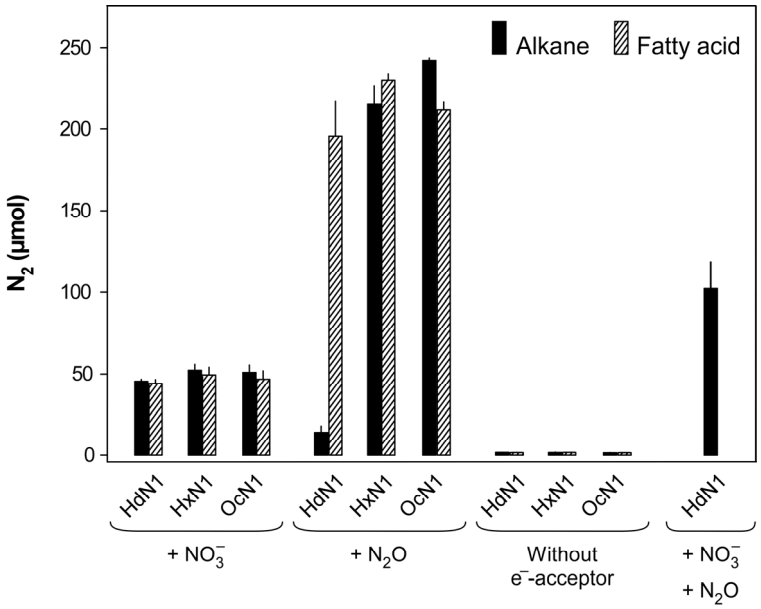

Fig. 14. N_2 formed in anaerobic cultures of strain HdN1, HxN1 and OcN1 with alkanes (black bars) or fatty acids (striated bars). A control experiment with strain HdN1 to exclude N_2O-toxicity received both, NO_3^- and N_2O. Here, more N_2 was formed than with NO_3^- alone. This indicated that not only NO_3^- but also N_2O was used by the respiratory chain if alkane degradation was enabled by NO_3^-. Data show that strain HdN1 could not use N_2O alone for alkane degradation, in contrast to the other strains. Negative controls (without electron acceptor) did not grow. Zedelius *et al*., 2011.

The puzzling inability of strain HdN1 to grow with alkanes and N_2O was scrutinized in time course experiments measuring formation of N_2 and CO_2 and reduction of N_2O with a surplus of alkane (*n*-hexadecane) or fatty acid (hexadecanoate) with either NO_3^- or N_2O and an argon atmosphere (Fig. 15). With NO_3^-, both substrates were utilized leading to production of N_2 and CO_2 (Fig. 15 A-D). The distinctive feature of strain HdN1 became apparent with N_2O, which was not reduced in cultures with hexadecane (Fig. 15 E).

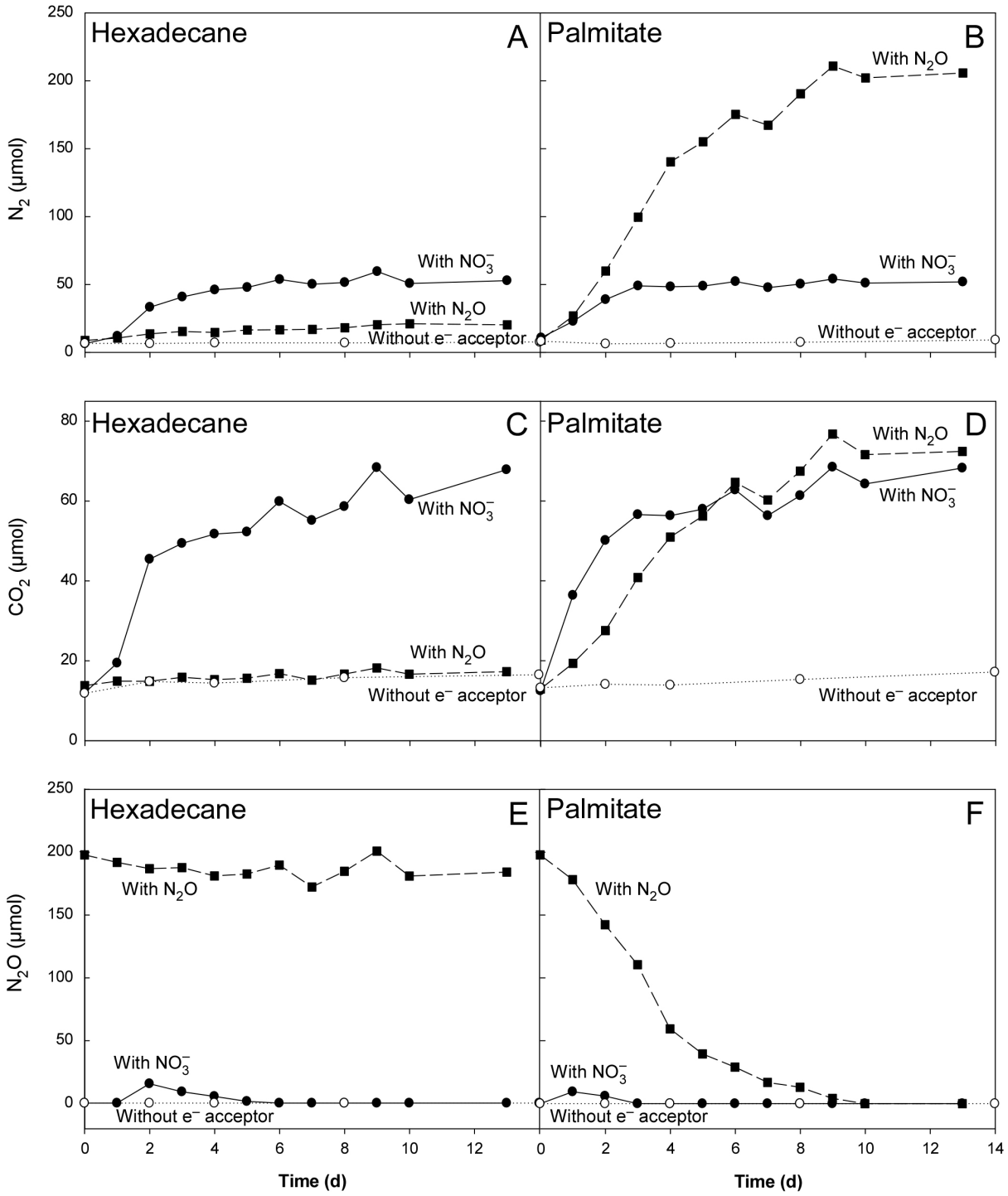

Fig. 15. Time courses of the formation of N_2 (A, B) CO_2 (C, D) and reduction of N_2O (E, F) in anaerobic cultures of strain HdN1 with *n*-hexadecane (A, C and E) or palmitate (B, D and F). The electron acceptors were added in stoichiometrically limiting amounts (100 mmol of NO_3^-; c. 250 mmol of N_2O) relative to the electron donor (171 mmol of hexadecane, 10 mmol of palmitate). Results show that alkane oxidation to CO_2 was not possible with N_2O, but readily occurred with NO_3^-. The functionalized compound, palmitate, was oxidized with N_2O. Zedelius *et al*., 2011.

Only a marginal increase in N_2 from reduction of N_2O and no production of CO_2 was detected (Fig. 15 A, C), while growth with palmitate entailed formation of N_2 and CO_2 (Fig. 15 B, D) and complete reduction of N_2O (Fig. 15 F). In cultures with NO_3^-, a transient accumulation of N_2O could be observed during the initial growth phase (Fig. 15 E-F). The initial amounts of NO_3^- and N_2O had been chosen so that an equal amount of reduction equivalents could be transferred from the carbon substrate to the respective electron acceptor. More N_2 production was thus expected if all N_2O was reduced (according to eq. 2 and 3) compared to a complete reduction of NO_3^- (according to eq. 4 and 5).

$$C_{16}H_{34} + 49\ N_2O \rightarrow 16\ HCO_3^- + 49\ N_2 + 1\ H_2O + 16\ H^+ \quad (2)$$

$$C_{16}H_{32}O_2^- + 46.5\ N_2O \rightarrow 16\ HCO_3^- + 46.5\ N_2 + 15\ H^+ + 0.5\ H_2O \quad (3)$$

$$C_{16}H_{34} + 19.6\ NO_3^- + 3.6\ H^+ \rightarrow 16\ HCO_3^- + 9.8\ N_2 + 10.8\ H_2O \quad (4)$$

$$C_{16}H_{32}O_2^- + 18.6\ NO_3^- + 3.6\ H^+ \rightarrow 16\ HCO_3^- + 9.3\ N_2 + 9.8\ H_2O \quad (5)$$

Nitrite succeeds nitrate during denitrification ($NO_3^- \rightarrow NO_2^- \rightarrow NO \rightarrow N_2O \rightarrow N_2$) and was detected as regular intermediate at transient low concentrations (≤ 1.5 mM; B.3.1). With alkanes and N_2O, addition of 'pulses' of NO_2^- led to clear production of N_2 and CO_2 (Fig. 16). Apparently growth with alkanes was enabled by these additions.

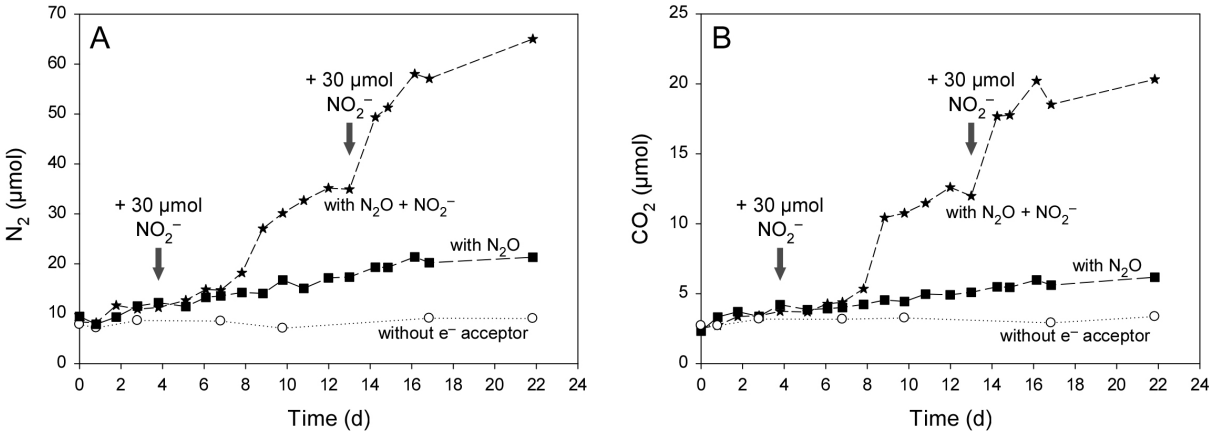

Fig. 16. N_2 (A) and CO_2 (B) formed in HdN1 cultures with alkanes and N_2O when NO_2^- (30 µmol) was added. The increase seen with N_2O alone can be explained by the oxidation of electron donors introduced with the inoculum. No formation of N_2 or CO_2 occurred without electron acceptor.

The formation of N_2 in cultures with only N_2O (Fig. 16 A) was as small as before (mind scale of y-axis) and apparently due to an endogenous electron donor introduced with the inoculum. Wax esters, and possibly other functionalized alkane metabolites stored within alkane grown

HdN1 cells (used here as inoculum), can be metabolized with N_2O and are thus good candidates for such electron donors. This also explains the formation of a small amount of N_2 with alkanes and N_2O seen in Fig. 15 A. The detection of wax ester-formation by strain HdN1 will be described in more detail in section B.4.4.

Strain HdN1 exhibited a unique physiology. Above results suggested that an intermediate from nitrate reduction 'before' N_2O was necessary for growth with alkanes. The crucial biochemical step during alkane degradation not sustained with N_2O could be the anaerobic activation reaction, since functionalized alkanes like alkanols and fatty acids were metabolized with this electron acceptor. Essentially, a small proportion of either NO_2^- or NO is suggested to be deviated from the respiratory chain for alkane activation (orange and red arrows in Fig. 17). Accordingly, the bulk of nitrogen compounds would follow the canonical denitrification pathway also in alkane cultures of strain HdN1. This hypothesis is supported by the finding that N_2O was a regular intermediate (Fig. 15 E-F; it accumulated only when N_2O reduction was inhibited; see Fig. 21) and N_2 was formed as metabolic end product.

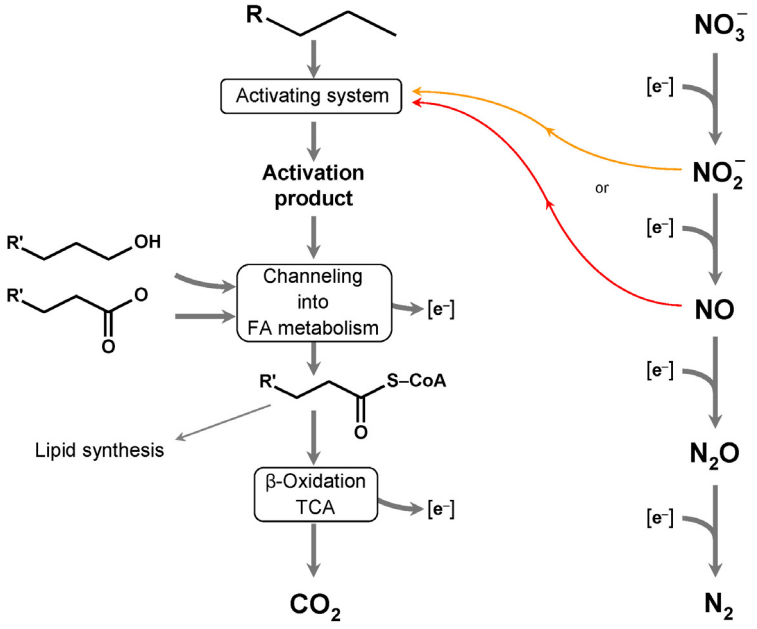

Fig. 17. Hypothetical involvement of N–O-compounds in alkane activation by strain HdN1. The scheme offers an explanation for the inability of strain HdN1 to utilize *n*-alkanes with N_2O alone. It is assumed that the unidentified activating system introduces a functional group to the inert hydrocarbon compound using a small proportion of NO_2^- (orange arrow) or NO (red arrow) that is deviated from the respiratory chain. These N–O compounds may be used for activation indirectly by yielding O_2 for a monooxygenases reaction, or by giving rise to another reactive factor or enzyme centre or directly as co-reactants introducing a polar group. The alkyl residue R′ may or may not be identical with the original residue R (depending on the activation mechanism and alkane C-atom being attacked). FA, fatty acid; TCA, tricarboxylic acid cycle. Zedelius *et al*., 2011.

A reactive compound known to enable alkane activation is O_2 (via monooxygenases; Britton, 1984). The possibility for intra-cellular oxygen production and utilization are discussed below and an overview of possible activation pathways is given in section B.5. Endergonic (energy rich) electron acceptors can in principle decompose with release of O_2 by thermodynamically feasible dismutation reactions (Table 2). While other reactions are purely hypothetical thus far, chlorite dismutation has been shown experimentally (van Ginkel *et al.,* 1996). Also NO dismutation into N_2 and O_2 was proposed due to detection of ^{18}O oxygen, the absence of a N_2O reductase from the genome (Ettwig *et al.,* 2010) and modifications to the potentially involved NO reductase of this strain (see section B.2.3 and Ettwig *et al.,* 2012). N_2O as the source for O_2 via dismutation (although thermodynamically feasible, see Table 2) is excluded for strain HdN1 since N_2O did not sustain anaerobic growth with alkanes.

Table 2. O_2 production by dismutation reactions of energy rich electron acceptors.

				$\Delta G'^{\circ}$ (kJ (mol O_2)$^{-1}$)
$2\ ClO_3^-$	→	$2\ Cl^- +$	$3\ O_2$	– 85.3
ClO_2^-	→	$Cl^- +$	O_2	– 148.4
$4\ NO_3^- + 4\ H^+$	→	$2\ N_2 +$	$5\ O_2 + 2\ H_2O$	+ 26.2[a]
$4\ NO_2^- + 4\ H^+$	→	$2\ N_2 +$	$3\ O_2 + 2\ H_2O$	– 55.2
$2\ NO$	→	$N_2 +$	O_2	– 173.1
$2\ N_2O$	→	$2\ N_2 +$	O_2	– 208.4
$2\ SO_4^{2-} + 4\ H^+$	→	$2\ S +$	$3\ O_2 + 2\ H_2O$	+ 391.6[a]

a Nitrate and sulfate do not allow dismutation reactions yielding oxygen in an exothermic fashion and are included only for comparison (grey).

Anaerobic alkane degradation with involvement of the electron acceptor in substrate activation has been described for strain *Pseudomonas chloritidismutans* – a strain that dismutates chlorite (Mehboob *et al.,* 2009). The O_2 from this dismutation was proposed to be employed by a monooxygenase and alkane oxidation activity was observed in whole cells grown anaerobically with chlorate and *n*-decane ($C_{10}H_{22}$). Production of intracellular O_2 and its utilization for anaerobic alkane activation was also proposed for '*Candidatus* Methylomirabilis oxyfera', the first described methanotroph coupling methane oxidation to NO_2^- reduction (Raghoebarsing *et al.,* 2006, Ettwig *et al.,* 2010). Since formation of O_2 would suggest a similar 'intra-aerobic' (Ettwig *et al.,* 2010) activation pathway, several attempts were made to detect traces of O_2 in denitrifying cultures of strain HdN1 during growth with alkanes (discussed in section B.3).

By an unresolved mechanism, NO_3^- and NO_2^- enabled growth with alkanes (while N_2O did not). This raised the question whether NO as subsequent denitrification intermediate could enable growth with alkanes or not. Several attempts to grow strain HdN1 provided only with NO as terminal electron acceptor failed. Either the applied concentrations (0.075%, v/v in the gas mixture) of this radical compound were toxic (Zumft, 1993), or not high enough (0.05%, v/v) to sustain a clear increase in cell density – the macroscopic indicator for growth. Therefore a new approach was started circumventing these complications by adding small (non-toxic) amounts of NO (gas saturated water) repeatedly to alkane cultures, where a large amount of N_2O was present. If NO enabled the activation reaction, reduction of N_2O as bulk electron acceptor would sustain oxidation of functionalized alkanes and thus a marked increase in N_2 should emerge (principle of the experiment Fig. 18 A). This setup made it possible to test whether NO could initiate alkane activation, without the need to add large (toxic) amounts of NO. If NO was simply respired, only stoichiometric amounts of N_2 would be formed (ratio NO:N_2 = 2:1; see equation 6 page 38). Positive controls received either O_2 or NO_2^-. Alkane metabolism was clearly functional with NO_2^- according to physiological experiments. Since proteomic data showed that the same monooxygenases were present under both aerobic and anaerobic conditions, I expected that added O_2 would be utilized for alkane functionalization even with cells from anoxic cultivation. The negative control had the same amount of N_2O and alkane, but did not receive any additions to verify that the alkane metabolism was not sustained with N_2O alone and to show that no ambient gases were introduced during acquisition of gas samples. The amounts of electron acceptors to be injected were chosen so that twice as much NO, NOC-18 (3,3-Bis(aminoethyl)-1-hydroxy-2-oxo-1-triazene (a slow-release NO-donor; structure see Fig. 18) or NO_2^- was added to the cultures as O_2.

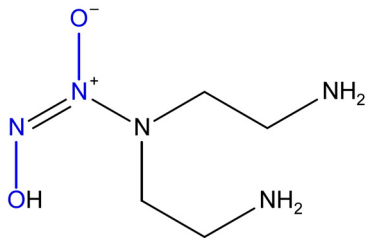

Fig. 18. Structure of NOC-18. The two NO-moieties (blue) are slowly released.

Repeated additions of small amounts of NO, NOC-18, NO_2^- or O_2 indeed caused more N_2- and CO_2-formation than expected from respiration of NO alone (Fig. 19 B). Accordingly, the reduction of N_2O was stronger in these cultures than in the control. The observed changes

were more pronounced with O_2 and NOC-18. The alkane activation, and thus N_2O dependent catabolism, was possibly very efficient from O_2 additions because expression of terminal oxidases for oxygen respiration was probably low due to anaerobic cultivation. Since NOC-18 releases two NO moieties, an increase in N_2 and CO_2 that was significantly higher than from NO-additions is not astonishing. The increases from NO- and NO_2^--additions were of comparable magnitude. This suggests that their role in accepting electrons (2 e^- for NO and 3 e^- for NO_2^-) was less important in this setup than their role in the initiation of the alkane catabolism. Calculated amounts of N_2 and CO_2 from a hypothetical oxidation of hexadecane coupled to NO-respiration (according to equation 6) were added to the curve of the negative control to visualize the respective increases that would be expected if additions of NO were simply respired and did not lead to alkane activation (Fig. 19 B).

$$2\ C_{16}H_{34} + 98\ NO \rightarrow 32\ CO_2 + 49\ N_2 + 34\ H_2O \quad (6)$$

Overall the outcome of this experiment suggested that O_2, NO_2^- and NO could initiate alkane activation. Presumably NO_2^- had been reduced to NO before its utilization. Still, a complete exclusion of NO_2^- as the pivotal compound is not possible, since NO could in principle dismutate yielding NO_2^- and N_2O according to eq. 7.

$$4\ NO + H_2O \rightarrow 2\ NO_2^- + N_2O \quad (\Delta G^{\circ\prime} = -40\ kJ\ mol_{NO}^{-1};\ \text{see Appendix S1 of Chapter D.3}) \quad (7)$$

Still, I favor NO as the actual functional compound (red arrow in Fig. 17) because of the versatile reactivity of this radical (·:N::O::), the strongly exergonic nature of potential reactions, and the presence of a phylogenetically particular type of NO reductase (discussed below).

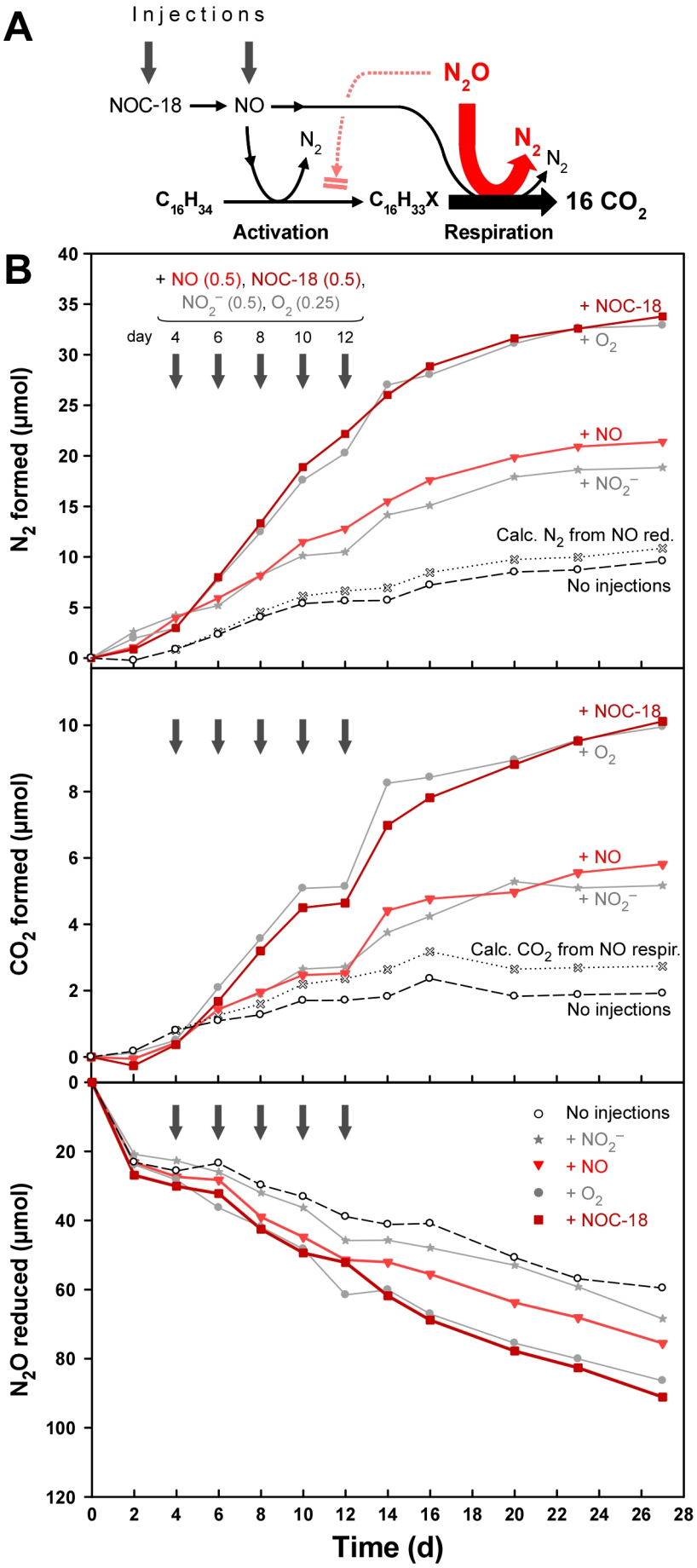
A
Injections
NOC-18
NO
N2O
N2
N2
N2
C16H34
C16H33X
16 CO2
Activation
Respiration
B
+ NO (0.5), NOC-18 (0.5),
NO2− (0.5), O2 (0.25)
day 4 6 8 10 12
+ NOC-18
+ O2
+ NO
+ NO2−
Calc. N2 from NO red.
No injections
N2 formed (µmol)
CO2 formed (µmol)
Calc. CO2 from NO respir.
N2O reduced (µmol)
Time (d)

Fig. 19. Effect of low concentrations of NO on the utilization of *n*-hexadecane by strain HdN1 incubated with N_2O as main electron acceptor for anaerobic respiration.
A. Principle of the experiment. NO but not N_2O allows alkane activation to a polar product (X, functional group) which then allows respiration of the abundantly present N_2O.
B. Amounts of formed N_2, CO_2 and reduced N_2O following five injections of NO or the NO donor NOC-18 (quantities indicated in µmol). Positive controls received O_2 or NO_2^- while the negative control received no additions. Experiments were performed in 156 ml serum bottles with 10 ml culture, 57 µmol (10 µl) *n*-hexadecane and 250 µmol anoxic N_2O. To ensure a metabolically active state that may better withstand adverse NO effects than a 'resting' state, cultures had been provided with a small (20 µmol) amount of NO_2^- directly before the experiment (before time point zero, not shown). Additions were injected when N_2 or CO_2 production with NO_2^- had ceased (details in Appendix S1 of Chapter D.2). The increase of CO_2 and N_2 production by NO or the NO-donor NOC-18 cannot be explained by their use only as respiratory electron-acceptors, but rather indicates alkane conversion to a product metabolizable with N_2O. Maximum amounts expected from a purely respiratory use of NO (0.5 N_2/NO; 0.327 CO_2/NO) are visualized as dotted line. Duplicates yielded the same results (not shown). Zedelius *et al*., manuscript completed (2012).

B.2.3 The divergent NO-reductase of strain HdN1

The usual reductive route for nitrate metabolites would be expected for strain HdN1, since NO_2^- and N_2O were found to be intermediates and all common genes for canonical denitrification were detected in the genome (see section B.2.1). In contrast, presented physiological results made it clear, that a specialized metabolism of N–O compounds is active in this organism on which its anaerobic *n*-alkane degrading capabilities depend. The strain grew with alkanes under anoxic conditions if it was supplied with NO_2^-, but not if it had only N_2O as electron acceptor. Despite the obvious physiological differences, the same was true for *Ca*. Methylomirabilis oxyfera. Thus, if both organisms indeed shared a common pathway for anaerobic alkane activation (possibly via NO dismutation), the responsible enzymes were expected to show a conspicuously high level of similarity in these evolutionary unrelated species due to a common function. Since a complete genome sequence was available for each strain, identification of genes for candidate enzymes was attempted via comparative genomics. All predicted protein sequences with more than 50 amino acids from both organisms and 794 other published bacterial genomes (a non-redundant set of all available complete genomes at NCBI; Sept. 2010) were included in this approach to assess the relative degree of similarity between proteins of *Ca.* M. oxyfera and strain HdN1 against the largest possible background (for details see Appendix S1 of Chapter D.3).

The two best scoring hits were a protein originally annotated as "nitric-oxide reductase, subunit B" and a regulator protein that was located in genomic proximity in both strains. The first qNor-like protein (gene locus tag HdN1F_02620) had two closely related homologues in *M. oxyfera* (gene locus tags DAMO_2434 and DAMO_2437) that had been shortlisted as pu-

tative NO dismutases before (Ettwig *et al*., 2010). To avoid confusion from inconsistent naming and although NO dismutase activity has not been shown in enzyme assays, these three enzymes will be called "Nod" in the following as suggested by Ettwig and coworkers (2012). Also in strain HdN1 this protein had been identified during proteomic analysis with high scores. The second protein featured a DNA-binding domain and a PAS-sensing domain that was related to the well-known O_2 sensor FixL. A regulator with the appropriate sensoric capacity within genomic proximity strengthens the case for a novel pathway involving chemogenic O_2. To assess the possibility that the identified qNor-like protein possessed a novel catalytic function its phylogenetic affiliation was investigated and key amino-acid residues were compared to those of canonical qNors. A phylogenetic tree was constructed with 536 representative amino acid sequences of heme-copper oxidases and the sequences from HdN1 and *M. oxyfera* (Fig. 20 A). The putative 'nitric oxide dismutases' formed a monophyletic clade, branching off from the ubiquinol dependent nitric oxide reductases (qNor). This branch was shared with proteins of *Muricauda* (Bruns *et al*., 2001)*, Cecembia* and *Indibacter* (Kumar *et al*., 2010, 2012), constituting an adjacent cluster. The metabolism of N–O compounds in these species has not been investigated and the significance of their phylogenetic affiliation with the putative dismutases is unclear. While the phylogenetic affiliation is only an indicator of limited functional significance, key amino acid identities can indeed hold clues on a specialized function. Several highly conserved amino acids were substituted in the HdN1 and *M. oxyfera* enzymes. In the active site, one of the twin-histidines (His246 in the canonical *Paracoccus* enzyme) expected to be required for binding of the Fe_B (that binds the NO in typical qNors; Matsumoto *et al*., 2012) was exchanged for an aspargine (alignment of helices VIII-X adjacent the active site see Fig. 20 B). Also a threonin (Thr243) and a glutamate (Glu257) in the proton channel, needed for H^+ transfer to the active site for NO reduction, were substituted by an isoleucine and a glutamine. Finally, the key residues constituting the quinol-binding site were converted to amino acids with dissimilar properties compared to the setup of the common Nors. As a result of these alterations, coordination of Fe_B could be impossible, while either a different kind of metal or a bulky amino acid might be accommodated in its usual spot. Also proton transfer to the active site and electron conduction from quinol could be hindered or completely prevented, as was also found by Ettwig *et al*. (2012). In conclusion, these internally consistent changes to conserved active site residues open the possibility that the modified enzymes really perform a different function.

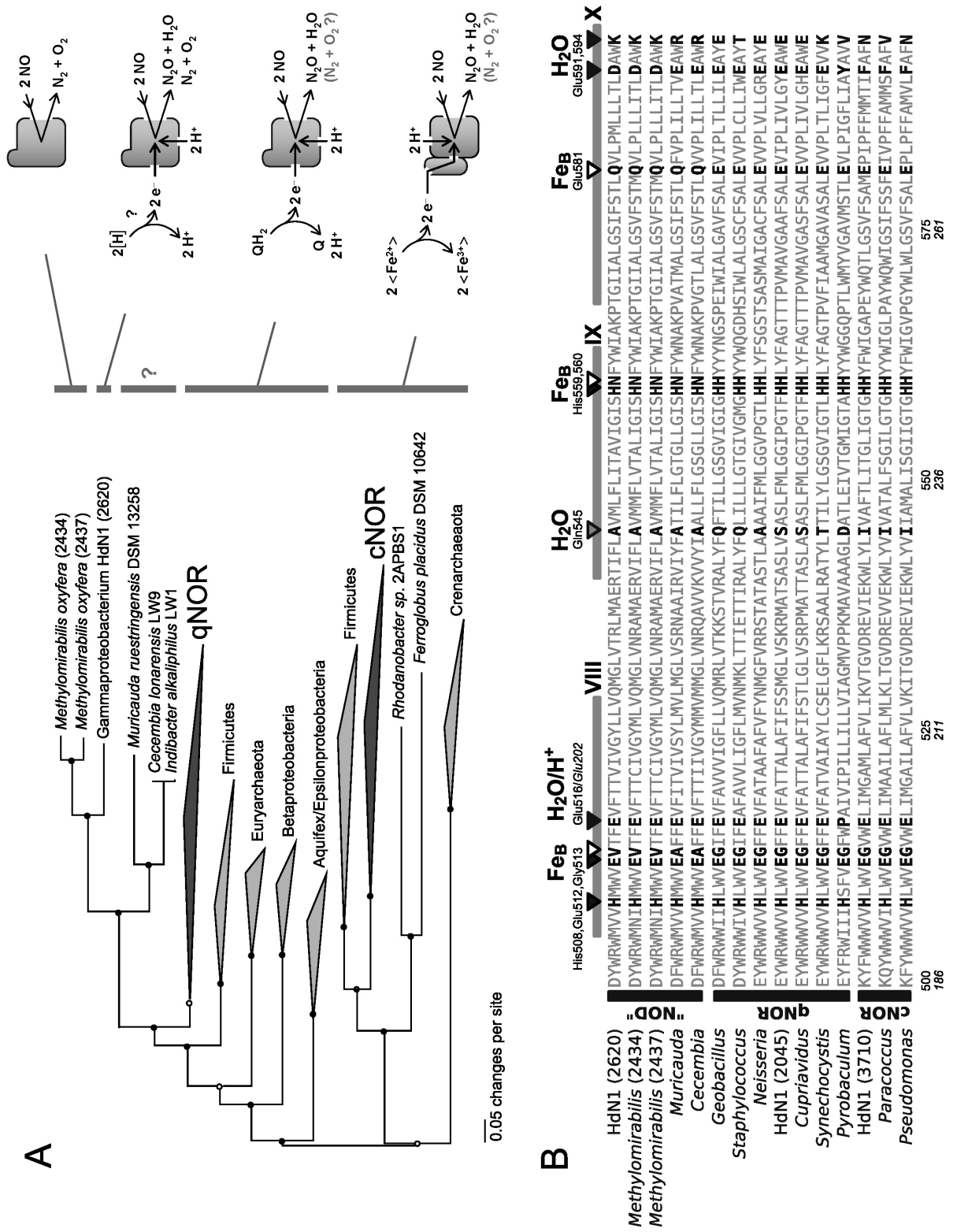

Fig. 20. Phylogenetic relationships (amino acid level) of NO reductases. A. Phylogenetic relationships of NO reductases and the reactions catalyzed. The candidate nitric oxide dismutases form a separate clade at the top. Circles at nodes symbolize the following gamma20 likelihoods: open (>70%), half-open (>95%), filled (>98%). Black triangles represent groups of canonical qNor and cNor protein sequences. B. Close up of part of the active site region (*Geobacillus stearothermophilus* position 500–494 and *Paracoccus* position 186–280) showing transmembrane helixes VIII–X and key conserved amino acids involved in the coordination of the Fe_B and the water/proton channel. Zedelius *et al*., manuscript completed (2012).

Interpretations are complicated for strain HdN1 due to proteomic and physiological findings. Only one of the three different NO-reductases detected during annotation of the complete genome (see Appendix S1 of chapter D.2) was also identified during proteomic analysis – the putative NO dismutase (HdN1F_02620). Neither the qNor (HdN1F_37100) nor the cNor (HdN1F_ 20450) and thus no 'typical' NO-reductase was formed. Since the probability of a so far undescribed enzyme catalyzing the reduction of NO to N_2O present in strain HdN1 (that would have been overlooked by proteogenomic analysis) is very low and since N_2O has been determined unambiguously as an intermediate during NO_3^- metabolism, only a dual function of the HdN1 'Nod' could explain our conflicting results. Thus, while the *M. oxyfera* enzymes would represent 'true' NO-dismutases the HdN1 protein would in contrast mainly function as NO reductase and only to a minor extent as a NO dismutase. Since only one O_2 was needed for activation, this would be sufficient for growth with alkanes. Accordingly this enzyme could be interpreted as a link between the classical NO reductases and NO dismutases. Simplified representations of the enzymes described above and their respective functions are depicted in Fig. 20 A.

If the quinol binding site was really non-functional in strain HdN1, the question arises how electrons for NO reduction to N_2O were possibly delivered to the enzyme. The gene for a small membrane protein (HdN1F_02610) related to b_{561} cytochromes that was detected directly adjacent the HdN1 Nod gene, could be involved in electron transfer to the enzyme. Since access of electrons is necessary for NO reduction, the hypothetical switch to NO dismutation could be regulated by affecting the binding of such transfer proteins to the enzyme.

B.3 Trace oxygen detection

Detection of O_2 formation in HdN1 cultures could be an indicator for NO dismutation. Although it cannot be completely excluded to be produced in metabolic reactions of energy rich N–O species as a byproduct irrelevant for alkane activation, several techniques were applied to find traces of O_2 as a potential key intermediate in the HdN1 alkane catabolism. First, an O_2 microsensor (lower detection limit of about 1 µmol l^{-1}; Revsbech, 1989) was inserted into a glass cylinder via gas-tight fitting and filled with N_2:CO_2, into which an anaerobically grown culture (in medium without reductant) was transferred. However, addition of NO or NO_2^- did not yield detectable amounts of O_2 (not shown). Secondly co-cultivation in brackish medium was attempted with luminous bacteria (related to *Photobacterium* or *Vibrio*) representing a

sensitive oxygen-biosensor, since the luminescence reaction is dependent on O_2 and the produced photons can be detected with high accuracy (Chance *et al*., 1978). But also with this setup no O_2-formation could be detected unambiguously. Third, a membrane-inlet mass-spectrometrometer setup (MIMS; Kana *et al*., 1994; Ettwig *et al*., 2010) which analyzes dissolved gases extracted from liquid samples was used to study metabolic activity and for potential detection of trace O_2. The setup consisted of a spherical glass container in which the culture was mixed by a magnetic stir bar and which was connected to a reservoir at the top. Via gas tight tubing, the setup could be filled with anaerobic cultures avoiding contact with air. A small liquid sample was constantly pumped to a tubular silicone membrane representing the inlet of the mass spectrometer (details of the setup are described in Appendix E.4.4). The abundance of several volatile compounds could be monitored simultaneously and in real-time. During identification of the compounds by their masses ambiguities from dissimilar compounds with the same masses had to be considered.

In first attempts, when only NO_2^- or NO was injected into anaerobic cultures grown with alkanes or fatty acids, O_2 was never detected (not shown). Since respiration and oxygenase activity would quickly reduce formed O_2, the absence of an electron donor was desirable. Thus, fresh cultures with alkanes (that had respired all added NO_3^- and NO_2^-) were pre-incubated with N_2O for two days to diminish stored organic intermediates (e.g. fatty acids or wax esters) within the cells by N_2O respiration – leaving the alkane substrate untouched. Under these circumstances, if the appropriate N–O compound was added, the cells would have to employ their alkane activating 'machinery' to enable further growth with N_2O. But this preparatory measure alone did not lead to O_2 detection. Furthermore, to slow down O_2 depletion, acetylene was added as a potential inhibitor of monooxygenases (Hamamura *et al.*, 1999; Yeager *et al.*, 1999). Since acetylene is also a long-known specific inhibitor of the N_2O reductase (Kristjanson and Hollocher, 1980), the canonical pathway for N_2 formation was blocked concomitantly. The experimental concept is shown in Fig. 21. Additions of NO were delicate due to potentially toxic effects of this radical N–O species (Zumft, 1993). During a number of experiments O_2 was either not detected upon NO addition or only at marginal concentrations ($\leq$ 0.5 µM) that vanished instantaneously. In contrast, upon addition of 50 µM NO_2^- the concentration of O_2 (mass 32) increased to 2 µM and formed a plateau for over 20 min (Fig. 22). This steady state can be interpreted as a dynamic equilibrium of formation and consumption. Three different amounts of O_2 in water were added subsequently to verify consumption. The pointed shape and short duration of the resulting O_2 peaks was so different from the peak fol-

lowing NO_2^- addition, that false positive results from inadvertent introduction of O_2 with the anoxic NO_2^- solution can be excluded. ^{15}N-labelled NO_2^- (98% purity) was used to also examine the fate of the N-compounds. The tentative O_2-precursor $^{15}N^{16}O$ (mass 31) increased and decreased together with O_2, but was detected only at very low concentrations. This suggests that NO from NO_2^- reduction is kept under close control, so that this potentially harmful compound does not accumulate. As expected, mostly $^{46}N_2O$ formed via reduction of $^{15}N^{16}O$ and accumulated due to the inhibition of the nitrous oxide reductase by acetylene. The slow decline in $^{46}N_2O$ concentration was explained by the constant liquid transport towards the mass spectrometer leading to a steady dilution due to influx from the untreated reservoir. The formation of $^{30}N_2$ concomitant with the observed O_2 production would be in line with the dismutation of NO into N_2 and O_2. Still it cannot be completely excluded that some residual reduction of N_2O to N_2 took place in spite of the added acetylene.

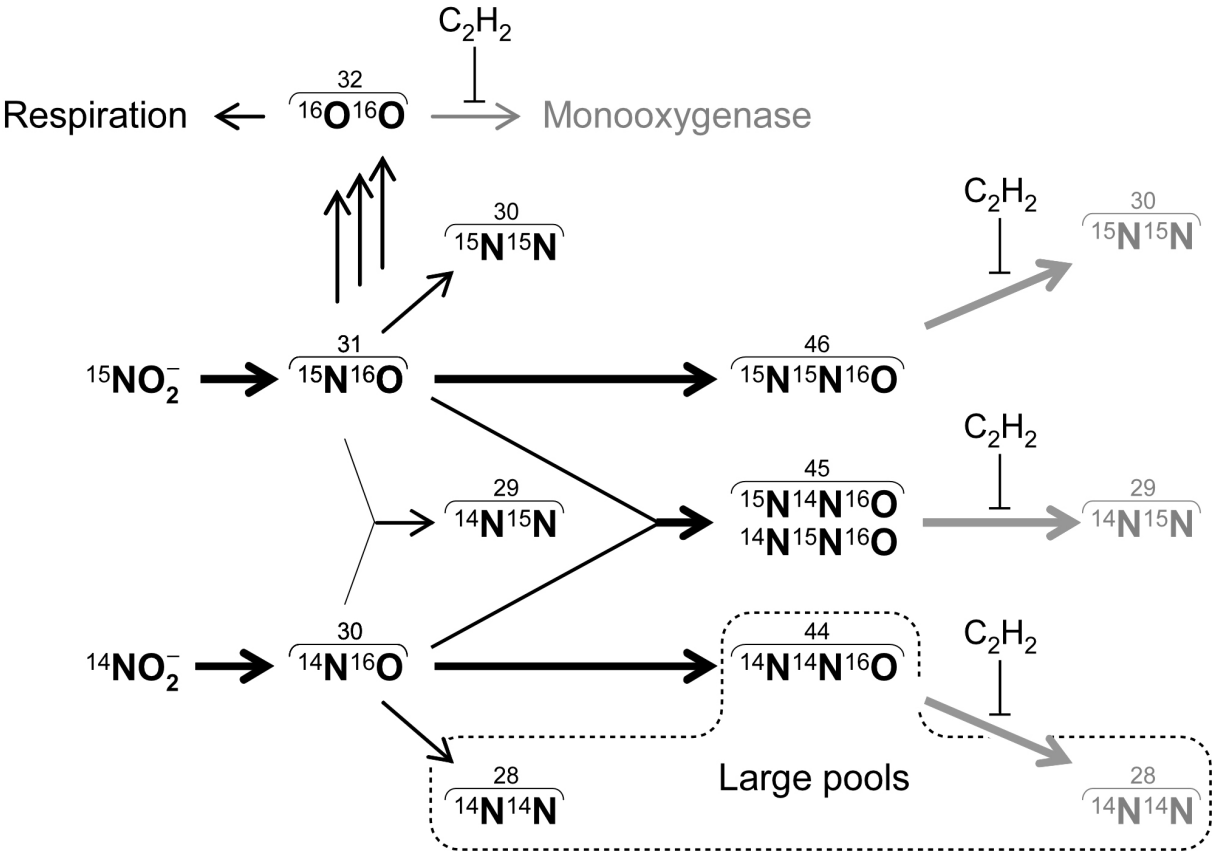

Fig. 21. Overview of the experimental concept for investigation of possible 'chemogenic' O_2 and volatile nitrogen species formed from NO_2^- by tetradecane-grown cells of strain HdN1. The concept includes acetylene inhibition of monooxygenase and N_2O reductase, and fate of ^{15}N-isotope label. The main reduction sequence is indicated in bold lines. N_2 isotopologues possibly formed by residual activity of the acetylene-impeded N_2O reductase are also indicated (grey). Unlabelled N_2O and N_2 are diluted in a large pool from pre-incubation. Zedelius *et al*., manuscript completed (2012).

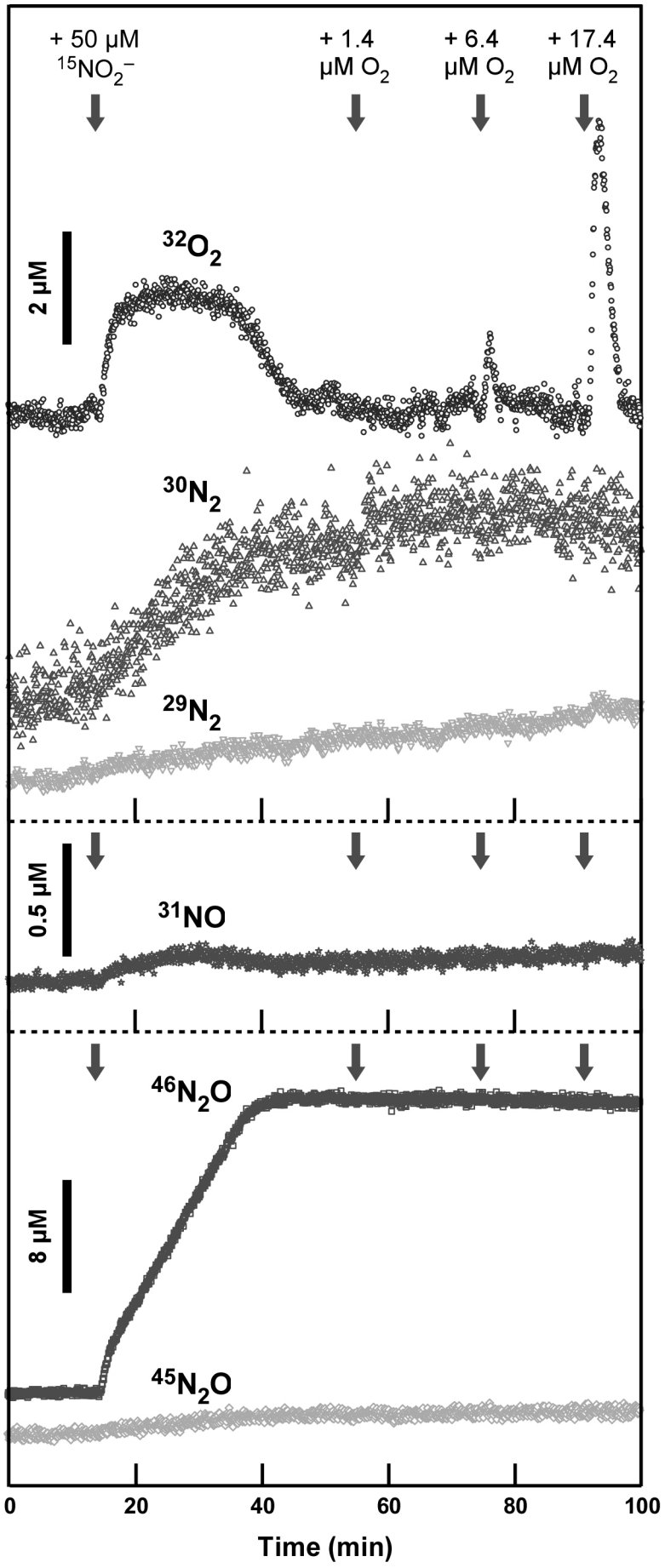

Fig. 22. Investigation of possible 'chemogenic' O_2 and volatile nitrogen species formed from NO_2^- by tetradecane-grown cells of strain HdN1. Chemical species attributed to masses of volatile compounds detectable by membrane-inlet mass spectrometry upon spiking of strain HdN1 with ^{15}N-NO_2^- (isotope purity, 98%). Detectable 'chemogenic' O_2 was consumed after several minutes due to respiration. Respiratory activity was also indicated by consumption of subsequently added O_2 from an aqueous solution. Prior to the depicted experiment, cells had been pre-incubated with N_2O (to diminish organic storage compounds) and acetylene (see text). Hence, there was a high background of unlabelled N_2O and N_2. Zedelius *et al*., manuscript completed (2012).

The curves for (unlabelled) $^{28}N_2$ and $^{44}N_2O$ were not shown due to high background from pre-cultivation and in case of $^{44}N_2O$ also due to interference with the signal from $^{44}CO_2$ (a table with some masses of compounds that potentially occur in biological MIMS samples and their respective identities can be found in Appendix E.4.4). Although these results are in line with putative anaerobic alkane oxidation with O_2 from NO dismutation, they do not prove this hypothesis. It can not be excluded, that some $^{30}N_2$ was formed due to leaky inhibition of the N_2O-reductase and the detected O_2 could have originated from a by-reaction of an uncharted kind of alkane activation with reactive N–O compounds not involving free O_2. Metabolite analysis from experiments with ^{18}O labeled compounds and activity assays with the putative NO-dismutase could further clarify these unresolved questions.

B.4 Aliphatic hydrocarbon metabolism

B.4.1 Proteogenomic information on growth with *n*-alkanes

Strain HdN1 is able to utilize a wide range of alkanes under aerobic and anaerobic conditions. Three monooxygenase genes were discovered in the genome: a cytochrome P450 alkane hydroxylase (*ahpG2*; HdN1F_17560) a di-iron alkane monooxygenase (*alkM*; HdN1F_04190) and a flavin dependent alkane monooxygenase (HdN1F_14540). The formation of all three was detected via shotgun proteomic analyses of cells grown aerobically or anaerobically with *n*-tetradecane, while they were absent in cultures with tetradecanoate (for details, see Table S2 in the appendix of Chapter D.3). The detection of monooxygenase-formation under anaerobic conditions (with high scores) was peculiar, but does not necessarily mean, that they were active and responsible for anaerobic alkane activation. Their expression could simply be regulated in dependence of the presence of alkanes. On the other hand, in cells grown aerobically or anaerobically with 1-tetradecene, the di-iron monooxygenase was not synthesized (responsible regulatory mechanisms were unknown), pointing to a more intricate regulation at least of this enzyme. Thus a potential role of these enzymes in anaerobic alkane functionalization was in the realm of possibility.

B.4.2 Growth with 1-alkenes

Strain HdN1 does not only degrade a wide range of saturated alkanes, but also some 1-alkenes (olefins) which in chemical terms would be the result of terminal alkane dehydrogenation.

Solubility in water is higher for alkenes and preliminary laboratory tests showed that they were more volatile and absorbed faster to butyl stoppers than alkanes of the same chain length. However if enough substrate was added, these properties did not constrain cultivation markedly. Sometimes growth with 1-alkenes started only after a lag-phase. This effect could be avoided by the application larger inocula taken from actively growing cultures. Metabolism of 1-alkenes was usually as fast as with alkanes (Fig. 23).

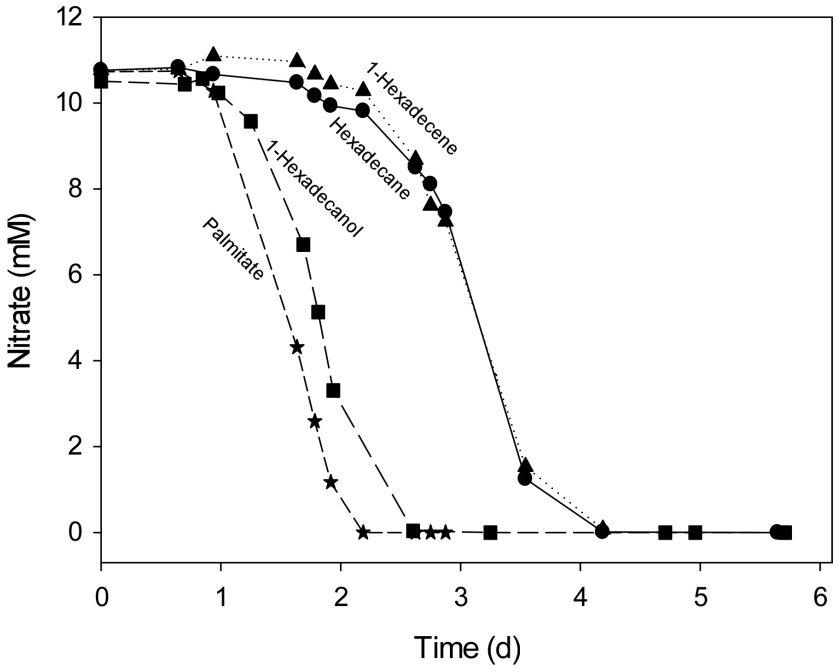

Fig. 23. Metabolic activity measured as reduction of NO_3^- (~ 10 mM) during anaerobic growth of strain HdN1 in cultures supplemented with *n*-hexadecane (●), 1-hexadecene (▲), 1-hexadecanol (■) or 1-hexadecanoate (palmitate;★).

Before the *n*-alkane activating mechanism via fumarate addition was discovered, it was discussed whether the anaerobic degradation of *n*-alkanes might be initiated via terminal desaturation (an O_2 independent but endergonic reaction with NAD^+, McKenna and Kallio, 1965) and subsequent addition of water to the double bond yielding a terminal or subtermial alcohol (Rehm and Reiff, 1981; Watkinson and Morgan, 1990). Since it was clear from our results with strain HdN1 and work with strain Hxd3 (Aeckersberg *et al*., 1998; Callaghan *et al*., 2006) that anaerobic alkane activation does not necessarily depend on fumarate addition, speculations on alternative biochemical pathways for 1-alkene degradation arose. The question was whether 1-alkenes were activated at the saturated side (similar to alkanes) or at the unsaturated side (activation at a 'central' carbon has not been described to date), so that the reactivity of the alkene double bond could be exploited for a different kind of activation reac-

tion. But strain HdN1 did not grow, if it had 1-hexadecene and only N_2O as electron acceptor (not shown) implying that activation of alkenes also depended on NO (or NO_2^-) and thus could be similar to the activation of alkanes. To determine whether strain HdN1 was in general able to activate terminal double bonds, 1,13-tetradecadiene (carrying a double bond at both ends) was added to anaerobic cultures in a suite of growth tests (structures of unsaturated alkane substrates are depicted in Fig. 24).

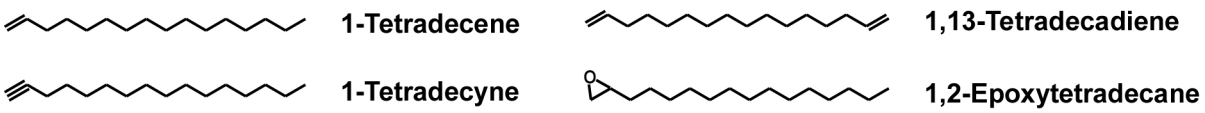

Fig. 24. Structures of 1-tetradecene, 1-tetradecyne, 1,13-tetradecadiene, 1,2-epoxytetradecane.

In incubations with the pure alkyldiene, growth only started after a long lag phase, whereas if it was added to a culture with *n*-tetradecane growth was impeded especially under anaerobic, but also under aerobic conditions. Cultures with a fatty acid and the α,ω-diene on the other hand grew well. Hence only growth with alkanes was affected. It remains unclear whether strain HdN1 can degrade 1-alkenes anaerobically via activation of the unsaturated side or not. The absence of growth with pure 1,13-tetradecadiene could be due to inhibition of a reaction later on the catabolic pathway. Results from analysis of cellular fatty acids (for details go to B.4.4), and the absence of the *alkM* monooxygenase in anaerobic cultures with 1-tetradecene (detected via proteomic; not shown), point to a difference in the degradation pathways of alkenes vs. alkanes that does not necessarily have to be the activation reaction.

Also 1,2-epoxytetradecane (structure see Fig. 24) inhibited growth with alkanes, but like 1,13-tetradecadiene it was metabolized in these cultures in the long run. Inhibition was even more pronounced with additions of 1-tetradecyne carrying a triple bond. Upon addition of this alkyne, growth with alkanes was completely inhibited, but growth with fatty acids was not affected. Results with added acetylene (HC≡CH) as potential inhibitor for alkane activation and N_2O reduction can be found in the appendix (Section E.1.4). Propylene (H_3C–$HC{=}CH_2$) for comparison did not inhibit anaerobic growth with alkanes or fatty acids (not shown).

Table 3. Growth tests with strain HdN1 and saturated or unsaturated alkanes or epoxides.

Electron acceptor	Growth substrate[a]	Additional substrate[b]	Growth[c]	
			Short term[d]	Long term[e]
NO_3^-	1-Decene (2% in HMN)		(+)	+
NO_3^-	1-Hexadecene		+	+
N_2O	1-Hexadecene		–	–
O_2	1-Tetradecene		+	+
NO_3^-	*n*-Tetradecane		+	+
NO_3^-	1,13-Tetradecadiene		–	+
NO_3^-	*n*-Tetradecane	1,13-Tetradecadiene	–	+
NO_3^-	Hexadecanoate	1,13-Tetradecadiene	+	+
O_2	*n*-Tetradecane		+	+
O_2	1,13-Tetradecadiene		–	n.d.
O_2	*n*-Tetradecane	1,13-Tetradecadiene	(+)	+
O_2	Pentanoate	1,13-Tetradecadiene	+	+
NO_3^-	1-Tetradecyne		–	–
NO_3^-	*n*-Tetradecane	1-Tetradecyne	–	–
NO_3^-	1-Tetradecene	1-Tetradecyne	–	+
NO_3^-	Tetradecanoate	1-Tetradecyne	+	+
N_2O	1-Tetradecanol	1-Tetradecyne	+	+
O_2	*n*-Tetradecane	1-Tetradecyne	–	n.d.
O_2	Tetradecanoate	1-Tetradecyne	+	+
NO_3^-	1,2-Epoxytetradecane		–	+
NO_3^-	*n*-Tetradecane	1,2-Epoxytetradecane	–	+
O_2	1,2-Epoxytetradecane		–	+
O_2	*n*-Tetradecane	1,2-Epoxytetradecane	–	+

a If not indicated otherwise, the substrates were added in their pure form. Amounts were: Liquid hydrocarbons ~10 µl, tetradecanoate 1 mmol l^{-1}, pentanoate 3 mmol l^{-1}, tetradecanol ~0.1 g.
b The same amounts of additional substrate and growth substrate were typically added.
c Growth was assessed as obvious turbidity indicated: + obvious growth, (+) little growth, – absence of growth, n.d. not determined.
d Short term was a time of 4 to 7 days.
e Long term was a time of more than 7 days.

Its addition to anaerobic cultures with alkanes did not lead to formation of propylene-oxide (Prior and Dalton, 1985; not shown). Thus, an assay for ^{18}O-labelled propylene from ^{18}O-H_2O and NO_2^- (Ettwig *et al*., 2010) is not possible with strain HdN1. Results are summarized in Table 3.

Apparently the double bond impeded the anaerobic activation reaction in strain HdN1 even though it was not toxic. Delayed growth could be explained by an enzymatic or abiotic saturation of the double bond prior to activation and subsequent degradation. From literature and from their proteomic detection in aerobic alkane cultures it was clear that monooxygenases were responsible for activation in the presence of O_2 (from air). These enzymes are known to often form epoxides when they encounter alkenes (Leak *et al*., 1992 and ref. therein). Formation of such alkyl-oxiranes that were not instantly degraded (possibly since appropriate enzymes for epoxide reduction were missing) could be an explanation for these observations. Epoxide-formation as potential evidence for the activity of monooxygenases will be discussed in section B.4.3. Alkynes appear to be even more problematic for activation reactions. Monooxygenases are known to be impeded or inhibited by addition of acetylene (Hyman and Arp, 1988). Alkynes (as their long chain structural analogs) possibly even represent ‘suicide substrates’ (Abeles and Maycock, 1976) for the anaerobic alkane activating enzymes. Here too covalent bonds might be formed at the active site when the enzyme ‘tries’ to functionalize them at the triple bond (Walsh, 1982). This might also be true in the case of the (1-methylalkyl)succinate synthase (MAS) enzymes for anaerobic alkane activation since growth with alkanes by strains HxN1 and OcN1 was inhibited by the addition of hexyne and octyne respectively (Grundmann and Webner personal communication). Due to the latter finding, inhibition of anaerobic growth by alkynes is not an appropriate tool to assess whether strain HdN1 utilizes monooxygenases for anaerobic alkane degradation or not.

B.4.3 Attempts to establish an epoxide-assay for detection of monooxygenase activity

Several monooxygenases have been shown to oxidize 1-alkenes to the corresponding 1,2-epoxides (Leak *et al*., 1992; Onumonu *et al*., 1994). Since growth of strain HdN1 on *n*-tetradecane via monooxygenases (detected by proteomics; Table S2 in the appendix of Chapter D.3) was impeded by 1,13-tetradecadiene in aerobic cultures with alkanes, the question arose whether formation of epoxides could be the reason for this impediment. Substrate tests showed that 1,2-epoxytetradecane did not sustain fast growth and thus was not quickly de-

graded even in aerobic cultures (Table 3). If epoxides were formed from 1-alkenes and were not degraded instantly, it could be possible to detect such alkyl-oxiranes as indicators for monooxygenase activity. This epoxide assay could then be applied to test whether monooxygenases were also catalyzing anaerobic alkane activation in strain HdN1. If this was the case, ^{18}O-oxygen could be traced due to exchange reactions (Friedman *et al*., 1986) from labeled water via NO_2^- or NO into the epoxide-bond (compare Ettwig *et al*., 2010). In contrast to the oxygen in a carboxyl-group, the oxygen within the epoxide bond is captured tightly and cannot exchange (via enzymatic activity) with the surrounding water (compare Scheller *et al*., 1998; de Bont *et al*., 1979).

Primarily, an aerobic whole cell assay for epoxide formation with 1-tetradecene was developed (details, see Appendix E.4.5) since it was obvious that under aerobic conditions monooxygenases would be active that could potentially form epoxides from 1-alkenes. In first trials only traces of epoxides were detected, but when ether extraction was repeated three times and the pooled fractions were evaporated and re-dissolved, a distinct peak of 1,2-epoxytetradecane could be detected via GCMS (Fig. 25). Sadly, all attempts for detection of epoxide formation upon alkene addition to anaerobic HdN1 cultures failed or where at best inconclusive (not shown). One reason for this could be a lower alkane functionalization activity in anaerobic cultures (which would also result in lower epoxide formation). This explanation would be plausible, since growth rates (limited by the pace of the initial activation reaction) are known to be higher with O_2 than with nitrate (Widdel and Musat, 2010), in line with respective growth rates of strain HdN1. Other reasons could be a higher rate of epoxide degradation in anaerobic cultures due to transformation reactions with N–O-compounds acting as nucleophiles or activity of epoxide transforming enzymes only expressed under anaerobic conditions. But an anaerobic activation of alkanes not involving monooxygenases would also be a possible explanation that can not be excluded (despite of their formation shown via proteomic analysis).

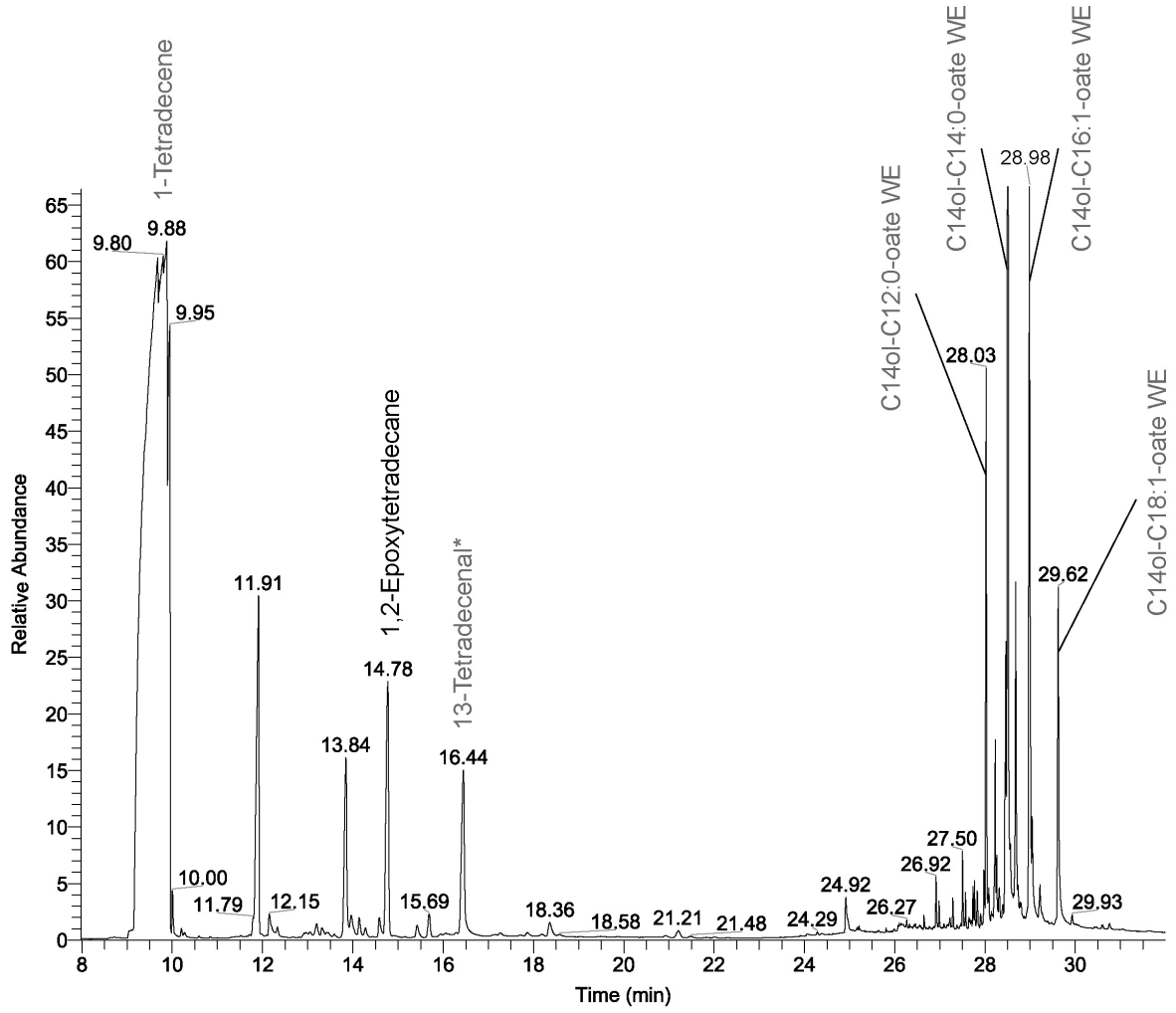

Fig. 25. Detection (GCMS) of 1,2-epoxytetradecane in aerobic cultures upon addition of 1 µl 1-tetradecene. Also detected and unambiguously identified were 1-tetradecene (peak frayed at top due to oversaturation) and the wax esters tetradecyl-dodecanoate, tetradecyl-tetradecanoate, tetradecyl-hexadecenoate and tetradecyl-octadecenoate. * Assignment of peak at 16.44 min as 13-tetradecenal was based on mass fingerprint only and thus preliminary due to missing comparison of retention time with that of an authentic standard.

B.4.4 Analysis of cellular fatty acid and wax ester patterns

Since presumably all pathways for long- and medium-chain alkane degradation lead into the fatty acid metabolism, building blocks for synthesis of cell membranes and in some cases for storage compounds like wax esters (Rontani, 2010) can be diverted from catabolism. Thus, the patterns of fatty acids found in membrane phospholipids can be analyzed (via preparation of fatty acid methyl esters, FAMEs) to deduce characteristics of the initial biochemical steps in alkane degradation. For example the comparison of such patterns in strain Hxd3 with patterns from other anaerobic alkane degraders utilizing fumarate addition indicated that this strain features a unique functionalization reaction (Aeckersberg, 1998; So *et al*., 2003).

Growth with odd-chain alkanes led to fatty acids with mostly even C-chains and vice versa. The addition of a C1-unit via carboxylation at the C3-position as the initial reaction has been suggested to explain these observations (So *et al*., 2003). During fumarate ($HO_2CHC=CHCO_2H$) addition, a C_4–unit is added to the subterminal C of the alkane. Due to the even number of the added carbon compound and subsequent C-skeleton rearrangement, even-chain fatty acids are created from even chain alkanes and odd chain fatty acids from odd chain alkanes. A similar result was obtained from analyses of the fatty acid patterns with odd or even alkane substrates in strain HdN1 (Ehrenreich, 1996). Hence, an activation reaction and a degradation pathway identical with that of strain Hxd3 can be excluded for strain HdN1. Although fumarate addition was also ruled out for this strain, judging solely from the analyzed FAME patterns, the introduction of a functional group with an even carbon number (at the C1- or C3-position) or an odd carbon number (at the C2-position) or no carbon at all is conceivable (results from FAME analyses of strain HdN1 obtained previously are summarized in Appendix Fig. E1). Examination of alkyl-groups detected in wax esters point to the introduction of a functional group devoid of carbon or a loss of the added C–unit directly after activation (see discussion below). The situation was different for growth with 1-alkenes, since the lengths of carbon chains detected in cellular fatty acids of alkene grown cells were independent of the chain-length of the growth substrate. Both 1-heptadecene and 1-hexadecene led to the same FAME pattern dominated by acids with an even C–chain (Appendix Fig. E2). This suggests that the anaerobic degradation of 1-alkenes was accomplished via a different pathway and potentially involving a different initial reaction compared to that of *n*-alkanes.

Long-chain alcohols are the product of aerobic alkane oxidation by monooxygenases (Britton, 1984). Thus it was not surprising to detect hexadecanol in aerobic hexadecane cultures (not shown). If NO-dismutation yielding O_2 in anaerobic alkane cultures was indeed taking place, such alcohols should also be produced by the monooxygenases present under anaerobic conditions (detected via proteomic analysis). Still, none of our attempts to find these alkanols in anaerobic cultures growing with alkanes by extraction of the organic components with ether followed by GC or GCMS analysis was successful (not shown). However, in an earlier work with strain HdN1, hexadecanol had been clearly detected in anaerobic hexadecane cultures during FAME analysis (Ehrenreich, 1996). This apparent contradiction could be explained, when unknown peaks with a high vaporization temperature that had appeared during GC-measurement of samples then, now could be identified as wax esters that hydrolyzed during the first step of the FAME preparation, releasing long-chain alcohols

(Fig. 26). So the alcohols detected previously did not derive directly from monooxygenase activity, but were released from waxes.

Since the free alcohol could not be detected in anaerobic cultures, could the presence of wax esters (made up of an alcohol and a fatty acid) still be an indicator for monooxygenase activity? In principle no, since such wax esters were also found in anaerobic cultures growing with long-chain fatty acids (e.g. hexadecanoate; Fig. E7). It is well known from wax esters synthesized by aerobic alkane degraders that the alcohol-moiety of wax esters always exhibits the same chain length as the substrate alkane (see Fig. 26 and Stewart and Kallio, 1959), while the fatty acid moiety is elongated or shortened by C_2-units (an indicator of β-oxidation). Although the same pattern was observed for strain HdN1 during anaerobic growth on alkanes, it turned out that this was also true for growth on fatty acid and could therefore not be interpreted unambiguously as a hint on monooxygenase activity.

Although the amount of wax esters formed in anaerobic cultures growing with alkanes might be higher than in cultures with fatty acids – which could possibly point to formation of alkanols from alkanes even under anaerobic conditions – but this one-time observation awaits further experimental substantiation in the future.

Intracellular lipid inclusions found in strain HdN1 can be compared to those found in aerobic alkane degraders. Cells of *Acinetobacter* grown with *n*-hexadecane under air exhibited inclusions of neutral lipids. These contained (in relative concentrations as %) wax ester (50.5), free fatty acid (5.8), free fatty alcohol (17.6), triglyceride (5.7), diglyceride (6.9), monoglyceride (1.3), *n*-hexadecane (12.0) as detected by Scott and Finnerty (1976). From ether extractions and analysis of cells grown with *n*-tetradecane vapors, the fraction of pure *n*-alkane is expected to be higher in strain HdN1 (not shown).

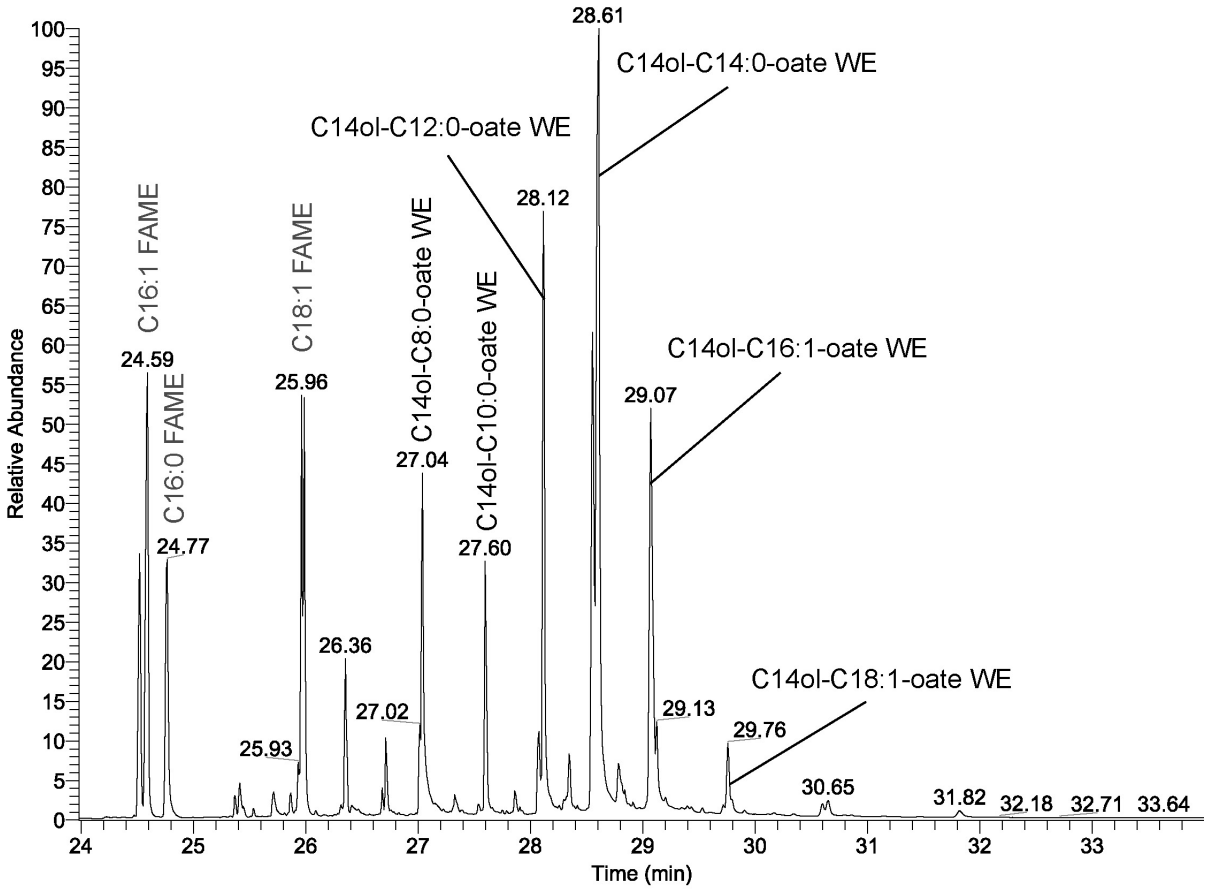

Fig. 26. Wax ester formation in anaerobic *n*-tetradecane cultures of strain HdN1 detected during FAME analysis via GCMS. Acid residues were either saturated (CX:0) or unsaturated (CX:1) mostly at the C_9-position. FAMEs released by hydrolysis from phospholipids and wax esters were also detected (grey).

During growth with Phenyl-alkanes (see also section B.4.5), phenylalkyl wax esters were synthesized under aerobic and anaerobic conditions (results from GCMS analysis see Appendix Fig. E11). Production of such phenyl-substituted waxes has been described only once previously in a culture of *Rhodococcus opacus* PD630 during aerobic growth with phenyldecane (Alvarez *et al*., 2002). Cells of strain HdN1 also produced wax esters, when they were grown with 1-alkenes. But no waxes (or FAMEs) with terminal double bonds were detected during growth with 1-tetradecene (not shown) meaning that this terminal double bond was saturated before their formation.

B.4.5 Analysis of metabolites from growth with 1-phenylalkanes

Since more than one century it is known, that fatty acids are degraded via β-oxidation. In his classical work, Franz Knoop (1904) fed phenyl-substituted fatty acids with even or odd side chain to dogs and later measured their degradation-products, phenylacetate and benzoate re-

spectively in the dog-urine. It was concluded, that as many C_2-units had been cleaved off as the phenyl-ring allowed. Thierfelder and Klenk (1924) found that phenylalkanes gave the same products – apparently after initial ω-oxidation of the alkyl side chain. The activity of the β-oxidation pathway in strain HdN1 is evident from the principal enzymes identified via genomic and proteomic (not shown), so phenylalkanes were in this case used to indirectly investigate the activation reaction. They are well suited for this task, since only one side of the alkyl side chain is available for a terminal (or subterminal) activation reaction since strain HdN1 is not able to degrade aromatics (i.e. doesn't grow with toluene or benzoate). Initial ω-oxidation followed by β-oxidation yields benzoate from phenyltridecane and phenylacetate from phenyltetradecane, when six C_2-units are cleaved off successively (structures see Fig. 27).

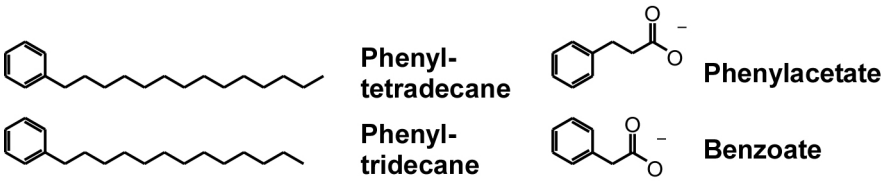

Fig. 27. Structures of phenylalkanes and phenyl-substituted carboxylic acids.

Benzoate had been detected as the only phenyl-substituted carboxylic acid in HdN1 cultures grown with phenyltridecane under nitrate reducing conditions. It was not detected in sterile controls or a control culture with hexadecane that had grown much faster (Ehrenreich, 1996). Since in contrast to 16 years ago, not only phenyltridecane, but also phenyltetradecane was commercially available, it was possible to compare metabolites formed during growth with both phenylalkanes with oxygen and under nitrate reducing conditions. Cultures were grown to high density and cells were removed from the aqueous medium by centrifugation and filtration before diluting it 1:10 prior to UPLC analysis.

In aerobic cultures, mostly benzoate was detected after growth with phenyltridecane and mostly phenylacetate was detected after growth with phenyltetradecane (Fig. 28 A). These metabolites suggest an aerobic degradation-pathway analogous to the classical one known for *n*-alkanes via ω-oxidation by a monooxygenases followed by two dehydrogenation steps and leading to β-oxidation. Oxidation at the subterminal C would have led to the opposite outcome.

Surprisingly, not only phenyltridecane, but also phenyltetradecane led to an accumulation of benzoate and only low amounts of phenylacetate were found in both anaerobically grown cultures (Fig. 28 B; detected amounts see Fig. E12 in the appendix). From this result with phenylalkanes, no conclusions can be drawn about the nature of the anaerobic activation of neither the alkyl side chain nor *n*-alkanes. A schematic overview on how these results could be explained with our current conception of strain HdN1's alkane-metabolism (involving the hypothetical NO-dismutation) can be found in the appendix (Fig. E13). Under anaerobic conditions the degradation of even-chain phenylalkanes possibly does not stop at phenylacetate, but removes another C_1-unit by α-oxidation (decarboxylation). The different metabolites from aerobic and nitrate-reducing cultures could stem from the expression of a different set of enzymes at each condition.

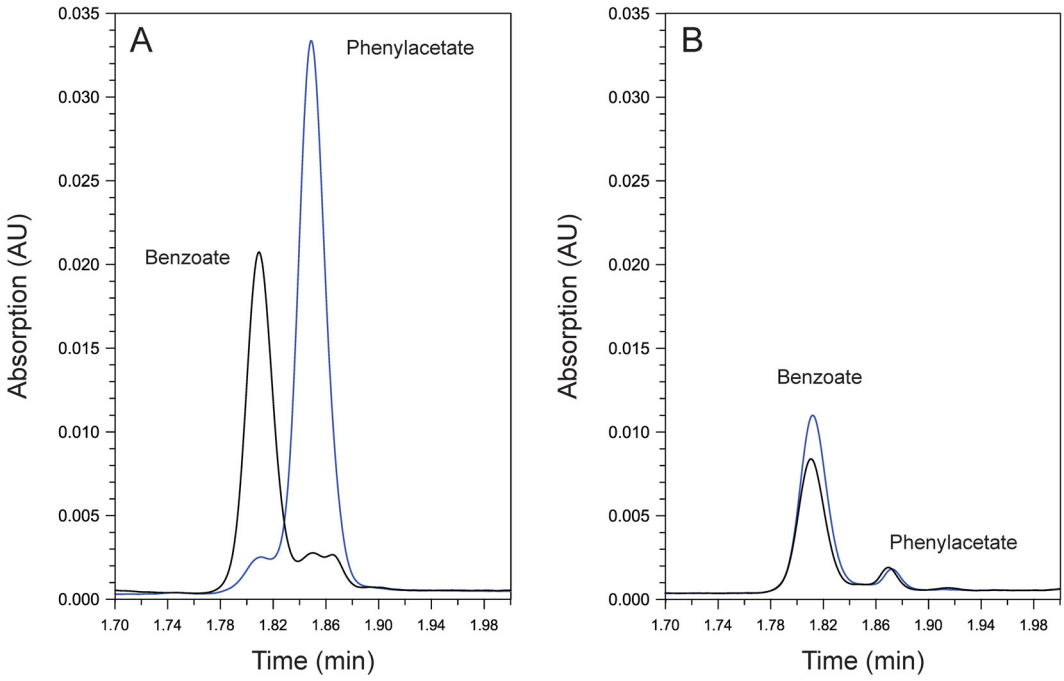

Fig. 28. UPLC-analysis of the aqueous phase of HdN1 cultures grown with phenylalkanes under aerobic (A) or nitrate-reducing (B) conditions presented as overlays of the chromatograms from cultures with 1-phenyltridecane (black) or 1-phenyltetradecane (blue). Benzoate and phenylacetate were detected via UV-Vis spectroscopy at 210 and 230 nm respectively and identified by their retention times.

B.5 Possible pathways for anaerobic alkane activation by strain HdN1

The identity of the enzymatic 'system' for anaerobic activation has not been elucidated, but the presented results allow speculations on its nature. Still a number of reactions are conceivable and consistent with the experimental data. It is expected that the functional group is added at the terminal or subterminal carbon. Two molecules of NO could be directly used by an unknown mechanism to introduce an oxygen atom into the alkane. This could either involve electrons for reduction of the nitrogen to N_2 thus also producing H_2O (Fig. 29, A) or if no external electrons are transferred to nitrogen, the reaction could produce N_2O but no H_2O (Fig. 29, B). This kind of activation reactions are conceivable but remain completely speculative since such a reaction has not been described to date. At least some conspicuous modifications to presently known enzymes would be expected to catalyze such a reaction (compare Ettwig *et al.,* 2012), but the three monooxygenase proteins detected by proteomic analyses did not show any phylogenetic peculiarities among other canonical monooxygenases (not shown).

Another hypothetical activation mechanism involving high valent metal centers appears to be more plausible since related pathways have been detected for anaerobic hydroxylation (not involving free O_2) of ethylbenzene and cholesterol by molybdoenzymes (Kniemeyer and Heider, 2001; Dermer and Fuchs, 2012). Following this hypothesis, the NO is needed to energize the catalytic metal of a metalloenzyme (so that it carries a high valence state) to activate a water molecule for hydroxylation of the alkane (Fig. 29, C). A related putative molybdoenzyme was detected in the genome of strain HdN1. Its alpha and beta subunits showed 55% and 31% amino acid sequence identity respectively with the alpha subunits and 64% and 52% identity (calculated by BLAST; Altschul *et al*., 1990) with the beta subunits of the two above mentioned cholesterol dehydrogenase of *Sterolibacterium denitrificans* and ethylbenzene dehydrogenase of *Aromatoleum aromaticum* strain EbN1. However reactive N–O compounds were not indicated to play a special role in catabolism of these substrates and the HdN1 enzyme was not identified during proteomic analysis of HdN1 cells grown aerobically or anaerobically with alkanes or alkenes, practically excluding its involvement in anaerobic alkane activation, since enzymes catalyzing such key reactions are expected to be highly expressed during growth with the inert substrate. Thus due to our findings from physiological experiments and proteome data, we favor the described hypothesis for dismutation of NO and usage of the formed O_2 by monooxygenases for alkane activation (Fig. 29, D).

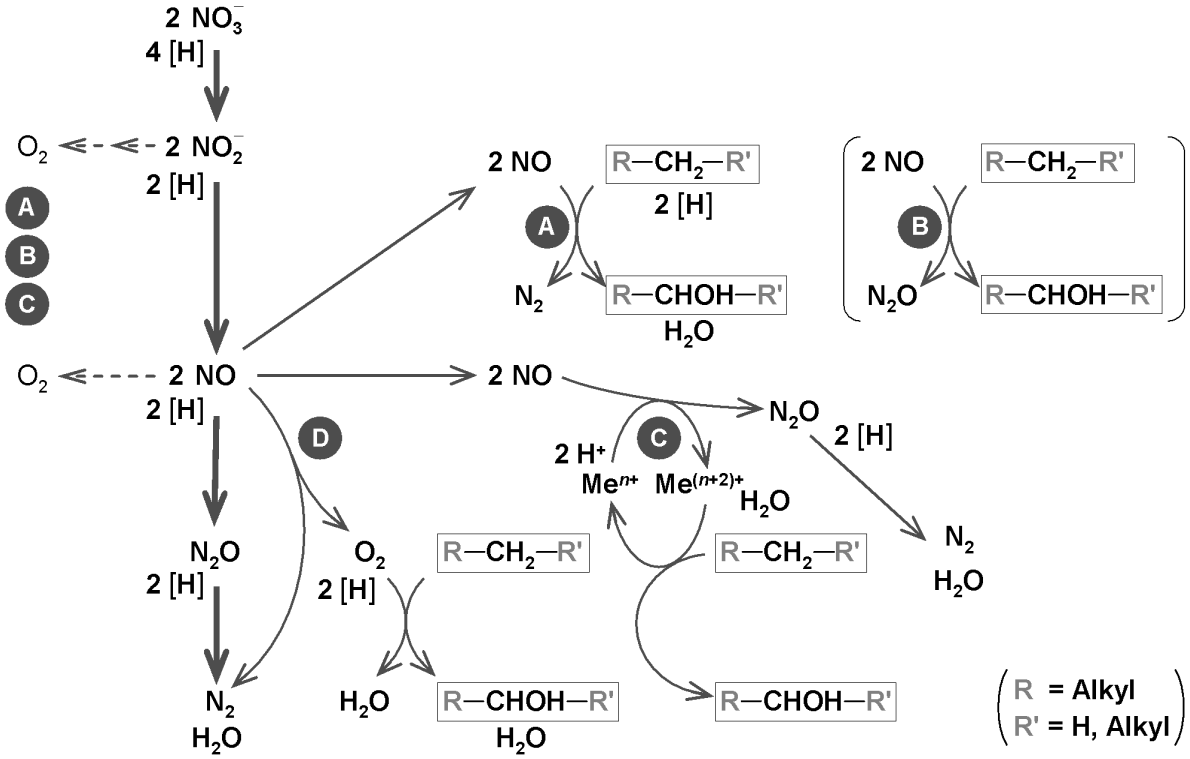

Fig. 29. Hypotheses of alkane activation with an NO_3^- -derived N–O species based on the experiments presented in this thesis. The scheme leaves open the site of alkane activation (primary or secondary carbon atom). The main route of the nitrogen in nitrate is always its respiratory reduction to N_2 via the canonical denitrification pathway (bold lines).
A. Part of NO as a reactive and endergonic ('energy-rich') compound is directly involved in alkane functionalization by an unknown enzyme and mechanism (purely speculative) requiring electrons. O_2 is formed in a by-reaction and may be used to some extent, but its formation is not significant for the catabolism.
B. As A, but without requirement for electrons.
C. Part of NO is used by a special reductase that couples NO-reduction specifically to the generation of another oxidant, a high-valent metal center. The metal center then introduces a hydroxyl group originating from water. Again, O_2 is formed in a by-reaction without catabolic significance.
D. The presently favored mechanism. Part of NO is converted to N_2 and O_2, the latter being used in a conventional monooxygenase reaction. Zedelius *et al*., manuscript completed (2012).

B.6 Conclusions and outlook

Strain HdN1 has a unique kind of anaerobic alkane metabolism. Knowledge on characteristics of its catabolism (e.g. range of degraded substrates) and anabolism (e.g. formation of wax esters) was advanced in this work. Evidence from physiological experiments presented here suggests that an N–O-compound (most probably nitric oxide) was diverted from the respiratory chain to enable the activation reaction, which involves the cleavage of a C–H bond of the alkane and yields a functionalized product. Although further experimental substantiation is necessary, results from MIMS experiments and comparative genomics hint on NO-dismutation into N_2 and O_2, the latter could be utilized by monooxygenases for alkane activa-

tion. The detection of alkane monooxygenases synthesized during anaerobic growth with alkanes via proteomic analysis fits nicely to this hypothesis.

Future investigations on the alkane-physiology of strain HdN1 could involve deuterated or ^{13}C-labelled alkane substrates since mass-spectrometrical analysis of labeled products could reveal additional structural information for deduction of the initial activation reaction. The use of ^{18}O-oxygen could allow for a deduction of the route of oxygen via N–O-compounds (by exchange with labeled water; Friedman *et al*., 1986) and in case of NO-dismutation for oxidation via monooxygenases into the alkane metabolites. The possibility for such an 'intra-aerobic' (Ettwig *et al*., 2010) pathway could also be probed with help of stable isotope fractionation assays again with deuterated or ^{13}C-labelled alkanes (Elsner, 2010). Values for the discrimination against heavy isotopes during anaerobic alkane degradation in strain HdN1 could be compared to kinetic isotope effect values known from literature (Sun *et al*., 2005, Kinnaman *et al*., 2007) as an indication on the nature of the applied activation mechanism.

The development of a genetic system with strain HdN1 would be another promising approach since physiological hypotheses could be tested with mutants lacking key enzymes. Obvious candidates for deletion are the monooxygenases and the putative NO-dismutase. Since the strain is able to grow with a broad range of non-alkane substrates it would be viable without a monooxygenase specific for the respective alkanes. In absence of the specialized NO-reductase (the putative NO-dismutase, HdN1F_02620) as the only NO-processing enzyme synthesized in anaerobically grown cells, this toxic compound would accumulate quickly to lethal concentrations during denitrification. If none of the other two NO-reductases would be upregulated in the absence of the NO-dismutase, a surrogate NO-detoxifying enzyme would have to be introduced (e.g. via an expression vector) additionally to test whether anaerobic alkane degradation was possible without the putative NO-dismutase.

In case the hypothesis for NO-dismutation is correct, a number of recalcitrant substrates could in principle be degraded by bacteria applying biochemical reactions so far considered to be feasible only under aerobic conditions. The process could potentially be used for bioremediation of recalcitrant pollutants and possibly in biotechnological applications involving O_2 dependent reactions.

C Literature

C.1 Literature from the introduction, results and discussion

Abbasnezhad, H., Gray, M., and Foght, J.M. (2011) Influence of adhesion on aerobic biodegradation and bioremediation of liquid hydrocarbons. *Appl Microbiol Biotechnol* **92**: 653–675.

Abeles, R.H., and Maycock, A.L. (1976) Suicide enzyme inactivators. *Acc Chem Res* **9**: 313–319.

Adams, J., Riediger, C., Fowler, M., and Larter, S. (2006) Thermal controls on biodegradation around the Peace River tar sands: Paleo-pasteurization to the west. *J Geochem Explor* **89**: 1–4.

Aeckersberg, F., Bak, F., and Widdel, F. (1991) Anaerobic oxidation of saturated-hydrocarbons to CO_2 by a new type of sulfate-reducing bacterium. *Arch Microbiol* **156**: 5–14.

Aeckersberg, F., Rainey, F.A., and Widdel, F. (1998) Growth, natural relationships, cellular fatty acids and metabolic adaptation of sulfate-reducing bacteria that utilize long-chain alkanes under anoxic conditions. *Arch Microbiol* **170**: 361–369.

Alexander, M. (1965) Biodegradation: problems of molecular recalcitrance and microbial fallibility. *Adv Appl Microbiol* **7:** 35–80.

Altschul, S.F., Gish, W., Miller, W., Myers, E.W., and Lipman, D.J. (1990) Basic local alignment search tool. *J Mol Biol* **215**: 403–410.

Amann, R., and Fuchs, B.M. (2008) Single-cell identification in microbial communities by improved fluorescence in situ hybridization techniques. *Nat Rev Microbiol* **6**: 339–348.

Atlas, R.M. (1981) Microbial degradation of petroleum hydrocarbons: an environmental perspective. *Microbiol Rev* **45**: 180–209.

Atlas, R.M., and Hazen, T.C. (2011) Oil biodegradation and bioremediation: A tale of the two worst spills in US history. *Environ Sci Technol* **45**: 6709–6715.

Ayala, M., and Torres, E. (2004) Enzymatic activation of alkanes: constraints and prospective. *Appl Catal Gen* **272**: 1–13.

Banat, I.M. (1995) Biosurfactants production and possible uses in microbial enhanced oil-recovery and oil pollution remediation – a review. *Bioresour Technol* **51**: 1–12.

Beyer H. and Walter W. (1988) Lehrbuch der organischen Chemie. Stuttgart, Germany: S. Hirzel Verlag.

Birch, L.D., and Bachofen, R. (1988) Microbial production of hydrocarbons. In *Biotechnology*. Vol 6b. Special Microbial Processes. Rehm, H.J., and Reed G. (eds). Weinheim, Germany: VCH Verlagsgesellschaft, pp. 71–99.

Boetius, A., Ravenschlag, K., Schubert, C.J., Rickert, D., Widdel, F., Gieseke, A. *et al.* (2000) A marine microbial consortium apparently mediating anaerobic oxidation of methane. *Nature* **407**: 623–626.

Bont, J.A.M.D., Attwood, M.M., Primrose, S.B., and Harder, W. (1979) Epoxidation of short chain alkenes in *Mycobacterium*-E20 - involvement of a specific monooxygenase. *FEMS Microbiol Lett* **6**: 183–188.

BP. *BP Statistical Review of World Energy June 2012* (BP, London, 2012); available at http://www.bp.com/statisticalreview.

Bragg, J. R., R. C. Prince, J. B. Wilkinson, and R. M. Atlas. (1992) Bioremediation for shoreline cleanup following the 1989 Alaska oil spill. Exxon Research and Engineering Company, Florham Park, New Jersey, USA.

Britton, L.N. (1984) Microbial degradation of aliphatic hydrocarbons. *In* Microbial degradation of organic compounds. Gibson, T.D. (ed.). New York, Marcel Dekker, pp 89–129.

Broda, E. (1977) 2 kinds of lithotrophs missing in nature. *Z Allg Mikrobiol* **17**: 491–493.

Bryant, M.P. (1972) Commentary on the Hungate technique for culture of anaerbic bacteria.: *Am J Clin Nutr* 1324–1328.

Bühler, M. and Schindler, J. (1984) Aliphatic hydrocarbons. In *Biotechnology*. Vol. 6a. Kieslich, K. (ed.). Weinheim, Germany: VCH Verlagsgesellschaft.

Callaghan, A.V., Gieg, L.M., Kropp, K.G., Suflita, J.M., and Young, L.Y. (2006) Comparison of mechanisms of alkane metabolism under sulfate-reducing conditions among two bacterial isolates and a bacterial consortium. *Appl Environ Microbiol* **72**: 4274–4282.

Callaghan, A.V., Wawrik, B., Chadhain, S.M.N., Young, L.Y., and Zylstra, G.J. (2008) Anaerobic alkane-degrading strain AK-01 contains two alkylsuccinate synthase genes. *Biochem Biophys Res Commun* **366**: 142–148.

Callaghan, A.V., Tierney, M., Phelps, C.D., and Young, L.Y. (2009) Anaerobic biodegradation of *n*-hexadecane by a nitrate-reducing consortium. *Appl Environ Microbiol* **75**: 1339–1344.

Chakraborty, R., and Coates, J.D. (2005) Hydroxylation and carboxylation-two crucial steps of anaerobic benzene degradation by *Dechloromonas* strain RCB. *Appl Environ Microbiol* **71**: 5427–5432.

Chance, B., Oshino, R., and Oshino, N. (1978) Sensitive oxygen assay method by luminous bacteria. *Methods Enzymol* **54**: 499–505.

Cheesbrough, T.M., and Kolattukudy, P.E. (1984) Alkane biosynthesis by decarbonylation of aldehydes catalyzed by a particulate preparation from *Pisum sativum*. *Proc Natl Acad Sci U S A* **81**: 6613–6617.

Christen, H.R. and Vögtle, F. (1985) Grundlagen der organischen Chemie. Frankfurt a.M., Germany: Salle and Sauerländer Verlag.

Cladera, A., Garcia-Valdes, E., and Lalucat, J. (2006) Genotype versus phenotype in the circumscription of bacterial species: the case of *Pseudomonas stutzeri* and *Pseudomonas chloritidismutans*. *Arch Microbiol* **184**: 353–361.

Coates, J.D., Chakraborty, R., Lack, J.G., O'Connor, S.M., Cole, K.A., Bender, K.S., and Achenbach, L.A. (2001) Anaerobic benzene oxidation coupled to nitrate reduction in pure culture by two strains of Dechloromonas. *Nature* **411**: 1039–1043.

Crabtree, R.H. (1985) The Organometallic Chemistry of Alkanes. *Chemical Rev* **85**: 245–269.

Dalsgaard, T., Canfield, D.E., Petersen, J., Thamdrup, B., and Acuna-Gonzalez, J. (2003) N_2 production by the anammox reaction in the anoxic water column of Golfo Dulce, Costa Rica. *Nature* **422**: 606–608.

Davies, M.J. (2003) Singlet oxygen-mediated damage to proteins and its consequences. *Biochem Biophys Res Commun* **305**: 761–770.

Dennis, M., and Kolattukudy, P.E. (1992) A cobalt-porphyrin enzyme converts a fatty aldehyde to a hydrocarbon and CO. *Proc Natl Acad Sci U S A* **89**: 5306–5310.

Dermer, J., Fuchs, G. (2012) Molybdoenzyme that catalyzes the anaerobic hydroxylation of a tertiary carbon atom in the side chain of cholesterol. *J Biol Chem*, doi: 10.1074/jbc.M112.407304.

Ehrenreich, P., Behrends, A., Harder, J., and Widdel, F. (2000) Anaerobic oxidation of alkanes by newly isolated denitrifying bacteria. *Arch Microbiol* **173**: 232–232.

Ehrenreich P. (1996) Anaerobes Wachstum neuartiger sulfatreduzierender und nitratreduzierender Bakterien auf *n*-Alkanen und Erdöl. *Ph.D.-thesis*, University Bremen.

Elshahed, M.S., Gieg, L.M., McInerney, M.J., and Suflita, J.M. (2001) Signature metabolites attesting to the in situ attenuation of alkylbenzenes in anaerobic environments. *Envl Sci Technoly* **35**: 682–689.

Elsner, M. (2010) Stable isotope fractionation to investigate natural transformation mechanisms of organic contaminants: principles, prospects and limitations. *J Environ Monit* **12**: 2005–2031.

Ettwig, K.F., Butler, M.K., Le Paslier, D., Pelletier, E., Mangenot, S., Kuypers, M.M.M. *et al.* (2010) Nitrite-driven anaerobic methane oxidation by oxygenic bacteria. *Nature* **464**: 543–548.

Ettwig, K.F., Speth, D.R., Reimann, J., Wu, M.L., Jetten, M.S.M. and Keltjens, J.T. (2012) Bacterial oxygen production in the dark. *Front Microbio* **3:**273. doi:10.3389/fmicb.2012.00273.

Finley, S.D., Broadbelt, L.J., and Hatzimanikatis, V. (2009) Thermodynamic analysis of biodegradation pathways. *Biotechnol Bioeng* **103**: 532–541.

Friedman, S.H., Massefski, W., Jr., and Hollocher, T.C. (1986) Catalysis of intermolecular oxygen atom transfer by nitrite dehydrogenase of *Nitrobacter agilis*. *J Biol Chem* **261**: 10538–10543.

Greenspan, P., Mayer, E.P., and Fowler, S.D. (1985) Nile Red - a selective fluorescent stain for intracellular lipid droplets. *J Cell Biol* **100**: 965–973.

Grimaud, R. (2010) Biofilm development at interfaces between hydrophobic organic compounds and water. In *Handbook of hydrocarbon and lipid microbiology*, Vol. 2. Timmis, K.N. (ed.). Heidelberg, Germany: Springer, pp. 1491–1500.

Grundmann, O., Behrends, A., Rabus, R., Amann, J., Halder, T., Heider, J., and Widdel, F. (2008) Genes encoding the candidate enzyme for anaerobic activation of *n*-alkanes in the denitrifying bacterium, strain HxN1. *Environ Microbiol* **10**: 376–385.

Hamamura, N., Storfa, R.T., Semprini, L., and Arp, D.J. (1999) Diversity in butane monooxygenases among butane-grown bacteria. *Appl Environ Microbiol* **65**: 4586–4593.

Hanselmann, K.W. (1991) Microbial energetics applied to waste repositories. *Experientia* **47**: 645–687.

Hasinger, M., Scherr, K.E., Lundaa, T., Brauer, L., Zach, C., and Loibner, A.P. (2012) Changes in *iso*- and *n*-alkane distribution during biodegradation of crude oil under nitrate and sulphate reducing conditions. *J Biotechnol* **157**: 490–498.

Heider, J. (2007) Adding handles to unhandy substrates: anaerobic hydrocarbon activation mechanisms. *Curr Opin Chem Biol* **11**: 188–194.

Helgeson, H.C., Owens, C.E., Knox, A.M., and Richard, L. (1998) Calculation of the standard molal thermodynamic properties of crystalline, liquid, and gas organic molecules at high temperatures and pressures. *Geochim Cosmochim Acta* **62**: 985–1081.

Hinrichs, K.U., Hayes, J.M., Bach, W., Spivack, A.J., Hmelo, L.R., Holm, N.G. *et al.* (2006) Biological formation of ethane and propane in the deep marine subsurface. *Proc Natl Acad Sci U S A* **103**: 14684–14689.

Hubert, C., Judd, A. (2010) Using microorganisms as prospecting agents in oil and gas exploration. In *Handbook of hydrocarbon and lipid microbiology*, Vol. 4. Timmis, K.N. (ed.). Heidelberg, Germany: Springer, pp. 2714–2723.

Hungate, R.E. (1969) A roll tube method for cultivation of strict anaerobes. In *Methods in Microbiology*. Vol. 3B. Norris, J.R., Ribbons, D.W. (ed.). London, England: Academic Press, pp.117–132.

Hyman, M.R., and Arp, D.J. (1988) Acetylene inhibition of metalloenzymes. *Anal Biochem* **173**: 207–220.

Ingraham, L., and Meyer, D. (1985) Singlet dioxygen. In *Biochemistry of dioxygen*: Springer US, pp. 21–43.

Kana, T.M., Darkangelo, C., Hunt, M.D., Oldham, J.B., Bennett, G.E., and Cornwell, J.C. (1994) Membrane Inlet Mass-Spectrometer for rapid high-precision determination of N_2, O_2, and Ar in environmental water samples. *Anal Chem* **66**: 4166–4170.

Kanamori, T., Rashid, N., Morikawa, M., Atomi, H., and Imanaka, T. (2002) *Oleomonas sagaranensis* gen. nov., sp nov., represents a novel genus in the *Alphaproteobacteria*. *FEMS Microbiol Lett* **217**: 255–261.

Kaplan, M.L., and Kelleher, P.G. (1971) Mechanism of polyethylene photodegradation – oxidation of terminal olefins and saturated centers with singlet oxygen. *J Polym Sci B* **9**: 565–568.

Kartal, B., Wessels, H.J.C.T., van der Biezen, E., Francoijs, K.J., Jetten, M.S.M., Klotz, M.G., and Stein, L.Y. (2012) Effects of nitrogen dioxide and anoxia on global gene and protein expression in long-term continuous cultures of *Nitrosomonas eutropha* C91. *Appl Env Microbiol* **78**: 4788–4794.

Kinnaman, F.S., Valentine, D.L., and Tyler, S.C. (2007) Carbon and hydrogen isotope fractionation associated with the aerobic microbial oxidation of methane, ethane, propane and butane. *Geochim Cosmochim Acta* **71**: 271–283.

Kniemeyer, O., Fischer, T., Wilkes, H., Glockner, F.O., and Widdel, F. (2003) Anaerobic degradation of ethylbenzene by a new type of marine sulfate-reducing bacterium. *Appl Env Microbiol* **69**: 760–768.

Kniemeyer, O., and Heider, J. (2001) Ethylbenzene dehydrogenase, a novel hydrocarbon-oxidizing molybdenum/iron-sulfur/heme enzyme. *J Biol Chem* **276**: 21381–21386.

Knoop, F. (1904) Der Abbau aromatischer Fettsäuren im Tierkörper. *Beitr Chem Physiol Pathol* **6**, 150–162.

Kristjansson, J.K., and Hollocher, T.C. (1980) 1st practical assay for soluble nitrous-oxide reductase of denitrifying bacteria and a partial kinetic characterization. *J Biol Chem* **255**: 704–707.

Kropp, K.G., Davidova, I.A., and Suflita, J.M. (2000) Anaerobic oxidation of *n*-dodecane by an addition reaction in a sulfate-reducing bacterial enrichment culture. *Appl Environ Microbiol* **66**: 5393–5398.

Kuenen, J.G. (2008) Anammox bacteria: from discovery to application. *Nat Rev Microbiol* **6**: 320–326.

Kumar, P.A., Srinivas, T.N.R., Madhu, S., Manorama, R., and Shivaji, S. (2010) Indibacter alkaliphilus gen. nov., sp nov., an alkaliphilic bacterium isolated from a haloalkaline lake. *Int J Syst Evol Microbiol* **60**: 721–726.

Kumar, P.A., Srinivas, T.N.R., Madhu, S., Sravan, R., Singh, S., Naqvi, S.W.A., *et al*. (2012) *Cecembia lonarensis* gen. nov., sp. nov., a haloalkalitolerant bacterium of the family *Cyclobacteriaceae*, isolated from a haloalkaline lake and emended descriptions of the genera *Indibacter, Nitritalea and Belliella*. *Int J Syst Evol Microbiol* **62:** (9) 2252–2258 doi: 10.1099/ijs.0.038604-0.

Kuypers, M.M.M., Sliekers, A.O., Lavik, G., Schmid, M., Jorgensen, B.B., Kuenen, J.G. *et al.* (2003) Anaerobic ammonium oxidation by anammox bacteria in the Black Sea. *Nature* **422**: 608–611.

Kvenvolden, K.A. (1988) Methane hydrate – a major reservoir of carbon in the shallow geosphere.

Chem Geol **71**: 41–51.

Kvenvolden, K.A., and Rogers, B.W. (2005) Gaia's breath – global methane exhalations. *Mar Petrol Geol* **22**: 579–590.

Lam, P., and Kuypers, M.M.M. (2011) Microbial nitrogen cycling processes in oxygen minimum zones. *Annu Rev Mar Sci* **3**: 317–345.

Leak, D.J., Aikens, P.J., and Seyedmahmoudian, M. (1992) The microbial production of epoxides. *Trends Biotechnol* **10**: 256–261.

Li, L., Liu, X., Yang, W., Xu, F., Wang, W., Feng, L. *et al.* (2008) Crystal structure of long-chain alkane monooxygenase (LadA) in complex with coenzyme FMN: Unveiling the long-chain alkane hydroxylase. *J Mol Biol* **376**: 453–465.

Lide, D.R. (ed.). CRC Handbook of Chemistry and Physics. 79th ed. 1998-1999. Boca Raton, USA: CRC Press Inc.

Lobachev, V.L., and Rudakov, E.S. (2005) Kinetics and mechanism of the oxidation of alkanes and alkenes with peroxynitrous acid in aqueous solution-gas phase systems. *Kinet Catal* **46**: 344–353.

López-Cortéz, N., Beloqui, A., Ghazi, A., Ferrer, M. (2010). Enzymatic functionalization of hydrocarbon-like molecules. In *Handbook of hydrocarbon and lipid microbiology*, Vol. 4. Timmis, K.N. (ed.). Heidelberg, Germany: Springer, pp. 2844–2855.

Lovley, D.R., Baedecker, M.J., Lonergan, D.J., Cozzarelli, I.M., Phillips, E.J.P., and Siegel, D.I. (1989) Oxidation of aromatic contaminants coupled to microbial iron reduction. *Nature* **339**: 297–300.

Ludwig, W., Strunk, O., Westram, R., Richter, L., Meier, H., Yadhukumar *et al*. (2004) ARB: a software environment for sequence data. *Nucleic Acids Res* **32**: 1363–1371.

Luesken, F.A., Wu, M.L., den Camp, H.J.M.O., Keltjens, J.T., Stunnenberg, H., Francoijs, K.J. *et al*. (2012) Effect of oxygen on the anaerobic methanotroph '*Candidatus* Methylomirabilis oxyfera': kinetic and transcriptional analysis. *Env Microbiol* **14:** 1024-1034.

Maeng, J.H., Sakai, Y., Tani, Y., and Kato, N. (1996) Isolation and characterization of a novel oxygenase that catalyzes the first step of *n*-alkane oxidation in Acinetobacter sp strain M-1. *J Bacteriol* **178**: 3695–3700.

McInerney, M.J., Hoehler, T., Gunsalus, R.P., Schink, B. Introduction to microbial hydrocarbon production: Bioenergetics (2010) In *Handbook of hydrocarbon and lipid microbiology*, Vol. 1. Timmis, K.N. (ed.). Heidelberg, Germany: Springer, pp. 321–336.

Matsumoto, Y., Tosha, T., Pisliakov, A.V., Hino, T., Sugimoto, H., Nagano, S. *et al.* (2012) Crystal structure of quinol-dependent nitric oxide reductase from *Geobacillus stearothermophilus*. *Nat Struct Mol Biol* **19**: 238–245.

Mckenna, E.J., and Kallio, R.E. (1965) Biology of hydrocarbons. *Annu Rev Microbiol* **19**: 183–208.

Mehboob, F., Junca, H., Schraa, G., and Stams, A.J.M. (2009) Growth of *Pseudomonas chloritidismutans* AW-1(T) on *n*-alkanes with chlorate as electron acceptor. *Appl Microbiol Biotechnol* **83**: 739–747.

Mulder, A., Vandegraaf, A.A., Robertson, L.A., and Kuenen, J.G. (1995) Anaerobic ammonium oxidation discovered in a denitrifying fluidized-bed reactor. *FEMS Microbiol Ecol* **16**: 177–183.

Mumma, M.J., DiSanti, M.A., DelloRusso, N., Fomenkova, M., MageeSauer, K., Kaminski, C.D., and Xie, D.X. (1996) Detection of abundant ethane and methane, along with carbon monoxide and water, in comet C/1996 B2 Hyakutake: Evidence for interstellar origin. *Science* **272**: 1310–1314.

Musat, F., and Widdel, F. (2008) Anaerobic degradation of benzene by a marine sulfate-reducing enrichment culture, and cell hybridization of the dominant phylotype. *Environ Microbiol* **10**: 10–19.

Niemann, H.B., Atreya, S.K., Bauer, S.J., Carignan, G.R., Demick, J.E., Frost, R.L. *et al.* (2005) The abundances of constituents of Titan's atmosphere from the GCMS instrument on the Huygens probe. *Nature* **438**: 779–784.

Novelli, G.D., ZoBell, C.E. (1944) Assimilation of petroleum hydrocarbons by sulfate reducing bacteria. *J Bacteriol* **47:** 447–448.

Ochsner, U.A., Hembach, T., and Fiechter, A. (1996) Production of rhamnolipid biosurfactants. *Adv Biochem Eng Biotechnol* **53**: 89–118.

Ollivier, B., Alazard, D. (2010) The oil reservoir ecosystem. In *Handbook of hydrocarbon and lipid microbiology*, Vol. 3. Timmis, K.N. (ed.). Heidelberg, Germany: Springer, pp. 2262–2268.

Onumonu, A.N., Colocoussi, A., Matthews, C., Woodland, M.P., and Leak, D.J. (1994) Microbial alkene epoxidation - merits and limitations. *Biocatalysis* **10**: 211–218.

Perfumo, A. (2010) Production and roles of biosurfactants and bioemulsifiers in accessing hydrophobic substrates. In *Handbook of hydrocarbon and lipid microbiology*, Vol. 2. Timmis, K.N. (ed.). Heidelberg, Germany: Springer, pp. 1501–1512.

Pinzon, N.M., Aukema, K.G., Gralnick, J.A., and Wackett, L.P. (2011) Nile Red detection of bacterial hydrocarbons and ketones in a high-throughput format. *Mbio* **2**.

Prince, R.C. (1993) Petroleum spill bioremediation in marine environments. *Crit Rev Microbiol* **19**: 217–242.

Prince, R.C. (2002) Petroleum and other hydrocarbons, biodegradation of. In *Encyclopedia of Environmental Microbiology*. Bitton, G., (ed.) New York, USA: John Wiley, pp. 2402–2416.

Pruesse, E., Quast, C., Knittel, K., Fuchs, B.M., Ludwig, W.G., Peplies, J., and Glockner, F.O. (2007) SILVA: a comprehensive online resource for quality checked and aligned ribosomal RNA sequence data compatible with ARB. *Nucleic Acids Res* **35**: 7188–7196.

Rabus, R., Wilkes, H., Behrends, A., Armstroff, A., Fischer, T., Pierik, A.J., and Widdel, F. (2001) Anaerobic initial reaction of *n*-alkanes in a denitrifying bacterium: Evidence for (1-methylpentyl)succinate as initial product and for involvement of an organic radical in n-hexane metabolism. *J Bacteriol* **183**: 1707–1715.

Rabus, R., Jarling, R., Lahme, S., Kuhner, S., Heider, J., Widdel, F., and Wilkes, H. (2011) Co-metabolic conversion of toluene in anaerobic *n*-alkane-degrading bacteria. *Environ Microbiol* **13**: 2576–2585.

Raghoebarsing, A.A., Pol, A., van de Pas-Schoonen, K.T., Smolders, A.J.P., Ettwig, K.F., Rijpstra, W.I.C. *et al.* (2006) A microbial consortium couples anaerobic methane oxidation to denitrification. *Nature* **440**: 918–921.

Rehm, H.J. and Reiff, I. (1981) Mechanisms and occurrence of microbial oxidation of long-chain alkanes. In *Advances in Biochemical Engineering/Biotechnology*, Vol. 19. Fiechter A. (ed.) Berlin, Germany: Springer 175–215. doi: 10.1007/3-540-10464-X_18.

Revsbech, N.P. (1989) An oxygen microsensor with a guard cathode. *Limnol Oceanogr* **34**: 474–478.

Rikken, G.B., Kroon, A.G.M., and vanGinkel, C.G. (1996) Transformation of (per)chlorate into chloride by a newly isolated bacterium: Reduction and dismutation. *Appl Microbiol Biotechnol* **45**: 420–426.

Rojo, F. (2009) Degradation of alkanes by bacteria. *Environ Microbiol* **11**: 2477-2490.

Rontani, J.F., (2010) Production of wax esters by bacteria. In *Handbook of hydrocarbon and lipid microbiology*, Vol. 1. Timmis, K.N. (ed.). Heidelberg, Germany: Springer, pp. 459–469.

Rosenfeld, W.D. (1947) Anaerobic oxidation of hydrocarbons by sulfate-reducing bacteria. *J Bacteriol* **54**: 664–665.

Saillard, J.-Y. (1990) Theoretical aspects of alkane C–H activation by organometallics. In *Selective hydrocarbon activation*. Davies, J.A., Watson, P.L.,Greenberg, A. and Liebmann, J.F. (eds.). Weinheim, Germany: VCH Verlagsgesellschaft.

Sakai, Y., Maeng, J.H., Tani, Y., and Kato, N. (1994) Use of long-chain *n*-alkanes (C-13-C-44) by an isolate, *Acinetobacter* Sp M-1. *Biosci Biotechnol Biochem* **58**: 2128–2130.

Salinero, K.K., Keller, K., Feil, W.S., Feil, H., Trong, S., Di Bartolo, G., and Lapidus, A. (2009) Metabolic analysis of the soil microbe *Dechloromonas aromatica* str. RCB: indications of a surprisingly complex life-style and cryptic anaerobic pathways for aromatic degradation. *BMC Genomics* **10**.

Samuels, L., Kunst, L., and Jetter, R. (2008) Sealing plant surfaces: Cuticular wax formation by epidermal cells. *Annu Rev Plant Biol* **59**: 683–707.

Scheller, U., Zimmer, T., Becher, D., Schauer, F., and Schunck, W.H. (1998) Oxygenation cascade in conversion of *n*-alkanes to alpha, omega-dioic acids catalyzed by cytochrome P450 52A3. *J Biol Chem* **273**: 32528–32534.

Schink, B. (1985) Degradation of unsaturated-hydrocarbons by methanogenic enrichment cultures. *FEMS Microbiol Ecol* **31**: 69–77.

Schmidt, I., and Bock, E. (1997) Anaerobic ammonia oxidation with nitrogen dioxide by *Nitrosomonas eutropha*. *Arch Microbiol* **167**: 106–111.

Schmidt, I., Zart, D., and Bock, E. (2001) Effects of gaseous NO_2 on cells of *Nitrosomonas eutropha* previously incapable of using ammonia as an energy source. *Anton Leeuw Int J G* **79**: 39–47.

Schreiber, F., Polerecky, L., and de Beer, D. (2008) Nitric oxide microsensor for high spatial resolution measurements in biofilms and sediments. *Anal Chem* **80**: 1152–1158.

Scott, C.C.L., and Finnerty, W.R. (1976) Characterization of intracytoplasmic hydrocarbon inclusions from hydrocarbon-oxidizing *Acinetobacter* species Ho1-N. *J Bacteriol* **127**: 481–489.

So, C.M., and Young, L.Y. (1999) Isolation and characterization of a sulfate-reducing bacterium that anaerobically degrades alkanes. *Appl Environ Microbiol* **65**: 2969–2976.

So, C.M., Phelps, C.D., and Young, L.Y. (2003) Anaerobic transformation of alkanes to fatty acids by a sulfate-reducing bacterium, strain Hxd3. *Appl Environ Microbiol* **69**: 3892–3900.

Söhngen, N.L. (1913) Benzin, Petroleum, Paraffinöl und Paraffin als Kohlenstoff– und Energiequelle für Mikroben. Zentralblatt für Bakteriologie, Parasitenkunde, Infenktionskrankheiten und Hygiene **37:** 595–609.

Spiekermann, P., Rehm, B.H.A., Kalscheuer, R., Baumeister, D., and Steinbuchel, A. (1999) A sensitive, viable-colony staining method using Nile red for direct screening of bacteria that accumulate polyhydroxyalkanoic acids and other lipid storage compounds. *Arch Microbiol* **171**: 73–80.

Stewart, J.E., and Kallio, R.E. (1959) Bacterial hydrocarbon oxidation 2. Ester formation from alkanes. *J Bacteriol* **78**: 726–730.

Sun, Y.G., Chen, Z.Y., Xu, S.P., and Cai, P.X. (2005) Stable carbon and hydrogen isotopic fractionation of individual *n*-alkanes accompanying biodegradation: evidence from a group of progressively biodegraded oils. *Org Geochem* **36**: 225–238.

Swannell, R.P.J., Lee, K., and McDonagh, M. (1996) Field evaluations of marine oil spill bioremediation. *Microbiol Rev* **60**: 342–365.

Thauer, R.K. (1998) Biochemistry of methanogenesis: a tribute to Marjory Stephenson. *Microbiology* **144**: 2377–2406.

Thauer, R.K., Jungermann, K., and Decker, K. (1977) Energy-conservation in chemotropic anaerobic bacteria. *Bacteriol Rev* **41**: 100–180.

Thauer, R.K., and Shima, S. (2008) Methane as fuel for anaerobic microorganisms. *Ann N Y Acad Sci* **1125**: 158–170.

Thierfelder, H., and Klenk, E. (1924) Further testings on the conduct of fatty aromatic compounds in the animal body. *H-S Z Physiol Chem* **141**: 13–28.

Tillman, J.A., Seybold, S.J., Jurenka, R.A., and Blomquist, G.J. (1999) Insect pheromones – an overview of biosynthesis and endocrine regulation. *Insect Biochem Mol Biol* **29**: 481–514.

Tindall, B.J., Rossello-Mora, R., Busse, H.J., Ludwig, W., and Kampfer, P. (2010) Notes on the characterization of prokaryote strains for taxonomic purposes. *Int J Syst Evol Micr* **60**: 249–266.

UNEP 2005: Marine Litter, an analytical overview.

Van Ginkel, C.G., Rikken, G.B., Kroon, A.G.M., and Kengen, S.W.M. (1996) Purification and characterization of chlorite dismutase: A novel oxygen-generating enzyme. *Arch Microbiol* **166**: 321–326.

Van Hamme, J.D., Singh, A., and Ward, O.P. (2003) Recent advances in petroleum microbiology. *Microbiol Mol Biol Rev* **67**: 503-549.

Vollhardt, P.C. (1990) Organische Chemie. Weinheim, Germany: VCH Verlagsgesellschaft.

Walsh, C. (1982) Suicide substrates – mechanism-based enzyme inactivators. *Tetrahedron* **38**: 871–909.

Wakett, L.P. (2010) Aliphatic hydrocarbon producers. In *Handbook of hydrocarbon and lipid microbiology*, Vol. 1. Timmis, K.N. (ed.). Heidelberg, Germany: Springer, pp. 609–614.

Watkinson, R.J., and Morgan, P. (1990) Physiology of aliphatic hydrocarbon-degrading microorganisms. *Biodegradation* **1**: 79–92.

Webner, K. (2012) Die Gene der (1-Methylalkyl)succinat-Synthase im anaeroben *n*-Alkanabbau des Betaproteobakteriums Stamm HdN1. *Ph.D.-thesis*, University Bremen.

Weelink, S.A.B., van Eekert, M.H.A., and Stams, A.J.M. (2010) Degradation of BTEX by anaerobic bacteria: physiology and application. *Rev Environ Sci Biotechnol* **9**: 359–385.

Whiteley, K.S., Heggs, T.G., Koch, H., Mawer, R.L., Immel, W. (2005) Polyolefins. In *Ullmann's Encyclopedia of Industrial Chemistry*, Weinheim, Germany: VCH Verlagsgesellschaft, pp. 2–95.

Whittington, D.A., Rosenzweig, A.C., Frederick, C.A., and Lippard, S.J. (2001) Xenon and halogenated alkanes track putative substrate binding cavities in the soluble methane monooxygenase hydroxylase. *Biochemistry* **40**: 3476–3482.

Wick, L.Y., de Munain, A.R., Springael, D., and Harms, H. (2002) Responses of *Mycobacterium* sp LB501T to the low bioavailability of solid anthracene. *Appl Microbiol Biotechnol* **58**: 378–385.

Widdel, F. (2010). Cultivation of anaerobic microorganisms with hydrocarbons as growth substrates. In *Handbook of hydrocarbon and lipid microbiology*, Vol. 5. Timmis, K.N. (ed.). Heidelberg, Germany: Springer, pp. 3787–3798.

Widdel, F. and Bak, F. (1992) Gram-negative mesophilic sulfate-reducing bacteria. In *The prokaryotes*. Balows, A., Trüper, H.G., Dworkin, M., Harder, W., and Schleifer, K.-H. (eds). New York: Springer, pp. 3352–3378.

Widdel, F. and Grundmann, O. (2010) Biochemistry of the anaerobic degradation of non-methane alkanes. In *Handbook of hydrocarbon and lipid microbiology*, Vol. 2. Timmis, K.N. (ed.). Heidelberg, Germany: Springer, pp. 909–924.

Widdel, F., Knittel, K., Galushko, A. (2010) Anaerobic hydrocarbon-degrading microorganisms: An overview. In *Handbook of hydrocarbon and lipid microbiology*, Vol. 3. Timmis, K.N. (ed.). Heidelberg, Germany: Springer, pp. 1997–2022.

Widdel, F. and Musat, F. (2010) Energetic and other quantitative aspects of microbial hydrocarbon utilization. In *Handbook of hydrocarbon and lipid microbiology*, Vol. 2. Timmis, K.N. (ed.). Heidelberg, Germany: Springer, pp. 731–764.

Wilkes, H., Kuhner, S., Bolm, C., Fischer, T., Classen, A., Widdel, F., and Rabus, R. (2003) Formation of *n*-alkane- and cycloalkane-derived organic acids during anaerobic growth of a denitrifying bacterium with crude oil. *Org Geochem* **34**: 1313–1323.

Wilkes, H., Rabus, R., Fischer, T., Armstroff, A., Behrends, A., and Widdel, F. (2002) Anaerobic degradation of *n*-hexane in a denitrifying bacterium: Further degradation of the initial intermediate (1-methylpentyl)succinate via C-skeleton rearrangement. *Arch Microbiol* **177**: 235–243.

Wilkes, H. and Schwarzbauer, J. (2010) Hydrocarbons: An introduction to structure, physico-chemical properties and natural occurrence. In *Handbook of hydrocarbon and lipid microbiology*, Vol. 1. Timmis, K.N. (ed.). Heidelberg, Germany: Springer, pp. 5–41.

Wilson, R.D., Monaghan, P.H., Osanik, A., Price, L.C., and Rogers, M.A. (1974) Natural marine oil seepage. *Science* **184**: 857–865.

Wolterink, A.F.W.M., Jonker, A.B., Kengen, S.W.M., and Stams, A.J.M. (2002) *Pseudomonas chloritidismutans* sp nov., a nondenitrifying, chlorate-reducing bacterium. *Int J Sysc Evol Micr* **52**: 2183–2190.

Wu, M.L., van Teeseling, M.C.F., Willems, M.J.R., van Donselaar, E.G., Klingl, A., Rachel, R. *et al*. (2012) Ultrastructure of the denitrifying methanotroph "*Candidatus* Methylomirabilis oxyfera," a novel polygon-shaped bacterium. *J Bacteriol* **194**: 284-291.

Yarza, P., Richter, M., Peplies, J., Euzeby, J., Amann, R., Schleifer, K.H. *et al.* (2008) The All-Species Living Tree project: a 16S rRNA-based phylogenetic tree of all sequenced type strains. *Syst Appl Microbiol* **31**: 241–250.

Yeager, C.M., Bottomley, P.J., Arp, D.J., and Hyman, M.R. (1999) Inactivation of toluene 2-monooxygenase in *Burkholderia cepacia* G4 by alkynes. *Appl Environ Microbiol* **65**: 632–639.

Yemashova, N.A., Murygina, V.P., Zhukov, D.V., Zakharyantz, A.A., Gladchenko, M.A., Appanna, V., and Kalyuzhnyi, S.V. (2007) Biodeterioration of crude oil and oil derived products: a review. *Rev Environ Sci Biotechnol* **6:** 315–337.

Zedelius, J., Rabus, R., Grundmann, O., Werner, I., Brodkorb, D., Schreiber, F., *et al.* (2011) Alkane degradation under anoxic conditions by a nitrate-reducing bacterium with possible involvement of the electron acceptor in substrate activation. *Environ Microbiol Reports* **3:** 125–135.

Zengler, K., Richnow, H.H., Rossello-Mora, R., Michaelis, W., and Widdel, F. (1999) Methane formation from long-chain alkanes by anaerobic microorganisms. *Nature* **401**: 266–269.

Zumft, W.G. (1993) The biological role of nitric-oxide in bacteria. *Arch Microbiol* **160**: 253–264.

Zumft, W.G. (1997) Cell biology and molecular basis of denitrification. *Microbiol Mol Biol Rev* **61**: 533–582.

D Publications

D.1 Overview of the manuscripts

Alkane degradation under anoxic conditions by a nitrate-reducing bacterium with possible involvement of the electron acceptor in substrate activation

Johannes Zedelius, Ralf Rabus, Olav Grundmann, Insa Werner, Danny Brodkorb, Frank Schreiber, Petra Ehrenreich, Astrid Behrends, Heinz Wilkes, Michael Kube, Richard Reinhardt and Friedrich Widdel

Author contributions

J.Z. and F.W. developed the concept with contributions by R.Ra.. J.Z. performed analysis of phylogeny and microbial activity. O.G. and I.W. revealed fumarate addition in strain OcN1. J.Z. conducted purity controls including microscopy and FISH. D.B. and J.Z. performed fatty alcohol analyses. F.S. conducted O_2-microsensor measurements. P.E. and A.B. investigated catabolic stoichiometry and electron acceptors. H.W. performed metabolite analyses. M.K., R.Re. and R.Ra. sequenced and annotated the genome. J.Z. designed and performed physiological gas measurements with contributions from F.W. F.W. contributed thermodynamic and energetic aspects. All authors discussed the results. F.W. and J.Z. wrote the manuscript.

Is there a key role of NO in *n*-alkane activation during growth of a Gammaproteobacterium (strain HdN1) by NO_3^- respiration?

Johannes Zedelius, Marcel M. M. Kuypers, Ralf Rabus, Frank Schreiber, Friedrich Widdel and Marc Strous

Author contributions

J.Z. and F.W. developed the concept with contributions by R.R. and M.S. J.Z. planned and performed physiological gas measurements. J.Z., F.S. and M.M.M.K. designed and conducted membrane-inlet mass spectrometry measurements. J.Z. revealed wax ester formation. R.R. performed proteomic analyses. M.S. conducted comparative genome and gene product analyses. F.W. contributed kinetic aspects as well as stoichiometric and ecophysiological considerations of NO metabolism. F.W. and J.Z. wrote the manuscript with input from all authors.

Chapter D.2

Alkane degradation under anoxic conditions by a nitrate-reducing bacterium with possible involvement of the electron acceptor in substrate activation

Johannes Zedelius,[1] Ralf Rabus,[1,2] Olav Grundmann,[1] Insa Werner,[1] Danny Brodkorb,[1] Frank Schreiber,[1] Petra Ehrenreich,[1] Astrid Behrends,[1] Heinz Wilkes,[3] Michael Kube,[4] Richard Reinhardt[5] and Friedrich Widdel[1]*

[1]*Max-Planck-Institut für Marine Mikrobiologie, Celsiusstraße 1, 28359 Bremen, Germany.*
[2]*Institut für Chemie und Biologie des Meeres, Universität Oldenburg, Carl-von-Ossietzky Str. 9-11, 26111 Oldenburg, Germany.*
[3]*GeoForschungsZentrum Potsdam, Telegrafenberg, 14473 Potsdam, Germany.*
[4]*Max-Planck-Institut für Molekulare Genetik, Ihnestraße 73, 14195 Berlin, Germany.*
[5]*Max-Planck-Institut für Pflanzenzüchtungsforschung, Carl-von-Linné-Weg 10, 50829 Köln, Germany.*

Manuscript *published* at

Environmental Microbiology Reports (2011)

Summary

Microorganisms can degrade saturated hydrocarbons (alkanes) not only under oxic but also under anoxic conditions. Three denitrifying isolates (strains HxN1, OcN1, HdN1) able to grow under anoxic conditions by coupling alkane oxidation to CO_2 with NO_3^- reduction to N_2 were compared with respect to their alkane metabolism. Strains HxN1 and OcN1, which are both Betaproteobacteria, utilized *n*-alkanes from C_6 to C_8 and C_8 to C_{12}, respectively. Both activate alkanes anaerobically in a fumarate-dependent reaction yielding alkylsuccinates, as suggested by present and previous metabolite and gene analyses. However, strain HdN1 was unique in several respects. It belongs to the Gammaproteobacteria and was more versatile towards alkanes, utilizing the range from C_6 to C_{30}. Neither analysis of metabolites nor of genes in the complete genome sequence of strain HdN1 hinted at fumarate-dependent alkane activation. Moreover, whereas strains HxN1 and OcN1 grew with alkanes and NO_3^-, NO_2^- or N_2O added to the medium, strain HdN1 oxidized alkanes only with NO_3^- or NO_2^- but not with added N_2O; but N_2O was readily used for growth with long-chain alcohols or fatty acids. Results suggest that NO_2^- or a subsequently formed nitrogen compound other than N_2O is needed for alkane activation in strain HdN1. From an energetic point of view, nitrogen-oxygen species are generally rather strong oxidants. They may enable enzymatic mechanisms that are not possible under conditions of sulfate reduction or methanogenesis and thus allow a special mode of alkane activation.

Introduction

Saturated hydrocarbons (alkanes) as major constituents of petroleum (Tissot and Welte, 1984) enter the environment via natural seeps or accidental spills, or due to the use of refined petroleum products. Furthermore, alkanes are wide-spread products of living organisms (Birch and Bachofen, 1988). Aerobic alkane biodegradation, in particular the initial O_2-dependent activation by monooxygenases, has been studied since many decades (Rojo, 2010). In recent years, alkanes were also shown to be degraded anaerobically with nitrate (Ehrenreich *et al*., 2000; Bonin *et al*., 2004; Grossi *et al*., 2008; Callaghan *et al*., 2009) or sulfate (Aeckersberg *et al*., 1991, 1998; So and Young, 1999; Cravo-Laureau *et al*., 2004; Davidova et al., 2006; Kniemeyer *et al*., 2007; Higashioka *et al*., 2009) as electron acceptor, or under conditions of methanogenesis (Zengler *et al*., 1999; Anderson and Lovley, 2000; Jones *et al*., 2008). The only well-established mechanism for anaerobic activation of alkanes to date is the radical-catalyzed addition to fumarate yielding alkylsuccinates (Kropp *et al*., 2000; Rabus *et al*., 2001; Heider, 2007). Genes [designated *mas*, for (1-methylalkyl)succinate synthase; or *ass*, for alkylsuccinate synthase] encoding the putative enzyme have been detected in a nitrate-reducing (Grundmann *et al*., 2008) and a sulfate-reducing (Callaghan *et al*., 2008) strain. Still, an alternative possibility for anaerobic alkane activation has been suggested on the basis of cell fatty acid and isotope labeling analysis (Aeckersberg *et al*., 1998; So *et al*., 2003; Callaghan *et al*., 2006).

Of three denitrifying strains, HxN1, OcN1, and HdN1, that were isolated with *n*-hexane, *n*-octane and *n*-hexadecane, respectively (Ehrenreich *et al.*, 2000), only the first one has been formerly studied with respect to its alkane metabolism (Rabus *et al*., 2001; Wilkes *et al*., 2002; Grundmann *et al*., 2008). A subsequent comparative study including the two other strains revealed that also strain OcN1 formed alkylsuccinates during growth with alkanes and harbored a gene apparently encoding the responsible enzyme. In contrast, alkylsuccinates were not detectable in strain HdN1, and its complete genome sequence did not reveal any gene likely to encode (1-methylalkyl)succinate or alkylsuccinate synthase. A unique physiological characteristic of strain HdN1 was that it did not grow with alkanes if N_2O was added instead of NO_3^-, whereas growth with alcohols and fatty acids readily occurred with N_2O. In contrast, strains HxN1 and OcN1 grew well with N_2O and alkanes. These findings suggest that alkane activation in strain HdN1 differs principally from alkane activation in strains HxN1 and OcN1 and requires an NO_3^--derived compound other than N_2O.

Results and discussion

Cultivation, phylogenetic relationships, morphology, and purity control

The focus of this study is on strain HdN1 and its apparently unusual physiology with respect to *n*-alkane utilization. The isolation of strain HdN1 along with strains OcN1 and HxN1, a few substrate tests, and the capacity for complete alkane oxidation in anoxic medium with NO_3^- have been documented previously (Ehrenreich *et al*., 2000). Unless indicated otherwise, the strains were grown in conventional HCO_3^-/CO_2-buffered defined medium (Rabus and Widdel, 1995) with alkanes as the only organic substrates.

The study of anaerobic microbial hydrocarbon utilization requires the strict exclusion of traces of O_2 from air which through monooxygenases could lead to hydroxyl compounds (that can be further degraded anaerobically). Hence, in addition to physical exclusion of air (Widdel and Bak, 1992), the presence of a reductant ("redox buffer") is advisable. Unlike sulfate-reducing bacteria that form a chemical reducing agent, sulfide, nitrate-reducing bacteria do not produce a reductant. Addition of sulfide (or other reducing sulfur compounds) is inappropriate because it is easily oxidized in by-reactions of the "high-potential" nitrate reduction pathway, or because it can inhibit denitrifiers (unpublished results). We therefore added ascorbate (4 mM) as a mild reductant (Rabus *et al*., 1993; Ehrenreich *et al*., 2000; Widdel, 2010). Ascorbate did not serve as substrate for growth and nitrate reduction, as revealed in control incubations with ascorbate alone. We also verified that ascorbate in our medium did not scavenge nitrite, the intermediate of nitrate reduction, by chemical reaction. If sterile medium with ascorbate (pH 7.2) and $NaNO_2$ (2 mM) was incubated for 10 days and analyzed by ion chromatography (Rabus *et al*., 1993), there was no noticeable decrease of the nitrite concentration. At low pH, reduction of the protonated form (HNO_2) by ascorbic acid to yield nitric oxide can be significant (Yamasaki, 2000). Furthermore, tests were carried out to exclude an adverse physiological effect of ascorbate. Strain HdN1 was grown with *n*-tetradecane and NO_3^- or NO_2^- in ascorbate-containing medium as well as in ascorbate-free medium deoxygenated by vigorous sparging with N_2. The cultures with and without ascorbate grew equally well.

Strain HdN1 affiliates with the Gammaproteobacteria, whereas strain OcN1 and HxN1 are members of the Betaproteobacteria (Fig. 1). Most nitrate-reducing bacteria enriched and isolated with various aromatic or saturated petroleum hydrocarbons are Betaproteobacteria

(Widdel *et al*., 2010). Some denitrifying strains that degrade petroleum hydrocarbons are Gammaproteobacteria; these also include alkane-degraders affiliating with *Marinobacter* sp. (Bonin *et al*., 2004) and *Pseudomonas balearica* (Grossi *et al*., 2008).

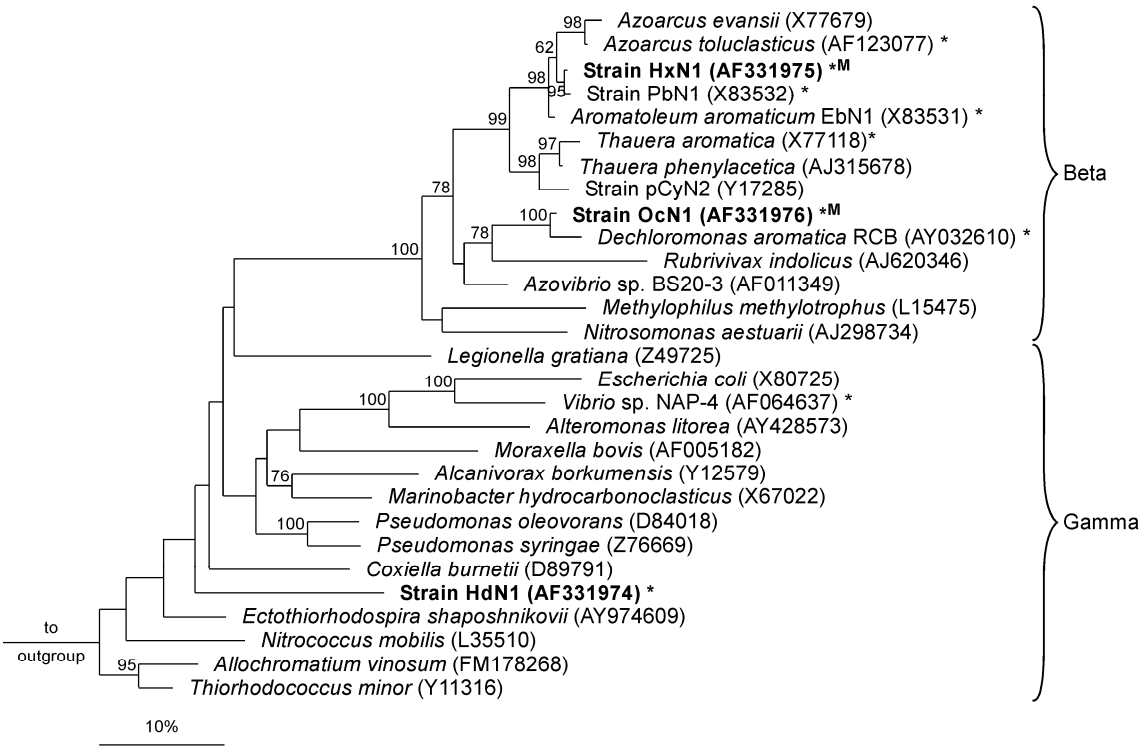

Fig. 1. Phylogenetic (16S rRNA-based) affiliation of strain HdN1 with selected Beta- and Gammaproteobacteria including other strains able to degrade aromatic or saturated petroleum hydrocarbons with nitrate (*). Strains able to degrade n-alkanes anaerobically are highlighted in bold; occurrence of (1-methylalkyl)succinate formation for alkane activation is also indicated (^{M}). Bootstrap values (%; only >60% shown) were obtained after 1000 resamplings. Scale bar, 10% estimated sequence divergence.

The cell shape of strain HdN1 was unusually variable and significantly influenced by the organic growth substrate (Ehrenreich *et al*., 2000). In particular long-chain alkanes caused swelling of a large fraction of the cells. In such cells, spacious inclusions resembling storage compounds could be seen at high magnification (Fig. 2A). However, polyhydroxyalkanoates were not detectable (A. Steinbüchel, pers. commun.) by gas chromatography following acidic hydrolysis and methylation of freeze-dried cells (Steinbüchel and Wiese, 1992). Cells in alkane cultures tended to grow in close contact with the overlying insoluble hydrocarbon phase. The bulk of alkane-grown cells was buoyant, possibly due to association with or storage of alkane droplets. Alkane storage and buoyancy is a phenomenon known from aerobic alkane degraders (Scott and Finnerty, 1976). This behavior rendered harvesting by centrifugation difficult. A minor fraction of the cells was motile.

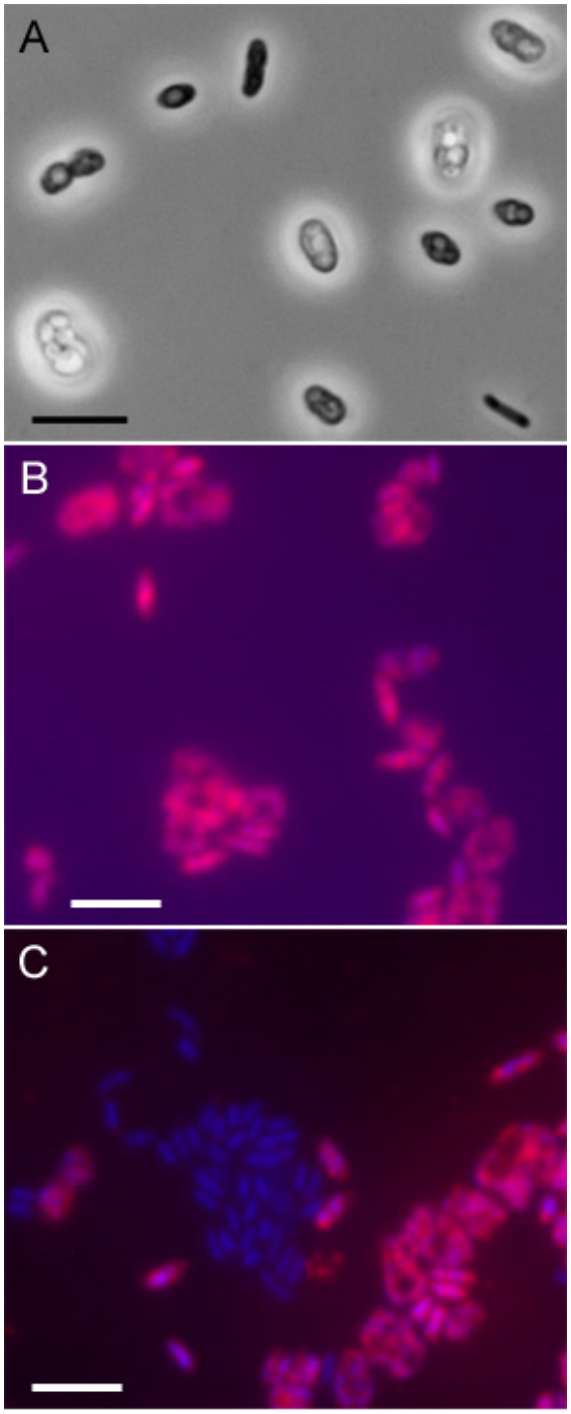

Fig. 2. Microscopic images of strain HdN1.
A. Highly variable cell forms of strain HdN1 grown anaerobically with hexadecane and nitrate. Phase contrast micrographs of viable cells. Bar, 5 µm.
B. Cells from a pure culture of strain HdN1 hybridized with a specific 16S rRNA-targeted oligonucleotide probe and stained with DAPI. The image represents an overlay of the probe and the DAPI signal. Bar, 5 µm.
C. Mixed cells of strains HdN1 and OcN1 hybridized, stained and visualized as in B. Bar, 5 µm.

Thorough purity tests excluded that cell heterogeneity in cultures of strain HdN1 was due to accompanying microorganisms. First, repeated aerobic and anaerobic (with NO_3^-) liquid dilution series (according to the most probable number technique) were carried out separately with *n*-tetradecane or *n*-valerate (*n*-pentanoate). All cultures derived from the highest positive dilution tubes were indistinguishable with respect to cell shapes and always able to use both, tetradecane and valerate. Second, cultures were streaked on agar plates containing valerate and yeast extract and incubated in a jar under air with 3% CO_2. All well separated valerate-grown colonies transferred to anoxic liquid media grew again with tetradecane, and cultures had the microscopic appearance as before. Third, strain HdN1 was mixed with strain OcN1, and a specific 16S rRNA-targeting fluorescent oligonucleotide probe (Appendix S1) was applied. Whereas in the pure culture all cells exhibited the specific hybridization signal (Fig. 2B), the mixed culture contained in addition the expected non-hybridizing cells that exhibited only the general fluorescent stain (Fig. 2C). Hence, strain HdN1 is in principle distinguishable from contaminants by specific probing.

Anaerobic growth tests with alkanes and alkanoates

The capability of strain HdN1 for complete hexadecane oxidation with nitrate according to $5\ C_{16}H_{34} + 98\ NO_3^- + 18\ H^+ \rightarrow 80\ HCO_3^- + 49\ N_2 + 54\ H_2O$ has been verified formerly with small, precisely quantifiable amounts of alkane (Ehrenreich *et al*., 2000). In all subsequent experiments, significantly higher amounts of alkanes were added than could be oxidized by the electron acceptor (10 mM NO_3^-). In this way, a large contact area between the insoluble hydrocarbon and aqueous phase was provided which favoured growth (Widdel, 2010). Alkanes with carbon chains $\leq C_{10}$ were provided as solutions in 2,2,4,4,6,8,8-heptamethylnonane (HMN) as an inert carrier phase to avoid toxic effects (Appendix S1). Further growth tests revealed that strain HdN1 utilized *n*-alkanes from C_6 (*n*-hexane) to C_{30} (*n*-triacontane) as carbon sources and electron donors (C_6 to C_{20}, C_{24}, C_{26}, C_{28}, C_{30}, C_{36} and C_{40} tested). Fastest growth was observed in the range from C_{14} (tetradecane) to C_{18} (octadecane). With an inoculum size of 1% (v/v), full growth and complete NO_3^- consumption occurred within seven days. A doubling time of 11 – 13 h during early growth was estimated from an analysis of the nitrate consumption curve (see also Ehrenreich *et al*., 2000). (Inhomogeneous growth and alkane droplets prevented measurement of the optical density as a growth parameter.) Growth with alkanes of shorter or longer chains was slower (two- to threefold time required for full

growth and NO_3^- consumption). The other strains, HxN1 and OcN1, utilized a significantly narrower range of alkanes, which was from C_6 to C_8 (*n*-octane) and C_8 to C_{12} (*n*-dodecane), respectively. Also alkane-utilizing sulfate-reducing bacteria utilized a narrower range (Rueter *et al*., 1994; Aeckersberg *et al*., 1998).

Strain HdN1 utilized monocarboxylic acids (sodium salts; method of preparation and addition given by Widdel and Bak, 1992; see also Appendix S1) from acetate to stearate (C_2 – C_{18}; higher fatty acids not tested), with best growth (roughly twice as fast as with alkanes) with valerate (C_5) and with fatty acids from *n*-decanoate (C_{10}) to stearate. Some primary linear alcohols were also tested (C_8 and C_{10} provided as solutions in HMN; C_{14} and C_{16} added as solid compounds). Strain HdN1 grew well with 1-decanol, 1-tetradecanol and 1-hexadecanol; growth with 1-octanol was poor, and no growth occurred with ethanol.

Growth tests with different electron acceptors

All three strains grew also aerobically with alkanes. Examination of strain HdN1 in more detail revealed that almost the same range of *n*-alkanes (and fatty acids) was oxidized with O_2 as in anoxic cultures with NO_3^-. Only *n*-hexane was not utilized so far with O_2. Another slight difference between aerobic and anaerobic alkane utilization was observed if cultures grown with hexadecane were transferred to medium medium with tridecane (C_{13}) or dodecane (C_{12}). Whereas aerobic cultures grew immediately with the lighter alkanes, anaerobic cultures exhibited a lag-phase of >10 days.

The transient formation by strain HdN1 of NO_2^- (not shown) and N_2O (Fig. 3A, B, lower curves) at low concentration during NO_3^- reduction and the detection of N_2 in all cultures grown under an argon atmosphere indicated the common denitrification pathway. To further examine the capability for efficient use of NO_2^- and N_2O, these electron acceptors were tested individually in the absence of NO_3^-.

Growth with alkanes also occurred with added NO_2^-, but was slightly slowed down if more than 5 mM NO_2^- was added. Furthermore, a lag phase of ca. two days was sometimes observed after inoculation of new medium with NO_2^-.

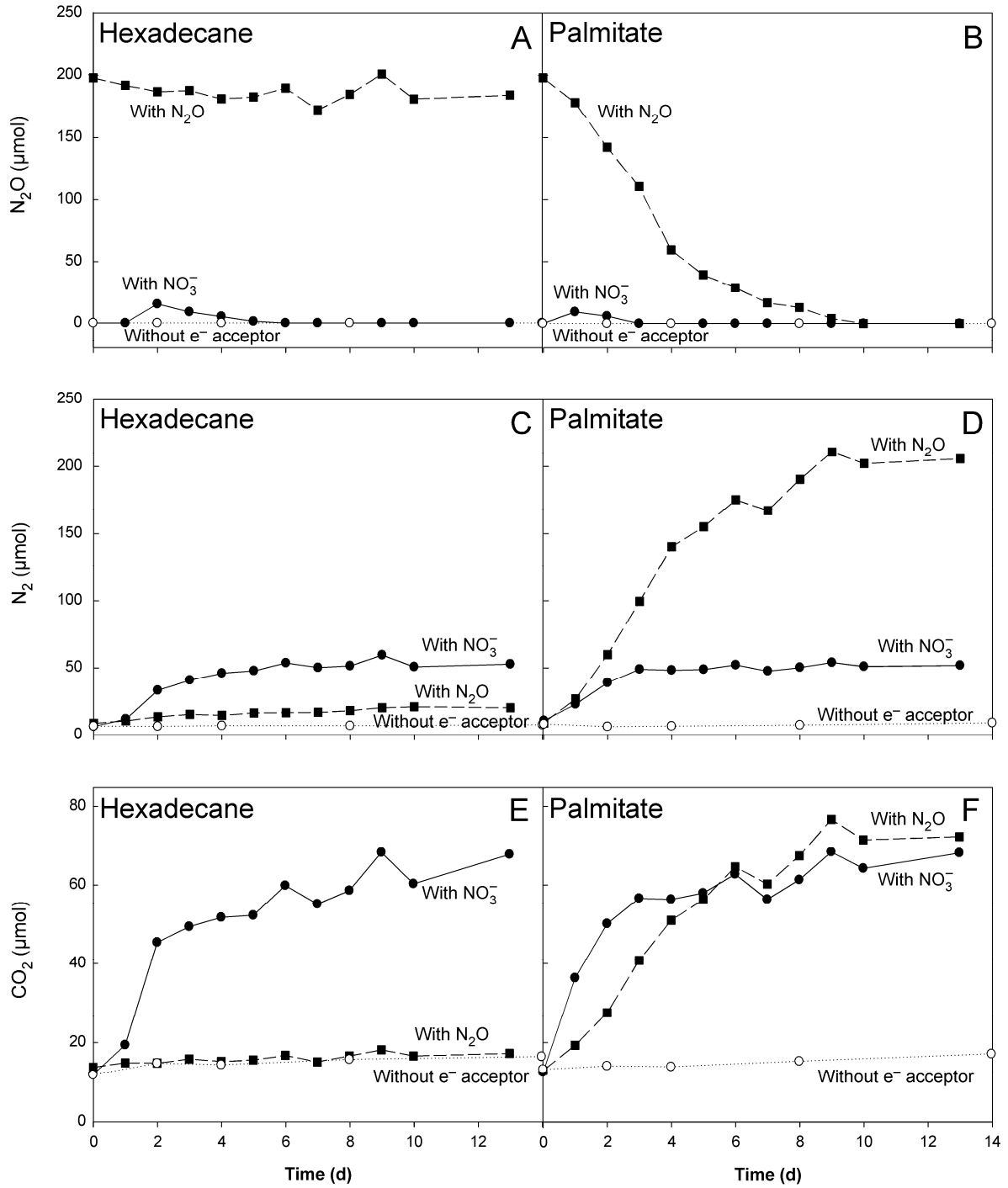

Fig. 3. Time courses of the formation of N_2O (A,B), N_2 (C,D) and CO_2 (E,F) in anaerobic cultures of strain HdN1 with n-hexadecane (A, C, E) or palmitate (B, D, F). The electron acceptors were added in stoichiometrically limiting amounts (100 µmol NO_3^-; ca. 250 µmol N_2O) relative to the electron donor (171 µmol hexadecane, advantage of large excess explained in text; 10 µmol palmitate). Results show that alkane oxidation to CO_2 was not possible with N_2O, but readily occurred with NO_3^-. The functionalized compound, palmitate, was oxidized with N_2O. Duplicates yielded the same results (not shown). Culture volumes of 10 ml (phosphate-buffered medium, pH ≈ 7.1, without addition of $NaHCO_3$; Appendix S1) were incubated in 165-ml serum bottles under an argon headspace. N_2O was injected as pure O_2-free gas. Cultures were very gently shaken for a few minutes per day. Vigorous shaking had to be avoided because it impeded growth. Samples from the headspace were analyzed with a gas chromatograph employing argon as carrier gas and a thermal conductivity detector. The calculated dissolved amounts of gases were added so as to obtain the total amounts in the bottles. Calculation was based on literature data (Stumm and Morgan, 1995; Wilhelm et al., 1977), assuming equilibrium (which may not have been fully reached due to limited agitation) and considering pH in the case of CO_2.

Surprisingly, strain HdN1 did not grow with alkanes in the growth tests with N_2O. In accordance with the lack of growth, N_2O was not consumed (Fig. 3A, upper curve), and N_2 (Fig. 3C) or CO_2 (Fig. 3E) were not formed. In contrast, growth with 1-tetradecanol, 1-hexadecanol or fatty acids was possible with added N_2O, and consumption of N_2O (Fig. 3B) as well as formation of N_2 (Fig. 3D) and CO_2 (Fig. 3F) was obvious.

A minor formation of N_2 from N_2O during incubation with hexadecane can be explained by reduction with an endogeneous electron source in the inoculum. The formation of N_2 from N_2O requires only 2 e^-, whereas formation of N_2 from NO_3^- requires 10 e^- from an electron donor. The lack of alkane utilization with N_2O was not due to specific inhibition. The same amount of N_2O added to a culture with hexadecane and NO_3^- did not inhibit growth. For physiological comparison, strains HxN1 and OcN1 were also incubated with N_2O as the only electron acceptor and utilizable alkanes (*n*-hexane and *n*-octane, respectively). These strains were able to grow with N_2O and alkanes. Results are summarized in Fig. 4. The inability for coupling alkane utilization to N_2O reduction is apparently unique for strain HdN1.

Other electron acceptors tested (concentrations in mM) but not utilized were sulfate (15), thiosulfate (5), sulfur (added as slurry), fumarate (10), and perchlorate (10). Toxic effects were excluded in controls containing in addition NO_3^-. In contrast, chlorate was toxic.

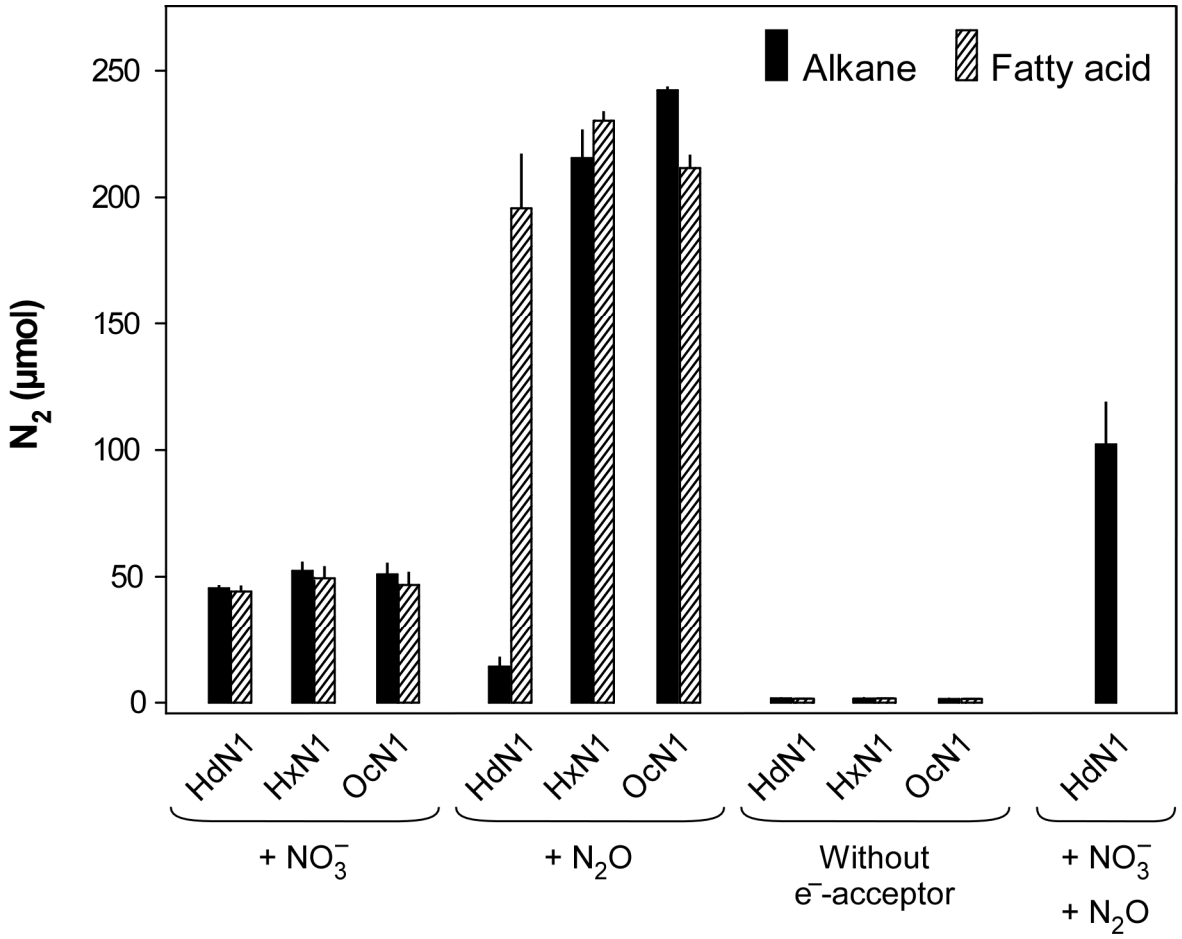

Fig. 4. N_2 formed in anaerobic cultures of strains HdN1, HxN1,and OcN1 with alkanes (black bars) or fatty acids (striated bars) and either NO_3^- (100 µmol) or N_2O (250 µmol). A control experiment with strain HdN1 for excluding N_2O-toxicity received both, NO_3^- and N_2O. Here, more N_2 was formed than with NO_3^- alone. This indicated that not only NO_3^- but also N_2O was used in the anaerobic respiratory chain if alkane degradation was enabled by NO_3^-. Data show that strain HdN1 could not use N_2O alone for alkane degradation, in contrast to the other strains. Culture volumes of 10 ml were incubated in 20-ml butyl-rubber sealed tubes. Strain HdN1 received 171 µmol pure n-hexadecane, or 10 µmol palmitate. Strain HxN1 received 38 µmol n-hexane (in 100 µl heptamethylnonane as carrier), or 30 µmol caproate. Strain OcN1 received 31 µmol n-octane (in 100 µl heptamethylnonane), or 30 µmol caproate. Tubes were incubated nearly horizontally while contact of the hydrocarbon phase with the stopper was avoided (Widdel, 2010) as far as possible. Gas samples were withdrawn 11 days after inoculation and analyzed (triplicates) as indicated in Fig. 3.

Search for metabolites and genes involved in alkane degradation

Investigation of metabolites and genes involved in alkane degradation via addition to fumarate have been reported for strain HxN1 (Rabus *et al*., 2001; Wilkes *et al*., 2002; Grundmann *et al*., 2008). The presently performed metabolite analysis of strain OcN1 upon growth with *n*-octane and NO_3^- revealed (1-methylheptyl)succinate (extraction, methylation and analysis as in Rabus *et al*., 2001; Wilkes *et al*., 2003), again indicating an activation via addition to fumarate. In contrast, alkyl-substituted succinates were never detectable in cultures and cells of strain HdN1. Another product searched for [by gas chromatography-mass spectrome-

try of extracts silylated with N,O-bis(trimethylsilyl)acetamide; Appendix S1] in anaerobic *n*-hexadecane cultures of strain HdN1 was 1-hexadecanol. If air was strictly excluded and if the culture was inactivated by heat (85 °C; Rabus *et al*., 2001) before extraction, 1-hexadecanol was not detectable. In contrast, 1-hexadecanol was detected if the anaerobically grown culture was exposed to air for 20–30 min (data not shown). Such 1-alkanol formation is a long-known indicator of monooxygenase activity (Britton, 1984). Metabolite analysis in anaerobic alkane degraders with facultative aerobic metabolism thus requires careful avoidance of artifacts due to reaction with O_2 from air.

The gene possibly encoding the alkane-activating enzyme in strain OcN1 was retrieved via polymerase chain reaction with degenerate primers for *mas* and *ass* genes, generation of a probe and screening of a genomic library, similar as described for strain HxN1 (Grundmann *et al*., 2008). The derived amino acid sequence (accession no. FN675935) revealed close relationships (Fig. S1) to the orthologue from strain HxN1 (Grundmann *et al*., 2008) and a sulfate-reducing bacterium (Callaghan *et al*., 2008). Attempts to amplify in an analogous manner *mas*- or *ass*-like genes from strain HdN1 failed. Therefore, a shotgun genomic library of strain HdN1 was established. This allowed assemblage of the complete genome sequence (4,587,455 bp; 3,762 coding sequences; accession no. FP929140; for some more details see Table S1). But neither this revealed *mas*- or *ass*-like genes (Table S2).

These findings suggested that the mechanism for alkane activation in strain HdN1, which has to involve the cleavage of a strong, apolar C–H-bond, differs basically from the mechanism with fumarate as co-substrate in the two other strains.

Linkage of alkane activation in strain HdN1 to the nitrate reduction pathway?

The distinctive results of the incubation experiments with either alkanes or functionalized (O-group-containing) substrates and N_2O may offer a clue as to how strain HdN1 could initiate alkane degradation under anoxic conditions. The electron acceptor tests with functionalized electron donors as well as identified genes (Table S3) indicate that strain HdN1 employs the common reduction sequence ($NO_3^- \rightarrow NO_2^- \rightarrow NO \rightarrow N_2O \rightarrow N_2$), viz. is in principle able to readily reduce N_2O. Also during growth with alkanes as organic substrates and NO_3^- or NO_2^- as electron acceptors, N_2O must have been a regular intermediate because N_2 rather than N_2O was the end product. However, N_2O added alone did not allow growth with alkanes. An early

reaction during alkane utilization must thus depend on an N-O-species other than N_2O. The early reaction could be the biochemically crucial activation of the alkane. The required N-O-species cannot be NO_3^-, because growth with alkanes was also possible if NO_2^- was added instead of NO_3^-. Hence, NO_2^- or NO (or a so far unknown product from NO_2^- reduction) may be essential for alkane activation. The basic hypothesis is depicted in Fig. 5.

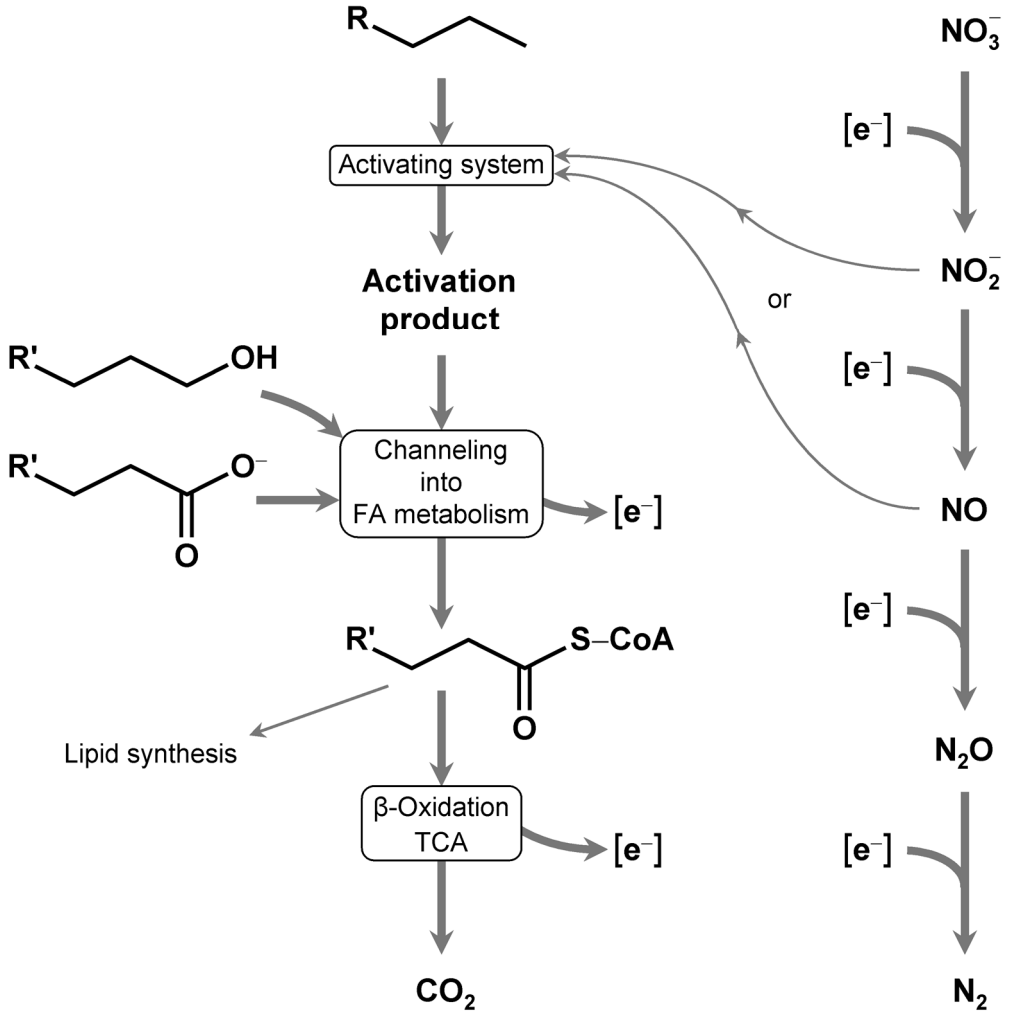

Fig. 5. Hypothetical involvement of denitrification intermediates in alkane activation. The scheme offers an explanation for the inability of strain HdN1 to utilize n-alkanes with N_2O alone (see Figs. 3 and 4). It is assumed that a small proportion of NO_2^- or NO is deviated from the respiratory chain for alkane activation. They may be used for activation indirectly (by yielding O_2 that is used by alkane monooxygenase; or by giving rise to another reactive factor or enzyme center) or directly (as co-reactants introducing a polar group). The alkyl residue R' may or may not be identical with the original residue R (depending on the activation mechanism and alkane C-atom being attacked). FA, fatty acid; TCA, tricarboxylic acid cycle.

In further experiments, added NO (prepared from acidified $NaNO_2$ and KI; Schreiber *et al*., 2008) turned out to be very toxic so that application of concentrations sufficient to achieve measurable growth was not possible; NO at a partial pressure of ca. 75 Pa [0.075% (v/v) in gas mixture of ambient pressure] in the headspace completely inhibited growth with NO_3^-. At

a partial pressure of 50 Pa (0.05%) NO did not completely inhibit growth with NO_3^-, albeit growth was retarded. To test whether such still tolerated NO concentration is sufficient to initiate alkane degradation and in this way allow growth, 500 ppmv NO was provided together with N_2O (17 mmol l^{-1}), the latter serving as main electron acceptor for anaerobic respiration. However, growth was not observed unless NO_3^- was added. It thus remains elusive whether NO_2^- or NO (or an unknown NO_2^--derived species) is actually required to initiate alkane degradation.

From a thermodynamic point of view, an involvement of N-O-species in alkane activation under anoxic conditions is an appealing hypothesis. N-O-species other than NO_3^- (Fig. 6A) are all metastable (Garrels and Christ, 1965; Thauer *et al*., 1977) and represent or can provide strong potential oxidants; this property could be enzymatically exploited to achieve alkane activation. An indirect use to form another reactive compound as well as a direct use of an N-O-species can be envisaged.

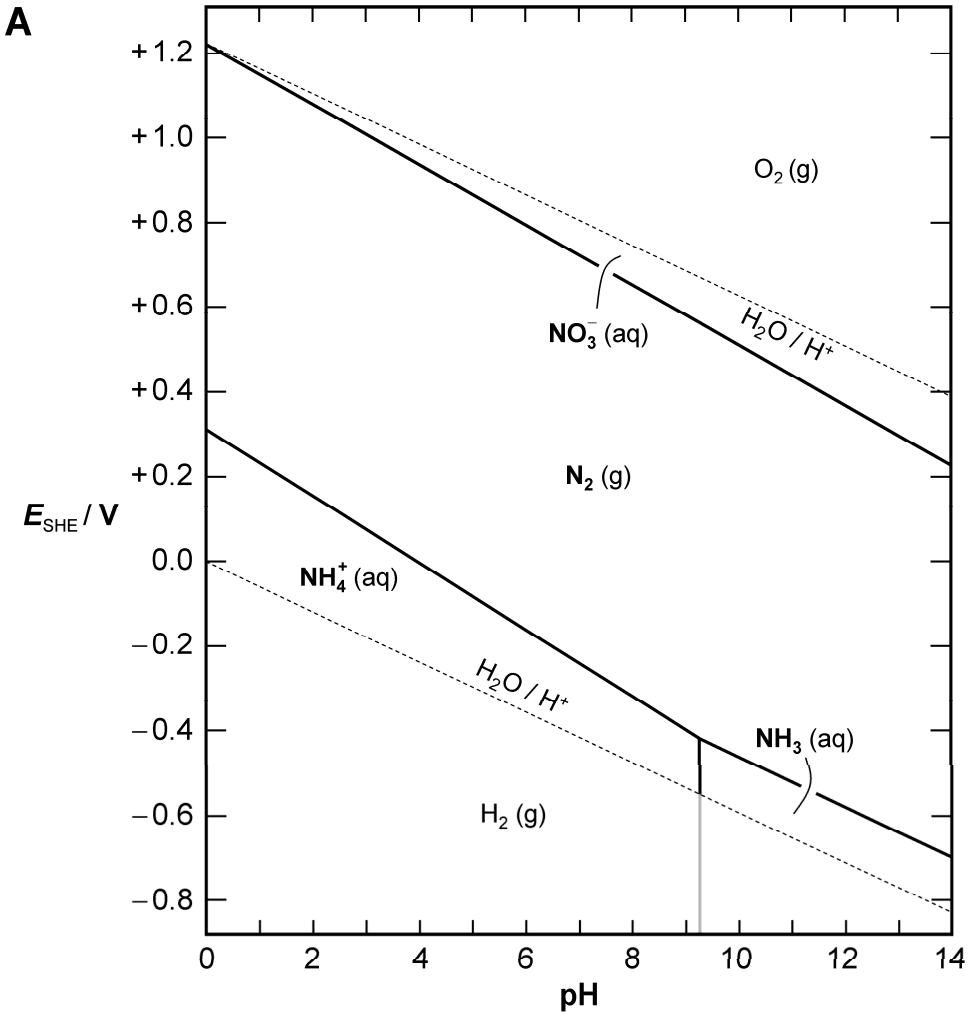
A
+1.2
+1.0
+0.8
+0.6
+0.4
+0.2
0.0
−0.2
−0.4
−0.6
−0.8
E_{SHE} / V
O_2 (g)
NO_3^- (aq)
H_2O / H^+
N_2 (g)
NH_4^+ (aq)
H_2O / H^+
NH_3 (aq)
H_2 (g)
0
2
4
6
8
10
12
14
pH

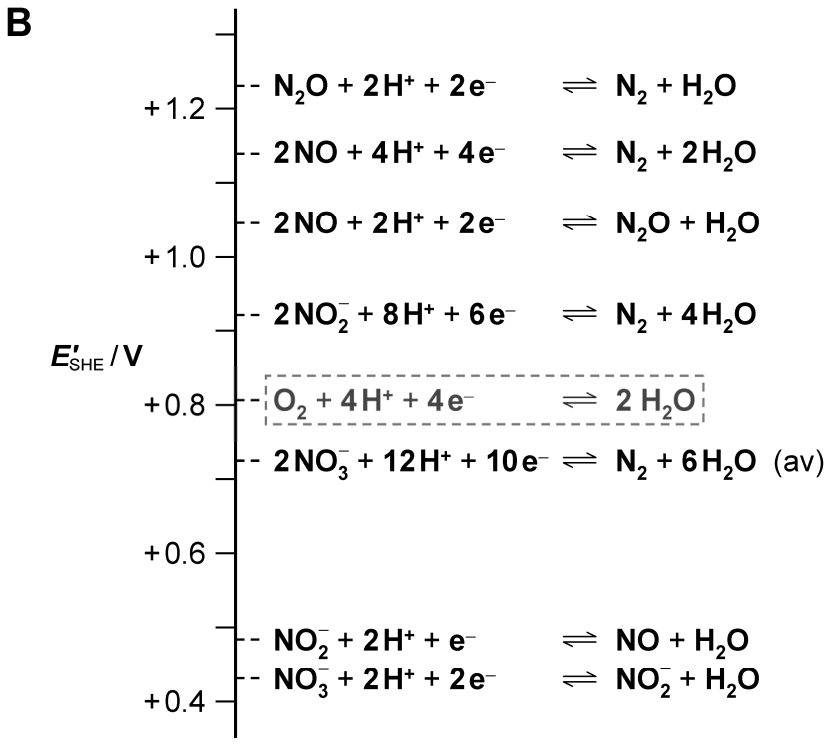
B
E'_{SHE} / V
+1.2
+1.0
+0.8
+0.6
+0.4
$N_2O + 2H^+ + 2e^- \rightleftharpoons N_2 + H_2O$
$2NO + 4H^+ + 4e^- \rightleftharpoons N_2 + 2H_2O$
$2NO + 2H^+ + 2e^- \rightleftharpoons N_2O + H_2O$
$2NO_2^- + 8H^+ + 6e^- \rightleftharpoons N_2 + 4H_2O$
$O_2 + 4H^+ + 4e^- \rightleftharpoons 2H_2O$
$2NO_3^- + 12H^+ + 10e^- \rightleftharpoons N_2 + 6H_2O$ (av)
$NO_2^- + 2H^+ + e^- \rightleftharpoons NO + H_2O$
$NO_3^- + 2H^+ + 2e^- \rightleftharpoons NO_2^- + H_2O$

Fig. 6. Some energetic aspects of N-O-species. Graphs are for the following activities or fugacities: $\{NO_3^-\}$, $\{NO_2^-\}$, $\{NH_3\,(g)\}$, $\{NH_4^+\} = 10^{-2}$; $\{N_2\,(g)\} = 10^{-0.1}$ (78% in air); $\{O_2\,(g)\} = 10^{-0.7}$ (21% in air); $\{H_2\} = 1$; $\{NO\,(g)\}$, $\{N_2O\,(g)\} = 10^{-4.3}$ (approximately corresponding to dissolved concentrations monitored under natural conditions; Schreiber et al., 2009).
A. E-pH (stability, Pourbaix) diagram of the system H-N-O. Only the lowest and highest oxidation states, NH_4^+, NH_3 and NO_3^- are thermodynamically stable. Other metabolically formed inorganic N-compounds are metastable (endergonic; e.g., eq. 1, 2) and can, in principle, spontaneously decompose (dismutate) into the species (including O_2) depicted in the diagram. Endergonic N-compounds can be metabolically formed because they appear as co-products besides H_2O (from reductive O-elimination).
B. Electrochemical half-reactions (including hypothetical ones) of N-O-species and O_2. If an endergonic N-compound does not react via dismutation (e.g., eqn. 2, 3) but in an electrochemical half-reaction (yielding the same product as dismutation), this half-reaction has a higher redox potential than that of $O_2/2H_2O$ ($E^{\circ\prime} = +0.815$ V). Again, this does not contradict the fact that NO_3^- and NO_2^- originate from a microbial oxidation process with O_2 (see under A; also, the reaction sequence in nitrification is different: $NH_4^+/NH_3 \rightarrow NH_2OH \rightarrow NO_2^-$). Generally, the redox potentials (E_i) of subsequent reduction steps (i = 1, 2, … m) of an overall reduction with free intermediates are linked to an average redox potential (E_{av}) according to $(n_1E_1 + n_2E_2 + \ldots + n_mE_m)/n_{tot} = E_{av}$; n_i is the number of electrons involved in an individual step and n_{tot} the total number of electrons. E_{av} is connected to the total free energy change, ΔG_{tot}, of the overall reduction with an electron-donating reaction of the redox potential E_{don} according to $E_{av} = -\Delta G_{tot}/(n_{tot}\,F) + E_{don}$, with F = 96,485 C mol^{-1} (explanation in Appendix S2). E_{av} of $2NO_3^-/N_2$ marks the borderline between the stability regions of NO_3^- and N_2 in the E-pH diagram (panel A). In a real metabolic process, a strong oxidant formed in a reduction sequence can only appear as free intermediate if its further reduction is enzymatically controlled and if unspecific reactions with reductants are slower or do not take place. Also, overall irreversibility is required, but this is naturally given (in an equilibrium system, redox pairs with different redox potential, e.g. NO_3^-/NO_2^- and NO_2^-/NO, cannot co-exist).
Calculations are based on standard free energy data (Garrels and Christ, 1965; Thauer et al., 1977). Derived standard redox potentials at pH = 7 ($E^{\circ\prime}$/V): NO_3^-/NO_2^-, +0.431; $2NO_3^-/N_2$, +0.747 (av); NO_2^-/NO, +0.347; $2NO_2^-/N_2$, +0.958; $2NO/N_2O$, +1.172; $2NO/N_2$, +1.264; N_2O/N_2; +1.355.

One mode of indirect use of NO_2^- and NO could be their dismutation (formally an "internal" reduction of N and oxidation of O) leading to O_2, according to the following equations:

$$4\ NO_2^- + 4\ H^+ \rightarrow 2\ N_2 + 3\ O_2 + 2\ H_2O;\ \Delta G^{\circ\prime} = -55.19\ \text{kJ (mol } O_2)^{-1} \quad (1)$$

$$2\ NO \rightarrow N_2 + O_2;\ \Delta G^{\circ} = -173.14\ \text{kJ (mol } O_2)^{-1} \quad (2)$$

O_2 could then be used for an alkane monooxygenase reaction (alkane hydroxylation). Also N_2O can in principle lead to O_2 [$2\ N_2O \rightarrow 2\ N_2 + O_2$; $\Delta G^{\circ} = -208.4$ kJ (mol $O_2)^{-1}$], but the present results exclude its use for an initiation of alkane degradation. There is indeed evidence for O_2 formation at very low concentration during NO_2^- reduction in a methane-utilizing enrichment culture dominated by '*Candidatus* Methylomirabilis oxyfera'. The enrichment grew under exclusion of air and depended on NO_2^- addition (Ettwig *et al.*, 2010). $^{18}O_2$ formation from $N^{18}O_2^-$ (indirectly labeled through $H_2{}^{18}O$) became detectable upon specific inhibition of methane monooxygenase. NO dismutation (eq. 2) was suggested as the underlying mechanism. Neither were NO_3^- or N_2O reduced, nor did the genome of the dominant bacterium harbor typical N_2O-reductase genes. Results therefore suggested that NO dismutation was a main reaction during NO_2^- reduction in '*Candidatus* M. oxyfera'. An earlier example of a metastable inorganic oxo-compound enabling biodegradative reactions through O_2 formation is chlorite, an intermediate of microbial chlorate reduction ($ClO_2^- \rightarrow Cl^- + O_2$; $\Delta G^{\circ\prime} = -148.4$ kJ mol^{-1}; Ginkel *et al*., 1996; Chackraborty and Coates, 2004; Tan *et al*., 2006; Weelink *et al*., 2008; Mehboob *et al*., 2009a, b). The presently investigated alkane-degrading strain HdN1 differs metabolically from 'M. oxyfera' in several respects. Strain HdN1 does not utilize methane, grows with NO_3^- and obviously involves the conventional reduction sequence via N_2O to N_2. If strain HdN1 would employ NO_2^-- or NO-derived O_2, the demand per hydrocarbon molecule utilized would be much lower than in ' *Candidatus* M. oxyfera'. Long-chain alkane activation would require only a minor withdrawal of NO_2^- or NO from the respiratory path that mainly leads to N_2 through N_2O. For instance, *n*-hexadecanol resulting from oxygenation of *n*-hexadecane ($C_{15}H_{31}CH_3 + O_2 + 2\ [H] \rightarrow C_{15}H_{31}CH_2OH + H_2O$) yields as many as 96 [H] ($C_{15}H_{31}CH_2OH + 31\ H_2O \rightarrow 16\ CO_2 + 96\ [H]$) per substrate molecule. With 2 [H] consumed for activation, each oxygenation event thus leaves 94 [H] per $C_{16}H_{34}$ for respiratory energy conservation. In contrast, each oxygenation event in methane utilization provides only 4 [H] per CH_4 for respiration. According to genomic data, strain HdN1 may form a di-iron monooxygenase, a P450-type monooxygenase and possibly a third type of monooxgenase

(Table S3). Multiple monooxygenases are not uncommon in aerobic alkane degraders (Rojo, 2010).

O_2 formation could not be detected so far in strain HdN1. We mixed a culture of strain HdN1 with a culture of luminous bacteria (isolated from herring using glycerol-peptone medium; Farmer and Hickman-Brenner, 2006) as sensitive O_2 indicators (Chance *et al*., 1978); both cultures had been adapted to brackish water (180 mM NaCl and 20 mM $MgSO_4$) medium. After extinction of luminescence due to oxygen consumption, neither addition of nitrate nor of nitrite or NO-saturated water caused the luminous reaction to resume (whereas air did immediately). Neither was oxygen detectable by means of an O_2-microelectrode (lower detection limit, 1 µM; Revsbech, 1989) in cultures supplied with NO_2^- or NO. Nevertheless, results do not rule out O_2 as an intermediate. A very low production rate and effective scavenging by alkane monooxygenase and competing respiratory enzymes (if present under anoxic conditions) such as high-affinity *cbb*$_3$-type oxidases (Pitcher and Watmough, 2004; predicted for strain HdN1; Table S5;) could maintain the O_2 concentration below detection level. Also, the produced alcohol may be consumed effectively by the subsequent reaction. Only upon sudden exposure to air, the anaerobically grown cells accumulated *n*-hexadecanol (see above).

The slight differences between the growth tests under oxic and anoxic conditions with alkanes of various chain lengths (see growth tests with different electron acceptors) do not necessarily contradict the hypothesis that monooxygenases are used under oxic as well as under anoxic cultivation conditions for alkane activation. There might be slight differences with respect to chain length specificity between the monooxygenase(s) formed in aerobic and denitrifying cultures.

Still, also other modes of an indirect use of N-O-species for alkane activation can be envisaged. For instance, they may serve as high-potential (strongly oxidizing) electron acceptors (half reactions in Fig. 6B) to generate by electron withdrawal an oxidized, active (reactive) state of a factor or an enzyme site involved in alkane activation.

Another hypothesis would be the direct involvement of an N-O-species in the activation reaction of the alkane. This would probably require a delicate mechanism. A direct biochemical linkage of the disintegration of an N-O-species to C–H-bond cleavage and formation of a functionalized product from an alkane would probably require an intricate mechanism.

Concluding remarks

In conclusion, results suggest a mechanistic alternative to the fumarate-dependent reaction for anaerobic alkane activation. Also a sulfate-reducing bacterium, strain Hxd3, metabolized long-chain *n*-alkanes obviously via an initial reaction different from that in other anaerobic alkane degraders (Aeckersberg *et al*., 1998; So *et al*. 2003; Callaghan *et al*., 2006). This raises the question whether nitrate-reducing strain HdN1 and sulfate-reducing strain Hxd3 employ basically the same reaction or different reactions to initiate alkane degradation. If they would employ essentially the same fumarate-independent activation reaction, strain HdN1 cannot involve an N-O-species or derived O_2 directly because they are excluded in strain Hxd3; the sulfate reducer was grown without nitrate. Also other ways to generate O_2 are essentially excluded in sulfate reducers; sulfate and its metabolites are all thermodynamically very stable and represent very weak oxidants. Hence, alkane activation by the same basic mechanism in strains HdN1 and Hxd3 would imply that the denitrifier uses an N-O-species or O_2 only indirectly to generate an alkane-activating factor, whereas the sulfate reducer would generate the same type of factor in a different manner. If strains HdN1 and Hxd3 use different mechanisms for alkane activation, which is more appealing to assume, the reaction in strain HdN1 would represent a third type of alkane activation under anoxic conditions, besides the fumarate-dependent mechanism and the speculative mechanism in strain Hxd3. More refined physiological experiments (preceded by an improved method for harvesting the buoyant cells associated with alkane) are needed to provide further hints as to the alkane activation mechanism in strain HdN1, with consideration of its apparently diverse monooxygenases.

Finally, the present results as well as the oxidation of methane with NO_2^- (Ettwig *et al*., 2010) indicate that NO_3^- or NO_2^- (either from NO_3^- reduction or directly from NH_4^+ oxidation) should not be merely considered as electron acceptors for anaerobic respiration. An intermediate formed during NO_3^- or NO_2^- reduction may function as or provide a co-reactant for the biochemical activation of various hydrocarbons or even of other chemically unreactive compounds. NO_3^- or NO_2^- in anoxic habitats could, in principle, promote or enable the degradation of certain organic fractions which tend to be refractory under conditions of sulfate reduction or methanogenesis.

Acknowledgements

We are indebted to Daniela Lange for experimental support, to Andreas Schummer for help with substrate tests, and to Alexander Steinbüchel for analysis of polyhydroxyalkanoic acids. This work was supported by the Max-Planck-Gesellschaft.

References

Aeckersberg, F., Bak, F., and Widdel, F. (1991) Anaerobic oxidation of saturated hydrocarbons to CO_2 by a new type of sulfate-reducing bacterium. *Arch Microbiol* **156:** 5–14.

Aeckersberg, F., Rainey, F.A., and Widdel, F. (1998) Growth, natural relationships, cell fatty acids and metabolic adaptation of sulfate-reducing bacteria that utilize long-chain alkanes under anoxic conditions. *Arch Microbiol* **170:** 361–369.

Anderson, R.T., and Lovley, D.R. (2000) Hexadecane decay by methanogenesis. *Nature* **404:** 722–723.

Birch, L.D., and Bachofen, R. (1988) Microbial production of hydrocarbons. In *Biotechnology*. Vol 6b. *Special Microbial Processes.* Rehm, H.J., and Reed G. (eds). Weinheim, Germany: VCH Verlagsgesellschaft, pp. 71–99.

Bonin, P.C., Cravo-Laureau, C., Michotey, V., Hirschler-Réa, A. (2004). The anaerobic hydrocarbon biodegrading bacteria: an overview. *Ophelia* **58**: 243–254.

Britton, L.N. (1984) Microbial degradation of aliphatic hydrocarbons. *In* Microbial degradation of organic compounds. Gibson, T.D. (ed.). New York, Marcel Dekker, pp 89–129.

Callaghan, A.V., Gieg, L.M., Kropp, K.G., Suflita, J.M., and Young, L.Y. (2006) Comparison of mechanisms of alkane metabolism under sulfate-reducing conditions among two bacterial isolates and a bacterial consortium. *Appl Environ Microbiol* **72:** 4274–4282.

Callaghan, A.V., Wawrik, B., Ní Chadhain, S.M., Young, L.Y., and Zylstra, G.J. (2008) Anaerobic alkane-degrading strain AK-01 contains two alkylsuccinate synthase genes. *Biochem Biophys Res Commun* **366:** 142–148.

Callaghan, A.V., Tierney, M., Phelps, C.D., and Young, L.Y. (2009) Anaerobic biodegradation of *n*-hexadecane by a nitrate-reducing consortium. *Appl Environ Microbiol* **75**: 1339–1344.

Chakraborty, R., and Coates, J.D. (2004) Anaerobic degradation of monoaromatic hydrocarbons. *Appl Microbiol Biotechnol* **64**: 437–446.

Chance, B., Oshino, R., and Oshino, N. (1978) Sensitive oxygen assay method by luminous bacteria. *Methods Enzymol* **54:** 499–505.

Cravo-Laureau, C., Matheron, R., Cayol, J.-L., Joulian, C., and Hirschler-Réa, A. (2004) *Desulfatibacillum aliphaticivorans* gen. nov., sp. nov., an n-alkane- and *n*-alkene-degrading, sulfate-reducing bacterium. *Int J Syst Evol Microbiol* **54:** 77–83.

Davidova, I.A., Duncan, K.E., Choi, O.K., and Suflita, J.M. (2006) *Desulfoglaeba alkanexedens* gen. nov., sp. nov., an *n*-alkane-degrading, sulfate-reducing bacterium. *Int J Syst Evol Microbiol* **56:** 2737–2742.

Ehrenreich, P., Behrends, A., Harder, J., and Widdel, F. (2000) Anaerobic oxidation of alkanes by newly isolated denitrifying bacteria. *Arch Microbiol* **173:** 58–64. (Erratum: *Arch Microbiol* **173:** 232).

Ettwig, K.F., Butler, M.K., Le Paslier, D., Pelletier, E., Mangenot, S., Kuypers, M.M.M., *et al*. (2010) Nitrite-driven anaerobic methane oxidation by oxygenic bacteria. *Nature* **464:** 543–548.

Farmer III, J.J., and Hickman-Brenner, F.W. (2006) The genera *Vibrio* and *Photobacterium*. In *The prokaryotes*, vol. 6. Dworkin, M., Falkow, S., Rosenberg, E., Schleifer, K.-H., and Stackebrandt, E. (ed.). New York, USA: Springer, pp. 508–563.

Garrels, R.M., and Christ, C.L. (1965) *Solutions, Minerals, and Equilibria*. New York, USA: Harper & Row.

Ginkel, C.G., Rikken, G.B., Kroon, A.G.M., and Kengen, S.W.M. (1996) Purification and characterization of chlorite dismutase: a novel oxygen-generating enzyme. *Arch Microbiol* **166:** 321–326.

Grossi, V., Cravo-Laureau, C., Guyoneaud, R., Ranchou-Peyruse, A., and Hirschler-Rea, A. (2008) Metabolism of *n*-alkanes and *n*-alkenes by anaerobic bacteria: A summary. *Org Geochem* **39**: 1197–1203.

Grundmann, O., Behrends, A., Rabus, R., Amann, J., Halder, T., Heider, J., and Widdel, F. (2008) Genes encoding the candidate enzyme for anaerobic oxidation of *n*-alkanes in the denitrifying bacterium, strain HxN1. *Environ Microbiol* **10:** 376–385.

Heider, J. (2007) Adding handles to unhandy substrates: anaerobic hydrocarbon activation mechanisms. *Curr Op Chem Biol* **11:** 188–194.

Higashioka, Y., Kojima, H., Nakagawa, T., Sato, S., and Fukui, M. (2009) A novel *n*-alkane-degrading bacterium as a minor member of *p*-xylene-degrading sulfate-reducing consortium. *Biodegradation* **20:** 383–390.

Jones, D.M., Head, I.M., Gray, N.D., Adams, J.J., Rowan, A.K., Aitken, C.M., Bennett, B., Huang, H., Brown, A., Bowler, B.F., Oldenburg, T., Erdmann, M., and Larter, S.R. (2008) Crude-oil biodegradation via methanogenesis in subsurface petroleum reservoirs. *Nature* **451:** 176–180

Kniemeyer, O., Musat, F., Sievert, S.M., Knittel, K., Wilkes, H., Blumenberg, M. *et al*. (2007) Anaerobic oxidation of short-chain hydrocarbons by marine sulphate-reducing bacteria. *Nature* **449**: 898–901.

Kropp, K.G., Davidova, I.A., and Suflita, J.M. (2000) Anaerobic oxidation of *n*-dodecane by an addition reaction in a sulfate-reducing bacterial enrichment culture. *Appl Environ Microbiol* **66:** 5393–5398.

Mehboob, F., Junca, H., Schraa, G., and Stams, A.J.M. (2009a) Growth of *Pseudomonas chloritidismutans* AW-1^T on *n*-alkanes with chlorate as electron acceptor. *Appl Microbiol Biotechnol* **83:** 739–747.

Mehboob, F., Wolterink, A.F., Vermeulen, A.J., Jiang, B., Hagedoorn, P.L., Stams, A.J., and Kengen, S.W. (2009b) Purification and characterization of a chlorite dismutase from *Pseudomonas chloriti-dismutans*. *FEMS Microbiol Lett* **293:** 115–121.

Pitcher, R.S., and Watmough, N.J. (2004) The bacterial cytochrome cbb_3 oxidases. *Biochim Biophys Acta* **1655:** 388–399.

Rabus, R., Nordhaus, R., Ludwig, W., and Widdel, F. (1993) Complete oxidation of toluene under strictly anoxic conditions by a new sulfate-reducing bacterium. *Appl Environ Microbiol* **59**: 1444–1451.

Rabus, R., and Widdel, F. (1995) Anaerobic degradation of ethylbenzene and other aromatic-hydrocarbons by new denitrifying bacteria. *Arch Microbiol* **163**: 96–103.

Rabus, R., Wilkes, H., Behrends, A., Armstroff, A., Fischer, T., Pierik, A.J., and Widdel, F. (2001) Anaerobic initial reaction of *n*-alkanes: evidence for (1-methylpentyl)succinate as initial product and for involvement of an organic radical in the metabolism of *n*-hexane in a denitrifying bacterium. *J Bacteriol* **183:** 1707–1715.

Revsbech, N. P. (1989) An oxygen microsensor with a guard cathode. *Limnol Oceanogr* **34:** 474–478.

Rueter, P., Rabus, R., Wilkes, H., Aeckersberg, F., Rainey, F.A., Jannasch, H.W., and Widdel, F. (1994) Anaerobic oxidation of hydrocarbons in crude-oil by new types of sulfate-reducing bacteria. *Nature* **372**: 455–458.

Rojo, F. (2010) Enzymes for aerobic degradation of alkanes. In *Handbook of Hydrocarbon and Lipid Microbiology*, vol. 2. Timmis, K.N. (ed.). Heidelberg, Germany: Springer, pp. 781–797.

Schreiber, F., Polerecky, L., de Beer, D. (2008) Nitric oxide microsensor for high spatial resolution measurements in biofilms and sediments. *Anal Chem* **80:** 1152–1158.

Schreiber, F., Loeffler, B., Polerecky, L., Kuypers, M.M., de Beer, D. (2009) Mechanisms of transient nitric oxide and nitrous oxide production in a complex biofilm. *ISME J* **3:**1301–1313.

Scott, C.C.L., and Finnerty, W.R. (1976) Comparative analysis of ultrastructure of hydrocarbon-oxidizing microorganisms. *J Gen Microbiol* **94**: 342–350.

So, C.M., and Young, L.Y. (1999) Isolation and characterization of a sulfate-reducing bacterium that anaerobically degrades alkanes. *Appl Environ Microbiol* **65:** 2969–2976.

So, C.M., Phelps, C.D., and Young, L.Y. (2003) Anaerobic transformation of alkanes to fatty acids by a sulfate-reducing bacterium, strain Hxd3. *Appl Environ Microbiol* **69:** 3892–3900.

Steinbüchel, A., and Wiese, S. (1992) A *Pseudomonas* strain accumulating polyesters of 3-hydroxybutyric acid and medium-chain-length 3-hydroxyalkanoic acids. *Appl Microbiol Biotechnol* **37:** 691–697.

Stumm, W., and Morgan, J.J. (1995) Aquatic chemistry. New York: John Wiley & Sons.

Tan, N.C., van Doesburg, W., Langenhoff, A.A., and Stams, A.J. (2006) Benzene degradation coupled with chlorate reduction in a soil column study. *Biodegradation* **17**: 113–119.

Thauer, R.K., Jungermann, K., and Decker, K. (1977) Energy conservation in chemotrophic anaerobic bacteria. *Bacteriol Rev* **41:** 100–180.

Tissot B.P., and Welte D.H. *Petroleum Formation and Occurrence*. Berlin, Germany: Springer, 1984.

Weelink, S.A., Tan, N.C., ten Broeke, H., van den Kieboom, C., van Doesburg, W., Langenhoff, A.A., *et al*. (2008) Isolation and characterization of *Alicycliphilus denitrificans* strain BC, which grows on benzene with chlorate as the electron acceptor. *Appl Environ Microbiol* **74:** 6672–6681.

Widdel, F. (2010) Cultivation of anaerobic microorganisms with hydrocarbons as growth substrates. In *Handbook of hydrocarbon and lipid microbiology*, vol. 2. Timmis, K.N. (ed.). Heidelberg, Germany: Springer, pp 3787–3798.

Widdel, F., and Bak, F. (1992) Gram-negative mesophilic sulfate-reducing bacteria. In *The prokaryotes*. Balows, A., Trüper, H.G., Dworkin, M., Harder, W., and Schleifer, K.-H. (eds). New York: Springer, pp. 3352–3378.

Widdel, F., Knittel, K., and Galushko, A. (2010) Anaerobic hydrocarbon-degrading microorganisms – an overview. In *Handbook of hydrocarbon and lipid microbiology*, vol. 2. Timmis, K.N. (ed.). Heidelberg, Germany: Springer, pp 1997–2021.

Wilhelm, E., Battino, R., and Wilcock, R.J. (1977) Low-pressure solubility of gases in water. *Chem Rev* 219–262.

Wilkes, H., Rabus, R., Fischer, T., Armstroff, A., Behrends, A., and Widdel, F. (2002) Anaerobic degradation of *n*-hexane in a denitrifying bacterium: further degradation of the initial intermediate (1-methylpentyl)succinate via C-skeleton rearrangement. *Arch Microbiol* **177:** 235–243.

Wilkes, H., Kühner, S., Bolm, C., Fischer, T., Classen, A., Widdel, F., and Rabus, R. (2003) Formation of *n*-alkane- and cycloalkane-derived organic acids during anaerobic growth of a denitrifying bacterium with crude oil. *Org. Geochem*. **34:** 1313–1323.

Yamasaki, H. (2000). Nitrite-dependent nitric oxide production pathway: Implications for involvement of active nitrogen species in photoinhibition in vivo. *Phil Trans R Soc Lond B Biol Sci* **355:** 1477–1488.

Zengler, K., Richnow, H.H., Roselló-Mora, R., Michaelis, W, and Widdel, F. (1999) Methane formation from long-chain alkanes by anaerobic microorganisms. *Nature* **401:** 266–269.

Appendix S1

Materials and methods

Origin of strains and regular cultivation

The denitrifying strain HdN1 was originally enriched with refined (aliphatic) mineral oil from freshwater mud and isolated with hexadecane (Ehrenreich *et al*., 2000). Strains HxN1 and OcN1 were enriched and isolated in the same study with hexane and octane, respectively. Cultures were maintained in the laboratory by transfer every 3 to 5 months, growth for approximately one week, and storage at 4 °C in the dark.

Anaerobic cultures were routinely grown in butyl rubber-sealed tubes (20 ml) or bottles (110 ml) with 10 ml and 80 ml anoxic medium, respectively (details in Widdel and Bak, 1992; Rabus and Widdel, 1995; Ehrenreich *et al*., 2000). Briefly, the medium for routine cultivation was prepared with 30 mM $NaHCO_3$ and a low phosphate concentration (3.7 mM). The reductant was ascorbate (4 mM) added from a filter-sterilized stock solution (prepared anaerobically from ascorbic acid and NaOH). Ascorbate did not serve as a substrate for growth. Usually, 10 mM $NaNO_3$ was added. The medium was overlaid with pure sterile (autoclaved under N_2) hexadecane (1.5 to 5 µl per ml medium, corresponding to 5.1 – 17.1 mmol l^{-1}).

Purity control

Cultures of strains grown with alkanes and other organic substrates were regularly checked by phase contrast microscopy. To verify absence of contaminants, cultures were also transferred to diagnostic liquid medium containing peptone (5 g l^{-1}) or yeast extract (5 g l^{-1}) and incubated anaerobically with NO_3^- or aerobically under air. In addition, cultures were streaked on agar plates prepared with fumarate (5 mM) or valerate (4 mM) and yeast extract (2.5 g l^{-1}) and incubated under air with 3% CO_2. Single, separate colonies were examined microscopically and tested for anaerobic growth with tetradecane.

Growth and growth tests with various electron donors and electron acceptors

The alkanes dodecane, tridecane and tetradecane were added like hexadecane (see above) as pure sterile liquids. Alkanes with shorter carbon chains, octanol and decanol were dissolved (pentane through octane, 5%; octanol, decanol, 1%; otherwise 20%) in 2,2,4,4,6,8,8-

heptamethylnonane as an inert and non-toxic carrier phase. The added volume of the alkane solutions was usually 50 µl per ml culture volume. Solid alkanes and solid long-chain alcohols were first added to empty culture tubes. Upon mild heating, the molten compounds were allowed to solidify while the tube was rotated so as to cover the glass wall with a thin layer. Then the tubes were flushed with oxygen-free gas while medium was added. Concentrations of monocarboxylic acid salts (in mM): formate, acetate, 10; propionate, butyrate, 5; valerate, 4; caproate, 3, heptanoate, 2; octanoate, 2; nonanoate, decanoate, dodecanoate, 1; tetradecanoate, 2, palmitate, 1.5; stearate, 1.5; long-chain fatty acid salts were added as molten solutions (Widdel and Bak, 1992). Ethanol was added at 10 mM.

Aerobic cultures were grown in sealed serum bottles with medium under air; the aqueous phase was one fifth or less of the bottle volume. The oxic medium without ascorbate contained only 2 mM $NaHCO_3$, while the headspace contained 1% CO_2.

Production of N_2, N_2O or CO_2, or consumption of N_2O was measured in cultures with more phosphate (KH_2PO_4, 8 mM, K_2HPO_4, 30 mM; pH ≈ 7.1) and without $NaHCO_3$ under a head space of pure argon.

Commercial N_2O (99.5%) for growth tests was incubated before application for at least two days at an overpressure of 100 kPa in a butyl-rubber sealed 165-ml serum bottle containing 5 ml of alkaline (pH 11) ascorbate (1 M) for scavenging traces of O_2. A volume of 0.61 ml was injected per ml of liquid culture volume (ca. 25 mmol l^{-1}).

NO was prepared from acidified $NaNO_2$ and KI as described previously (Schreiber *et al*., 2008) and stored in butyl rubber-sealed 5-ml glass tubes. Small volumes were withdrawn by means of a microliter syringe and injected into culture vials with large anoxic headspace (165 ml) and small aqueous volumes (10 ml) so as to achieve partial pressures of 50 – 100 Pa (0.05 – 0.1% in an atmosphere of ambient pressure).

Sequence analysis of 16S rRNA genes

Extraction of genomic DNA from strains HdN1, HxN1 and OcN1, amplification of 16S rRNA genes by PCR, and purification of PCR products were carried out using established procedures (Rainey *et al.,* 1996). Purified PCR products were sequenced using the Taq DyeDeoxy Terminator Cycle Sequencing Kit (Applied Biosystems, Foster City, Calif., USA) and the 373S instrument (Applied Biosystems).

Sequences were aligned with those of the SILVA SSU database (www.arb-silva.de, August 2009; Pruesse *et al*., 2007). The phylogenetic tree was constructed by means of the RAxML (maximum likelihood) program (7.0.3, release March 2008; Stamatakis *et al.*, 2005) of the ARB package (Ludwig *et al*., 2004) by applying position-variability and termini filters. Bootstrap values were obtained after 1000 resamplings. Only high quality sequences (>1200 bp) were used for tree construction. The 16S rRNA sequences of strains HdN1, HxN1 and OcN1 are available from the EMBL database under accession numbers Y17827, Y17826 and Y17828 respectively.

Cell hybridization assay

Fluorescent "*in-situ*" (whole-cell) hybridizations (FISH) for purity controls was carried out as described (Musat *et al.*, 2008) using the newly designed oligonucleotide probe HdN1_112 (5'-TTCCTGCGCTATCCTCAC-3', 60% formamide) which is specific for strain HdN1. The highest stringency yielding hybridization was obtained with 60% formamide. None of the 16S rRNA sequences in the SILVA SSU database (www.arb-silva.de, release August 2009; Pruesse *et al*., 2007) exhibited less than four mismatches.

Genomic analysis

DNA was isolated with the Genomic DNA kit (Qiagen, Hildesheim, Germany) according to the manufacturer's instructions and sonified. Shotgun fragments were ligated into the pUC/SmaI vector (Fermentas, St. Leon-Rot, Germany) and electroporated into *Escherichia coli* strain K12 substrain DH10B. Insert sizes were between 1.5 and 2.5 kb. In addition, a fosmid library (CopyControl™ Fosmid Library Production Kit, Epicentre, Madison, U.S.A.) was constructed for data finishing and confirmation of the assembly. Recombinant DNA was sequenced using the ABI3730XL instrument (ABI, Darmstadt, Germany). Gaps and regions of insufficient quality were completed by resequencing and primer walking. Sequences were assembled with PhredPhrap (http://www.phrap.org). The Consed package (Gordon, 2003) was used for final sequence editing. An 11-fold sequencing coverage was reached, resulting in a sequence quality of less than 1 error per 100,000 bases (average). Genes that may encode glycyl radical enzymes, enzymes of the known denitrification pathway, oxygenases, and cbb_3-type oxidases were searched for using the BLASTP-program (Altschul *et al*., 1997) and the HTGA-system (Rabus *et al*., 2002).

Chemical analyses

Nitrate and nitrite were measured by high-performance liquid chromatography (Sykam, Gliching/Munich, Germany) as described (Rabus und Widdel, 1995).

N_2, CO_2 and N_2O were analyzed in the culture headspace (see above) by gas chromatography using a GC-8A instrument (Shimadzu, Duisburg, Germany) equipped with a thermal conductivity detector. The gases were separated on a CP PoraPLOT Q (3 mm × 2 mm; Agilent, Waldbronn, Germany) or HP-PLOT MoleSieve (0.53 mm × 0.32 mm; Agilent, Waldbronn, Germany) column at 40°C using argon as carrier gas at a flow rate of 15.0 ml min^{-1}. Headspace samples were withdrawn with a gas-tight syringe equipped with a gas valve.

Organic acids were extracted from heat-inactivated (85 °C) and acidified cultures with dichloromethane, methylated, and analyzed by gas chromatography-mass spectrometry as described (Rabus *et al*., 2001). Long-chain alcohols were extracted with diethylether. After evaporation the residue was silylated with N,O-bis(trimethylsilyl)acetamide (Supelco, product specification T496017A) and analyzed by gas chromatography-mass spectrometry using a GCQ instrument (ThermoQuest Finnigan, Bremen, Germany) equipped with an Optima-5 column (Macherey-Nagel, Düren, Germany); the carrier gas was helium.

References

Altschul, S.F., Madden, T.L., Schäffer, A.A., Zhang, J., Zhang, Z., Miller, W., and Lipman, D.J. (1997) Gapped BLAST and PSI-BLAST: a new generation of protein database search programs. *Nucleic Acids Res* **25:** 3389–3402.

Ehrenreich, P., Behrends, A., Harder, J., and Widdel, F. (2000) Anaerobic oxidation of alkanes by newly isolated denitrifying bacteria. *Arch Microbiol* **173:** 58–64. (Erratum: *Arch Microbiol* **173:** 232).

Gordon, D. (2003) Viewing and editing assembled sequences using Consed. Current Protocols in Bioinformatics. Chapter 11, Unit 11 12.

Ludwig, W., Strunk, O., Westram, R., Richter, L., Meier, H., Yadhukumar et al. (2004) ARB: A software environment for sequence data. *Nucleic Acids Res* **32**: 1363–1371.

Musat, F., and Widdel, F. (2008) Anaerobic degradation of benzene by a marine sulfate-reducing enrichment culture, and cell hybridization of the dominant phylotype. *Env Microbiol* **10**: 10–19.

Pruesse, E., Quast, C., Knittel, K., Fuchs, B.M., Ludwig, W.G., Peplies, J., and Glöckner, F.O. (2007) SILVA: a comprehensive online resource for quality checked and aligned ribosomal RNA sequence data compatible with ARB. *Nucleic Acids Res* **35**: 7188–7196.

Rabus, R., Kube, M., Beck, A., Widdel, F., and Reinhardt, R. (2002) Genes involved in the anaerobic degradation of ethylbenzene in a denitrifying bacterium, strain EbN1. *Arch Microbiol* **178:** 506–516.

Rabus, R., Wilkes, H., Behrends, A., Armstroff, A., Fischer, T., Pierik, A.J., and Widdel, F. (2001) Anaerobic initial reaction of *n*-alkanes: evidence for (1-methylpentyl)succinate as initial product and for involvement of an organic radical in the metabolism of *n*-hexane in a denitrifying bacterium. *J Bacteriol* **183:** 1707–1715.

Rabus, R., and Widdel, F. (1995) Anaerobic degradation of ethylbenzene and other aromatic-hydrocarbons by new denitrifying bacteria. *Arch Microbiol* **63**: 96–103.

Rainey, F.A., WardRainey, N., Kroppenstedt, R.M., and Stackebrandt, E. (1996) The genus *Nocardiopsis* represents a phylogenetically coherent taxon and a distinct actinomycete lineage: Proposal of Nocardiopsaceae fam nov. *Int J Syst Bacteriol* **46**: 1088–1092.

Schreiber, F., Polerecky, L., de Beer, D. (2008) Nitric oxide microsensor for high spatial resolution measurements in biofilms and sediments. *Anal Chem* **80:** 1152–1158.

Stamatakis, A., Ludwig, T., and Meier, H. (2005) RAxML-III: a fast program for maximum likelihood-based inference of large phylogenetic trees. *Bioinformatics* **21**: 456–463.

Widdel, F., and Bak, F. (1992) Gram-negative mesophilic sulfate-reducing bacteria. In *The prokaryotes*. Balows, A., Trüper, H.G., Dworkin, M., Harder, W., and Schleifer, K.-H. (eds). New York: Springer, pp. 3352–3378.

Appendix S2

Redox potentials of subsequent reduction steps, and average redox potential

If an electron acceptor A_{ox} is reduced stepwise to A_{red} via m subsequent steps involving free intermediates (I_i), the reaction can be written as follows (n_i, number of electrons):

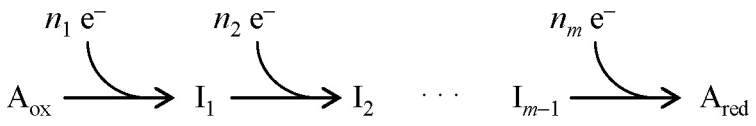

With an electron donor of a given redox potential, E_{don}, and the redox potential E_i of a reduction step (definition of which is originally based on a reversible reaction), the free energy change of an individual step is $-\Delta G_i = n_i F \Delta E_i = n_i F (E_i - E_{don})$; $F = 96{,}485$ C mol^{-1} (Faraday constant). The free energy change of the total reduction reaction is

$$-\Delta G_{tot} = n_1 F (E_1 - E_{don}) + n_2 F (E_2 - E_{don}) + \ldots + n_m F (E_m - E_{don}) \quad (1)$$

$$= F [(n_1E_1 + n_2E_2 + \ldots + n_mE_m) - (n_1 + n_2 + \ldots + n_m)E_{don}] \quad (2)$$

The sum $n_1 + n_2 + \ldots + n_i$ is the total number of electrons, n_{tot}, so that

$$-\Delta G_{tot} = F [(n_1E_1 + n_2E_2 + \ldots + n_mE_m) - n_{tot}E_{don}] . \quad (3)$$

Rearrangement leads to

$$\frac{-\Delta G_{tot}}{n_{tot} F} + E_{don} = \frac{n_1E_1 + n_2E_2 + \ldots + n_mE_m}{n_{tot}} . \quad (4)$$

The term $-\Delta G_{tot}/(n_{tot} F)$ expresses a redox potential difference. Because it includes only parameters referring to the total reaction, it can be defined as the average redox potential difference, ΔE_{av}, of the total reaction:

$$\frac{-\Delta G_{tot}}{n_{tot} F} = \Delta E_{av} . \quad (5)$$

Because ΔE_{av} is relative to the redox potential of the donor reaction, (5) necessarily defines also an average redox potential by $\Delta E_{av} = E_{av} - E_{don}$. We can thus write (4) as

$$(E_{av} - E_{don}) + E_{don} = E_{av} = \frac{n_1E_1 + n_2E_2 + \ldots + n_mE_m}{n_{tot}} \quad (6)$$

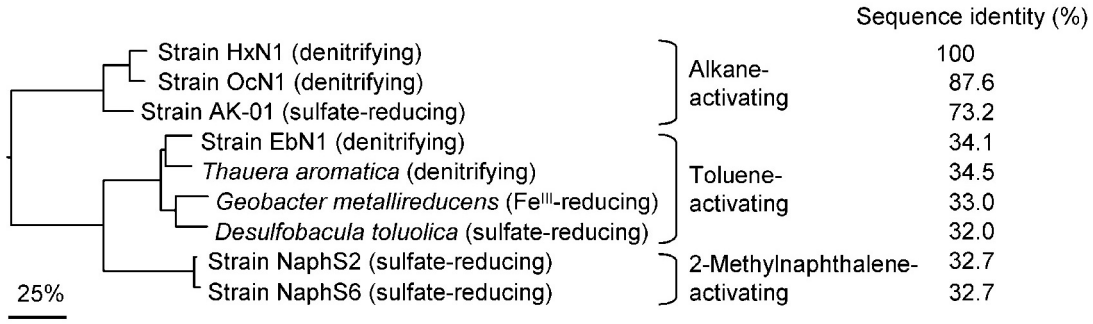

Fig. S1. Relationship of the assumed catalytic (large) subunit (MasD) of the *n*-alkane-activating enzyme in strain OcN1 to other enzymes activating hydrocarbons via addition to fumarate. Bar, 25% amino acid exchange.
Accession numbers: HxN1, CAO03074.1; OcN1, FN675935; AK-01, ABH11460.1; EbN1, YP_158060.1; *T. aromatica*, AAC38454.1; *G. metallireducens*, AAM34597.1; *D. toluolica*, ABM92935.1; NaphS2, CAO72219.1; NaphS6, CAO72222.1.

Table S1. General genome[a] features of strain HdN1.

Size (bp)	4,587,455	
G + C content (mol%)	53.26	
Stable RNAs		
rRNAs	9	(3 operons)
tRNAs	47	
Protein-coding sequences (CDS)[b]	3,763	
Coding (%)	89.2	
Average length (bp)	1,088	
Pseudo genes	45	

[a] Accession no. FP929140
[b] Without "pseudo"-qualifier

Table S2. Genome-based TBLASTN-search for genes (*bssA* and homologues) that may encode fumarate-dependent glycyl radical enzymes for anaerobic alkane activation.

Query				Best TBLASTN-hit in genome of strain HdN1			
Gene name	**Acc. no.**	**Amino acids**	**Predicted function, organism**	**Position**	**E-value**	**Identities**	**Positives**
bssA	CAI07159	861	α-Subunit, benzylsuccinate synthase, denitrifying Betaproteobacterium strain EbN1	762,138 – 761,950	1.2	20/70 (29%)	30/70 (43%)
masD	CAO03074	839	α-Subunit, (1-methylalkyl)succinate synthase, denitrifying Betaproteobacterium strain HxN1	1,510,228 – 1,510,115	0.3	16/38 (42%)	24/38 (63%)
nmsA	CAO72219	828	α-Subunit, (2-naphthylmethyl)succinate synthase, sulfate-reducing Deltaproteobact. strain NaphS2	1,591,168 – 1,591,049	1.1	15/40 (38%)	20/40 (50%)
dhaB1	CAJ67970	790	Glycerol dehydratase, *Clostridium difficile* 630	235,877 – 235,695	4.1	22/73 (30%)	31/73 (42%)
pflB	P09373	760	Pyruvate formate lyase, *Escherichia coli* K12	2,685,988 – 2,686,473	0.27	41/170 (24%)	74/170 (44%)
nrdD	P28903	712	Anaerobic ribonucleotide reductase, *Escherichia coli* K12	1,500,318 – 1,500,040	2.1	25/95 (26%)	41/95 (43%)

TBLASTN was performed as described by Altschul, S.F., Madden, T.L., Schaffer, A.A., Zhang, J., Zhang, Z., Miller, W., and Lipman, D.J. (1997) Gapped BLAST and PSI-BLAST: a new generation of protein database search programs. *Nucleic Acids Res* **25:** 3389–3402.

Table S3. Genome-based prediction of enzymes for the common denitrification pathway in strain HdN1.

Predicted gene (product) of strain HdN1					BLASTP hit used for annotation			
Gene name	**Identifier**	**Start (bp)**	**Amino acids**	**Predicted function**	**Gene**	**Organism** [a]	**E-value**	**Acc. no.**
Cluster I (1,639,227 – 1,652,317)								
narL	HDN1F_13190	1,639,865	213	Nitrate/nitrite 2-component response regulator	*narL*	Pseae	1e-59	O54039
narX	HDN1F_13210	1,641,736	624	Nitrate/nitrite 2-component sensor kinase	*narX*	Pseae	1e-94	O54040
narK1	HDN1F_13220	1,642,206	453	Nitrate/proton symporter	*narK1*	Pseae	7e-98	O54041
narK2	HDN1F_13230	1,643,621	556	Nitrate/nitrite antiporter	*narK2*	Azose	0.0	Q5NYZ3
narG	HDN1F_13240	1,645,636	1250	Nitrate reductase, alpha subunit	*narG*	Azose	0.0	Q5NYZ4
narH	HDN1F_13250	1,649,402	510	Nitrate reductase, beta subunit	*narH*	Azose	0.0	Q5NYZ5
narJ	HDN1F_13260	1,650,937	230	Nitrate reductase, delta subunit	*narJ*	Pseae	3e-42	O54045
narI	HDN1F_13270	1,651,640	226	Nitrate reductase, gamma subunit	*narI*	Pseae	3e-72	O54046
Cluster II (4,472,792 – 4,479,005)								
nirM	HDN1F_37060	4,472,792	104	Cytochrome *c*, monohaem	*nirM*	Pseae	3e-22	P00099
nirS	HDN1F_37070	4,474,578	585	Dissimilatory cytochrome cd_1 nitrite reductase precursor	*nirS*	Azose	0.0	Q5P7W3
norD	HDN1F_37080	4,476,628	631	Predicted nitric oxide reductase activation protein	*norD*	Pseae	1e-120	O51484
norQ	HDN1F_37090	4,477,453	273	Putative chaperone required for maturation of nitric oxide reductase	*norQ*	Azose	9e-95	Q5P8Y1
norB	HDN1F_37100	4,478,983	470	Nitric oxide reductase subunit B	*norB*	Azose	0.0	Q5P8Y4
norC	HDN1F_37110	4,479,430	142	Nitric oxide reductase subunit C	*norC*	Azose	2e-59	Q5P8Y5
Cluster III (4,522,585 – 4,528,867)								
nosL	HDN1F_37530	4,522,585	129	Predicted lipoprotein involved in nitrous oxide reduction (COG4314)	-	-	-	-
nosY	HDN1F_37540	4,523,550	271	Probable transmembrane protein	*nosY*	Azose	2e-74	Q5NZ06
nosF	HDN1F_37550	4,524,502	308	Putative ATP-binding protein	*nosF*	Azose	6e-94	Q5NZ05
nosD	HDN1F_37560	4,525,925	448	Nitrous oxidase accessory protein precursor	*nosD*	Azose	1e-149	Q5NZ04
nosR	HDN1F_37570	4,528,549	875	Domain, 4Fe-4S ferredoxin, iron-sulfur binding, FMN-binding	-	-	-	-
nosZ	HDN1F_37580	4,530,828	654	Nitrous oxide reductase	*nosZ*	Azose	0.0	Q5NZ01

[a] Abbreviations for organisms: Pseae, *Pseudomonas aeruginosa*; Azose, *Azoarcus*-related denitrifying Betaproteobacterium strain EbN1.

Table S4. Genome-based prediction of alkane monooxygenases (alkane hydroxylases) in strain HdN1.

Predicted gene (product) of strain HdN1					BLASTP hit used for annotation			
Identifier	**Start (bp)**	**Amino acids**	**Predicted function**	**InterPro [a]**	**Gene**	**Organism [b]**	**E-value**	**Acc. no.**
Cyt P450 monooxygenase *(accessory proteins[c] in grey)*								
HDN1F_17550	2,213,848	106	Ferredoxin	IPR001041		Alcbo	2e-44	Q5ca10
HDN1F_17560	2,214,183	471	Cytochrom P450 alkane hydroxylase	IPR001128	*ahpG2*	Alcbo	0	Q5K133
HDN1F_17570	2,215,803	410	Ferredoxin reductase	IPR001327		Alcbo	0	Q5ca08
Alkane-1-monooxygenase *(di-iron enzyme)*								
HDN1F_04180	517,699	314	Transcriptional regulator, AlkR	IPR000005	*alkR*	Acica	4e-71	Q9xdp8
HDN1F_04190	517,997	423	Alkane 1-monoxygenase, AlkM (di-iron)	IPR012145		Aciba	1e-138	ZP_05827357
Alkane-1-monooxygenase *(flavin enzyme)*								
HDN1F_14540	1,814,074	505	Alkane 1-monoxygenase (flavin)	IPR000960		Alcbo	9e-167	YP_692002
HDN1F_17470	2,204,606	500	Alkane 1-monoxygenase (flavin)	IPR000960		Alcbo	0	YP_692002
HDN1F_17580	2,218,527	512	Alkane 1-monoxygenase (flavin)	IPR000960		Alcbo	0	YP_691914
HDN1F_30030	3,708,484	495	Alkane 1-monoxygenase (flavin)	IPR000960		Alcbo	2e-178	YP_692002
HDN1F_36680	4,423,219	511	Alkane 1-monoxygenase (flavin)	IPR000960		Alcbo	3e-159	YP_691914

[a] IPR001041: domain, ferredoxin; IPR001128: family, cytochrome P450; IPR001327: domain, FAD-dependent pyridine nucleotide-disulfide oxidoreductase; IPR000005: domain, helix-turn-helix, AraC type; IPR012145: family, alkane 1-monooxygenase; IPR000960: family, flavin-containing monooxygenase FMO.
[b] Abbreviations for organisms: Aciba, *Acinetobacter baumannii*; Acica, *Acinetobacter calcoaceticus*; Alcbo, *Alcanivorax borkumensis*.
[c] Genes for accessory proteins in direct proxemity to the predicted oxygenase-related genes.

Table S5. Genome-based prediction of *cbb*$_3$-type oxidases (oxidases with high O_2-affinity) in strain HdN1.

Predicted gene (product) of strain HdN1						BLASTP hit used for annotation			
Gene name	**Identifier**	**Start (bp)**	**Amino acids**	**Predicted function**	**InterPro [a] COG [b,c]**	**Gene**	**Organism [d]**	**E-value**	**Acc. no.**
ccoP	HDN1F_11960	1,483,054	298	Cytochrome *c* oxidase *cbb*$_3$-type, subunit III	IPR004678 COG2010	*ccoP*	Azose	1e-65	Q5P0X3
ccoQ	HDN1F_11970	1,483,947	76	Probable cytochrome *c* oxidase, subunit CcoQ	IPR008621 COG4736	*ccoQ*	Azose	1e-04	Q5P0X4
ccoO	HDN1F_11980	1,484,180	207	Cytochrome *c* oxidase, *cbb*$_3$-type, subunit II	IPR003468 COG2993	-	-	-	-
ccoN	HDN1F_11990	1,484,818	480	Cytochrome *c* oxidase, *cbb*$_3$-type, subunit I	IPR004677 COG3278	-	-	-	-
ccoN	HDN1F_27210	3,357,106	498	Cytochrome-*cbb*$_3$ oxidase, subunit I	IPR004677	*ccoN*	Azose	1e-145	Q5P0X6
ccoO	HDN1F_27220	3,358,613	216	Cytochrome-*cbb*$_3$ oxidase, subunit I	IPR003468 COG2993	*ccoO*	Azose	3e-54	Q5P0X5
ccoQ	HDN1F_27230	3,359,260	63	Cytochrome *c* oxidase subunit	IPR008621	-	-	-	-
ccoP	HDN1F_27240	3,359,444	307	Cytochrome-*cbb*$_3$ oxidase, subunit III	IPR004678 COG2010	*ccoP*	Azose	2e-48	Q5P0X3

[a] IPR003468: family, cytochrome *c* oxidase, mono-heme subunit; IPR004677: family, cytochrome *c* oxidase *cbb*$_3$-type, subunit I; IPR004678: family, cytochrome *c* oxidase *cbb*$_3$-type, subunit III; IPR008621: family, *cbb*$_3$-type cytochrome oxidase, cytochrome *c* subunit.

[b] COG, cluster of orthologous groups.

[c] COG2010: CccA, cytochrome *c*, mono- and diheme variants; COG2993: CcoO, *cbb*$_3$-type cytochrome oxidase, cytochrome *c* subunit; COG3278: CcoN, *cbb*$_3$-type cytochrome oxidase, subunit I; COG4736: *cbb*$_3$-type cytochrome oxidase, subunit 3.

[d] Abbreviation for organism: Azose, *Azoarcus*-related denitrifying Betaproteobacterium strain EbN1.

Chapter D.3

Is there a key role of NO in *n*-alkane activation during growth of a Gammaproteobacterium (strain HdN1) by NO_3^- respiration?

Johannes Zedelius,[1] Marcel M. M. Kuypers,[1] Ralf Rabus,[1,2] Frank Schreiber,[1,3]
Friedrich Widdel[1]* and Marc Strous[1,4]

[1]*Max Planck Institute for Marine Microbiology, Celsiusstraße 1, D 28359 Bremen, Germany.*
[2]*Institute for Chemistry and Biology of the Marine Environment, University of Oldenburg, Carl-von-Ossietzky-Straße 911, D 26111 Oldenburg, Germany.*
[3]*EAWAG – Swiss Federal Institute of Aquatic Science and Technology, Department of Environmental Microbiology, Überlandstrasse 133, CH-8600 Dübendorf, Switzerland.*
[4]*Institute for Genome Research and Systems Biology, Center for Biotechnology, University of Bielefeld, Universitätsstraße 27, D-33615 Bielefeld, Germany.*

Manuscript *finished* (2012)

Summary

The Gammaproteobacterium HdN1 grows anaerobically by NO_3^- or NO_2^- reduction to N_2 with *n*-alkanes. N_2O however, albeit allowing growth with fatty acids, cannot sustain growth with alkanes, suggesting that NO_2^- or NO is essential for alkane activation. If cells were incubated with alkanes and N_2O and small 'pulses' of NO were added, more N_2 was formed than could be derived from NO alone. This indicated that NO yielded an alkane-derived product oxidizable through N_2O respiration. Apparently, NO is crucial for alkane activation, as previously also suggested for the NO_2^--reducing methanotroph Candidatus *Methylomirabilis oxyfera*. Proteomic analysis of strain HdN1 grown with NO_3^- revealed a distinct type of NO-reductase with active-site amino acid modifications predicted from the genomes of both organisms. Mass spectrometry revealed trace O_2 formation by strain HdN1 provided with NO_2^-. It is possible that the modified NO reductase converts NO to N_2 and O_2. The latter may have a dual role by serving for alkane activation and contributing to respiration. Still, other activation mechanisms of alkanes with NO_3^--derived intermediates can be envisaged, in which case O_2 would be only a by-product.

Introduction

Alkanes (saturated hydrocarbons) are naturally wide-spread compounds originating either directly from living organisms (Birch and Bachofen, 1988) or, in high structural diversity, from petroleum (Tissot and Welte, 1984) and petroleum-derived fuels. Despite low chemical reactivity, alkanes are metabolized by diverse microorganisms, so as to serve as electron donor for respiratory energy conservation, and as carbon source for cell synthesis. The long-known aerobic alkane-degrading microorganisms employ monooxygenases which involve an O_2-derived, highly reactive O-species to overcome the C─H-bond stability and lead to alcohols for further metabolism (Britton 1984; Groves, 2006). More recently, anaerobic alkane-utilizing microorganisms have been described which reduce NO_3^- (or NO_2^-), SO_4^{2-} or H^+-ions to N_2, H_2S, or H_2 (for methanogenic partners) respectively (Widdel *et al*., 2010). A unique process is the SO_4^{2-}-dependent oxidation of the simplest alkane, methane, by distinct archaea associated with Deltaproteobacteria (Knittel and Boetius, 2009). The apparently most common activation mechanism of non-methane alkanes is a radical enzyme-catalyzed addition (Heider, 2007) of the alkane at carbon-2 to fumarate yielding (1-methylalkyl)succinate (Kropp *et al*., 2000; Rabus *et al*., 2001; Widdel and Grundmann, 2010; Jarling *et al*., 2012). Still, other mechanisms have been envisaged (Aeckersberg *et al*., 1998; So *et al*., 2003) in sulfate-reducing bacteria.

In the previous study (Zedelius *et al*., 2011), it remained open whether NO_2^- or NO was the crucial N-O-compound needed for alkane metabolism, and whether the N-O-compound may lead to 'chemogenic' O_2 as a co-substrate for alkane monooxygenase. In the present study, we attempted to further limit the possibilities. We tested possible NO-dependent initiation of alkane oxidation, searched for traces of formed O_2, and used a proteomic approach to detect the presence of a phylogenetically distinct type of NO-reductase that is predicted by comparison of the genomes of strains HdN1 (Zedelius *et al*., 2011) and Candidatus *M. oxyfera* and may form O_2 (Ettwig *et al*., 2010, 2012). The present study also includes a detailed stoichiometric model of a variable, ‘branched’ use of generated O_2 in both, hydrocarbon functionalization and respiratory reactions.

Results

NO enabling alkane oxidation during incubation with N_2O

If NO can be shown to allow alkane oxidation, this would rule out the 'upstream' intermediate NO_2^- as the crucial compound (unless NO yields NO_2^- by dismutation; see Discussion), leaving NO as a direct precursor of the postulated O_2. In view of the high toxicity of NO (Zumft, 1993; Zedelius *et al*., 2011) at the concentrations that would be theoretically (stoichiometrically) needed for serving as the only electron acceptor and clearly revealing alkane oxidation, we incubated strain HdN1 with N_2O as non-toxic bulk electron acceptor for respiration and added only small 'pulses' of NO. If this would lead to alkane activation (in addition to possibly serving as electron acceptor for respiration), the functionalized product should be metabolizable with N_2O. Indeed, there was more N_2 production than could be accounted for by NO reduction alone, indicating that the alkane metabolism was initialized by NO or a subsequent product other than N_2O and then proceeded via N_2O reduction (Fig. 1; Appendix S1).

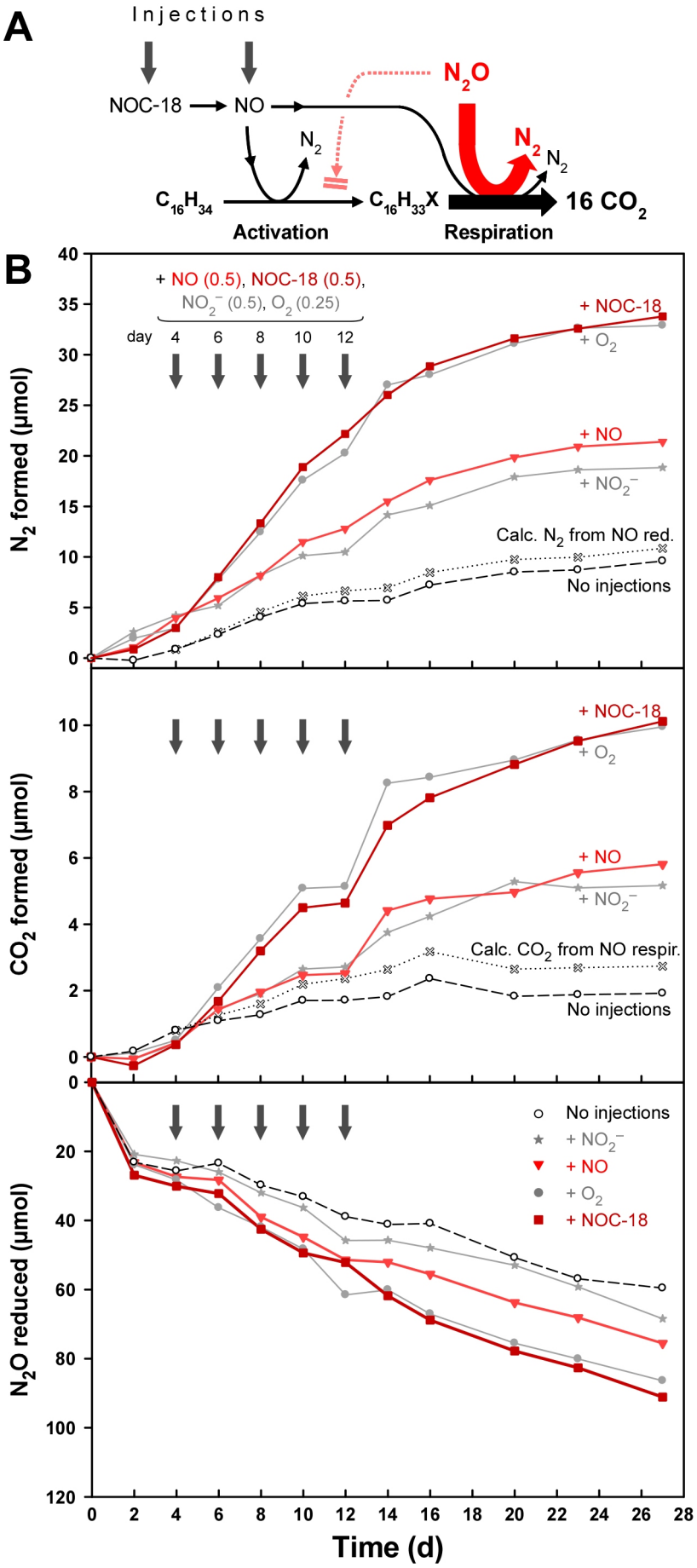
A
Injections
NOC-18
NO
N2O
N2
N2
N2
C16H34
C16H33X
16 CO2
Activation
Respiration
B
+ NO (0.5), NOC-18 (0.5),
NO2− (0.5), O2 (0.25)
day 4 6 8 10 12
+ NOC-18
+ O2
+ NO
+ NO2−
Calc. N2 from NO red.
No injections
N2 formed (µmol)
Calc. CO2 from NO respir.
CO2 formed (µmol)
N2O reduced (µmol)
Time (d)

Fig. 1. Effect of low concentrations of NO on the utilization of *n*-hexadecane by strain HdN1 incubated with N_2O as main electron acceptor for anaerobic respiration.
A. Principle of the experiment. NO but not N_2O allows alkane activation to a polar product (X, functional group) which then allows respiration of the abundantly present N_2O.
B. Amounts of formed N_2, CO_2 and reduced N_2O following five injections of NO or the NO donor NOC-18 (quantities indicated in µmol). Positive controls received O_2 or NO_2^- while the negative control received no additions. Experiments were performed in 156 ml serum bottles with 10 ml culture, 57 µmol (10 µl) n-hexadecane and 250 µmol anoxic N_2O. To ensure a metabolically active state that may better withstand adverse NO effects than a 'resting' state, cultures had been provided with a small (20 µmol) amount of NO_2^- directly before the experiment (before time point zero, not shown). Additions were injected when N_2 or CO_2 production with nitrite had ceased (details in Appendix S1). The increase of CO_2 and N_2 production by NO or the NO-donor NOC-18 cannot be explained by their use only as respiratory electron-acceptors, but rather indicates alkane conversion to a product metabolizable with N_2O. Maximum amounts expected from a purely respiratory use of NO (0.5 N_2/NO; 0.327 CO_2/NO; equations in Appendix S1) are visualized as dotted line. Duplicates yielded the same results (not shown).

Detection of O_2 formation from NO_3^--derived intermediates

For attempts to detect O_2 as an intermediate that could be the agent for alkane functionalization, formation of volatile compounds was analyzed by membrane-inlet mass spectrometry (MIMS) during a time course experiment with freshly grown cultures of strain HdN1 provided with NO or NO_2^-. NO_2^- was ^{15}N-labelled to follow also the fate of nitrogen. On the one hand, O_2 would probably be scavenged by both respiration and alkane oxygenation, so that absence of organic substrate would be desirable. On the other hand, reduction of NO_2^- requires reducing equivalents. As an attempt, tetradecane-grown cells were pre-incubated with N_2O, assuming that this would diminish stored alkane-derived intermediates while still leaving enough reducing equivalents for the reduction of the small amount of nitrite.

O_2 was undetectable when only NO_2^- or NO were added. Therefore, acetylene was added as a (potential) monooxygenase inhibitor (Hamamura *et al*., 1999; Yeager *et al*., 1999). Acetylene also inhibits N_2O reductase (Kristjansson and Hollocher, 1980). The experimental concept is shown in Fig. 2. Experiments with direct injection of NO as a toxic compound were obviously delicate; in different experiments, O_2 formation was either not detectable, or appeared only at marginal concentration (≤ 0.5 µM) that disappeared almost instantaneously. However, injection of 50 µM NO_2^- as a less toxic compound did result in the formation of 2 µM O_2 (Fig. 3). This amount was appropriate to also reveal subsequent consumption with residual substrate. The short 'plateau' of formed O_2 is interpreted as a steady state between formation and consumption. Subsequent injection of an aqueous solution of O_2 confirmed its consumption. The tentative precursor, NO, was detectable at very low concentration. Release of O_2 was not detected in sterile control experiments.

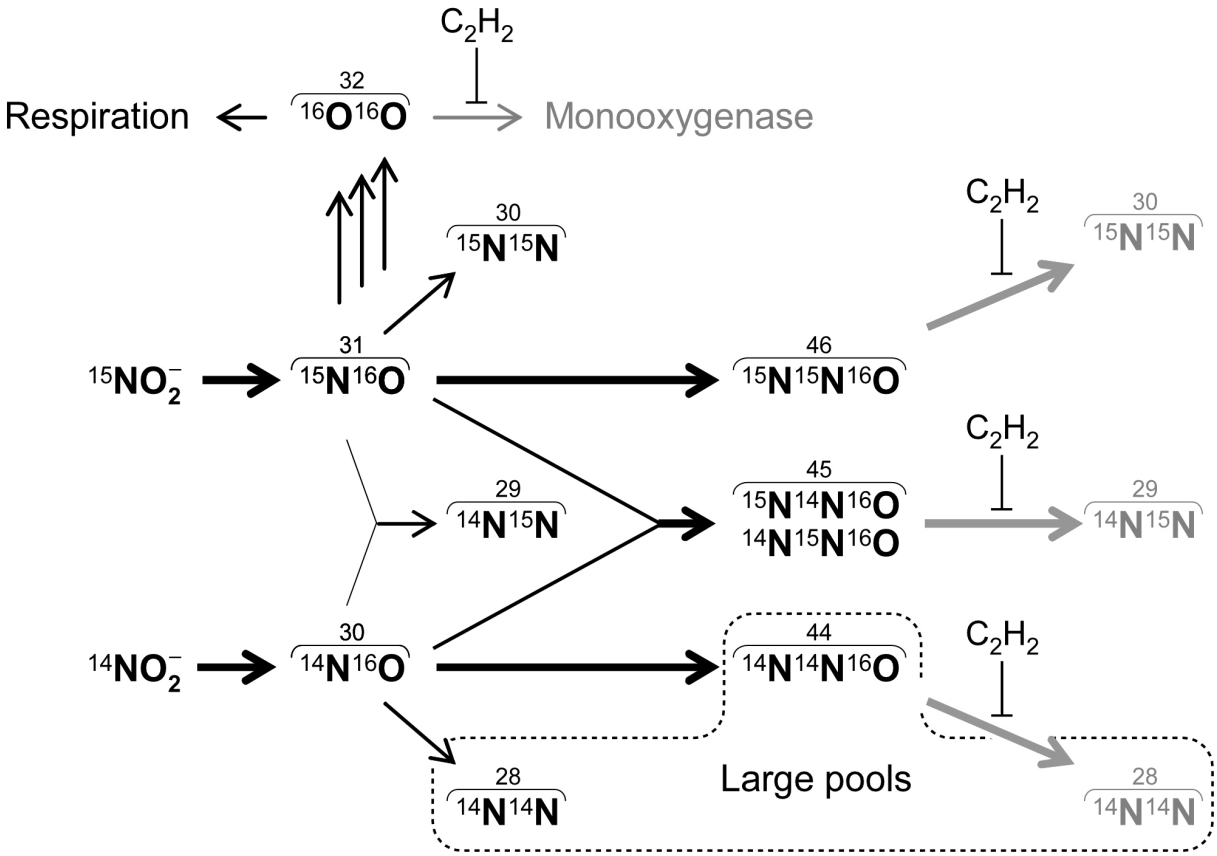

Fig. 2. Overview of the experimental concept for investigation of possible 'chemogenic' O_2 and volatile nitrogen species formed from NO_2^- by tetradecane-grown cells of strain HdN1. The concept includes acetylene inhibition of monooxygenase and N_2O reductase, and fate of ^{15}N-isotope label. The main reduction sequence is indicated in bold lines. N_2 isotopologues possibly formed by residual activity of the acetylene-impeded N_2O reductase are also indicated (grey). Unlabelled N_2O and N_2 are diluted in a large pool from pre-incubation.

As expected, N_2O accumulated in the acetylene-treated cultures and revealed the single or double label of ^{15}N from nitrite (Fig. 3). Formation of unlabelled N_2O is not depicted because it includes the high background concentration (around 1 mM) left from pre-incubation. The slight decrease of the N_2O concentration with time is explained by the dilution due to the constant flow of medium through the incubation vessel to the mass-spectrometer. There was a marked increase of N_2, as shown for the $^{15}N^{14}N$ and $^{15}N^{15}N$ isotopologue (Fig. 3; unlabeled N_2 not depicted because of transferred background from preculture).

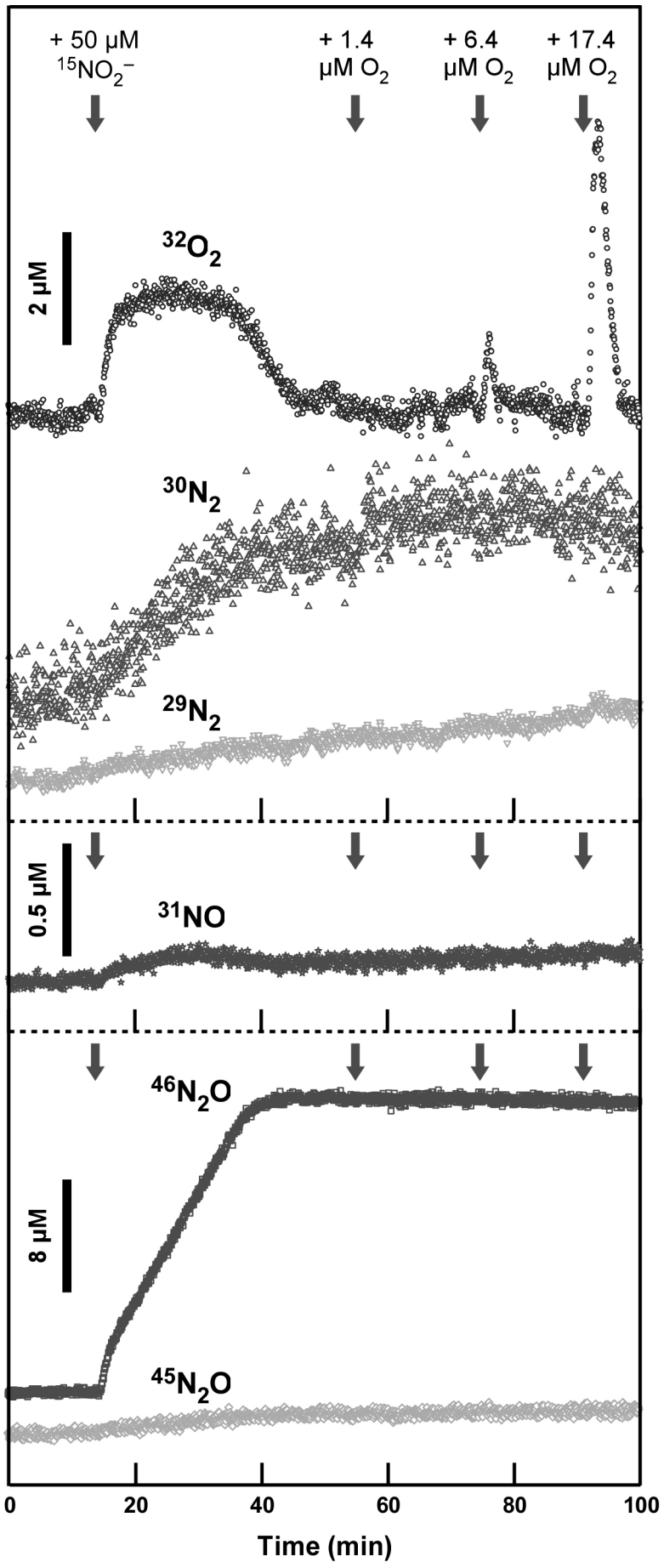

Fig. 3. Investigation of possible 'chemogenic' O_2 and volatile nitrogen species formed from NO_2^- by tetradec-ane-grown cells of strain HdN1. Chemical species attributed to masses of volatile compounds detectable by membrane-inlet mass spectrometry upon spiking of strain HdN1 with ^{15}N-NO_2^- (isotope purity, 98%). Detectable 'chemogenic' O_2 was consumed after several minutes due to respiration. Respiratory activity was also indicated by consumption of subsequently added O_2 from an aqueous solution. Prior to the depicted experiment, cells had been pre-incubated with N_2O (to diminish organic storage compounds) and acetylene (see text). Hence, there was a high background of unlabelled N_2O and N_2.

Proteogenomic evidence for formation of a unique NO-metabolizing enzyme in strain HdN1

Because strain HdN1 and *M. oxyfera* are phylogenetically (with respect to 16S rRNA) unrelated, any top-scoring hits from a comparison of their previously sequenced genomes (Ettwig *et al*., 2010; Zedelius *et al*., 2011) are likely to indicate functional similarity. For this comparison, the predicted proteins of strain HdN1 were blasted against a database with the predicted proteins of 794 reference genomes including *M. oxyfera*. Seventeen high-scoring shared proteins were discovered (Table S1; Appendix S1). Fifteen of these could be dismissed based on both inappropriate functional annotation and very low transcription levels in *M. oxyfera*, thus leaving two candidate gene products involved in a particular catabolism of N–O-compounds.

One gene product in strain HdN1 was a predicted NO-reductase (HDN1F_02620), representing the closest relative of two (DAMO_2437, DAMO_2434) of the three NO-reductases predicted for *M. oxyfera* (Ettwig *et al*., 2012). These enzymes form a distinct, monophyletic sister clade to the canonical quinol-dependent NO-reductases, which are all integral membrane proteins with 14 transmembrane helices. Fig. 4A shows the phylogenetic relationships as well as their basic building units, electron donors and reactions (for assumed reactions see Discussion). Similar proteins were also present in the genome *Muricauda ruestringensis* (Huntemann *et al*., 2012) and two other members of the Cytophaga/Flavobacteria superphylum. *M. ruestringensis* was originally isolated from an aerobic enrichment with hexadecane but subsequently revealed to be unable to use alkanes (Bruns *et al*., 2001).

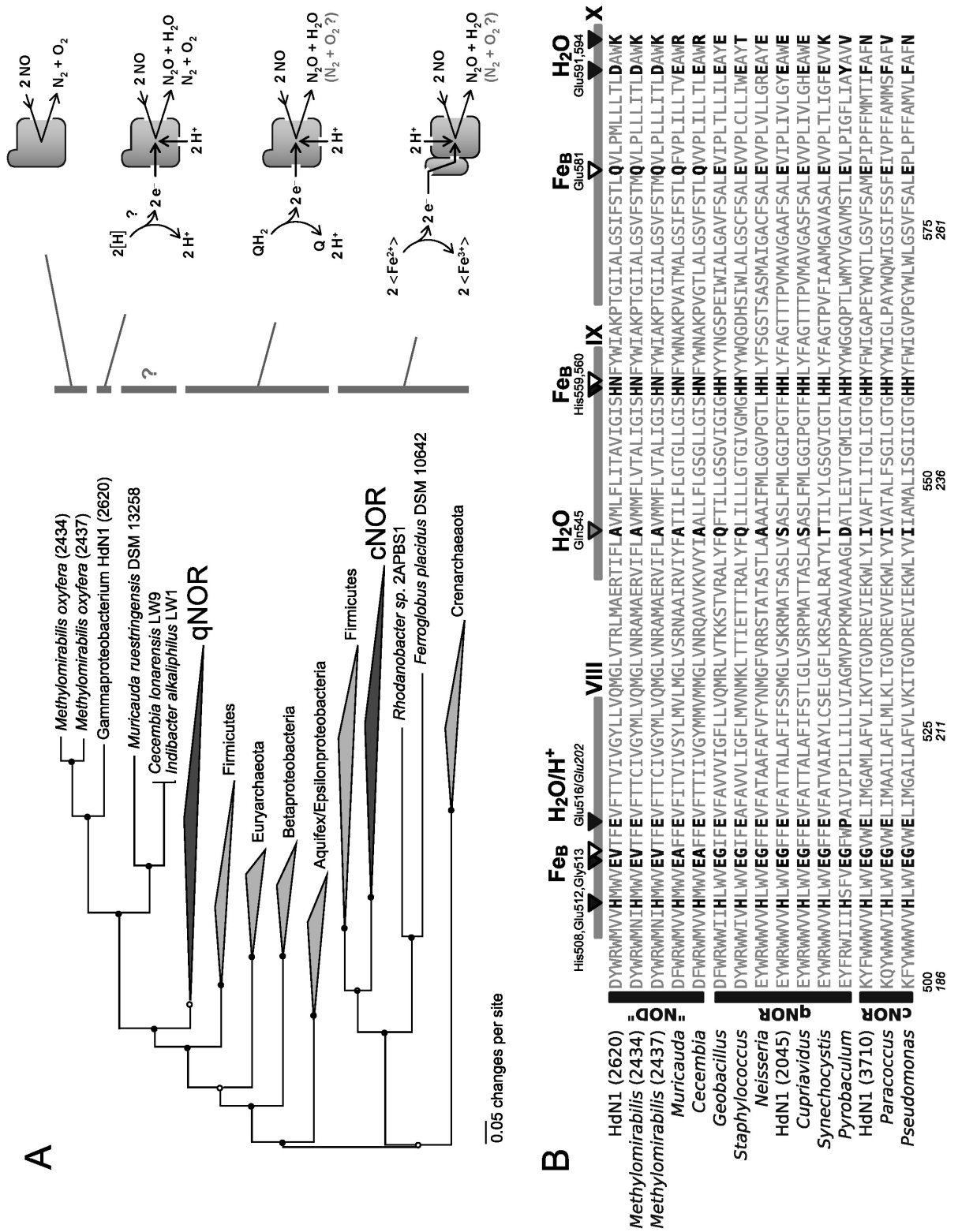

Fig. 4. Phylogenetic relationships (amino acid level) of NO reductases.

A. Phylogenetic relationships of NO reductases and the reactions catalysed. The candidate nitric oxide dismutases form a separate clade at the top. Circles at nodes symbolize the following gamma20 likelihoods: open (>70%), half-open (>95%), filled (>98%). Black triangles represent groups of canonical qNor and cNor protein sequences.

B. Close up of part of the active site region (Geobacillus stearothermophilus position 500-494 and Paracoccus position 186–280) showing transmembrane helixes VIII–X and key conserved amino acids involved in the coordination of the Fe_B and the water/proton channel.

The second gene product of interest was a predicted regulator encoded by HDN1F_02670 and DAMO_2439; this protein was present in the same gene cluster as the abovementioned NO-reductase. The regulator consisted of a DNA-binding domain and a PAS sensing domain that is also part of the well known oxygen sensor FixL. The FixL-like regulator was not detected in the genome of *M. ruestringensis*.

Fig. 4B shows an alignment of the amino acids that constitute the active site of the NO-reductases in strain HdN1, *M. oxyfera* and other microorganisms (see also alignment by Ettwig *et al*., 2012). Most of the functional aspects of the protein appeared to be conserved; the coordination of the heme *b* and heme b_3, the hydrophobic but empty cytochrome *c* binding pocket, the putative water channel and the putative proton channel. However, the coordination of the non-heme Fe_B was totally altered. In nitric oxide reductase Fe_B is coordinated by three histidines (His508/559/560, *Geobacillus stearothermophilus* positions) and two glutamates (Glu512/581; Matsumoto *et al*., 2012). Mutation of these residues leads to a non-functional enzyme. In the enzymes of strain HdN1, *M. oxyfera,* and *M. ruestringensis*, His-560 was mutated into Asn, Glu-581 into Gln, and the conserved Gly-513, necessary for the correct positioning of Glu-512, was mutated into a bulkier Val or Ala. With respect to the key residues of the quinol binding site, the enzymes from strain HdN1, *M. oxyfera* and 'typical' NO-reductases (having His-328, Glu-332 and Asp-746) did not have any amino acid with related properties in common, as was also found by Ettwig *et al*. (2012).

In the previous study (Zedelius *et al*., 2011), prediction of enzymes involved in the nitrate or oxygen respiration pathways, or potentially relevant for alkane functionalization was exclusively genome-based. Here, we also studied differential proteome profiles across several substrate-adapted cells by a shotgun approach. Of the three different predicted Nor proteins, the above unique protein resembling the *M. oxyfera* NO-reductase with proposed NO-dismutase function (NOD) was detected and identified with high score in cells grown anaerobically with *n*-tetradecane, 1-tetradecene or tetradecanoate. The enzyme was not detectable in aerobically grown cells. The other predicted qNor (HdN1F_02450) and the cNor (HdN1F_37100) were not detectable via the present proteomic approach (Table S2; Appendix S1).

Furthermore, genomic reading frames predicted di-iron (AlkM) as well as P450 type monooxygenases (AbpG). While both proteins were present in cells grown with alkane and O_2 or NO_3^-, AbpG was also formed by cells grown with an alkene and O_2 or NO_3^-. Neither

AlkM nor AbpG could be detected (Table S2; Appendix S1) in myristate-uilizing cells (with O_2 or NO_3^-).

Further growth experiments with organic substrates

Further substrate tests in addition to previous ones (Ehrenreich *et al*., 2000; Zedelius *et al*., 2011) showed growth of strain HdN1 with *n*-alkanes from C_6 to C_{30}, the higher of which ($\geq C_{18}$) are solid at incubation temperature (28 °C).

During growth with alkanes, many cells of the population assumed a 'swollen', somewhat irregular shape with droplet-like inclusions. Because polyhydroxyalkanoates were not detectable (Zedelius *et al*., 2011), the droplets were assumed to represent intracellular alkane, a phenomenon also observed in aerobic alkane degraders (Scott and Finnerty, 1976). An additional analysis revealed the presence of waxes, i.e. esters of long-chain alcohols and fatty acids. Such waxes were also detected in cells consecutively cultivated with long-chain fatty acids under oxic or anoxic conditions. This indicated the capability for reductive alcohol formation, i.e. independent alkane hydroxylation.

Discussion

Likely key role of NO and derived O_2 in alkane activation

The present study further favors the hypothesis that strain HdN1 in anoxic surroundings deviates an NO_3^--derived intermediate from the respiratory path into alkane functionalization. This intermediate is most likely NO, according to the 'pulse' experiments (Fig. 1). Still, NO_2^- cannot be completely excluded as the more directly needed agent. For instance NO could, in principle, dismutate according to $4NO + H_2O \rightarrow 2NO_2^- + 2H^+ + N_2O$ ($\Delta G°' = -40$ kJ mol_{NO}^{-1}; Appendix S1]. Still, we presently favor a key role of NO because of the versatile reactivity of this radical (·:N::O::), the strongly exergonic nature of potential reactions, and the presence of a phylogenetically particular type of NO-reductase.

Conditions for revealing O_2 formation directly from NO by mass spectrometry are still delicate. It is unknown whether NO at the added, artificially increased concentration could contribute to O_2 scavenging according to $4NO + O_2 + 2H_2O \rightarrow 4H^+ + 4NO_2^-$ (Lewis and Deen, 1994). However, nitrite addition caused accumulation of a molecular mass of 32 match-

ing that of O_2 (Fig. 3; further discussion of mass 32 in Appendix S1). The formation of $^{14}N^{15}N$ and $^{15}N^{15}N$ is in agreement with an assumed NO dismutation. Nevertheless, we cannot exclude that the acetylene-impeded N_2O reductase exhibits some residual activity and forms at least some of the labeled N_2 (Fig. 2).

The observed formation of O_2 is not a definite proof of its key role in alkane activation. O_2 could be a minor, physiologically insignificant by-product of another reaction of an N-O-species, whereas the actual activation reaction involves NO in a different manner. Any reaction would result in the same overall stoichiometry of alkane oxidation with nitrate (principle of element and electron conservation).

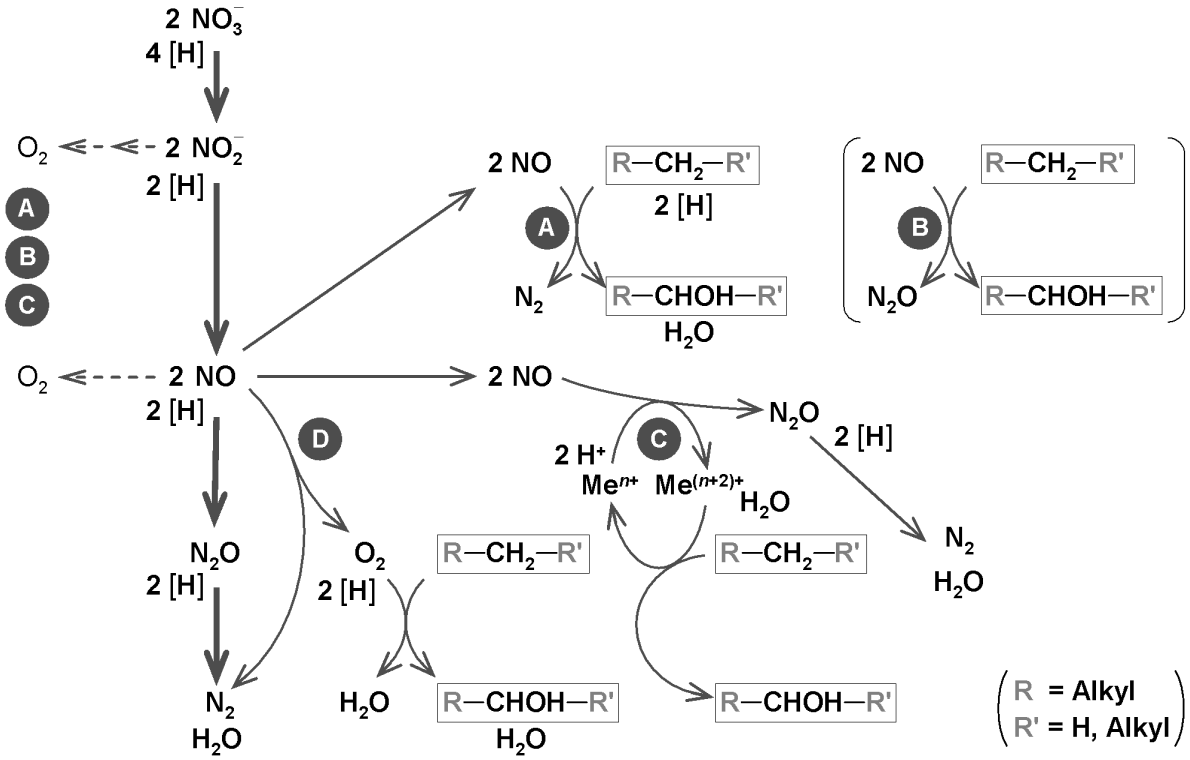

Fig. 5. Hypotheses of alkane activation with an NO_3^--derived N-O-species based on the present experiments. The scheme leaves open the site of alkane activation (primary or secondary carbon atom). The main route of nitrate is always its respiratory reduction to N_2 via the canonical denitrification pathway (bold lines).
A. Part of NO as a reactive and endergonic ('energy-rich') compound is directly involved in alkane functionalization by an unknown enzyme and mechanism (purely speculative) requiring electrons. O_2 is formed in a by-reaction and may be used to some extent, but its formation is not significant for the catabolism.
B. As A, but without requirement for electrons.
C. Part of NO is used by a special reductase that couples NO-reduction specifically to the generation of another oxidant, a high-valent metal center. The metal center then introduces a hydroxyl group originating from water. Again, O_2 is formed in a by-reaction without catabolic significance.
D. The presently favored mechanism. Part of NO is converted to N_2 and O_2, the latter being used in a conventional monooxygenase reaction.

Fig. 5 summarizes envisaged possibilities in addition to O_2 formation. The most appealing alternative to an involvement of O_2 would be a specific 'electronic' coupling between NO reduction and the generation of a high-valent metal center which then introduces a hydroxyl group into the alkane chain, i.e acts as alkane dehydrogenase. A metal for such a center could be molybdenum, analogous to ethylbenzene dehydrogenase in '*Aromatoleum aromaticum*' strain EbN1, and C25 dehydrogenase in *Sterolibacterium denitrificans*. The enzymes in these denitrifiers dehydrogenate the alkyl side chain of the benzene ring (Kloer *et al*., 2006) at C2, or a tertiary carbon position (C25) in the sterol side chain (Dermer and Fuchs, 2012) respectively. Also dehydrogenation of an *n*-alkane in particular at a secondary carbon atom to yield a secondary alcohol appears well feasible in a denitrifier. The redox potential (details in Appendix S1) of secondary alcohol formation ($R_1R_2HCOH/R_1R_2HCH + H_2O$; $E°' \approx +0.027$ V; R designates alkyl) is only somewhat higher than of tertiary alcohol formation ($R_1R_2R_3COH/R_1R_2R_3CH + H_2O$; $E°' \approx -0.02$ V; other value, −0.14 V). However, if such a reaction would be consequently hypothesized also for Candidatus *M*. *oxyfera,* this assumption would be confronted with the very unreactive C–H-bonds of methane. From a purely thermodynamic point of view, the redox potential of a 'methane dehydrogenase' ($CH_3OH/CH_4 + H_2O$; $E°' = +0.17$ V) appears achievable during nitrate reduction. Still, the most consistent hypothesis based on present knowledge is hydrocarbon activation by chemogenic O_2. Also, the broad range of used alkanes (C_6 to C_{30}) resembles that of typical aerobic alkane degraders (Table S3). Anaerobic alkane degraders are more specific with respect to the ranges of utilizable chain lengths (Widdel *et al*., 2010).

Structural and mechanistic aspects of NO reductases and possible substrate dismutation

NO-reductases from denitrifying bacteria belong to the heme copper oxidase super family. Functionally, this relationship may be reflected by some NO-reductases able to reduce O_2 (Fujiwara and Fukumori, 1996) and oxidases able to reduce NO (Giuffre *et al*., 1999; Hayashi *et al*., 2009). Heme copper oxidases themselves are complex, multimeric membrane proteins (Michel, 1999) in mitochondria and bacteria. They couple O_2 reduction with the build-up of a transmembrane H^+-gradient by vectorial electron flow and additional proton pumping (in opposite direction). The active (O_2-binding) site of the most wide-spread type, aa_3-oxidase (complex IV), contains heme a_3 and juxtaposed copper (so-called Cu_B). The high-affinity cbb_3 oxidases contain heme b_3. NO reductases, which are also membrane-embedded, are much

simpler. They are heterodimeric or monomeric and contain non-heme iron, Fe_B (instead of Cu) juxtaposed to heme *b* in the active site. A special type contains copper which, however, is not in the active site but in the accessory (small) subunit for electron uptake. Nomenclature is complicated because two abbreviations, NOR as functional term and Nor for gene product, are in use, with prefixes or suffixes. The NO reductases in strain HdN1 and *M. oxyfera* represent a distinct lineage branching off from monomeric NO reductases termed qNOR ('q' referring to quinol specificity). These enzymes have much in common with the catalytic (large) subunit, NorB, of heterodimeric NO reductases, termed cNOR ('c' referring to cytochrome specificity), and show in addition some motifs of the small subunit, NorC, of cNOR. For this reason, qNOR has also been designated NorB, unfortunately making this term ambiguous. To avoid confusion, consistent use of a formerly established designation, NorZ (Cramm *et al*., 1997) has been recommended for qNOR (more details in Zumft 2005). Even though NO reduction is more exergonic than O_2 reduction, NO reductases do not conserve energy by proton pumping. Enzyme-internal vectorial electron transport as another mechanism for energy conservation may occur in certain NO reductases (Matsumoto *et al*., 2012). In any case, NO reductases in denitrifiers enable energy conservation during the electron transport towards them (Simon *et al*., 2008).

According to recent insights (Matsumoto *et al*., 2012, Blomberg and Siegbahn, 2012), oxidized (EPR-silent) nitric oxide reductase is characterized by an oxo-bridge in the "binuclear center", b_3–O–Fe_B. Uptake of 2 e^- and 2 H^+ replaces this bridge by one NO-molecule orientated in the manner b_3–NO–Fe_B. Addition of the other NO-molecule leads (via the "cis" mechanism) to coordinated hyponitrite ($HON=NO^-$), thus forming the dinitrogen bond. Both oxygen atoms then interact with Fe_B, and rotation of hyponitrite releases N_2O, leaving one O-atom which again bridges heme b_3 and Fe_B (more details in cited literature). At higher concentrations (micromolar range) of NO, this may react with the oxo-bridged state of the enzyme and lead to NO_2^- and reduced heme b_3.

The observed changes of functional amino acids may suggest mechanisms for NO dismutation, the principle of which may be according to

$$2\ NO \rightarrow [ON=NO] \rightarrow N_2 + O_2. \qquad (1)$$

If the quinol binding site is non-functional (Ettwig *et al*. 2012), the binuclear center will presumably be in the oxidized form. The O-atom of one NO-molecule could thus combine with

the oxo-bridge to form the di-oxygen bond while the other NO-molecule could replace the oxo-bridge with its O-atom and simultaneously complete the N_2 molecule. If, alternatively, one would assume functionality of the quinol binding site (despite the marked amino acid changes), i.e. a mechanism similar as for NO-reduction with transient reduction of the binuclear center, 'reducing power' would have to flow back to quinone (net reaction is electron-neutral). Even though, as an interesting hypothesis, an H_2O molecule could replace Glu-581 as Fe_B-ligand and provide the second O-atom for O_2, backflow of electrons with the more positive redox potential to quinone appears energetically problematic. Alternatively, a small membrane protein related to b_{561} cytochromes, the gene of which is adjacent the HdN1 Nor gene, might play a role in electron transfer for NO reduction. From a thermodynamic point of view, even 'electronic' coupling of NO reduction ($4NO + 4e^- + 4H^+ \rightarrow 2N_2O + 2H_2O$; $E°' = 1.172$ V) to water cleavage ($2H_2O \rightarrow O_2 + 4e^- + 4H^+$; $E°' = 0.815$ V) would be feasible.

If the special NO-reductases of strain HdN1 and *M. oxyfera* are indeed O_2 evolving enzymes, the formation of the former protein revealed by proteomic analysis suggests additional function in respiration. There was no evidence for formation of a 'conventional' respiratory NO-reductase which would be expected in view of the significant N_2O production if this cannot be accounted for by the special, novel type of NO-reductase. Such dual function would urge upon the question whether there might be various transitions between 'conventional' NO-reductases and the exclusively NO-dismutating form of *M. oxyfera*, or whether most if not all NO reductases have, in principle, some more or less pronounced tendency for liberating O_2. If access of H^+ and e^- is not limiting, reduction to N_2O and H_2O is kinetically by far dominant. Only particular bacteria such as *M. oxyfera* or strain HdN1 make use of the dismutation reaction and promote this by slightly altered enzyme architecture to generate O_2. Besides impeded or 'controlled', sub-stoichiometric access of H^+ and e^- to the reaction center, also the exchange of the histidine usually coordinating Fe_B could alter catalysis. It is presently unknown whether this site is occupied by Fe or by another metal.

From an evolutionary point of view, it remains an open question whether the primeval function of NO reductases was dismutation or reduction. In any case, harboring an enzyme for O_2 generation may be advantageous especially for the metabolism of hydrocarbons in otherwise anoxic surroundings. Alkane functionalization by monooxygenases is in principle faster (as evident from rapidly growing aerobes) than through the obligately anaerobic enzymes such as the nickel-containing reverse methyl-coenzyme M reductase (Shima *et al.*, 2012) or

the radical-harboring (1-methylalkyl)succinate synthase (Rabus *et al*., 2001). Microorganisms involving the latter enzymes obviously compensate for their slowness by high enzyme concentrations (Krüger *et al*., 2003; Grundmann *et al*., 2008; Schmitt, Grundmann and Widdel, unpublished data). The ability for O_2 generation during denitrification offers the advantage of maintaining the hydrocarbon metabolism from oxic conditions by involving a modified variant of a single, rather ubiquitous enzyme if conditions become anoxic. A similar 'minimalistic' enzymatic outfit allowing versatile growth with hydrocarbons in oxic and anoxic surroundings is represented by perchlorate or chlorate reduction with cleavage of the intermediate, ClO_2^- into Cl^- and O_2 (de Geus *et al*., 2009; Mehboob *et al*., 2009; Oosterkamp *et al*., 2011). Another mechanism for chemogenic O_2, H_2O_2 dismutation by catalase, is, essentially for detoxification.

Kinetic aspects of NO utilization

Any involvement of the toxic NO as an intermediate (Zumft, 1993) and reactant requires maintenance at very low, compatible level even if its precursor, NO_2^-, builds up. An inherent kinetic feature of NO utilization may contribute to such control. NO reduction and dismutation, in contrast to NO_3^-, NO_2^- or N_2O reduction, is bimolecular with respect to the N-substrate. If enzyme concentration is considered as constant and (in case of NO reduction to N_2O) proton and electron supply not rate-limiting, the kinetic behavior is governed by the NO concentration in second power, viz. by $[NO]^2$. Because any reaction of NO is highly exergonic, a kinetic model can be formulated here in case of NO dismutation, as $2\,NO + E \rightleftarrows E(NO)_2 \rightarrow E + N_2 + O_2$; the model would be the same for canonical NO reduction. The rate of NO consumption, v_{NO}, as a function of the NO concentration in steady state follows the equation (details in Appendix S1)

$$v_{NO} = v_{NO\cdot max}\ \frac{[NO]^2}{K_m + [NO]^2}\ . \qquad (2)$$

K_m is a composite of three rate constants (for substrate binding, substrate release and product formation). The other characteristic, $v_{NO\cdot max}$, is the 'maximum' rate which v_{NO} approaches asymptotically for $[NO] \rightarrow \infty$. There is some similarity with the classical monomolecular enzymatic reaction (generally with substrate A and product P), $A + E \rightleftarrows EA \rightarrow E + P$, which yields the typical Michaelis-Menten equation

$$v = v_{max} \frac{[A]}{K_m + [A]} \quad (3)$$

However, reaction kinetics of NO (eq. 2) differs from eq. (3) in two respects. First, function (2) is sigmoidal (Fig. 6), viz. it passes from second-order behavior at [NO] << K_m through first-order behavior at medium concentration to approximate zero-order behavior at [NO] >> K_m (enzyme almost saturated). In contrast, eq. (3) passes from first-order type kinetics at low [A] towards zero-order kinetics at very high [A]. Second, even though there are similar kinetic characteristics (v_{max}, half-saturation concentration, and K_m), they are not fully equivalent. K_m in eq. (2) has the dimension mol^2 l^{-2}, whereas in eq. (3) the dimension is mol l^{-1}. Furthermore, the half-saturation concentration, i.e. the substrate concentration yielding $v_{max}/2$ and termed $[NO]_{v_{max}/2}$, is formally not identical with K_m in eq. (2); rather $[NO]_{v_{max}/2} \equiv \sqrt{K_m}$ (details in Appendix S1). In contrast, in eq. (3) $[A]_{v_{max}/2} \equiv K_m$.

There is a concentration range with a particularly sharp response of v to changing [NO]. Such a range does not exist in eq. (3). If the enzyme operates in the range of such pronounced slope, it can sensitively react by significantly increased NO scavenge if nitrite reduction accidentally becomes too fast.

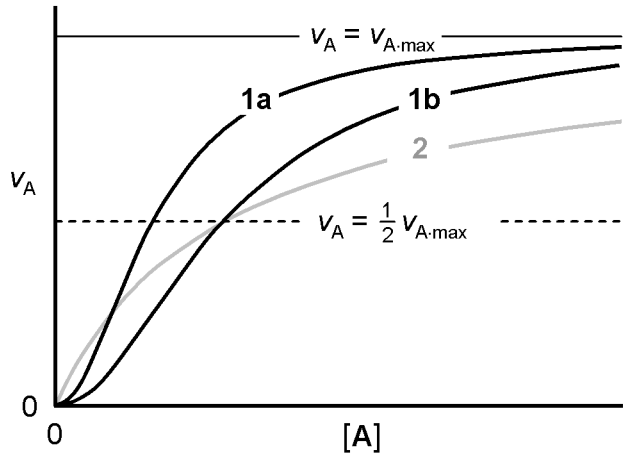

Fig. 6. Rate as a function of substrate concentration for homo-bimolecular (1a, 1b) and monomolecular (2) reaction of a substrate at an enzyme. For convenience, all reactions are displayed with 'normalized' $v_{A\cdot max}$. Reaction (1a) has the same numeric K_m-value and reaction (1b) the same $[A]_{vmax/2}$ as reaction (2).

Stoichiometric aspects of proposed NO dismutation in carbon metabolism

Despite the proposed common principle of NO dismutation as an O_2 source for hydrocarbon functionalization in strain HdN1 and *M. oxyfera*, there are interesting, delicate differences due

to their unequal carbon substrates. CH_4-derived CH_3OH provides from one molecule 6 e^-, whereas a long-chain alcohol such as $C_{16}H_{33}OH$ formed from hexadecane provides 96 e^- (Zedelius *et al*., 2011). Hence, the relative withdrawal of e^- for substrate functionalization in *M. oxyfera* is much higher. Fig. 7 compares NO utilization, O_2 production and the flow of electrons and carbon in both organisms.

If, for simplified treatment, cell synthesis is ignored, strain HdN1 performs the net reaction

$$5\ C_{16}H_{34} + 98\ NO_3^- + 18\ H^+$$

$$\rightarrow 80\ HCO_3^- + 49\ N_2 + 54\ H_2O. \qquad (4)$$

Activation of 5 $C_{16}H_{34}$ requires 10 e^- and 5 O_2. Production of the latter needs 10 NO. Because the electrons can only come from the functionalized product, hexadecanol, electrons equivalent to $^5/_{48}$ $C_{16}H_{33}OH$ ($\equiv {}^5/_{48} \times 96\ e^- = 10\ e^-$) are fully sacrificed for functionalization without the possibility for build-up of a proton gradient. The remaining $4^{43}/_{48}$ $C_{16}H_{33}OH$ ($\equiv 470\ e^-$) are for NO_3^- respiration. If O_2 formation for functionalization would be exactly stoichiometric, a moiety of 10 NO_3^- would be reduced only to the level of NO providing O_2, thus consuming 30 e^-. The remaining bulk of 88 NO_3^- would be reduced further via N_2O and thus consume 440 e^-. On the other hand, an exact 'stoichiometric fit' of O_2 production appears unlikely in view of other scavenging reactions; rather, a variable amount of O_2, in Fig. 7 designated *a*, may be consumed by oxidases even if their expression is low in anoxic surroundings. Hence, somewhat more than 10 NO, i.e. (10 + 2*a*) NO may be dismutated.

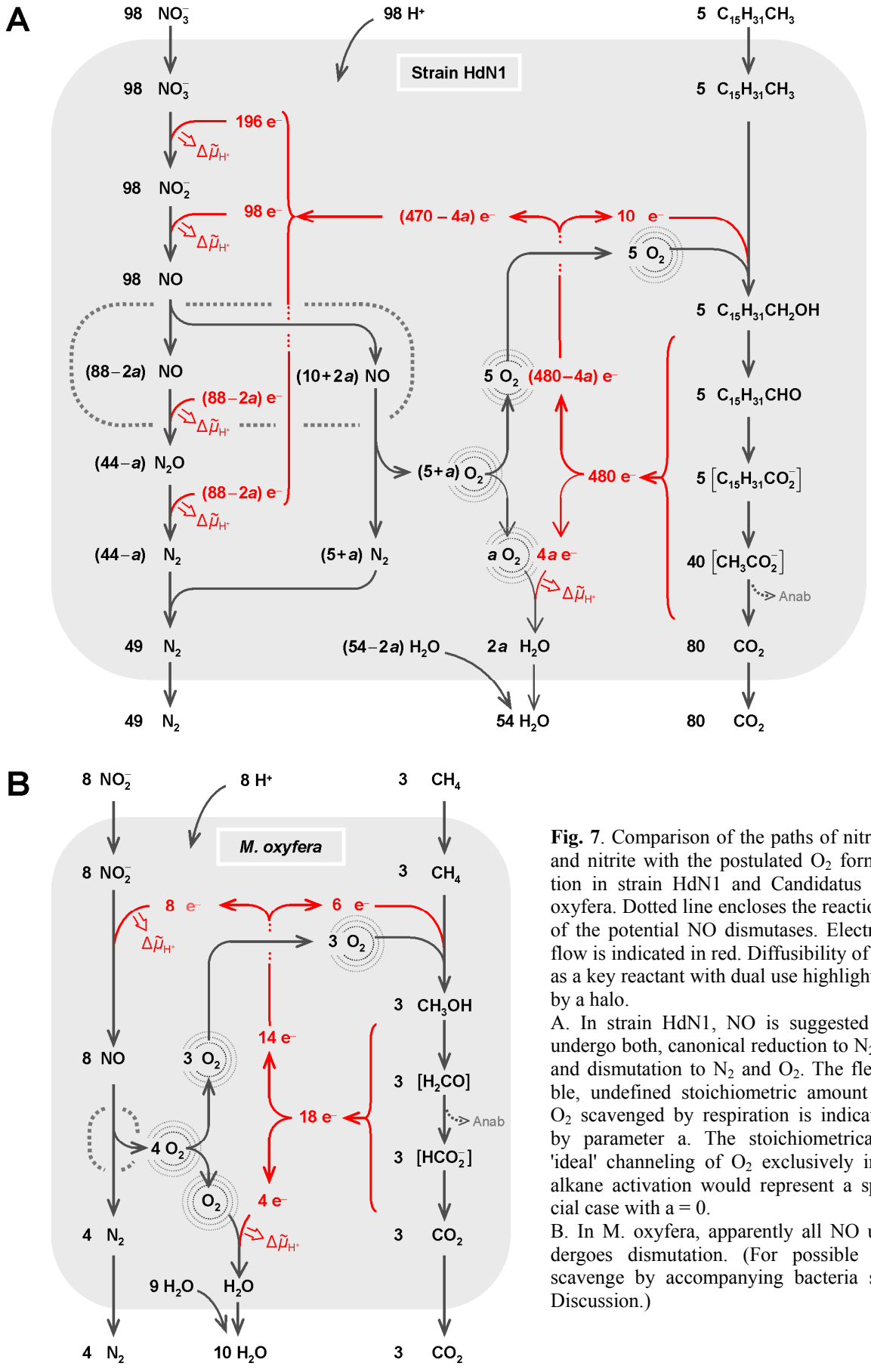

Fig. 7. Comparison of the paths of nitrate and nitrite with the postulated O_2 formation in strain HdN1 and Candidatus M. oxyfera. Dotted line encloses the reactions of the potential NO dismutases. Electron flow is indicated in red. Diffusibility of O_2 as a key reactant with dual use highlighted by a halo.

A. In strain HdN1, NO is suggested to undergo both, canonical reduction to N_2O, and dismutation to N_2 and O_2. The flexible, undefined stoichiometric amount of O_2 scavenged by respiration is indicated by parameter a. The stoichiometrically 'ideal' channeling of O_2 exclusively into alkane activation would represent a special case with a = 0.

B. In M. oxyfera, apparently all NO undergoes dismutation. (For possible O_2 scavenge by accompanying bacteria see Discussion.)

M. oxyfera performs the net reaction

$$3\ CH_4 + 8\ NO_2^- + 8\ H^+$$

$$\rightarrow 3\ CO_2 + 4\ N_2 + 10\ H_2O. \quad (5)$$

Activation of 3 CH_4 requires 6 e^- and 3 O_2. Production of these 3 O_2 needs 6 NO. Because again the electrons can only come from the functionalized product, methanol, 1 CH_3OH (6 e^-) is sacrificed for functionalization. The remaining 2 CH_3OH provide 12 e^- for respiratory purposes and build-up of a proton gradient. Because all 8 NO_2^- are reduced only to the level of 8 NO that yield 4 O_2, this reduction consumes 8 e^-, thus leaving 4 e^-. This number of electrons exactly reduces the remaining 1 O_2 that does not enter the monooxygenase reaction (Wu *et al*., 2011). Growth with methane through nitrate reduction according to

$$5\ CH_4 + 8\ NO_3^- + 3\ H^+$$

$$\rightarrow 5\ HCO_3^- + 4\ N_2 + 9\ H_2O \quad (6)$$

would not be possible via internal O_2 formation and a monoxygenase reaction because the reduction of 8 NO_3^- to 8 NO needs as many as 24 e^-. Fuctionalization of 5 CH_4 would need in addition 10 e^-. The resulting total demand of 34 e^- cannot be met by the 5 CH_3OH formed, oxidation of which to 5 CO_2 yields only 30 e^-. Hence, an organism with the present type of methane functionalization would need an additional electron donor, or partner bacteria providing NO_2^- from NO_3^- reduction with another electron donor (Deutzmann and Schink, 2011). Methane catabolism according to eq. (6) would be only possible via monooxygenase-independent functionalization such as involvement of methyl-coenzyme M reductase operating in opposite direction to methanogenesis (Scheller, *et al*., 2010; Thauer, 2011). However, it is unknown whether this enzyme, which involves low-valent, strongly reducing states of nickel (Thauer, *et al*., 1998), would be compatible with a cellular environment largely governed by high-potential denitrification biochemistry.

Considering interactions with other microorganisms

Microorganisms *in situ* capable of utilizing compounds that are not metabolizable by other community members may loose intermediates that foster accompanying bacteria (commensals). This is also possible with nitrate-derived intermediates. Whereas numerous denitrifying

bacteria produce and consume, i.e. share pools of NO_2^-, N_2O and possibly also of NO (Schreiber *et al*., 2008), only a few may form O_2. Its leakage could favor commensals including non-denitrifying aerobes or microaerobes that are unable to produce O_2 but able to scavenge this with high affinity. For the producer, diffusive loss of O_2 would implicate a lesser stoichiometric need of electron donor. Formal treatment by 'parametric' stoichiometry is simplest for methane-utilizing *M. oxyfera*. The principle can be extended to any electron donor and also intermediates of nitrate reduction scavenged by accompanying bacteria. If an undefined number of *b* O_2 is lost to the community, eq. (5) is modified to

$$(3–0.5b)\ CH_4 + 8\ NO_2^- + 8\ H^+$$

$$\rightarrow (3–0.5b)\ CO_2 + 4\ N_2 + (10–b)\ H_2O + b\ O_2. \qquad (7)$$

Formally, $0 \le b \le 6$ ($b = 6$ would mean nitrite dismutation). However, in the metabolism of Candidatus *M. oxyfera*, the upper limit of O_2 loss would be much lower. Because CH_4 is activated to CH_3OH ($\equiv 6\ e^-$), and because 2 e^- are needed for methane activation, 4 e^- remain for NO_2^- reduction to NO. Hence, there must be ≥ 2 CH_4 per 8 NO_2^- in eq. (7), so that $(3–0.5b) \ge 2$ and $b \le 2$, i.e. $0 \le b \le 2$. One borderline case ($b = 0$) of eq. (7) is eq. (5), the other (b = 2) is eq. (8),

$$CH_4\ (g) + 4\ NO_2^- + 4\ H^+$$

$$\rightarrow CO_2\ (g) + 2\ N_2 + 4\ H_2O + 2\ O_2\ (g), \qquad (8)$$

[$\Delta G°' = –246$ kJ (mol $NO_2^-)^{-1}$], which would still allow respiratory energy conservation by NO_2^- reduction.

Outlook

The proposed chemogenic O_2 as a functionalizing agent may neither be restricted to denitrification-coupled hydrocarbon utilization nor to strain HdN1 and *M. oxyfera*. For instance, chemogenic O_2 could allow post-synthetic lipid modification by acyl-chain desaturase (Aguilar and de Mendoza, 2006) maintaining membrane fluidity if temperature decreases. Also, the O_2-dependent synthesis of the dehydrogenase cofactor, pyrroloquinoline quinone (PQQ; Magnusson *et al*., 2004) would be enabled under conditions of denitrification. *Muricauda ruestringensis* may also employ an NO reductase with dismutating capability (Fig. 4; Huntemann *et al*., 2012). However, *M. ruestringensis* has not been investigated with respect to a dissimilatory nitrate metabolism. The genomic search did not reveal related NO reductases in *Dechloromonas aromatica* strain RCB, a facultatively anaerobe reducing nitrate (or chlorate) aromatic compounds even though its genome lacks typical enzymes for metabolizing the latter anaerobically (Salinero *et al*., 2009). However, its genome did not reveal an enzyme related to NO-reductase of strains HdN1 or *M. oxyfera* that could explain the metabolism of aromatics. On the other hand, certain phylogenetically unrelated NO reductases may also dismutate NO.

In conclusion, NO dismutation would further underscore the biological versatility of this toxic and amazingly simple compound. Other established usages and reactions are, besides reduction to N_2O common to denitrifiers, reduction to hydrazine ($H_2N–NH_2$) as key intermediate in anaerobic ammonium oxidation (Kartal *et al*., 2011), complete (possibly accidental) reduction to NH_4^+ by a multiheme enzyme (Costa *et al*., 1990), reduction to N_2O for the purpose of detoxification (Arkenberg *et al*., 2011 and references therein), and its wide-ranging significance as a signaling compound in higher organisms (Ignarro, 2002; Besson-Bard *et al*., 2008).

Experimental procedures

Gas analyses

N_2, N_2O and CO_2 in experiments revealing alkane utilization were analyzed by gas chromatography and thermal conductivity detection as described (Zedelius *et al*., 2011; Appendix S1).

Analysis of trace gases including those with isotope label was performed in a headspace-free incubation vial (370 ml) connected directly to a membrane-inlet mass spectrometer (MIMS; Kana *et al*., 1994, Ettwig *et al*., 2010). Cells grown with *n*-tetradecane and NO_3^- were first pre-incubated for two days with N_2O and then for one day with additional acetylene. The culture was anoxically transferred to the reaction vial, also filling a connected, not-intermixed reservoir. A slow (0.6 ml min^{-1}) flow transported the stirred culture liquid from the vial 'online' to the MIMS inlet. Solutes were injected with He-flushed syringes.

Experiments with NO

NO gas was liberated by reduction of $NaNO_2$ with KI in H_2SO_4, trapped and used to saturate anoxic H_2O (*c*. 1.9 mM NO at ambient pressure) as described (Schreiber *et al*., 2008). The NO-solution was injected. Alternatively the slow-release NO-donor 3,3-Bis(aminoethyl)-1-hydroxy-2-oxo-1-triazene (NOC-18) (Sigma Aldrich) in anoxic, Ar-saturated H_2O was applied (details in Appendix S1).

Comparative genomics and gene analysis

For enzyme search, sequences (≥50 amino acids) of all predicted open reading frames of strain HdN1 were blasted (cutoff $E > 10^{-10}$) against 794 non-redundant genomes (one per genus) selected from 1493 completely sequenced bacterial genomes (ftp://ftp.ncbi.nih.gov/genomes/bacteria/all.gbk.tar.gz). Only the best 20 hits were kept. Among these, eight open reading frames revealing a protein of Candidatus *M. oxyfera* were further inspected manually.

For sequence comparison, 1962 full length amino acid sequences of heme-copper oxidase family members (CCD206949) were obtained with text and homology searches from Genbank. The sequences were analyzed with UCLUST (Edgar, 2010) to generate clusters with

≥70% amino acid identity. Using a representative from each cluster (536 in total), sequences were aligned with MAFFT (Katoh *et al*., 2002). A phylogenetic tree based on an approximate maximum likelyhood algorithm was created with FastTree2 (Price *et al*., 2010). All sequences (112) belonging to the phylogenetic clade that contained the canonical nitric oxide reductases (encoded by *norB* and *norZ*) were extracted and realigned more precisely (MAFFT, maxiterate 1000 option). The alignment was inspected manually with JalView (Waterhouse *et al*., 2009). After applying a 10% conservation filter reducing the alignment from 1473 to 755 columns (the most conserved ones), a phylogenetic tree was created with FastTree2. Robustness of bifurcations (instead of "bootstrap" values; Price *et al*., 2010) were estimated using gamma20 likelihoods.

Shotgun proteomic analysis

Medium with cells (400 ml) of strain HdN1 growing with tetradecane, tetradecene or tetradecanoate by NO_3^--respiration or under air was separated from the carbon substrate by a separatory funnel or by filtration (Whatman, grade 595) and subsequently harvested by centrifugation. Hydrocarbon-grown cells were partly buoyant (Zedelius *et al*., 2011) so that the pellet yield was low. The problem was overcome by repeating the addition of (10 mM) nitrate. Pellets were washed with anoxic Tris-buffer, shock-frozen with liquid N_2 and stored at −80°C until further analysis. Cell breakage by ultrasonication, cysteine alkylation, protein digestion by trypsin or ApsN, peptide separation by 1D-nano-LC (Ettan MDLC, GE Healthcare) and identification with a linear ion trap mass spectrometer (Thermo LTQ, Thermo Fischer) were performed by Toplab (Martinsried, Germany) as described (Trautwein *et al*., 2012).

Fatty acid methyl ester (FAME) and wax ester analysis

Cellular fatty acids were converted to methyl esters (FAMEs) and separated by gas chromatography as described (Sasser *et al*., 1990). Individual FAMEs were identified by their retention times and those of authentic standards. Long-chain wax esters were analyzed via gas chromatography-mass spectrometry, based on their retention times and mass fingerprints in comparison to those of an authentic hexadecyl hexadecanoate standard (Appendix S1).

Acknowledgements

We thank Gaute Lavik and Jens Harder for helpful discussion, and Katharina Ettwig for kindly providing information about Candidatus *M. oxyfera*. This research was supported by the Max-Planck-Gesellschaft.

References

Aeckersberg, F., Rainey, F.A., Widdel, F. (1998) Growth, natural relationships, cellular fatty acids and metabolic adaptation of sulfate-reducing bacteria that utilize long-chain alkanes under anoxic conditions. *Arch Microbiol* **170:** 361–369.

Aguilar, P.S., de Mendoza, D. (2006) Control of fatty acid desaturation: a mechanism conserved from bacteria to humans. *Mol Microbiol* **62:**1507–1514.

Arkenberg, A., Runkel, S., Richardson, D.J., and Rowley, G. (2011) The production and detoxification of a potent cytotoxin, nitric oxide, by pathogenic enteric bacteria. *Biochem Soc Trans* **39:** 1876–1879.

Besson-Bard, A., Pugin, A., and Wendehenne, D. (2008) New insights into nitric oxide signaling in plants. *Annu Rev Plant Biol* **59:** 21–39.

Birch, L.D., and Bachofen, R. (1988) Microbial production of hydrocarbons. In *Biotechnology*. Rehm, H.J. (ed). Weinheim: Verlag Chemie, pp. 71–99.

Blomberg, M.R., Siegbahn, P.E. (2012) Mechanism for N_2O generation in bacterial nitric oxide reductase: a quantum chemical study. *Biochemistry* **51:** 5173–5186.

Britton, L.N. (1984) Microbial degradation of aliphatic hydrocarbons. *In* Microbial degradation of organic compounds. Gibson, T.D. (ed.). New York, Marcel Dekker, pp 89–129.

Bruns, A., Rohde, M., Berthe-Corti, L. (2001) *Muricauda ruestringensis gen. nov., sp nov*., a facultatively anaerobic, appendaged bacterium from German North Sea intertidal sediment. *Int J Syst Evol Microbiol* **51:** 1997–2006.

Costa, C., Macedo, A., Moura, I., Moura, J.J.G., Legall, J., Berlier, Y. *et al*. (1990) Regulation of the hexaheme nitrite nitric-oxide reductase of *Desulfovibrio desulfuricans*, *Wolinella succinogenes* and *Escherichia coli* – a mass-spectrometric study. *FEBS Lett* **276:** 67–70.

Cramm, R., Siddiqui, R.A., Friedrich, B. (1997) Two isofunctional nitric oxide reductases in *Alcaligenes eutrophus* H16. *J Bacteriol* **179:** 6769–6777.

de Geus, D.C., Thomassen, E.A.J., Hagedoorn, P.L., Pannu, N.S., van Duijn, E., Abrahams, J.P. (2009) Crystal structure of chlorite dismutase, a detoxifying enzyme producing molecular oxygen. *J Mol Biol* **387:** 192–206.

Dermer, J., Fuchs, G. (2012) Molybdoenzyme that catalyzes the anaerobic hydroxylation of a tertiary carbon atom in the side chain of cholesterol. *J Biol Chem*, doi: 10.1074/jbc.M112.407304.

Deutzmann, J.S., Schink, B. (2011) Anaerobic oxidation of methane in sediments of lake Constance, an oligotrophic freshwater lake. *Appl Environ Microbiol* **77:** 4429–4436

Edgar, R.C. (2010) Search and clustering orders of magnitude faster than BLAST. *Bioinformatics* **26:** 2460–2461.

Ehrenreich, P., Behrends, A., Harder, J., Widdel, F. (2000) Anaerobic oxidation of alkanes by newly isolated denitrifying bacteria. *Arch Microbiol* **173:** 232–232.

Ettwig, K.F., Butler, M.K., Le Paslier, D., Pelletier, E., Mangenot, S., Kuypers, M.M.M., *et al.* (2010) Nitrite-driven anaerobic methane oxidation by oxygenic bacteria. *Nature* **464:** 543–548.

Ettwig, K.F., Speth, D.R., Reimann, J., Wu, M.L., Jetten, M.S.M. and Keltjens, J.T. (2012) Bacterial oxygen production in the dark. *Front. Microbio.* 3:273. doi:10.3389/fmicb.2012.00273

Fujiwara, T. and Fukumori, Y. (1996) Cytochrome *cb*-type nitric oxide reductase with cytochrome *c* oxidase activity from *Paracoccus denitrificans* ATCC 35512. *J Bacteriol* **178:** 1866–1871.

Giuffre, A., Stubauer, G., Sarti, P., Brunori, M., Zumft, W.G., Buse, G. and Soulimane, T. (1999) The heme-copper oxidases of Thermus thermophilus catalyze the reduction of nitric oxide: Evolutionary implications. *Proc Natl Acad Sci* USA **96:** 14718–14723.

Groves, J.T. (2006) High-valent iron in chemical and biological oxidations. *J Inorg Biochem* **100:** 434–447.

Grundmann, O., Behrends, A., Rabus, R., Amann, J., Halder, T., Heider, J., Widdel, F. (2008) Genes encoding the candidate enzyme for anaerobic activation of *n*-alkanes in the denitrifying bacterium, strain HxN1. *Environ Microbiol* **10:** 376–385.

Hamamura, N., Storfa, R.T., Semprini, L., Arp, D.J. (1999) Diversity in butane monooxygenases among butane-grown bacteria. *Appl Environ Microbiol* **65:** 4586–4593

Hayashi, T., Lin, M.T., Ganesan, K., Chen, Y., Fee, J.A., Gennis, R.B. and Moenne-Loccoz, P. (2009) Accommodation of two diatomic molecules in cytochrome bo_3: insights into NO reductase activity in terminal oxidases. *Biochemistry* **48:** 883–890.

Heider, J. (2007) Adding handles to unhandy substrates: anaerobic hydrocarbon activation mechanisms. *Curr Opin in Chem Biol* **11:** 188–194.

Huntemann, M., Teshima, H., Lapidus, A., Nolan, M., Lucas, S., Hammon, N., *et al.* (2012) Complete genome sequence of the facultatively anaerobic, appendaged bacterium *Muricauda ruestringensis* type strain (B1T). *Stand Genomic Sci* **6:** 185–193.

Ignarro, L.J. (2002) Nitric oxide as a unique signaling molecule in the vascular system: a historical overview. *J Physiol Pharmacol* **53:** 503–514.

Ishige, T., Tani, A., Sakai, Y.R., Kato, N. (2003) Wax ester production by bacteria. *Curr Opin Microbiol* **6:** 244–250.

Jarling, R., Sadeghi, M., Drozdowska, M., Lahme, S., Buckel, W., Rabus, R., *et al.* (2012) Stereochemical investigations reveal the mechanism of the bacterial activation of *n*-alkanes without oxygen. *Angew Chem Int Ed Engl* **51:** 1334–1338.

Kana, T.M., Darkangelo, C., Hunt, M.D., Oldham, J.B., Bennett, G.E., and Cornwell, J.C. (1994) Membrane Inlet Mass-Spectrometer for Rapid High-Precision Determination of N-2, O-2, and Ar in Environmental Water Samples. *Anal Chem* **66:** 4166–4170.

Kartal, B., Maalcke, W.J., de Almeida, N.M., Cirpus, I., Gloerich, J., Geerts W., *et al.* (2011) Molecular mechanism of anaerobic ammonium oxidation. *Nature* **479:** 127–130.

Katoh, K., Misawa, K., Kuma, K., Miyata, T. (2002) MAFFT: a novel method for rapid multiple sequence alignment based on fast Fourier transform. *Nucleic Acids Res* **30:** 3059-3066

Kloer, D.P., Hagel, C., Heider, J., Schulz, G.E. (2006) Crystal structure of ethylbenzene dehydrogenase from *Aromatoleum aromaticum*. *Structure* **14:** 1377–1388.

Knittel, K., Boetius, A. (2009) Anaerobic oxidation of methane: progress with an unknown process. *Annu Rev Microbiol* **63:** 311–334.

Kristjansson, J.K., Hollocher, T.C. (1980) 1st practical assay for soluble nitrous-oxide reductase of denitrifying bacteria and a partial kinetic characterization. *J Biol Chem* **255:** 704–707.

Kropp, K.G., Davidova, I.A., and Suflita, J.M. (2000) Anaerobic oxidation of n-dodecane by an addition reaction in a sulfate-reducing bacterial enrichment culture. *Appl Environ Microbiol* **66:** 5393–5398.

Krüger, M., Meyerdierks, A., Glockner, F.O., Amann, R., Widdel, F., Kube, M., *et al.* (2003) A conspicuous nickel protein in microbial mats that oxidize methane anaerobically. *Nature* **426:** 878–881.

Lewis, R.S., Deen, W.M. (1994) Kinetics of the reaction of nitric-oxide with oxygen in aqueous-solutions. *Chem Res Toxicol* **7:** 568–574.

Magnusson, T.O., Toyama, H., Saeki, M., Rojas, A., Reed, J.C., Liddington, R.C., *et al.* (2004) Quinone biogenesis: Structure and mechanism of PqqC, the final catalyst in the production of pyrroloquinoline quinone. *Proc Natl Acad Sci* USA **101:** 7913–7918.

Matsumoto, Y., Tosha, T., Pisliakov, A.V., Hino, T., Sugimoto, H., Nagano, S. *et al*. (2012) Crystal structure of quinol-dependent nitric oxide reductase from Geobacillus stearothermophilus. *Nat Struct Mol Biol* **19:** 238–245.

Mehboob, F., Junca, H., Schraa, G., Stams, A.J.M. (2009) Growth of *Pseudomonas chloritidismutans* AW-1(T) on *n*-alkanes with chlorate as electron acceptor. *Appl Microbiol Biotechnol* **83:** 739–747.

Michel, H. (1999) Cytochrome *c* oxidase: Catalytic cycle and mechanisms of proton pumping – a discussion. *Biochemistry* **38:** 15129–15140.

Oosterkamp, M.J., Mehboob, F., Schraa, G., Plugge, C.M., Stams, A.J.M. (2011) Nitrate and (per)chlorate reduction pathways in (per)chlorate-reducing bacteria. *Biochem Soc Trans* **39:** 230–235.

Price, M.N., Dehal, P.S., Arkin, A.P. (2010) FastTree 2-approximately maximum-likelihood trees for large alignments. *PLoS One* **5:** e9490.

Rabus, R., Wilkes, H., Behrends, A., Armstroff, A., Fischer, T., Pierik, A.J., Widdel, F. (2001) Anaerobic initial reaction of *n*-alkanes in a denitrifying bacterium: Evidence for (1-methylpentyl)succinate as initial product and for involvement of an organic radical in *n*-hexane metabolism. *J Bacteriol* **183:** 1707–1715.

Salinero, K.K., Keller, K., Feil, W.S., Feil, H., Trong, S., Di Bartolo, G., Lapidus, A. (2009) Metabolic analysis of the soil microbe *Dechloromonas aromatica* str. RCB: indications of a surprisingly complex life-style and cryptic anaerobic pathways for aromatic degradation. *BMC Genomics* **10:** 351

Sasser, M. (1990) Identification of bacteria by gas chromatography of cellular fatty acids. *Newsletter US Fed Cul Coll*: 1–6.

Scheller, S., Goenrich, M., Boecher, R., Thauer, R.K., Jaun, B. (2010) The key nickel enzyme of methanogenesis catalyses the anaerobic oxidation of methane. *Nature* **465:** 606–608.

Schreiber, F., Polerecky, L., de Beer, D. (2008) Nitric oxide microsensor for high spatial resolution measurements in biofilms and sediments. *Anal Chem* **80:** 1152–1158.

Scott, C.C.L., Finnerty, W.R. (1976) Characterization of intracytoplasmic hydrocarbon inclusions from hydrocarbon-oxidizing *Acinetobacter* species Ho1-N. *J Bacteriol* **127:** 481–489.

Shima, S., Krueger, M., Weinert, T., Demmer, U., Kahnt, J., Thauer, R.K., Ermler, U. (2012) Structure of a methyl-coenzyme M reductase from Black Sea mats that oxidize methane anaerobically. *Nature* **481:** 98–101.

Simon, J., van Spanning, R.J.M., and Richardson, D.J. (2008) The organisation of proton motive and non-proton motive redox loops in prokaryotic respiratory systems. *Biochim Biophys Acta-Bioenergetics* **1777:** 1480–1490.

So, C.M., Phelps, C.D., Young, L.Y. (2003) Anaerobic transformation of alkanes to fatty acids by a sulfate-reducing bacterium, strain Hxd3. *Appl Environ Microbiol* **69**: 3892–3900.

Stewart, J.E., Kallio, R.E. (1959) Bacterial hydrocarbon oxidation 2. Ester formation from alkanes. *J Bacteriol* **78:** 726–730.

Thauer, R.K. (1998) Biochemistry of methanogenesis: a tribute to Marjory Stephenson. *Microbiology-UK* **144:** 2377–2406.

Thauer, R.K. (2011) Anaerobic oxidation of methane with sulfate: on the reversibility of the reactions that are catalyzed by enzymes also involved in methanogenesis from CO_2. *Curr Opin Microbiol* **14:** 292–299.

Tissot, B.P., Welte, D.H. (1984) *Petroleum formation and occurence*. 2nd edn, New York, USA: Springer.

Trautwein, K., Lahme, S., Wöhlbrand, L., Feenders, C., Mangelsdorf, K., Harder, J., *et al*. (2012) Physiological and proteomic adaptation of "*Aromatoleum aromaticum*" EbN1 to low growth rates in benzoate-limited, anoxic chemostats. *J Bacteriol* **194:** 2165–2180.

Waterhouse, A.M., Procter, J.B., Martin, D.M.A., Clamp, M., Barton, G.J. (2009) Jalview version 2 – a multiple sequence alignment editor and analysis workbench. *Bioinformatics* **25:** 1189–1191.

Widdel, F., Grundmann, O., (2010) Biochemistry of the anaerobic degradation of non-methane alkanes. In *Handbook of hydrocarbon and lipid microbiology*, Vol. 2. *Timmis, K.N.* (ed.). Heidelberg, Germany: Springer, pp. 909–924.

Widdel, F., Knittel, K., Galushko, A. (2010) Anaerobic hydrocarbon-degrading microorganisms: An overview. In *Handbook of hydrocarbon and lipid microbiology*, Vol. 2. *Timmis, K.N.* (ed.). Heidelberg, Germany: Springer, pp. 1998–2015.

Wu, M.L., de Vries, S., van Alen, T.A., Butler, M.K., den Camp, H.J.M.O., Keltjens, J.T., *et al*. (2011) Physiological role of the respiratory quinol oxidase in the anaerobic nitrite-reducing methanotroph 'Candidatus *Methylomirabilis oxyfera'*. *Microbiology* **157:** 890–898.

Yeager, C.M., Bottomley, P.J., Arp, D.J., Hyman, M.R. (1999) Inactivation of toluene 2-monooxygenase in Burkholderia cepacia G4 by alkynes. *Appl Environ Microbiol* **65:** 632–639.

Zedelius, J., Rabus, R., Grundmann, O., Werner, I., Brodkorb, D., Schreiber, F., *et al.* (2011) Alkane degradation under anoxic conditions by a nitrate-reducing bacterium with possible involvement of the electron acceptor in substrate activation. *Environ Microbiol Reports* **3:** 125–135.

Zumft (1993) The biological role of nitric oxide in bacteria. *Arch Microbiol* **160:** 253–264.

Zumft, W.G. (2005) Nitric oxide reductases of prokaryotes with emphasis on the respiratory, heme-copper oxidase type. *J Inorg Biochem* **99:** 194–215.

Appendix S1

Supporting Information for Results

Calculated N_2 and CO_2 formation from NO-respiration with hexadecane

Respiratory consumption of NO with hexadecane as electron donor according to

$$2\ C_{16}H_{34} + 98\ NO \rightarrow 32\ CO_2 + 49\ N_2 + 34\ H_2O, \qquad (S1)$$

leads to $^{1}/_{2}$ N_2 / NO and $^{16}/_{49} \approx 0.327$ CO_2 / NO. Thus, exclusive respiratory use of the addition of 5×0.5 µmol NO = 2.5 µmol NO would have yielded 1.25 µmol N_2 and 0.816 µmol CO_2. In Fig. 1, these amounts were graphically added on top of the respective time courses of the control experiment without injection of NO.

Table S1. Comparative genomics of strain HdN1 and Candidatus *Methylomirabilis oxyfera* on the level of translated amino acid sequences[a].

Strain HdN1	***M. oxyfera***	**Annotation**	**Pos.[b]**	**Identity**	**Length**	**Transcription level[c]**
identifier	identifier			(%)		(× cov.)
HDN1F	DAMO					
_01080	_0255	Haloacid dehalogenase-like hydrolase	1	37	1081	0.5
_02620	**_2437**	**NO reductase**	**1**	**60**	**787**	**353.0**
	_2434		**2**	**59**	**787**	**78.0**
_02670	**_2439**	**O_2 / light sensor, transcriptional regulator**	**1**	**39**	**217**	**12.0**
_06090	_0203	Glycosyl transferase	4	34	242	0.2
_07920	_1661	Tryptophan tryptophylquinone biosynthesis enzyme	6	42	353	0.6
_14990	_2509	Antitoxin of toxin-antitoxin stability system	1	72	85	1.4
_19430	_1222	Membrane protein involved in aromatic hydrocarbon degradation	2	32	424	0.2
_21280	_2380	Cysteine desulfurase	3	57	416	2.0
_22750	_1582	Plasmid maintenance system antidote protein	8	48	91	0.0
_25900	_2194	Transcriptional regulator	7	67	91	1.7
_25910	_2193	Phage derived protein Gp49-like (DUF891)	4	59	97	3.6
_27170	_0773	C_4-dicarboxylate transporter	1	56	330	0.6
_31800	_0361	Hypothetical protein (OsmC-like)	3	40	148	0.2
_33430	_1265	Hypothetical protein	8	30	147	0.1
_35720	_0450	Lytic murein transglycosylase	5	42	203	1.9
_36560	_1264	TonB-dependent receptor	1	35	682	0.6
_37120	_1304	Hypothetical patatin/ phospholipase	5	36	460	1.1

a. Alignment via BLAST

b. Position of the hit among the best hits.

c. Transcription level indicates the sequencing coverage of the gene in the *Methylomirabilis* transcriptomic study (Ettwig *et al*, 2010).

Table S2. Detected proteins in strain HdN1 possibly involved in alkane degradation and denitrification. Cells were grown anaerobically or aerobically with *n*-tetradecane or *n*-tetradecanoic acid

Identifier	By relationship annotated as		Average score of protein[c] in strain HdN1			
HDN1F						
	Name	**Function[a]**	**NO_3^- (– O_2)**		**O_2 (– NO_3^-)**	
			$C_{14}H_{30}$	**$C_{13}H_{27}CO_2^-$**	**$C_{14}H_{30}$**	**$C_{13}H_{27}CO_2^-$**
Denitrification						
_13240	NarG	NO_3^- reductase, alpha subunit	2391	2954	1001	91
_13250	NarH	NO_3^- reductase, beta subunit	991	896	592	98
_13260	NarJ	NO_3^- reductase, delta subunit	120[d]	n.d.	94[e]	n.d.
_13270	NarI	NO_3^- reductase, gamma subunit	n.d.	84[e]	n.d.	n.d.
_37070	NirS	Dissimil. cytochrome cd_1 NO_2^- reductase precursor	2038	1923	2046	1955
_02620	'Nod' [b]	Candidate NO dismutase	**1100**	488	**n.d.**	**n.d.**
_20450	NorZ	NO reductase (qNor)	n.d.	n.d.	n.d.	n.d.
_37100	NorB	NO reductase (cNor), subunit B	n.d.	n.d.	n.d.	n.d.
_37110	NorC	NO reductase (cNor), subunit C	n.d.	85	113[e]	116
_37580	NosZ	N_2O reductase	335[d]	1327	571	844
Alkane degradation						
_17550	–	Ferredoxin	138	n.d.	108[d]	n.d.
_17560	AhpG	Cyt. P450 alkane hydroxylase	1608	n.d.	464	n.d.
_17570	–	Ferredoxin reductase	487	n.d.	n.d.	n.d.
_04190	AlkM	Alkane monooxygenase	670	n.d.	598	n.d.
_12450	–	Dioxygenase ferredoxin reductase component	79	n.d.	n.d.	n.d.
_14540	–	Monooxygenase flavoprotein	569	n.d.	327	n.d.
_26430	–	2-Nitropropane dioxygenase	405	347	431	303
_30550	CypX	Cytochrome P450	120	63[e]	n.d.	n.d.

a. Proteins colored grey are indirectly related to oxygenases by chromosomal proximity or functional prediction

b. Gene designation "*nod*" adapted from Ettwig *et al*. (2012)

c. Listed proteins have been identified in three independent biological replicates (except for **d**: identified twice; **e**: identified once) n.d. not detected

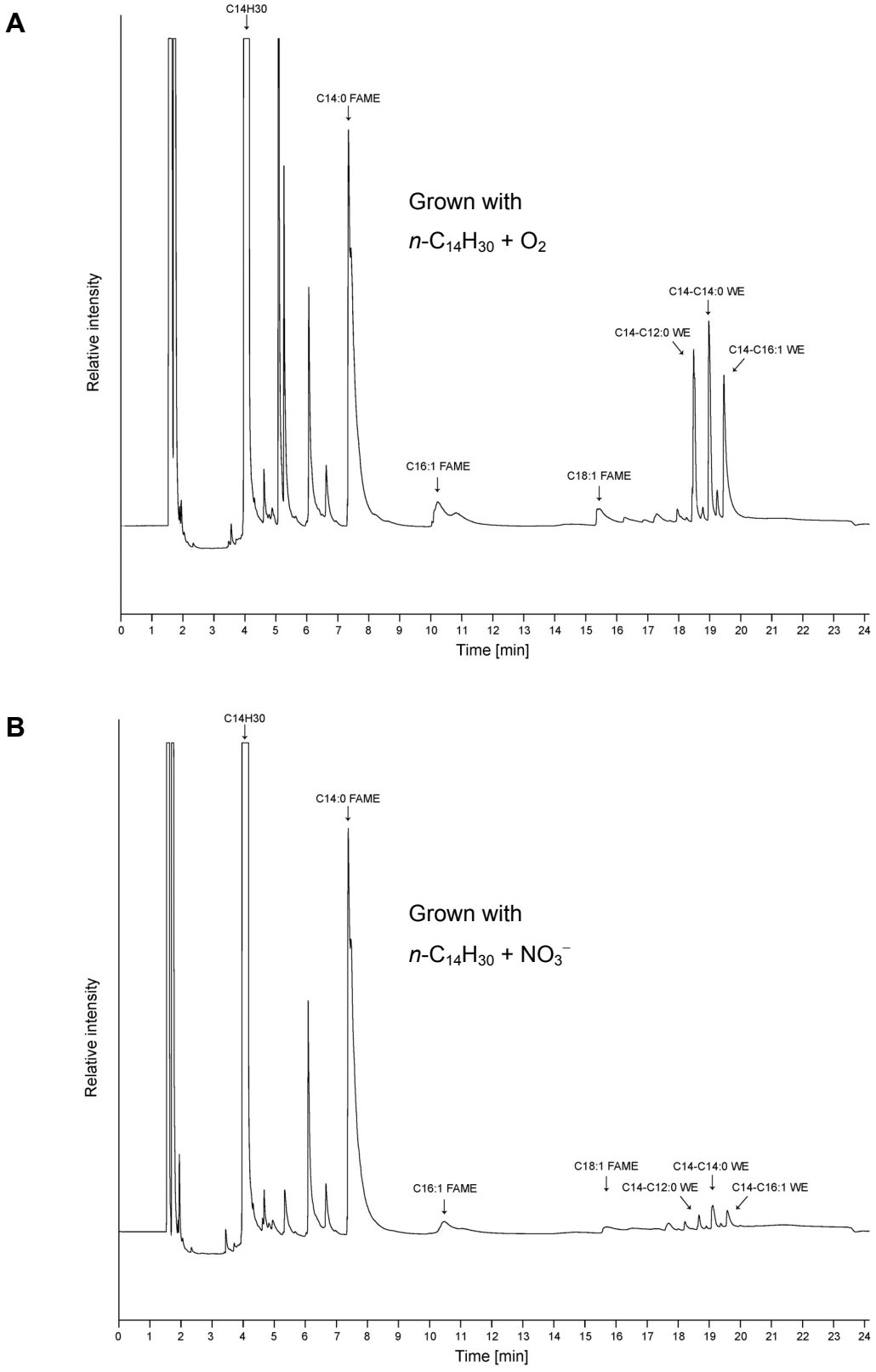
A
C14H30
C14:0 FAME
Grown with
n-C14H30 + O2
C14-C14:0 WE
C14-C12:0 WE
C14-C16:1 WE
C16:1 FAME
C18:1 FAME
Relative intensity
Time [min]
B
C14H30
C14:0 FAME
Grown with
n-C14H30 + NO3−
C18:1 FAME
C14-C14:0 WE
C16:1 FAME
C14-C12:0 WE
C14-C16:1 WE
Relative intensity
Time [min]

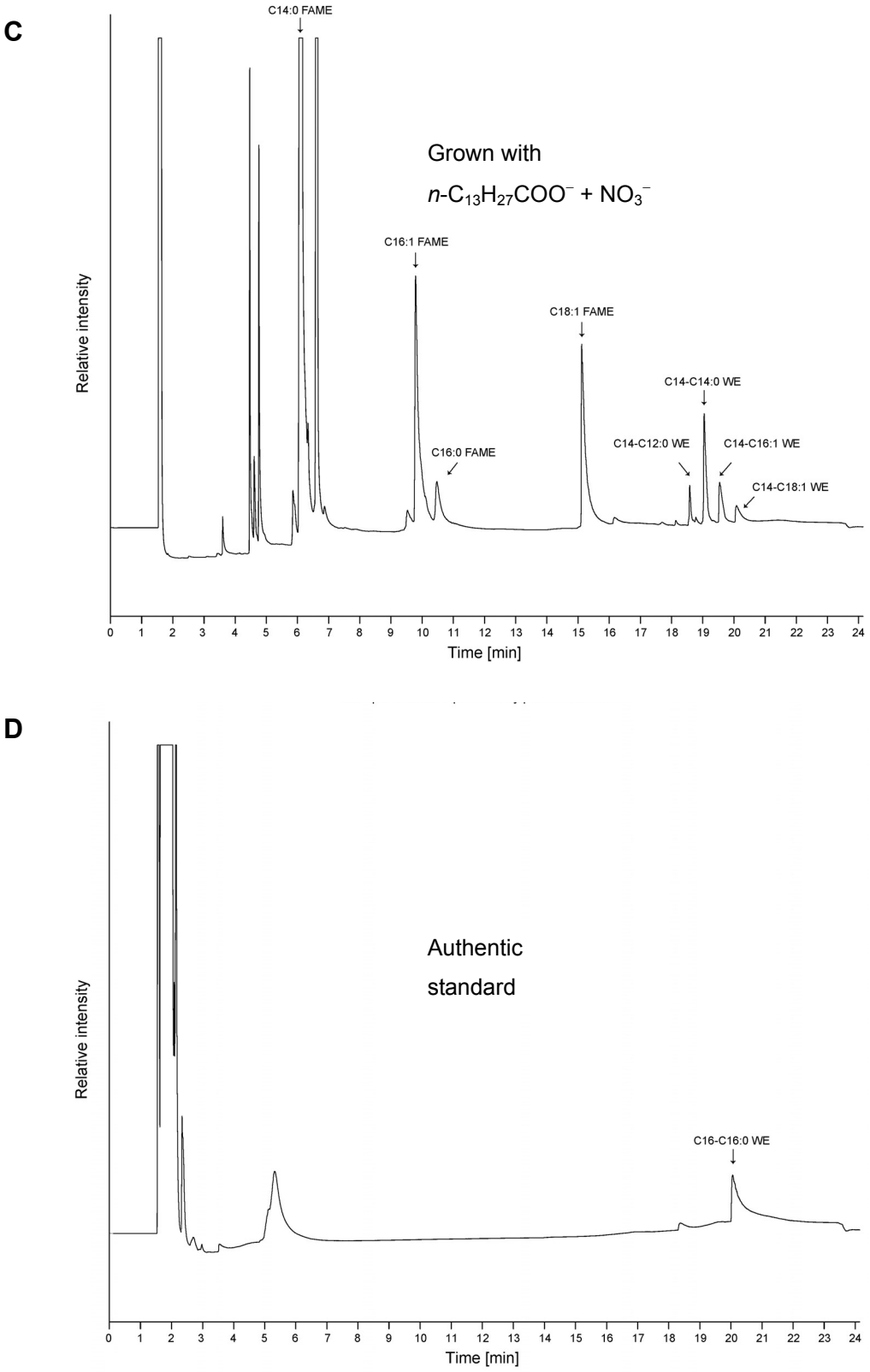

Fig. S1. Identification of wax esters in strain HdN1 upon aerobic (A) or denitrifying (B) growth with *n*-tetradecane. For comparison, a culture grown anaerobically with *n*-tetradecanoate was included (C). Saturation or unsaturation is indicated for the fatty acid moiety (acyl chain). The authentic standard (D) was cetyl-palmitat (hexadecyl-hexadecanoate, C16-C16:0 WE).

Supporting Information for Discussion

Hypothetical dismutation of NO-Dismutation to NO_2^- and N_2O

If external NO is added, the reverse nitrite reductase reaction could generate electrons of rather favorable potential ($2\ NO + 2\ H_2O \rightarrow 2\ NO_2^- + 4\ H^+ + 2\ e^-$; $E°' = +0.347$ V) for reducing another part of NO to N_2O ($2\ NO + 4\ H^+ + 2\ e^- \rightarrow N_2O + H_2O$; $E°' = +1.172$ V), resulting in dismutation (redox potentials in Thauer *et al*., 1977; Zedelius *et al*., 2011)

$$4\ NO + H_2O \rightarrow 2\ NO_2^- + 2\ H^+ + N_2O \qquad \text{(S2)}$$

$\Delta G°' = -40$ kJ $(\text{mol NO})^{-1}$

Interpretation of mass 32

Other biogenic compounds of mass 32 would be methanol (CH_3OH), hydrazine (N_2H_4) and hydrogen sulfide (H_2S). However, their formation upon nitrite addition to cells adapted to denitrification with long-chain alkanes is not expected.

Calculation of redox potentials of alcohol / alkane couples

Redox potentials given in the text as $E°'$ (i.e. for $pH = 7$) for dehydrogenation of saturated hydrocarbons to alcohols,

$$\text{AlkH} + H_2O \rightleftarrows \text{Alk–OH} + 2\ e^- + H^+,$$

$$\text{short form: AlkOH / AlkH} + H_2O \qquad \text{(S3)}$$

(Alk = prim., sec., tert. Alkyl)

at primary, secondary and tertiary carbon atoms were calculated from $\Delta_f G°$-values of the respective alcohols and alkanes (Table S4).

Table S4. Free energy of formation of selected alkanes and alcohols.

Compound	$\Delta_f G°$ / kJ mol^{-1}	Reference
CH_4 (g)	−50.75	(Thauer *et al*., 1977)
CH_3OH (aq)	−175.39	(Thauer *et al*., 1977)
$CH_3–CH_2–CH_3$ (g)	−17.2	(Speight, 2005)
$CH_3–CHOH–CH_3$ (aq)	−177.0	(Thauer *et al*., 1977)
$CH_3–CH_2–(CH_3)CH–CH_3$ (lq)	−13.71	[a]
	−14.6	(D'Ans Lax, 1983)
$CH_3–CH_2–(CH_3)OH–CH_3$ (lq)	−175.3	(Speight, 2005)
	−199	(D'Ans Lax, 1983)

[a] The $\Delta_f G°$-value of 2-methylbutane (lq) was calculated from $\Delta_f H°$ = 178.4 kJ mol^{-1} (Speight, 2005) and entropy of formation, $\Delta_f S°$ = −552.4 J K^{-1} mol^{-1}, as $\Delta_f G° = \Delta_f H° - T\,\Delta_f S°$ (T = 298 K). $\Delta_f S°$ was calculated from (the absolute) $S°$-values of $C_{graphite}$, H_2 (g) and 2-methylbutane (lq), which are 5.74, 130.68 and 260.4 J K^{-1} mol^{-1} respectively (Speight, 2005).

2-Methylbutan-2-ol (lq) was chosen because data for tertiary alcohols in aqueous (aq) reference state were not found. 2-Methylbutan-2-ol has limited solubility in H_2O so that liquid (lq) and aqueous (aq) state can be in equilibrium, i.e. reactions of aqueous state are energetically similar as reactions of liquid state. Values for 2-Methylbutan-2-ol (aq) based on Speight (2005) and D'Ans Lax (1983) deviate significantly, thus yielding rather different $E°$'-values for tertiary carbon dehydrogenation of −0.022 and −0.140 V, respectively.

Table S3. Range of *n*-alkanes used by some known aerobic bacteria

Acinetobacter sp. strain Ths	C_{13}–C_{30}
Alkanivorax borkumensis	C_9 –C_{32}
Marinobacter hydrocarbonoclasticus	C_{16}–C_{30}
Oleiphilius messinensis	C_{11}–C_{20}
Oleispira antarctica	C_{10}–C_{18}
Thalassolituus oleivorans	C_7 –C_{20}

Rate of the homo-bimolecular reaction of NO

Because NO_2 dismutation is strongly exergonic, there is essentially no reverse reaction so that the kinetic model with one lumped enzyme-bound state is

$$\mathbf{2\ NO} + \mathrm{E} \underset{v_{-1},\, k_{-1}}{\overset{v_{+1},\, k_{+1}}{\rightleftharpoons}} \mathrm{E}\,\mathbf{(NO)_2} \xrightarrow{v_{+2},\, k_{+2}} \mathbf{N_2 + O_2} \qquad \text{(S4)}$$

with k designating rate constants (rate coefficients assumed to be concentration-independent) and v the concentration dependent rates. In a steady state (no change of concentration of enzyme and enzyme-substrate complex), the rate of complex formation must equal the sum of the rates of complex decomposition, i.e.

$$v_{+1} = v_{-1} + v_{+2}\ , \qquad \text{(S5)}$$

or with corresponding rate constants and concentrations

$$k_{+1}[\mathrm{NO}]^2[\mathrm{E}] = k_{-1}[\mathrm{E(NO)_2}] + k_{+2}[\mathrm{E(NO)_2}]\ . \qquad \text{(S6)}$$

Because the net rate, which equals v_{+2}, is of interest, the concentration of the enzyme-substrate complex, $[E(NO)_2]$, must be known.

This is achieved by substituting $[E] = [E_t] - [E(NO)_2]$, where $[E_t]$ is total enzyme, and solving for $[E(NO)_2]$:

$$k_{+1}[\mathrm{NO}]^2([\mathrm{E_t}] - [\mathrm{E(NO)_2}]) = k_{+2}[\mathrm{E(NO)_2}] + k_{-1}[\mathrm{E(NO)_2}] \qquad \text{(S7)}$$

$$k_{+1}[\mathrm{NO}]^2[\mathrm{E_t}] = [\mathrm{E(NO)_2}](k_{-1} + k_{+2} + k_{+1}[\mathrm{NO}]^2) \qquad \text{(S8)}$$

$$[\mathrm{E(NO)_2}] = \frac{k_{+1}[\mathrm{NO}]^2[\mathrm{E_t}]}{k_{-1} + k_{+2} + k_{+1}[\mathrm{NO}]^2} = \frac{[\mathrm{NO}]^2[\mathrm{E_t}]}{\frac{k_{-1} + k_{+2}}{k_{+1}} + [\mathrm{NO}]^2}\ . \qquad \text{(S9)}$$

Then the rate is calculated as

$$v_{\mathrm{NO}} = \mathrm{k_{+2}}\,[\mathrm{E(NO)_2}] = \frac{[\mathrm{NO}]^2 k_{+2}[\mathrm{E_t}]}{\frac{k_{-1} + k_{+2}}{k_{+1}} + [\mathrm{NO}]^2}\ . \qquad \text{(S10)}$$

The product k_{+2} [E_t] is the maximum rate, v_{max}, that would be achieved with fully saturated enzyme. The expression ($k_{-1} + k_{+2}$)/k_{+1} is defined as another constant (composite constant), K_m, so that

$$v_{NO} = \frac{v_{max}[NO]^2}{k_m + [NO]^2} . \quad (S11)$$

There is an NO concentration that yields half of the maximum rate, $v_{max}/2$, and which is designated $[NO]_{v_{max}/2}$. Hence, this is calculated as

$$0.5\, v_{max} = \frac{v_{max}[NO]^2_{v_{max}/2}}{K_m + [NO]^2_{v_{max}/2}} \quad (S12)$$

$$0.5 = \frac{[NO]^2_{v_{max}/2}}{K_m + [NO]^2_{v_{max}/2}} \quad (S13)$$

$$[NO]_{v_{max}/2} = \sqrt{K_m} . \quad (S14)$$

The 'classical' equation of a monomolecular reaction of a compound A (or a bimolecular reaction with co-reactants of constant concentration) is

$$v_A = \frac{v_{max}[A]}{K_m + [A]} . \quad (S15)$$

Here, the half-maximum rate is

$$0.5\, v_{max} = \frac{v_{max}[A]_{v_{max}/2}}{K_m + [A]_{v_{max}/2}} , \quad (S16)$$

so that

$$[A]_{v_{max}/2} = K_m . \quad (S17)$$

Details of Experimental Procedures

Preparation of solutions of NO and slow-release NO-donor

NO gas was prepared by reduction of $NaNO_2$ with KI in aqueous H_2SO_4,

$$2\ NO_2^- + 2\ I^- + 4\ H^+ \rightarrow 2\ NO\uparrow + I_2 + 2\ H_2O, \qquad \text{(S18)}$$

dissolved in anoxic H_2O to saturation (1.9 mM NO at ambient pressure) as described (Schreiber *et al*., 2008), and stored in butyl-rubber sealed glass tubes or serum bottles. A solution of the slow-release (half-life time, *c*. 57 h; Hrabie *et al*., 1993) NO-Donor 3,3-bis(aminoethyl)-1-hydroxy-2-oxo-1-triazene (Fig. S2; NOC-18, Sigma Aldrich) was prepared by dissolving 1 mg in 1 ml of phosphate buffer (0.1 M, *pH* = 7.4) in a tube (4.5 ml). The tube was sealed with a butyl rubber septum and deoxygenated by passing Ar for 15 min via hypodermic needles through the septum.

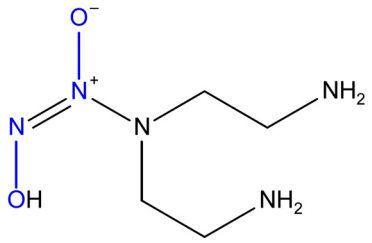

Fig. S2. The two NO-moieties (blue) of NOC-18 are slowly released as NO.

Headspace gas analysis

N_2, CO_2 and N_2O levels in the headspace of anoxic cultures were measured using a GC 8A gas chromatograph (Shimadzu) equipped with a thermal conductivity detector (TCD) and a Porapak Q column (Sigma-Aldrich, St. Luis, USA). Argon was used as carrier with a flowrate of 15 ml min^{-1}. Cultures which received the additions were pre-incubated with 20 µmol NO_2^- to ensure a metabolically active state. Additions were injected when N_2 or CO_2 production with nitrite had ceased. Amounts of N_2 and CO_2 present at this point (day zero) were subtracted to consider only the production from the additions. Controls did not receive any addi-

tions and were not pre-incubated with nitrite. For calculation of absolute amounts, the dissolved fraction was accounted for as described before (Zedelius *et al*., 2011). Serum bottles (165 ml) were filled with 10 ml phosphate-buffered anoxic medium under an atmosphere of argon and closed with butyl rubber stoppers and aluminum crimps. Duplicates for each culture condition were prepared and measured twice at each sampling point.

Culture preparation for membrane-inlet mass spectrometry (MIMS)

HdN1 cultures were grown anaerobically in 500 ml rubber-stoppered glass bottles with 10 mM $NaNO_3$ and 500 µl *n*-tetradecane in 400 ml He-saturated, phosphate buffered (30 mM) medium at 28°C. When all nitrate was reduced (as checked with Merckoquant test strips; Merck), 50 ml of N_2O gas (Air Liquide) was added to the culture headspace. Two days later, acetylene-saturated water was injected (10%, vol/vol). After 12 h incubation, the cells were anoxically transferred into the MIMS-setup by application of an Ar-overpressure. The setup had been deoxygenated before by flushing with He.

Setup for membrane-inlet mass spectrometry (MIMS)

The MIMS-setup was essentially as described by (Ettwig *et al*., 2010). In short, it consisted of a gas-tight round reactor without headspace connected to a membrane-inlet for mass spectrometric analysis (Fig. S3). The reactor was constantly mixed by a glass-coated stir bar. Liquid from the reactor was pumped constantly at ~0.7 ml min^{-1} to the membrane-inlet via gas tight tubing. When the pumped liquid reached the silicone membrane, volatile non-ionic compounds diffused into the quadrupole mass spectrometer (GAM 200, InProcess Instruments, Bremen, Germany) via a cold-trap (−20°C) to remove water. The reactor was connected to a culture reservoir which was connected to a helium-line, thus excluding suction of air if the culture level dropped. Dissolved compounds were injected into the reactor via stoppers by means of anoxic syringes. Mixing with the reservoir was marginal because the connection was narrow (3–5 mm) and long (115 mm).

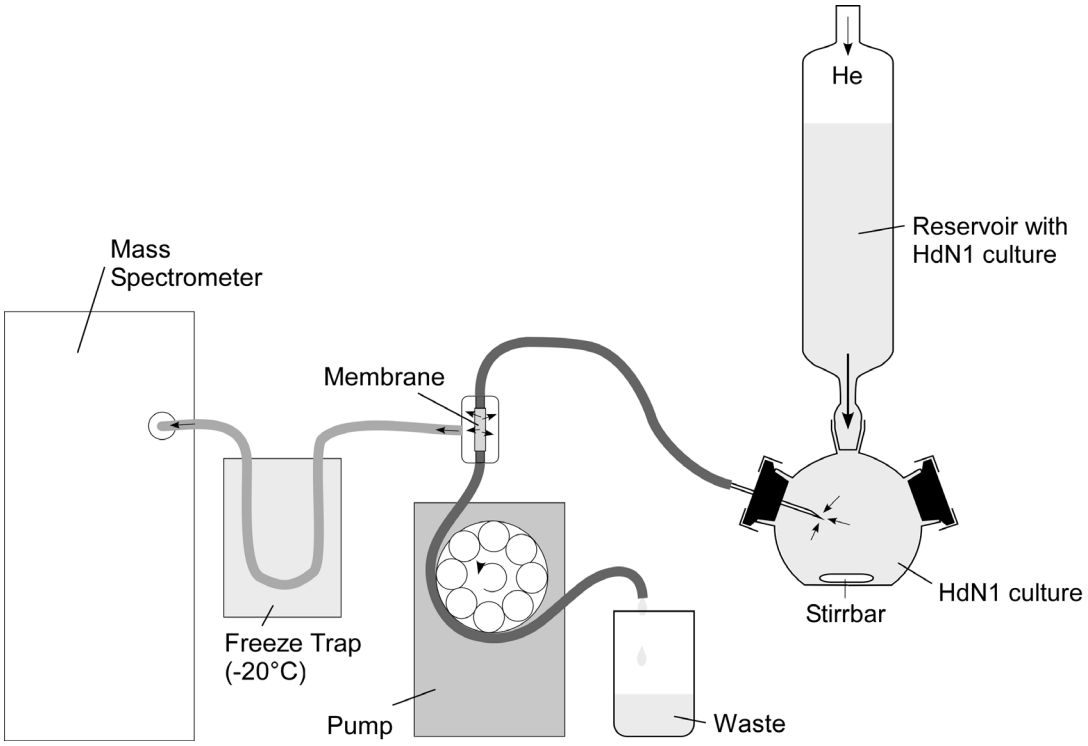

Fig. S3. MIMS setup for real-time analyses of volatile compounds dissolved in the culture liquid.

Analysis of fatty acid methyl (FAME) and wax esters

Cellular fatty acids were converted to fatty acid methyl esters (FAMEs) and analyzed by gas chromatography (GC) or gas chromatography mass spectrometry (GCMS) as described (Sasser *et al*., 1990). Cells (*c*. 0.2 g wet mass) were aerobically or anaerobically grown in 400 ml medium with the indicated carbon and electron source and harvested by centrifugation. In tetradecane and tetradecanoate cultures, the organic substrate was removed as described for the preparation of shotgun proteomic analysis (Experimental procedures). Long-chain wax esters were co-extracted during FAME-extraction and appeared in the same chromatograms. FAMEs analyzed via GC were identified by their retention times and those of standards in published chromatograms. Wax esters analyzed via GCMS were identified by their mass fingerprints and by their retention times; an authentic hexadecyl-hexadecanoate standard was included.

Samples (1 µl) for GC were analyzed via flame ionization (FID) on an Auto System gas chromatograph (PerkinElmer, Überlingen, Germany). Compounds were separated on an Op-

tima-5 column (film thickness, 0.25 µm; i.d., 0.32 mm; length, 50 m; Macherey-Nagel). The following temperature program was applied: The injection port temperature was 250°C, and the column start temperature was 90°C (held for 2 min). The column temperature was first increased to 155°C at a rate of 5°C min^{-1}, subsequently to 320°C at a rate of 30°C min^{-1}, and held at 320°C for 4 min. The detection temperature was 350°C. The split ratio was 1:10.

Samples for GC-MS (1 µl) were analyzed on a Trace GCMS (Thermo Finnigan, Waltham, USA). Separation was performed on a HP-5 column (25 m x 0.2 mm x 0.33 µm; Agilent, Santa Clara, USA). The following temperature program was applied: The injection port temperature was 290°C. The initial column temperature was 90°C (held for 2 min). This was increased to 155°C at a rate of 5°C min^{-1}, subsequently to 320°C at a rate of 30°C min^{-1}, and then held at 320°C for 20 min.

References

D'Ans Lax (1983) Taschenbuch für Chemiker und Physiker. 4. Aufl., Bd. II. Springer.

Ettwig, K.F., Butler, M.K., Le Paslier, D., Pelletier, E., Mangenot, S., Kuypers, M.M.M., *et al.* (2010) Nitrite-driven anaerobic methane oxidation by oxygenic bacteria. *Nature* **464:** 543–548.

Ettwig, K.F., Speth, D.R., Reimann, J., Wu, M.L., Jetten, M.S.M. and Keltjens, J.T. (2012) Bacterial oxygen production in the dark. *Front. Microbio.* **3:** 273. doi:10.3389/fmicb.2012.00273

Hrabie, J.A., Klose, J.R., Wink D.A., and Keefer L.K. (1993) New nitric oxide-releasing zwitterions derived from polyamines. *J Org Chem* **58:** 1472–1476.

Sasser, M. (1990) Identification of bacteria by gas chromatography of cellular fatty acids. Newsletter *US Fed Cul* Coll: 1–6.

Schreiber, F., Polerecky, L., and de Beer, D. (2008) Nitric oxide microsensor for high spatial resolution measurements in biofilms and sediments. *Anal Chem* **80:** 1152–1158.

Speight, J.G. (2005) *Lange's Handbook of Chemistry*, 16th edn. New York: McGraw-Hill.

Thauer , R.K., Jungermann, K., and Decker, K. (1977) Energy conservation in chemotrophic anaerobic bacteria. *Bacteriol Rev* **41:** 100–180.

Zedelius, J., Rabus, R., Grundmann, O., Werner, I., Brodkorb, D., Schreiber, F., *et al.* (2011) Alkane degradation under anoxic conditions by a nitrate-reducing bacterium with possible involvement of the electron acceptor in substrate activation. *Environ Microbiol Reports* **3:** 125–135.

D.4 Further contributions as a co-author:

Nitrite-driven anaerobic methane oxidation by oxygenic bacteria

Katharina F. Ettwig, Margaret K. Butler, Denis Le Paslier, Eric Pelletier, Sophie Mangenot, Marcel M. M. Kuypers, Frank Schreiber, Bas E. Dutilh, Johannes Zedelius, Dirk de Beer, Jolein Gloerich, Hans J. C. T. Wessels, Theo van Alen, Francisca Luesken, Ming L. Wu, Katinka T. van de Pas-Schoonen, Huub J. M. Op den Camp, Eva M. Janssen-Megens, Kees-Jan Francoijs, Henk Stunnenberg, Jean Weissenbach, Mike S. M. Jetten and Marc Strous

Author contributions

Genome sequencing and assembly from enrichment culture ‘Twente’ was performed by D.L.P., E.P., S.M. and J.W. M.S., E.M.J.-M., K.-J.F. and H.S. performed the sequencing and initial assembly of sequence from enrichment culture ‘Ooij’. Mapping of sequences from enrichment culture ‘Ooij’ to ‘Twente’ was performed by B.E.D. and M.S. B.E.D. and E.P. performed SNP and coverage analyses. Genome annotation and phylogenetic analysis were conducted by M.K.B. H.J.M.O.d.C. provided support with alignments. Sample preparation for proteome analysis was performed by M.K.B. and M.W., with LC–MS/MS and protein identification performed by J.G. and H.J.C.T.W. Material for transcriptome analysis was prepared by T.v.A. and F.L., with sequencing performed by E.M.J.-M., K.-J.F. and H.S. Continuous cultures were set up and maintained by K.F.E. and K.T.v.d.P.-S. Experiments for nitrogenous intermediates were designed and performed by K.F.E., M.M.M.K., F.S., D.d.B. and J.Z., and those for methane activation were designed and performed by K.F.E. Pilot experiments were conducted by K.F.E., F.L., M.K.B., K.T.v.d.P.-S, T.A. and M.S. K.F.E., M.K.B., M.S.M.J. and M.S. conceived the research. K.F.E., M.K.B. and M.S. wrote the paper with input from all other authors.

Vol 464|25 March 2010|doi:10.1038/nature08883 nature

ARTICLES

Nitrite-driven anaerobic methane oxidation by oxygenic bacteria

Katharina F. Ettwig[1]*, Margaret K. Butler[1]*†, Denis Le Paslier[2,3,4], Eric Pelletier[2,3,4], Sophie Mangenot[2], Marcel M. M. Kuypers[5], Frank Schreiber[5], Bas E. Dutilh[6], Johannes Zedelius[5], Dirk de Beer[5], Jolein Gloerich[7], Hans J. C. T. Wessels[7], Theo van Alen[1], Francisca Luesken[1], Ming L. Wu[1], Katinka T. van de Pas-Schoonen[1], Huub J. M. Op den Camp[1], Eva M. Janssen-Megens[8], Kees-Jan Francoijs[8], Henk Stunnenberg[8], Jean Weissenbach[2,3,4], Mike S. M. Jetten[1] & Marc Strous[1,5,9]

Only three biological pathways are known to produce oxygen: photosynthesis, chlorate respiration and the detoxification of reactive oxygen species. Here we present evidence for a fourth pathway, possibly of considerable geochemical and evolutionary importance. The pathway was discovered after metagenomic sequencing of an enrichment culture that couples anaerobic oxidation of methane with the reduction of nitrite to dinitrogen. The complete genome of the dominant bacterium, named '*Candidatus* Methylomirabilis oxyfera', was assembled. This apparently anaerobic, denitrifying bacterium encoded, transcribed and expressed the well-established aerobic pathway for methane oxidation, whereas it lacked known genes for dinitrogen production. Subsequent isotopic labelling indicated that '*M. oxyfera*' bypassed the denitrification intermediate nitrous oxide by the conversion of two nitric oxide molecules to dinitrogen and oxygen, which was used to oxidize methane. These results extend our understanding of hydrocarbon degradation under anoxic conditions and explain the biochemical mechanism of a poorly understood freshwater methane sink. Because nitrogen oxides were already present on early Earth, our finding opens up the possibility that oxygen was available to microbial metabolism before the evolution of oxygenic photosynthesis.

With the ubiquitous use of fertilizers in agriculture, nitrate (NO_3^-) and nitrite (NO_2^-) have become major electron acceptors in freshwater environments[1]. The feedback of eutrophication on the atmospheric methane (CH_4) budget is poorly understood, with many potential positive and negative feedback loops acting in concert[2]. This previously prompted us to investigate the possibility of anaerobic oxidation of methane coupled to denitrification (reduction of NO_3^- and NO_2^- through nitric oxide (NO) to nitrous oxide (N_2O) and/or dinitrogen gas (N_2)), and microbial communities that perform this process were enriched from two different freshwater ecosystems in The Netherlands[3,4], and recently from mixed Australian freshwater sources by others[5]. All independent enrichment cultures were dominated by the same group of bacteria representing a phylum (NC10) defined only by environmental 16S ribosomal RNA gene sequences[6]. Although many surveys have found these sequences in a variety of aquatic habitats worldwide, reports on the natural activity of these bacteria are scarce (summarized in ref. 4).

Methane is one of the least reactive organic molecules[7]. Aerobic methanotrophs overcome its high activation energy by a reaction with molecular oxygen[8]. Anaerobic sulphate-reducing microbial consortia activate methane by a reversal of its biological production, using a homologue of the methane-releasing enzyme (methyl-coenzyme M reductase) of methanogens[9]. These consortia usually consist of distinct archaea related to methanogens and sulphate-reducing bacteria[10]. Initially, it was hypothesized that anaerobic oxidation of methane coupled to denitrification proceeded in a similar manner, with archaea conducting reverse methanogenesis in association with denitrifying bacterial partners[3]. However, it was subsequently shown that the complete process could also be performed by the bacteria in the total absence of archaea[4,11]. The overall reaction of methane with nitrite (and nitrate) is thermodynamically feasible[3,7]:

$$3CH_4 + 8NO_2^- + 8H^+ = 3CO_2 + 4N_2 + 10H_2O$$

$$(\Delta G^{\circ\prime} = -928\ \mathrm{kJ\ mol^{-1}}\ CH_4)$$

However, so far no known biochemical mechanism has been able to explain the activation of methane in the absence of oxygen or (reversed) methanogens.

Genome assembly from enrichment cultures

We addressed the unknown mechanism of nitrite-dependent anaerobic methane oxidation by metagenomic sequencing of two enrichment cultures described previously: one enriched from Twentekanaal sediment[3,11], here designated 'Twente', and a culture from Ooijpolder ditch sediment[4], designated 'Ooij'. Both enrichments were 70–80% dominated by populations of the same bacterial species (minimum 97.5% 16S rRNA gene identity; for microdiversity in culture 'Ooij' see ref. 4). In the present study we propose to name this species '*Candidatus* Methylomirabilis oxyfera'. The metagenome of culture 'Twente' was

[1]Radboud University Nijmegen, IWWR, Department of Microbiology, Heyendaalseweg 135, 6525 AJ, Nijmegen, The Netherlands. [2]CEA Genoscope, [3]CNRS-UMR 8030, 2 rue Gaston Crémieux, [4]Université d'Evry Val d'Essonne, Boulevard François Mitterrand CP 5706, 91057 Evry, France. [5]Max Planck Institute for Marine Microbiology, Celsiusstrasse 1, D-28359 Bremen, Germany. [6]Radboud University Nijmegen Medical Centre, Centre for Molecular and Biomolecular Informatics, Nijmegen Centre for Molecular Life Sciences, Geert Grooteplein 28, [7]Radboud University Nijmegen Medical Centre, Nijmegen Proteomics Facility, Department of Laboratory Medicine, Laboratory of Genetic, Endocrine and Metabolic Diseases, Geert Grooteplein-Zuid 10, [8]Radboud University Nijmegen, Department of Molecular Biology, Nijmegen Centre for Molecular Life Sciences, Geert Grooteplein-Zuid 26, 6525 GA, Nijmegen, The Netherlands. [9]Centre for Biotechnology, University of Bielefeld, Postfach 10 01 31, D-33501 Bielefeld, Germany. †Present address: Australian Institute for Bioengineering and Nanotechnology, University of Queensland, Brisbane, 4072, Australia.
*These authors contributed equally to this work.

Table 1 | Databases of genomic, proteomic and transcriptomic data

Enrichment culture	Approach	Molecule type	Amount of data obtained	NCBI-database, accession number
'Twente'	454 pyrosequencing	DNA	90,353,824 nt	Short Read Archive, SRR023516.1
	Illumina sequencing	DNA	196,814,368 nt	Short Read Archive, SRR022749.2
	Assembled genome	DNA	2,752,854 nt	GenBank, FP565575
	Paired-end plasmid (10 kb) sequencing	DNA	16,440,000 nt (trimmed)	Project ID 40193 (linked to FP565575)
	Illumina sequencing	RNA	198,977,152 nt	Gene Expression Omnibus, GSE18535
	nLC LIT FT–ICR MS/MS	Protein	–	Peptidome, PSE127
'Ooij'	Illumina sequencing	DNA	188,099,392 nt	Short Read Archive, SRR022748.2
	nLC LIT FT–ICR MS/MS	Protein	–	Peptidome, PSE128

nLC LIT FT-ICR MS/MS, nanoflow liquid chromatography linear ion-trap Fourier-transform ion cyclotron resonance MS/MS analysis; nt, nucleotides.

obtained by 454 pyrosequencing, Illumina sequencing and paired-end Sanger sequencing of a 10-kilobase (kb) insert plasmid library (Table 1 and Supplementary Fig. 1). Binning based on GC content and coverage indicated that almost 60% of the metagenomic data from pyrosequencing were associated with '*M. oxyfera*'. These data were initially assembled into five scaffolds that could then be joined into a single circular chromosome (2,753 kb; see Supplementary Table 1 for more properties) by long-range PCR amplification.

Consistent with previous work[11], combined metagenomic data contained no evidence for the presence of the archaea that were originally suggested to form a consortium with the dominant bacterium[3]. Out of roughly 365,000 reads obtained by pyrosequencing, only 78 gave a Blast hit with a bacterial 16S or 23S rRNA gene sequence distinct from '*M. oxyfera*', and none matched archaeal sequences (Supplementary Table 2). No other single species constituted a numerically significant part of the overall enriched community to enable the assembly of more than very small (most less than 2 kb) fragments.

Short-read (32 base pairs) Illumina sequencing of culture 'Ooij' revealed that, in contrast with the near-clonal population dominating culture 'Twente' (for single nucleotide polymorphism (SNP) frequency see Supplementary Fig. 2), a more diverse population of '*M. oxyfera*' inhabited this culture, as commonly observed by metagenomic sequencing of microbial populations[12]. In the present case the estimated number of SNPs in culture 'Ooij' was more than threefold that in culture 'Twente'. Because of this microdiversity, assembly of larger contigs for culture 'Ooij' was impossible and the short reads were mapped directly onto the complete genome of '*M. oxyfera*'. Although the two enrichment cultures were dominated by the same species, the sequences were apparently too dissimilar to enable mapping by the currently available approaches[13]. A new mapping algorithm based on iterated Blast searches was therefore developed[14]. This allowed us to construct consensus sequences for genes of the '*M. oxyfera*' populations dominating enrichment culture 'Ooij'. By proteomic detection of peptides predicted from this consensus, the procedure was validated experimentally (Supplementary Table 3). The average identity of the partial genome obtained from enrichment culture 'Ooij' to the complete genome of '*M. oxyfera*' was 91.1% at the DNA level (open reading frames (ORFs) and RNAs), and the SNP frequency among the Ooij populations was at least 3.45% (Supplementary Fig. 2).

To facilitate the mechanistic interpretation of the genomic sequence information, the transcription and expression of predicted genes was investigated by Illumina sequencing of RNA and by liquid chromatography–tandem mass spectrometry (LC–MS/MS) of extracted proteins (Table 1).

Paradoxical predictions from the genome

Both enrichment cultures were grown anoxically and performed methane oxidation coupled to the complete denitrification of nitrite to N_2 (refs 3, 4, 11). We therefore inspected the genome, transcriptome and proteome for homologues of known genes involved in denitrification[15]. '*M. oxyfera*' apparently lacked some genes necessary for complete denitrification (Fig. 1a and Supplementary Table 4). Genes for the reduction of nitrate to nitrite (*narGHJI*, *napAB*), nitrite to NO (*nirSJFD/GH/L*) and NO to N_2O (*norZ* = q*nor*) were present in the genome, and expression as proteins could be demonstrated for Nap, Nir and Nor. However, with the exception of the accessory gene *nosL*, the gene cluster encoding enzymes for the reduction of N_2O to N_2 (*nosZDFY*) was missing. Previous studies have shown that N_2O was not the main product of denitrification but was only produced in trace amounts[4,11]. However, on the basis of the analysis of the data sets outlined in Table 1 and the fact that the '*M. oxyfera*' genome sequence seems complete, we judge it highly unlikely that genes encoding canonical N_2O reductase were overlooked and escaped proper assembly. Because complete denitrification can also be achieved by the combined action of multiple species, we could not yet rule out the possibility that the missing catalytic activity was complemented by other bacteria.

In a similar fashion, we searched for homologues of anaerobic alkane activation enzymes, such as fumarate-adding glycyl-radical enzymes[16] and the methyl-coenzyme M reductase of reverse methanogens[9]. Consistent with the absence of archaea, the metagenome contained no homologue of methyl-coenzyme M reductase. However, alkane-activating glycyl radical enzymes, which had been proposed to activate methane in these organisms[7], were also missing. Instead, the genome did encode the complete pathway for aerobic methane oxidation (Fig. 1b and Supplementary Table 5). This well-known pathway proceeds through methanol (CH_3OH), formaldehyde (CH_2O) and formate (HCOOH) to carbon dioxide (CO_2)[8]. In the

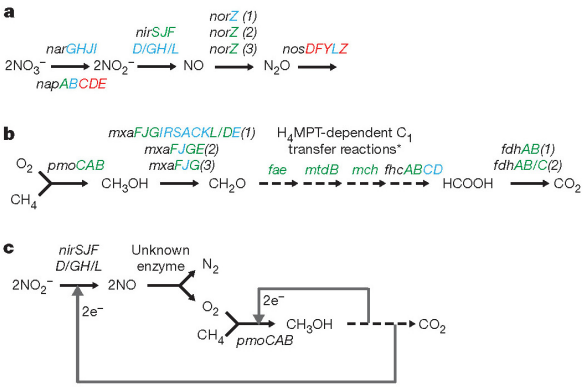

Figure 1 | Significant pathways of *Methylomirabilis oxyfera*. Canonical pathways of denitrification (**a**), aerobic methane oxidation (**b**) and proposed pathway of methane oxidation with nitrite (**c**). *narGHJI*, nitrate reductase; *napABCDE*, periplasmic nitrate reductase; *nirSJFD/GH/L*, nitrite reductase; *norZ*, nitric oxide reductase; *nosDFYLZ*, nitrous oxide reductase; *pmoCAB*, particulate methane monooxygenase; *mxaFJGIRSACKL/DE*, methanol dehydrogenase; *fae*, formaldehyde-activating enzyme; *mtdB*, methylene-tetrahydromethanopterin (H_4MPT) dehydrogenase; *mch*, methenyl-H_4MPT cyclohydrolase; *fhcABCD*, formyltransferase/hydrolase; *fdhABC*, formate dehydrogenase. Genes in red are absent from the genome, those in blue are present in the genome and those genes in green are present in both the proteome and the genome. Asterisk, H_4MPT-dependent reactions involve the intermediates methylene-H_4MPT, methenyl-H_4MPT and formyl-H_4MPT.

first step of this pathway, methane is hydroxylated by a reaction with oxygen, yielding methanol and water. This reaction is catalysed by the enzyme methane mono-oxygenase (MMO). Both metagenomes contained one set of *pmoCAB* genes encoding the particulate (membrane-bound) form of this enzyme complex (pMMO); genes encoding the soluble form were absent. Although the amino-acid sequences were phylogenetically distant from all homologous sequences currently in the databases (Fig. 2 and Supplementary Fig. 3), *pmoA* signature residues and those important for function were well conserved (Supplementary Fig. 4). The complete aerobic methanotrophic pathway was found to be transcribed and expressed in both anaerobic enrichment cultures (Supplementary Table 5), including the complete tetrahydromethanopterin-dependent C_1 transfer module. The phylum NC10 is thus only the fifth phylogenetic group known to harbour this potentially primordial metabolic module[17]. Phylogenetic analysis indicated that '*M. oxyfera*' represents a deeply branching lineage of this C_1 pathway (data not shown).

We were therefore faced with two anaerobic, denitrifying microbial communities that were dominated by the same species, an apparently aerobic methanotroph incapable of complete denitrification. To resolve this puzzle, we investigated whether '*M. oxyfera*' produced N_2 by means of a previously unknown mechanism. Figure 1c shows a possible mechanism that could resolve the conflict between the genetic and experimental evidence; it is based on the conversion of two molecules of NO into O_2 and N_2. This reaction is thermodynamically favourable ($\Delta G^{\circ\prime} = -173.1\,kJ\,mol^{-1}\,O_2$) but kinetically difficult[18]. No catalyst operating at biologically relevant temperatures (0–100 °C) is known, although for higher temperatures several catalysts (for example copper zeolites) have been developed that decompose NO from industrial and automobile exhaust fumes[19]. The production of oxygen as a metabolic intermediate is not completely new to biology: dismutation of the toxic intermediate chlorite ($ClO_2^- \rightarrow Cl^- + O_2$) by chlorate-reducing bacteria prevents cell damage and yields oxygen for chemo-organotrophic respiration[20], or possibly for mono-oxygenase-dependent biosynthesis[21].

The pathway outlined in Fig. 1c would require only one new enzyme, an 'NO dismutase', to catalyse a thermodynamically feasible reaction and replace N_2O reductase. The oxygen produced would become available to oxidize methane aerobically, explaining the presence of genes for aerobic methane oxidation in the '*M. oxyfera*' genome and the insensitivity of the cultures to oxygen[4]. In this model, the function of the putative quinol-dependent NO reductases (norZ) could be the detoxification of NO rather than respiration, which is consistent with its function in most other known bacteria[22]. Alternatively, together with two multi-copper oxidases encoded in the genome, they are hypothetical candidates for catalysing the oxygen production from NO.

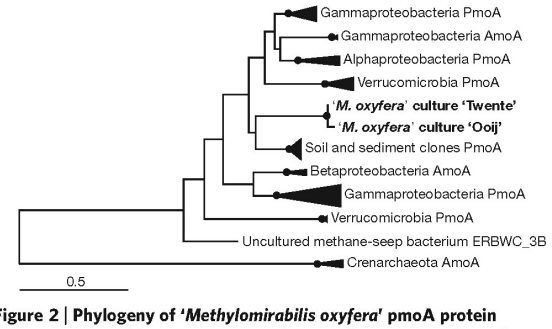

Figure 2 | Phylogeny of '*Methylomirabilis oxyfera*' pmoA protein sequences. Neighbour-joining tree showing the position of enrichment cultures 'Twente' and 'Ooij' (in bold) relative to other pmoA and amoA sequences. The distance tree was computed with the Dayhoff matrix-based method, and bootstrapping of 100 replicates was performed within the neighbour-joining, minimum-evolution, maximum-parsimony and maximum-likelihood evolutionary methods. Bootstrapping results are summarized on the tree, with filled circles representing branch points at which all four methods give greater than 70% support. The scale bar represents 50 amino-acid changes per 100 amino acids. See also Supplementary Fig. 3 for more detailed tree and bootstrap values.

Experimental evidence for the proposed pathway

The operation of the new pathway was addressed experimentally in a series of experiments performed with culture 'Ooij'. Its activity was higher than that of culture 'Twente', and it was less sensitive to experimental handling. To corroborate the coupling of nitrite reduction to methane oxidation, we first incubated 380 ml of the enrichment culture with ^{13}C-labelled methane and with nitrate (2 mM) as the only electron acceptor while monitoring the concentration and isotopic composition of the dissolved gases. With nitrate only, no methane oxidation was detectable and no N_2 was produced. On addition of ^{15}N-labelled nitrite, methane oxidation began and labelled N_2 was formed in stoichiometric amounts (Fig. 3a). Together, these results showed unambiguously that methane oxidation by '*M. oxyfera*' cultures proceeded in the absence of extracellular oxygen: the oxygen concentration remained below the detection limit (0.3 μM), the activity was dependent on the presence of nitrite, and the stoichiometry of the reaction indicated that no electrons were lost to other electron acceptors (theoretical stoichiometry $3CH_4/4N_2$; measured stoichiometry 3/3.87). The experiment also confirmed that denitrification was complete, despite the lack of genes encoding N_2O reductase in the genome of '*M. oxyfera*'. Similar results were obtained after the addition of ^{15}NO (Supplementary Fig. 5). This indicated that NO was an intermediate of '*M. oxyfera*', and the results are consistent with the presence and expression of nitrite reductase.

To test whether N_2 production by '*M. oxyfera*' proceeded through N_2O as an intermediate, the enrichment culture was incubated with $^{13}CH_4$, nitrate and N_2O, but without nitrite. Under these conditions, neither methane nor N_2O was consumed (Fig. 3b). Consistent with the genomic inventory, N_2O was apparently not a suitable electron acceptor for methane oxidation. Again, methane was oxidized only after the addition of $^{15}NO_2^-$, and almost all (93%) of the label was recovered in N_2. Only a small amount (7%) of the $^{15}NO_2^-$ was converted to N_2O, presumably by community members other than '*M. oxyfera*'. Because a large amount of unlabelled N_2O was present from the start, it can be assumed to have fully penetrated the microbial cells, even those residing in aggregates. For this reason we would expect that if N_2O had been turned over as an intermediate during nitrite reduction by '*M. oxyfera*', most ^{15}N label would have been recovered as N_2O, because the cells would mainly reduce the unlabelled N_2O to N_2. Hence, the ^{15}N label would be 'trapped' in the N_2O 'pool', and definitely so for a model in which the missing genes for N_2O reductase would be complemented by other bacteria in the enrichment culture. However, it is still a possibility that in '*M. oxyfera*' N_2O production and reduction are extremely strictly coupled. Given the absence of genes for a conventional N_2O reductase[23], N_2 production would depend on the presence and activity of an as yet unknown functional analogue. Thus, even in this conservative model it is likely that a novel enzyme produces N_2 in '*M. oxyfera*'.

N_2O reductase is inhibited by acetylene (C_2H_2) at millimolar concentrations[15], and the addition of acetylene would therefore be a straightforward method of providing further evidence for the absence of this enzyme. However, acetylene also inhibits pMMO at much lower concentrations (micromolar range)[24]. Thus because the genomic and proteomic analyses suggested that pMMO was the methane-activating enzyme in '*M. oxyfera*', a complete inhibition of total activity by acetylene would be expected for this organism. Indeed, experiments with culture 'Twente' suggested complete inhibition of methane oxidation activity at concentrations as low as 10 μM acetylene (data not shown).

To provide more evidence for the potential role of pMMO in anaerobic methane oxidation, we used an established assay for

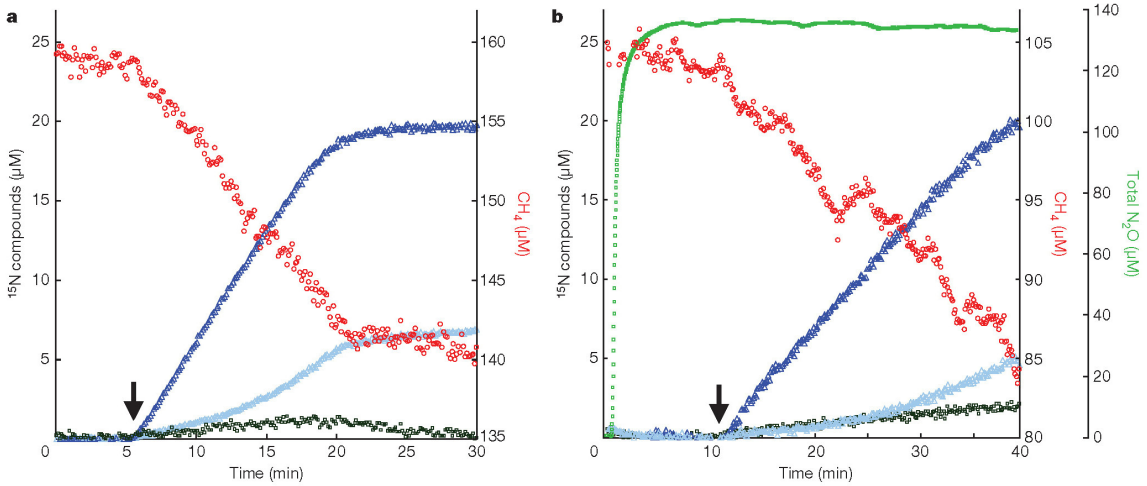

Figure 3 | Coupling of methane oxidation and nitrite reduction in enrichment cultures of *'Methylomirabilis oxyfera'*. Methane is oxidized only after addition of ^{15}N-labelled nitrite (50 μM, arrow), which is converted to ^{15}N-labelled dinitrogen gas in the presence of about 2,000 μM ^{14}N-nitrate (**a**) or 2,000 μM ^{14}N-nitrate and 135 μM ^{14}N-N$_2$O (**b**). Experiments were performed with 380 ml of anoxic, stirred enrichment culture 'Ooij' (protein content 147 ± 11 mg). Red circles, CH_4; dark blue triangles, $^{15,15}N_2$; light blue triangles, $^{15,14}N_2$; green squares, total N_2O; dark green squares, $^{14,15}N_2O$ and $^{15,15}N_2O$.

pMMO activity, the oxidation of propylene (propene, C_3H_6)[24]. In this assay, pMMO adds one oxygen atom from O_2 to propylene, yielding propylene oxide (propylene epoxide, C_3H_6O). In incubations of enrichment culture 'Ooij' with propylene, formate and oxygen, aerobic pMMO activity occurred at a rate of 0.54 nmol C_3H_6O min^{-1} per mg protein. Next, nitrite was added instead of oxygen. Interestingly, in the presence of nitrite propylene was oxygenated more rapidly (0.94 nmol min^{-1} per mg protein) than in the presence of oxygen. No activity above background levels was detected with N_2O or nitrate. Also in this experiment, the pMMO activity was completely inhibited by 0.15 mM acetylene. To exclude the possibility that contaminating oxygen could explain the observed pMMO activity, we used ^{18}O labelling to trace the oxygen atoms of nitrite into propylene oxide. The direct use of ^{18}O-labelled nitrite proved impossible, because the ^{18}O was quickly exchanged with the unlabelled ^{16}O from water, presumably through the activity of nitrite reductase[25] (Supplementary Fig. 4). To overcome this problem, we generated ^{18}O-labelled nitrite in the incubations themselves by adding ^{18}O-labelled water. In this way, incorporation of the ^{18}O from nitrite into propylene oxide was shown (74–88% originating from nitrite). In line with theoretical expectations, control incubations confirmed that O was not exchanged between water and O_2 or propylene oxide, and that ^{18}O-labelled water did not lead to propylene oxide formation in the absence of nitrite. Control incubations with aerobic methanotrophs were not active with nitrite and did not incorporate ^{18}O from nitrite.

In theory, two mechanisms could explain this result: first, the direct use of NO by pMMO, or second, the production of oxygen by pMMO or a separate enzyme followed by consumption of the produced oxygen by pMMO (Fig. 1c). The divergent position of the '*M. oxyfera*' pMMO (Fig. 2) may argue for the first possibility; however, most residues typical for pMMOs were conserved (Supplementary Fig. 4). The 3:8 methane:nitrite stoichiometry observed renders the second possibility more likely, because apparently not all NO is reduced through pMMO. With the second possibility the remaining oxygen (25%) may be consumed by terminal oxidases.

We addressed these two possibilities experimentally by measuring the production of ^{18}O-labelled oxygen in the incubations with propylene. Indeed, a small amount of labelled oxygen was released in anoxic incubations with propylene, nitrite and ^{18}O-labelled water (0.15 nmol min^{-1} per mg protein; Fig. 4). In control incubations of aerobic methanotrophs in the presence of ^{18}O-labelled water and ^{18}O-labelled nitrite, no labelled oxygen was detectable, ruling out chemical or non-specific reactions with pMMO. In addition, production of oxygen by enzymes for the detoxification of reactive oxygen species, for example catalase or superoxide dismutase, is unlikely, because reactive oxygen species are not known to be produced in the absence of oxygen, even when NO is present[26]. Furthermore, these enzymes are presumably more active in aerobically grown methanotrophs, which did not produce oxygen from nitrite. When methane was used instead of propylene, no oxygen was released by '*M. oxyfera*'. This may be explained by the roughly 2–3-fold higher enzymatic rates

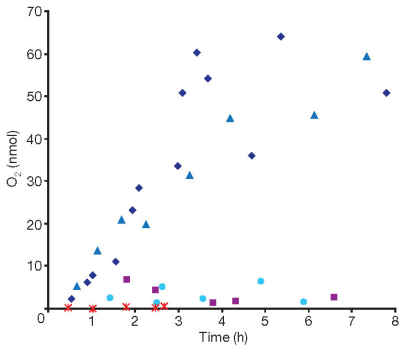

Figure 4 | Oxygen production from nitrite in *'Methylomirabilis oxyfera'*. Whole cells of enrichment culture 'Ooij' were incubated in buffer containing nitrite and 25% ^{18}O-labelled water, leading to 90% O exchange within 30 min. Total oxygen production from this indirectly labelled $N^{18}O_2^-$ was inferred from the measured concentration of $^{16,18}O_2$ and $^{18,18}O_2$ in the helium headspace with the following additions: propylene (dark blue diamonds), propylene and acetylene (blue triangles), methane (purple squares) and oxygen (light blue circles). Anaerobic control incubations of *Methylosinus acidophilus* (red asterisks) with ^{18}O-labelled nitrite did not produce measurable amounts of oxygen. Cells were concentrated to obtain similar maximum rates of propylene oxidation activity; 1.15 nmol min^{-1} (with NO_2^-, 1.22 mg of protein) for '*M. oxyfera*', and 1.68 nmol min^{-1} (with O_2, 0.046 mg of protein) for *M. acidophilus*.

with methane (Fig. 3 and ref. 4) than with propylene; the lower activity of pMMO with propylene allowed some oxygen to escape.

Conclusions and perspectives

We have described the discovery of a new 'intra-aerobic' pathway of nitrite reduction. This pathway resembles the original proposal for the mechanism of denitrification. After its discovery in the nineteenth century, it was generally assumed that denitrification proceeded by the production of oxygen from nitrate, which could subsequently be used for respiration (reviewed in ref. 27). It therefore seems that an old hypothesis may have been brushed aside too easily.

The new pathway of 'intra-aerobic denitrification' is not necessarily restricted to methane-oxidizing bacteria: with all currently available assays for denitrification the process would either be overlooked (for example with the acetylene-block technique) or lumped together with conventional denitrification (for example with isotope pairing). Under dynamic oxic/anoxic conditions and with recalcitrant substrates (aromatic compounds, alkanes and alkenes) the process may certainly offer ecological advantages.

The production of oxygen from nitrogen oxides is also of interest for ordering the evolution of metabolic pathways on early Earth, which are mostly believed to have proceeded from reduced (for example fermentation) to oxidized (for example aerobic respiration) pathways[28,29]. In this model, the pathway presented here may have evolved to exploit newly formed pools of nitrogen oxides after the oxygenation of the atmosphere. Alternatively, on the basis of enzyme phylogenies, respiration has been discussed as a primordial pathway[30,31] that originally depended on nitrogen oxides that were most probably present on early Earth[31], although whether they were quantitatively important is under debate[28,32]. Our study adds a new aspect to this debate, because it is tempting to speculate that intra-aerobic denitrification may have preceded oxygen production by photosynthesis, or extended the niches for the evolution of aerobic pathways in a still predominantly anaerobic environment before the Great Oxidation Event about 2.45 Gyr ago[33]. The intra-aerobic pathway presented here would have enabled microorganisms to thrive on the abundant methane in the Archaean atmosphere[34] without direct dependence on oxygenic photosynthesis, causing ^{13}C-depleted sedimentary carbon that has so far been attributed to aerobic methanotrophs[35].

'*Candidatus* Methylomirabilis oxyfera'

Etymology. *methyl* (modern Latin): the methyl group; *mirabilis* (Latin): astonishing, strange; *oxygenium* (Latin): oxygen; *fera* (Latin): carrying, producing. The name alludes to the substrate methane, which is oxidized by a surprising combination of pathways, involving oxygen as an intermediate.

Locality. Enriched from freshwater sediments of the Twentekanaal and Ooijpolder ditches, The Netherlands.

Properties. Methane-oxidizing and nitrite-reducing bacterium of the candidate division NC10. Grows anaerobically, but produces oxygen for the aerobic oxidation of methane. Reduces nitrite to dinitrogen gas without a nitrous oxide reductase. Gram-negative rod with a diameter of 0.25–0.5 μm and a length of 0.8–1.1 μm. Mesophilic with regard to temperature and pH (enriched at 25–30 °C and pH 7–8). Slow growth (doubling time 1–2 weeks).

METHODS SUMMARY

Molecular methods. DNA from both enrichment cultures was isolated as described[36], with modifications, and used as a template for pyrosequencing[37], construction of a 10-kb insert plasmid library (enrichment culture 'Twente') and single-end Illumina sequencing (both cultures). Coding sequences of the closed genome were predicted, and automatic functional annotation was performed with MaGe[38]. Selected annotations (Supplementary Tables 4 and 5) were confirmed manually.

Short reads resulting from Illumina sequencing of enrichment culture 'Ooij' were mapped onto the completed genome of '*M. oxyfera*' (culture 'Twente') with an algorithm based on iterated Blast searches and validated by comparison with proteomics results (ref. 14 and Supplementary Table 3).

Protein extracts from both enrichment cultures were separated by SDS–PAGE, trypsin-digested and analysed by LC–MS/MS[39]. Mass spectrometric data files were searched against a database of predicted '*M. oxyfera*' protein sequences.

Total RNA from enrichment culture 'Twente' was reverse-transcribed and sequenced by the single-end Illumina technique.

Activity experiments. All incubations were performed at 30 °C and pH 7.3 with cell suspensions from culture 'Ooij'[4]. For measurement of nitrogenous intermediates, 380 ml containing 2 mM NO_3^- and 100 μM CH_4 was incubated anaerobically while measuring the concentration and isotopic composition of CH_4, O_2 and nitrogenous gases with microsensors[40–42] and membrane-inlet mass spectrometry. N_2O, $^{15}NO_2^-$ and ^{15}NO were added as specified. Propylene oxidation and oxygen production assays were performed with 0.5 ml of tenfold concentrated cells. NO_2^-, formate and gases were added in combinations specified in Results. ^{18}O-labelled NO_2^- was generated in '*M. oxyfera*' incubations by O-equilibration with 25% ^{18}O-labelled water in the medium[25]. For *Methylosinus acidophilus* (DQ076754) controls, ^{18}O-labelled NO_2^- was used in addition to ^{18}O-labelled water. Propylene oxide in headspace samples was quantified by gas chromatography[11], and formation of $^{18}O_2$ and incorporation of ^{18}O into propylene oxide was determined by coupled gas chromatography–mass spectrometry as described[4], with modifications.

Full Methods and any associated references are available in the online version of the paper at www.nature.com/nature.

Received 8 October 2009; accepted 5 February 2010.

1. Galloway, J. N. *et al.* Transformation of the nitrogen cycle: recent trends, questions, and potential solutions. *Science* **320,** 889–892 (2008).
2. Bodelier, P. L. E. & Laanbroek, H. J. Nitrogen as a regulatory factor of methane oxidation in soils and sediments. *FEMS Microbiol. Ecol.* **47,** 265–277 (2004).
3. Raghoebarsing, A. A. *et al.* A microbial consortium couples anaerobic methane oxidation to denitrification. *Nature* **440,** 918–921 (2006).
4. Ettwig, K. F., van Alen, T., van de Pas-Schoonen, K. T., Jetten, M. S. M. & Strous, M. Enrichment and molecular detection of denitrifying methanotrophic bacteria of the NC10 phylum. *Appl. Environ. Microbiol.* **75,** 3656–3662 (2009).
5. Hu, S. *et al.* Enrichment of denitrifying anaerobic methane oxidizing microorganisms. *Envir. Microbiol. Rep.* **1,** 377–384 (2009).
6. Rappé, M. S. & Giovannoni, S. J. The uncultured microbial majority. *Annu. Rev. Microbiol.* **57,** 369–394 (2003).
7. Thauer, R. K. & Shima, S. Methane as fuel for anaerobic microorganisms. *Ann. NY Acad. Sci.* **1125,** 158–170 (2008).
8. Trotsenko, Y. A. & Murrell, J. C. Metabolic aspects of aerobic obligate methanotrophy. *Adv. Appl. Microbiol.* **63,** 183–229 (2008).
9. Krüger, M. *et al.* A conspicuous nickel protein in microbial mats that oxidize methane anaerobically. *Nature* **426,** 878–881 (2003).
10. Knittel, K. & Boetius, A. Anaerobic oxidation of methane: progress with an unknown process. *Annu. Rev. Microbiol.* **63,** 311–334 (2009).
11. Ettwig, K. F. *et al.* Denitrifying bacteria anaerobically oxidize methane in the absence of *Archaea*. *Environ. Microbiol.* **10,** 3164–3173 (2008).
12. Wilmes, P., Simmons, S. L., Denef, V. J. & Banfield, J. F. The dynamic genetic repertoire of microbial communities. *FEMS Microbiol. Rev.* **33,** 109–132 (2009).
13. Farrer, R. A., Kemen, E., Jones, J. D. G. & Studholme, D. J. *De novo* assembly of the *Pseudomonas syringae* pv. *syringae* B728a genome using Illumina/Solexa short sequence reads. *FEMS Microbiol. Lett.* **291,** 103–111 (2009).
14. Dutilh, B. E., Huynen, M. A. & Strous, M. Increasing the coverage of a metapopulation consensus genome by iterative read mapping and assembly. *Bioinformatics* **25,** 2878–2881 (2009).
15. Zumft, W. G. Cell biology and molecular basis of denitrification. *Microbiol. Mol. Biol. Rev.* **61,** 533–616 (1997).
16. Heider, J. Adding handles to unhandy substrates: anaerobic hydrocarbon activation mechanisms. *Curr. Opin. Chem. Biol.* **11,** 188–194 (2007).
17. Chistoserdova, L., Kalyuzhnaya, M. G. & Lidstrom, M. E. C1-transfer modules: from genomics to ecology. *ASM News* **71,** 521–528 (2005).
18. Howard, C. S. & Daniels, F. Stability of nitric oxide over a long time interval. *J. Phys. Chem.* **62,** 360–361 (1958).
19. Parvulescu, V. I., Grange, P. & Delmon, B. Catalytic removal of NO. *Catal. Today* **46,** 233–316 (1998).
20. van Ginkel, C. G., Rikken, G. B., Kroon, A. G. M. & Kengen, S. W. M. Purification and characterization of chlorite dismutase: a novel oxygen-generating enzyme. *Arch. Microbiol.* **166,** 321–326 (1996).
21. Bab-Dinitz, E., Shmuely, H., Maupin-Furlow, J., Eichler, J. & Shaanan, B. *Haloferax volcanii* PitA: an example of functional interaction between the Pfam chlorite dismutase and antibiotic biosynthesis monooxygenase families? *Bioinformatics* **22,** 671–675 (2006).
22. Zumft, W. G. Nitric oxide reductases of prokaryotes with emphasis on the respiratory, heme–copper oxidase type. *J. Inorg. Biochem.* **99,** 194–215 (2005).
23. Zumft, W. G. & Kroneck, P. M. H. in *Advances in Microbial Physiology* Vol. 52 (ed. Poole, R. K.) 107–227 (Academic, 2007).

24. Prior, S. D. & Dalton, H. Acetylene as a suicide substrate and active-site probe for methane monooxygenase from *Methylococcus capsulatus* (Bath). *FEMS Microbiol. Lett.* **29,** 105–109 (1985).
25. Kool, D. M., Wrage, N., Oenema, O., Dolfing, J. & Van Groenigen, J. W. Oxygen exchange between (de)nitrification intermediates and H_2O and its implications for source determination of NO_3^- and N_2O: a review. *Rapid Commun. Mass Spectrom.* **21,** 3569–3578 (2007).
26. Demicheli, V., Quijano, C., Alvarez, B. & Radi, R. Inactivation and nitration of human superoxide dismutase (SOD) by fluxes of nitric oxide and superoxide. *Free Radic. Biol. Med.* **42,** 1359–1368 (2007).
27. Allen, M. B. & van Niel, C. B. Experiments on bacterial denitrification. *J. Bacteriol.* **64,** 397–412 (1952).
28. Broda, E. The history of inorganic nitrogen in the biosphere. *J. Mol. Evol.* **7,** 87–100 (1975).
29. Fenchel, T. *Origin and Early Evolution of Life* (Oxford Univ. Press, 2002).
30. Castresana, J. in *Respiration in Archaea and Bacteria: Diversity of Prokaryotic Electron Transport Carriers* Vol. 15 (ed. Zannoni, D.) 1–14 (Springer, 2004).
31. Ducluzeau, A. L. *et al.* Was nitric oxide the first deep electron sink? *Trends Biochem. Sci.* **34,** 9–15 (2009).
32. Chapman, D. J. & Schopf, J. W. *Biological and Biochemical Effects of the Development of an Aerobic Environment* (Princeton Univ. Press, 1983).
33. Holland, H. D. The oxygenation of the atmosphere and oceans. *Phil. Trans. R. Soc. B* **361,** 903–915 (2006).
34. Pavlov, A. A., Kasting, J. F., Brown, L. L., Rages, K. A. & Freedman, R. Greenhouse warming by CH_4 in the atmosphere of early Earth. *J. Geophys. Res. Planets* **105,** 11981–11990 (2000).
35. Hayes, J. M. in *Earth's Earliest Biosphere* (ed. Schopf, J. W.) 291–301 (Princeton Univ. Press, 1983).
36. Zhou, J., Bruns, M. A. & Tiedje, J. M. DNA recovery from soils of diverse composition. *Appl. Environ. Microbiol.* **62,** 316–322 (1996).
37. Margulies, M. *et al.* Genome sequencing in microfabricated high-density picolitre reactors. *Nature* **437,** 376–380 (2005).
38. Vallenet, D. *et al.* MaGe: a microbial genome annotation system supported by synteny results. *Nucleic Acids Res.* **34,** 53–65 (2006).
39. Wilm, M. *et al.* Femtomole sequencing of proteins from polyacrylamide gels by nano-electrospray mass spectrometry. *Nature* **379,** 466–469 (1996).
40. Andersen, K., Kjær, T. & Revsbech, N. P. An oxygen insensitive microsensor for nitrous oxide. *Sens. Actuators B Chem.* **81,** 42–48 (2001).
41. Revsbech, N. P. An oxygen microsensor with a guard cathode. *Limnol. Oceanogr.* **34,** 474–478 (1989).
42. Schreiber, F., Polerecky, L. & de Beer, D. Nitric oxide microsensor for high spatial resolution measurements in biofilms and sediments. *Anal. Chem.* **80,** 1152–1158 (2008).

Supplementary Information is linked to the online version of the paper at www.nature.com/nature.

Acknowledgements We thank F. Stams and N. Tan for sharing their ideas on NO decomposition; D. Speth and L. Russ for pilot experiments; N. Kip for providing *M. acidophilus* cultures; A. Pierik for electron paramagnetic resonance analysis; G. Klockgether and G. Lavik for technical assistance; and B. Kartal, J. Keltjens, A. Pol, J. van de Vossenberg and F. Widdel for helpful discussions. M.M.M.K., F.S., J.Z. and D.d.B. were supported by the Max Planck Society, M.S.M.J. by European Research Council grant 232937, M.S., K.F.E. and M.K.B. by a Vidi grant to M.S. from the Netherlands Organisation for Scientific Research (NWO), and M.L.W. and B.D. by a Horizon grant (050-71-058) from NWO.

Author Contributions Genome sequencing and assembly from enrichment culture 'Twente' was performed by D.L.P., E.P., S.M. and J.W. M.S., E.M.J.-M., K.-J.F. and H.S. performed the sequencing and initial assembly of sequence from enrichment culture 'Ooij'. Mapping of sequences from enrichment culture 'Ooij' to 'Twente' was performed by B.E.D. and M.S. B.E.D. and E.P. performed SNP and coverage analyses. Genome annotation and phylogenetic analysis were conducted by M.K.B. H.J.M.O.d.C. provided support with alignments. Sample preparation for proteome analysis was performed by M.K.B. and M.W., with LC–MS/MS and protein identification performed by J.G. and H.J.C.T.W. Material for transcriptome analysis was prepared by T.v.A. and F.L., with sequencing performed by E.M.J.-M., K.-J.F. and H.S. Continuous cultures were set up and maintained by K.F.E. and K.T.v.d.P.-S. Experiments for nitrogenous intermediates were designed and performed by K.F.E., M.M.M.K., F.S., D.d.B. and J.Z., and those for methane activation were designed and performed by K.F.E. Pilot experiments were conducted by K.F.E., F.L., M.K.B., K.T.v.d.P.-S, T.A. and M.S. K.F.E., M.K.B., M.S.M.J. and M.S. conceived the research. K.F.E., M.K.B. and M.S. wrote the paper with input from all other authors.

Author Information Sequencing and proteomic data are deposited at the National Centre for Biotechnology Information under accession numbers FP565575, SRR023516.1, SRR022749.2, GSE18535, SRR022748.2, PSE127 and PSE128. Reprints and permissions information is available at www.nature.com/reprints. The authors declare no competing financial interests. Correspondence and requests for materials should be addressed to K.F.E. (k.ettwig@science.ru.nl) or M.S. (mstrous@mpi-bremen.de).

doi:10.1038/nature08883 nature

METHODS

DNA preparation. DNA from both enrichment cultures was isolated as described[36], with modifications. After incubation of biomass in DNA extraction buffer for 2 h, 0.7 vol. of phenol/chloroform/3-methylbutan-1-ol (25:24:1, by volume) was added and the mixture was incubated for 20 min at 65 °C. The aqueous phase was recovered by centrifugation and another treatment with phenol/chloroform/3-methylbutan-1-ol was performed. The aqueous phase was then mixed with an equal volume of chloroform/3-methylbutan-1-ol (24:1, v/v) and the DNA was precipitated and cleaned as described[36].

Sequencing methods. We performed 454 pyrosequencing on total genomic DNA from enrichment culture 'Twente' with the Roche Genome Sequencer FLX system by Keygene N.V.[37]. Sequencing of the single-end Illumina samples was performed with total genomic DNA from both enrichment cultures, as described. The samples were prepared in accordance with the manufacturer's protocol (Illumina). Subsequent sequencing was conducted on a genome Analyser II (Illumina). A 10-kb insert plasmid library of total genomic DNA from enrichment culture 'Twente' was constructed; clones were picked and bi-directionally sequenced by using standard protocols. Sequence data resulting from the plasmid library and pyrosequencing were combined, and a preliminary global assembly, performed with both Phrap[43] and Newbler (454 Life Sciences) assembly softwares, resulted in five scaffolds containing seven contigs. Gaps were closed and the genome was made circular with a combination of several methods, such as sequencing of a transposon-shotgun library of plasmids overlapping the assembly gaps (with 3,229 validated sequences obtained), and PCR amplification and subsequent sequencing of regions between scaffold ends (297 validated sequences). Identified in the genome were 47 transfer RNAs representing all amino acids, 3 small RNAs and 1 ribosomal RNA operon, as well as all of the 63 conserved clusters of orthologous groups, confirming the completeness of the genome. Gene prediction was performed with AMIGene software. Coding sequences were predicted (and assigned a unique identifier prefixed with 'DAMO'), and automatic functional annotation was performed as described previously with the MaGe system[38]. Annotations for selected genes (Supplementary Tables 4 and 5) were confirmed manually.

Phylogenetic analysis of PmoA and AmoA protein sequences. An alignment of selected bacterial and archaeal PmoA and AmoA amino-acid sequences was generated with MEGA version 4 (http://www.megasoftware.net), and conservation of important residues was judged by comparison with refs 44, 45. There were a total of 178 amino-acid positions in the final data set. A distance tree was generated in MEGA, using the neighbour-joining method. Bootstrap values of 100 replicates were generated for neighbour-joining, minimum evolution and maximum parsimony, with the Dayhoff matrix-based method. PhyML 3.0 (www.atgc-montpellier.fr/phyml/) was used to generate maximum-likelihood bootstrap values.

Proteomics. A cell-free extract from the biomass of enrichment culture 'Twente' was prepared by concentrating a sample of the biomass in 20 mM phosphate buffer and bead-beating for 2 min. The supernatant was then boiled for 10 min in sample buffer. For a cell-free extract from enrichment culture 'Ooij', a sample of the biomass was concentrated in 20 mM phosphate buffer containing 1 mM phenylmethylsulphonyl fluoride, protease inhibitor cocktail and 1% SDS, and the sample was boiled for 7 min. Both cell-free extracts were then loaded on an SDS–PAGE gel, prepared with standard methods, with about 50 μg protein per lane. After separation of proteins and staining with colloidal Coomassie blue, the gel lane was cut into four slices, each of which was destained by three cycles of washing with, successively, 50 mM ammonium bicarbonate and 50% acetonitrile. Protein reduction, alkylation and digestion with trypsin were performed as described[39]. After digestion, the samples were desalted and purified as described[46]. Sample analysis by LC–MS/MS was performed with an Agilent nanoflow 1100 liquid chromatograph coupled online through a nano-electrospray ion source (Thermo Fisher Scientific) to a 7-T linear ion-trap Fourier transform ion cyclotron resonance mass spectrometer (Thermo Fisher Scientific). The chromatographic column consisted of a 15-cm fused silica emitter (PicoTip Emitter, tip 8 ± 1 μm, internal diameter 100 μm; New Objective) packed with 3-μm C_{18} beads (Reprosil-Pur C_{18} AQ; Dr Maisch GmbH)[47]. After the peptides had been loaded on the column in buffer A (0.5% acetic acid), bound peptides were gradually eluted with a 67-min gradient of buffer B (80% acetonitrile, 0.5% acetic acid). First, the concentration of acetonitrile was increased from 2.4% to 8% in 5 min, followed by an increase from 8% to 24% in 55 min, and finally an increase from 24% to 40% in 7 min. The mass spectrometer was operated in positive-ion mode and was programmed to analyse the top four most abundant ions from each precursor scan by using dynamic exclusion. Survey mass spectra (m/z 350–2,000) were recorded in the ion cyclotron resonance cell at a resolution of $R = 50{,}000$. Data-dependent collision-induced fragmentation of the precursor ions was performed in the linear ion trap (normalized collision energy 27%, activation $q = 0.250$, activation time 30 ms). Mass spectrometric datafiles were searched against a database containing the predicted protein sequences from the '*M. oxyfera*' genome and known contaminants, such as human keratins and trypsin. Database searches were performed with the database search program Mascot version 2.2 (Matrix Science Inc.). To obtain factors for the recalibration of precursor masses, initial searches were performed with a precursor-ion tolerance of 50 p.p.m. Fragment ions were searched with a 0.8-Da tolerance and searches were allowed for one missed cleavage, carbamidomethylation (C) as fixed modification, and deamidation (NQ) and oxidation (M) as variable modifications. The results from these searches were used to calculate the m/z-dependent deviation, which was used to recalibrate all precursor m/z values. After recalibration of the precursor masses, definitive Mascot searches were performed with the same settings as above, but with a precursor-ion tolerance of 15 p.p.m. In addition, reverse database searches were performed with the same settings. Protein identifications were validated and clustered with the PROVALT algorithm to achieve a false-discovery rate of less than 1% (ref. 48).

Transcriptomics. Total cell RNA was extracted from enrichment culture 'Twente' biomass with the RiboPure-Bacteria Kit (Ambion) in accordance with the manufacturer's instructions. An additional DNase I treatment was performed (provided within the RiboPure-Bacteria Kit). RNA quality was checked by agarose-gel electrophoresis, and the RNA concentration was measured with a Nanodrop ND-1000 spectrophotometer (Isogen Life Science). First-strand cDNA was generated with RevertAid H Minus M-MuLV Reverse Transcriptase (Fermentas Life Sciences), in accordance with the manufacturer's protocol. Second-strand cDNA synthesis was performed with RNase H (Fermentas Life Sciences) and DNA polymerase I (Fermentas Life Sciences) in accordance with the manufacturer's protocol. Purification of the double-stranded DNA for sequencing was performed with the Qiaquick PCR Purification Kit (Qiagen) in accordance with the manufacturer's instructions, and single-end Illumina sequencing was performed as described above.

Short-read sequence mapping. Reads resulting from the Illumina sequencing of enrichment culture 'Ooij' were mapped onto the complete genome of '*M. oxyfera*' (enrichment culture 'Twente') with an algorithm based on iterated Blast searches[14]. In brief, the 32-nt Illumina reads were mapped to the 'Twente' reference genome by composing a majority-vote consensus. This initial consensus assembly was then taken to remap all short reads iteratively, improving the assembly coverage and bringing the genome closer to the consensus of the sequenced population 'Ooij'. Three different programs were used to map the short reads to the reference genome (Maq, Blast and MegaBlast), and with each program at least 12 iterations were constructed. For Blast and MegaBlast several different word lengths were also tried, ultimately yielding a total of 87 potential consensus genomes for the 'Ooij' culture Illumina reads (see Supplementary Table in ref. 14). To test empirically which of these assemblies best described the '*M. oxyfera*' 'Ooij' population, the ORF coordinates from the complete 'Twente' genome were mapped to each of these assemblies (the reads were mapped without gaps, so the genomic coordinates are identical) and all ORFs were translated into protein. Subsequently, the peptides obtained by LC–MS/MS (see above) were mapped to these translated ORFs with Mascot (see above). It was found that the Blast-based assembly with a word length of 8 could explain the largest number of peptides (Supplementary Table 3). As the number of peptides reached a plateau after seven iterations, we chose iteration 7 as the optimal sequence for the '*M. oxyfera*' 'Ooij' consensus genome. Positions at which SNPs occurred were identified by mapping the Illumina reads of the two enrichment cultures to their respective genomes with Maq (default settings). Sites with a polymorphic consensus were designated as SNP sites.

Activity measurements. All activity experiments were performed at 30 °C and pH 7.3 (10 mM MOPS) with whole cells from enrichment culture 'Ooij'. For measurement of nitrogenous intermediates (Fig. 3), 380 ml of enrichment culture containing 147 ± 11 mg of protein, about 2 mM NO_3^- (to maintain the redox potential) and 100 μM CH_4 were incubated in a modified Schott glass bottle without headspace and stirred with a glass-coated magnet (Supplementary Fig. 7). Microsensors for O_2 (ref. 41), N_2O (ref. 40) and NO (ref. 42), prepared and calibrated as described previously, were inserted into the culture through Teflon-coated rubber. The concentration and isotopic composition of methane and nitrogenous gases were measured in liquid withdrawn through a sintered glass filter by membrane-inlet mass spectrometry, with a quadrupole mass spectrometer (GAM 200; IP Instruments). To compensate for the liquid loss, the setup was coupled to a helium-flushed medium reservoir. N_2O was added in gas-saturated anaerobic medium, and ^{15}N-labelled NO_2^- as anaerobic stock solution. The ^{15}NO stock solution was prepared by adding H_2SO_4 to a solution containing ^{15}N-labelled NO_2^- and KI, and capturing the evolved NO gas in anaerobic water[42].

Propylene oxidation and oxygen production assays (Fig. 4) were performed (at least in duplicate) with 0.5 ml of tenfold concentrated whole cells from enrichment culture 'Ooij' in 3-ml Exetainers (Labco). Biomass was centrifuged anaerobically, washed once and resuspended in anaerobic, MOPS-buffered

doi:10.1038/nature08883 nature

(pH 7.3, 10 mM) medium[4] without NO_2^- and NO_3^-. Control incubations were performed with the aerobic, methanotrophic α-Proteobacterium *Methylosinus acidophilus* in NO_3^--free M2 medium[49]. Samples were preincubated anaerobically for at least 4 h with a helium headspace containing 6% CH_4 to deplete a cellular store of electron acceptors. Pilot experiments had shown that rates of propylene oxidation with and without added electron acceptors were otherwise identical for up to 5 h. After removal of the CH_4 from the headspace by six cycles of vacuum and helium (0.5 bar) supply, a combination specified in the Results section of the following salts (as anaerobic stock solutions) and gases (purity 99% or greater) were added: ^{15}N-labelled NO_2^- (3 mM final concentration), O_2 (6.5% in headspace, resulting in about 84 μM in solution), formate (5 mM final concentration), propylene (16% in headspace), acetylene (0.4% in headspace, resulting in 150 μM). $N^{18}O_2^-$ was not added directly to '*M. oxyfera*' incubations because the ^{18}O in it was quickly equilibrated with O in water by the activity of nitrite reductase[25], leading to 96% equilibration with O in NO_2^- within 30 min (Supplementary Fig. 6). Instead, unlabelled NO_2^- was used in combination with medium containing 25% ^{18}O-labelled water (more than 97% ^{18}O; Cambridge Isotope Laboratories). For control incubations of *M. acidophilus*, ^{18}O-labelled NO_2^- (produced as described[50] and checked by mass spectrometry after conversion to N_2O as described[51]) was used in addition to ^{18}O-labelled water, because no nitrite reductase activity can be expected. Samples were horizontally incubated at 30 °C on a shaker (250 r.p.m.). Headspace samples were taken every 30–60 min with a gas-tight glass syringe. Propylene oxide and CH_4 were quantified by gas chromatography as described previously[11], with increased temperatures of oven (150 °C), injection port and detector (180 °C). Oxidation rates were calculated from the linear part of the graphs ($R^2 \geq 0.9$), using at least three measuring points. Samples not exceeding the rate of controls without added electron acceptor (see above) were considered negative.

Formation of $^{18}O_2$ was measured by coupled GC–MS as described previously[4], detecting the masses 32–36 Da. Calibration for small amounts of oxygen was performed with known amounts of $^{18,18}O_2$ in helium and the $^{16,18}O_2$ and $^{18,18}O_2$ content of air, taking into account the average isotopic composition of atmospheric O_2. The lower limit for the accurate quantification of $^{18,18}O_2$ was 0.1 nmol ml^{-1}. Air contamination was minimized by flushing the inlet area of the gas chromatograph with helium, and the measured values of $^{16,18}O_2$ and $^{18,18}O_2$ were corrected for their abundance in contaminating air, assessed by the amount of $^{16,16}O_2$ and $^{14,14}N_2$. Incorporation of ^{18}O into propylene oxide was measured with a modification of the above method at a higher column temperature (150 °C) and detecting the masses 58–60 Da.

43. Gordon, D., Abajian, C. & Green, P. *Consed*: a graphical tool for sequence finishing. *Genome Res.* **8,** 195–202 (1998).
44. Hakemian, A. S. & Rosenzweig, A. C. The biochemistry of methane oxidation. *Annu. Rev. Biochem.* **76,** 223–241 (2007).
45. Stoecker, K. *et al.* Cohn's *Crenothrix* is a filamentous methane oxidizer with an unusual methane monooxygenase. *Proc. Natl Acad. Sci. USA* **103,** 2363–2367 (2006).
46. Rappsilber, J., Ishihama, Y. & Mann, M. Stop and go extraction tips for matrix-assisted laser desorption/ionization, nanoelectrospray, and LC/MS sample pretreatment in proteomics. *Anal. Chem.* **75,** 663–670 (2003).
47. Ishihama, Y., Rappsilber, J., Andersen, J. S. & Mann, M. Microcolumns with self-assembled particle frits for proteomics. *J. Chromatogr. A* **979,** 233–239 (2002).
48. Weatherly, D. B. *et al.* A heuristic method for assigning a false-discovery rate for protein identifications from Mascot database search results. *Mol. Cell. Proteomics* **4,** 762–772 (2005).
49. Raghoebarsing, A. A. *New Directions in Microbial Methane Oxidation*. PhD thesis, Radboud Univ. Nijmegen (2006).
50. Friedman, S. H., Massefski, W. & Hollocher, T. C. Catalysis of intermolecular oxygen atom transfer by nitrite dehydrogenase of *Nitrobacter agilis*. *J. Biol. Chem.* **261,** 538–543 (1986).
51. McIlvin, M. R. & Altabet, M. A. Chemical conversion of nitrate and nitrite to nitrous oxide for nitrogen and oxygen isotopic analysis in freshwater and seawater. *Anal. Chem.* **77,** 5589–5595 (2005).

E Appendix

This appendix is a compilation of supplementary figures and data, some media compositions and detailed method descriptions that were not part of manuscripts and their respective appendices, but are of relevance to the overall thesis.

E.1 Supplementary figures and data

E.1.1 Detailed substrate spectrum of strain HdN1 (tabular)

Table E1. Compounds tested as electron donors and carbon sources with strain HdN1 under **aerobic** conditions. Gaseous alkanes were added to the headspace with the indicated pressure. Liquid or solid alkanes were added purely or dissolved in HMN (% in brackets, vol/vol).

Substrate tests (+ 4,4 mmol air ≡ 0,93 mmol O_2)	**added amount**	**growth**	**Day after inoculation when growth was detected by turbidity**
n-*Alkanes*[a]			
Methane	1 bar	−	
Ethane	1 bar	−	
Propane	1 bar	−	
Butane	1 bar	−	
Pentane	(5%)	−	
Hexane	(5, 20%)	−	
Heptane	(5, 20%)	−	
Octane	(20%)	+	3
Nonane	(20%)	+	3
Decane	(5%)	+	3
Undecane	(5%)	+	3
Dodecane	pure	+	2
Tridecane	pure	+	2
Tetradecane	pure	+	2
Pentadecane	pure	+	2
Hexadecane	pure	+	2
Heptadecane	pure	+	2
Octadecane	pure	+	2
Eisane	pure	+	4
Tetracosane	pure	+	4
Hexacosane	pure	+	4
Octacosane	pure	+	4
Triacontane	pure	+	6
Tetracontane	pure	−	

a Gaseous n-alkanes were added to the head space with CO_2, according to Ehrenreich *et al.* (2000). Liquid *n*-Alkanes (C_6-C_{18} at 25°C) were added dissolved in HMN up to C_{11}, higher alkanes added as pure substances. Solid *n*-Alkanes (≥C_{20} at 25°C) were melted and cooled to line the reaction-tubes prior to addition of the medium.

Table E2. Compounds tested as electron donors and carbon sources with strain HdN1 under **aerobic** conditions. Fatty acid substrates were added to the indicated concentrations (mM).

Substrate tests (+ 4,4 mmol air ≡ 0,93 mmol O_2)	**Added amount**	**Growth**
Fatty acids		
Formiate[a]	(10, 20 mM)	−
Acetate	(10, 20 mM)	+
Propionate	(5 mM)	(+)
Butyrate	(5, 10 mM)	+
Valerianate	(4, 8 mM)	+
Caproate	(3, 6 mM)	+
Heptanoate	(4 mM)	+
Octanoate	(4 mM)	+
Nonanoate	(1, 2 mM)	(+)
Decanoate	(0,5 1 mM)	(+)
Dodecanoate	(2 mM)	+
Tetradecanoate	(2 mM)	+
Palmitate	(1, 2 mM)	+
Stearate	(1, 2 mM)	+

a Cultures with formiate were amended with 1 mM acetate as C-source.

Table E3. Compounds tested as electron donors and carbon sources with strain HdN1 under **anaerobic** conditions. Gaseous substrates were added to the headspace with the indicated pressure. Hydrophobic substrates were added purely or dissolved in HMN (% in brackets, vol/vol).

Substrate tests (+ 10 mM nitrate)	**Added amount**	**Growth**	**day after ino. when growth was visible**
n-*Alkanes*			
Methane[b]	1 bar	−	
Ethane[b]	1 bar	−	
Propane[b]	1 bar	−	
Butane[b]	1 bar	−	
Hexane	(2%)	(+)	4
Heptane	(2, 4%)	(+)	4
Octane	(2, 5%)	(+)	5
Nonane	(2, 5%)	(+)	5
Decane	(5%)	(+)	6
Undecane	(5%)	(+)	5
Dodecane	pure	(+)	22
Tridecane	pure	(+)	22
Tetradecane	pure	+	2
Pentadecane	pure	+	2
Hexadecane	pure	+	2
Heptadecane	pure	+	3
Octadecane	pure	+	3
Eisane	pure	+	4
Tetracosane	pure	+	4
Hexacosane	pure	+	4
Octacosane	pure	+	4
Triacontane	pure	+	7
Tetracontane	pure	−	
1-Alkenes			
1-Decene	(2%)	(+)	
1-Tetradecene	pure	+	
1-Hexadecene	pure	+	
1-Heptadecene	pure	+	

a Liquid *n*-alkanes (C_6-C_{18} at 25°C) were added dissolved in HMN up to C_{11}, higher alkanes were added as pure substances. Solid *n*-alkanes (≥C_{20} at 25°C) were melted and cooled to line the reaction-tubes prior to addition of the medium.
b Gaseous n-alkanes added to the head space with CO_2, according to Ehrenreich et al. (2000).

Table E4. Compounds tested as electron donors and carbon sources with strain HdN1 under **anaerobic** conditions. Gaseous substrates were added to the headspace with the indicated pressure. Hydrophobic substrates were added purely or dissolved in HMN (% in brackets, vol/vol). Hydrophilic substrates were added to the indicated concentrations (mM).

Substrate tests (+ 10 mM nitrate)	**added amount**	**growth**
Aromatics		
Benzoate	(1 mM)	−
Phenyl-acetate	(1 mM)	−
Phenyl	(0.5 mM)	−
Toluene	(1, 2%)	−
Aldehydes		
Decanal	(0.5, 1%)	+
Alcohols		
Methanol	(10 mM)	−
Ethanol	(10 mM)	−
1-Propanol	(5, 10 mM)	−
2-Propanol	(5, 10 mM)	−
1-Butanol	(5, 10 mM)	−
2-Butanol	(5, 10 mM)	−
1-Octanol	(0.5, 1%)	(+)
1-Decanol	(1, 2%)	+
1-Tetradecanol	pure	+
1-Hexadecanol	pure	+
2-Hexadecanol	pure	(+)
Phenyl-alkanes		
1-Phenyldecane	(1, 2%)	−
1-Phenyldodecane	(1, 2%)	−
1-Phenyltridecane	(1, 2%)	(+)
1-Phenyltetradecane	pure	+

Table E5. Compounds tested as electron donors and carbon sources with strain HdN1 under **anaerobic** conditions. Hydrophobic substrates were added purely or dissolved in HMN (% in brackets, vol/vol). Hydrophilic substrates were added to the indicated concentrations (mM).

Substrate tests (+ 10 mM nitrate)	**added amount**	**growth**
2-Methylheptane	(2, 4%)	−
3-Methylheptane	(2, 4%)	−
4-Methylheptane	(2, 4%)	−
2-Methyloctane	(2, 4%)	−
3-Methyloctane	(2, 4%)	−
4-Methyloctane	(2, 4%)	−
2-Methylnonane	(2, 4%)	−
3-Methylnonane	(2, 4%)	−
Liquid paraffin low density	pure	+
Liquid paraffin high density	pure	+
Paraffin wax	pure	+
Cyclohexane	(1, 2%)	−
Ethylcyclohexane	(1, 2%)	−
Monocarboxylic Acids		
3-Methylbutyrate	(2, 4 mM)	+
Fatty acids		
Formiate	(10, 20 mM)	−
Acetate	(10, 20 mM)	+
Propionate	(5, 10 mM)	+
Butyrate	(5, 10 mM)	+
Valerianate	(4, 8 mM)	+
Caproate	(3, 6 mM)	+
Heptanoate	(4 mM)	+
Octanoate	(4 mM)	+
Nonanoate	(1, 2 mM)	(+)
Decanoate	(0,5 1 mM)	(+)
Undecanoate	(0,5 1 mM)	+
Dodecanoate	(1, 2 mM)	+
Tridecanoate	(1, 2 mM)	+
Tetradecanoate	(1, 2 mM)	+
Pentadecanoate	(1, 2 mM)	+
Palmitate	(1, 2 mM)	+
Heptadecanoate	(1, 2 mM)	+
Stearate	(1, 2 mM)	+

Table E6. Compounds tested as electron donors and carbon sources with strain HdN1 under **anaerobic** conditions. Hydrophilic substrates were added at the indicated concentrations (mM or g l^{-1}).

Substrate tests (+ 10 mM nitrate)	**added amount**	**growth**
Other compounds		
Tartrate	(5, 10 mM)	−
Lactate	(10 mM)	−
Pyruvate	(10 mM)	(+)
Succinate	(5, 10 mM)	−
Fumarate	(5, 10 mM)	−
Malate	(5, 10 mM)	−
Citrate	(5, 10 mM)	−
Glutarate	(5, 10 mM)	−
Mannose	(5, 10 mM)	−
Fructose	(2.5 mM)	−
Glucose	(5, 10 mM)	−
Ascorbate	(4, 8 mM)	−
Gluconate	(5, 10 mM)	−
Glycine	(5 mM)	−
Alanine	(10 mM)	−
Glutamate	(5 mM)	−
Serine	(5 mM)	−
Aspartate	(5 mM)	−
Yeast Extract	(5 g/l)	−
Peptone	(5 g/l)	−

E.1.2 HdN1 FAME Patterns

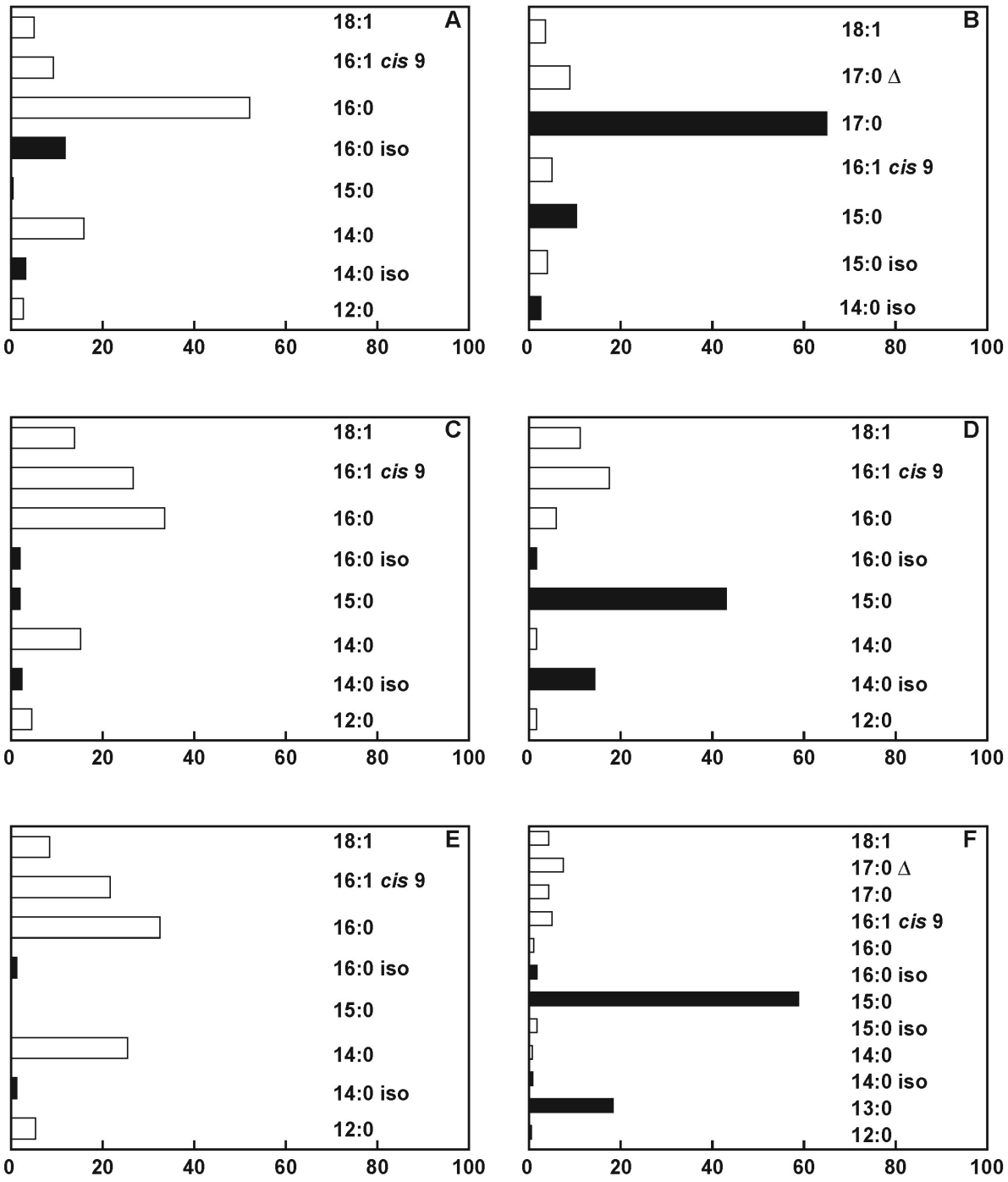

Fig. E1. Reproduced from Ehrenreich, 1996. Distribution (%) of analyzed cell fatty acids of strain HdN1 in cells grown anaerobically with hexadecanoate (A), heptadecanoate (B), *n*-hexadecane (C) and *n*-pentadecane (D) as well as in cells grown aerobically with *n*-hexadecane (E), *n*-pentadecane (F). Black bars (■) indicate fatty acids with an odd number of C-atoms in the carbon-backbone, white bars (□) indicate fatty acids with an even number of C-atoms in the carbon-backbone.

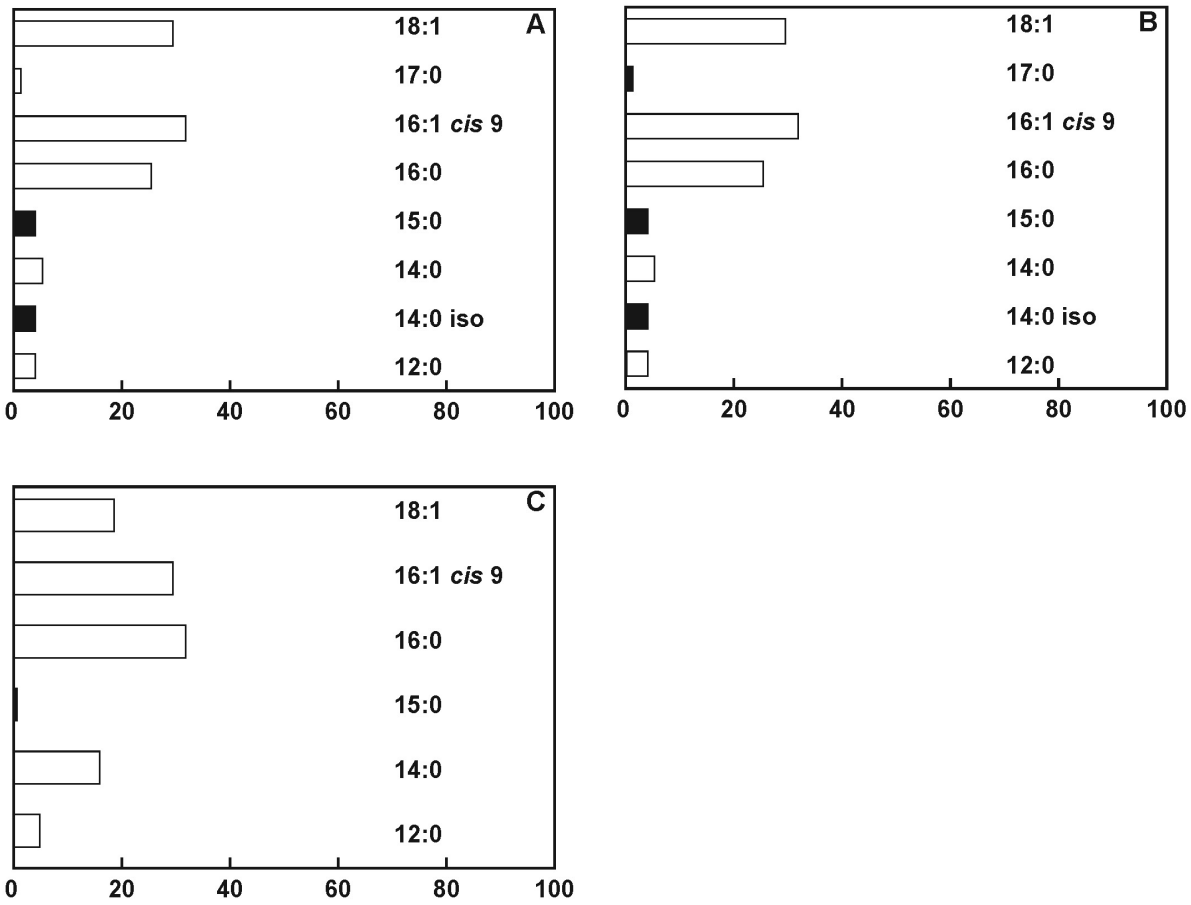

Fig. E2. Reproduced from Ehrenreich, 1996. Distribution (%) of analyzed cell fatty acids of strain HdN1 in cells grown anaerobically with 1-hexadecene (A), 1-heptadecene (B) or 1-hexadecanol (C). Black bars (■) indicate fatty acids with an odd number of C-atoms in the carbon-backbone, white bars (□) indicate fatty acids with an even number of C-atoms in the carbon-backbone.

E.1.3 Wax ester production by strain HdN1

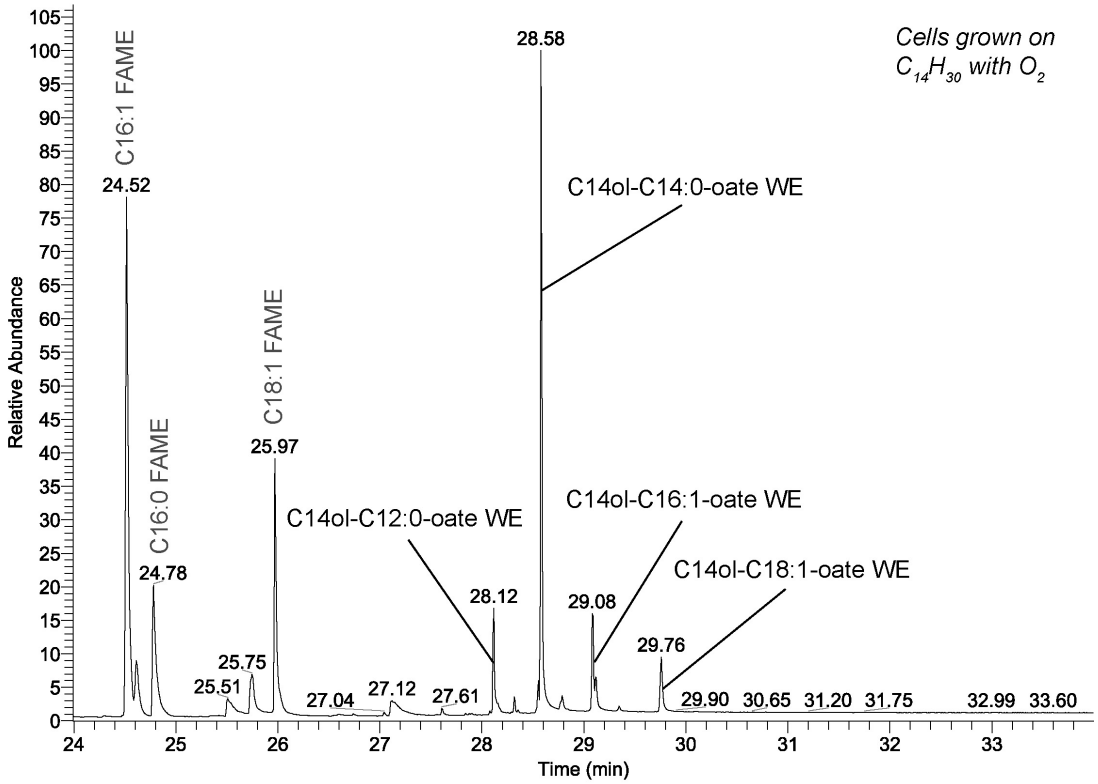

Fig. E3. Wax esters and FAMEs (grey caption) detected during FAME analysis. Cells of strain HdN1 were grown with *n*-tetradecane ($C_{14}H_{30}$) under air (with O_2).

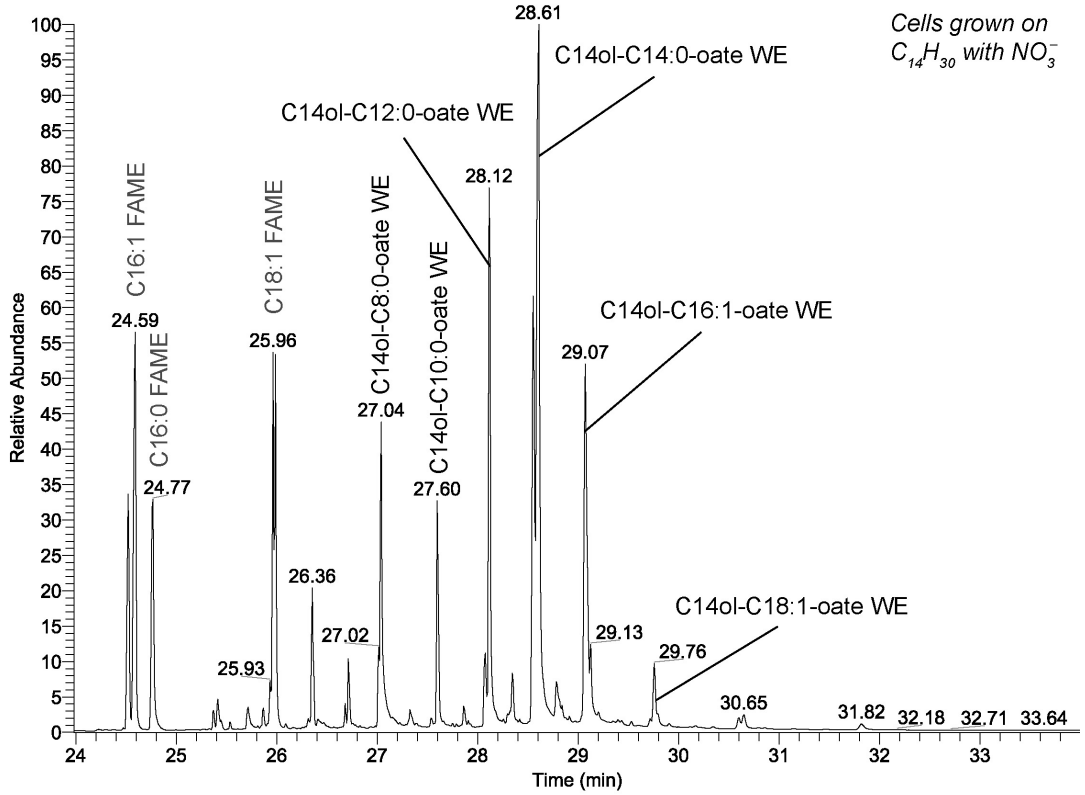

Fig. E4. Wax esters and FAMEs (grey caption) detected during FAME analysis. Cells of strain HdN1 were grown with *n*-tetradecane ($C_{14}H_{30}$) and nitrate (NO_3^-).

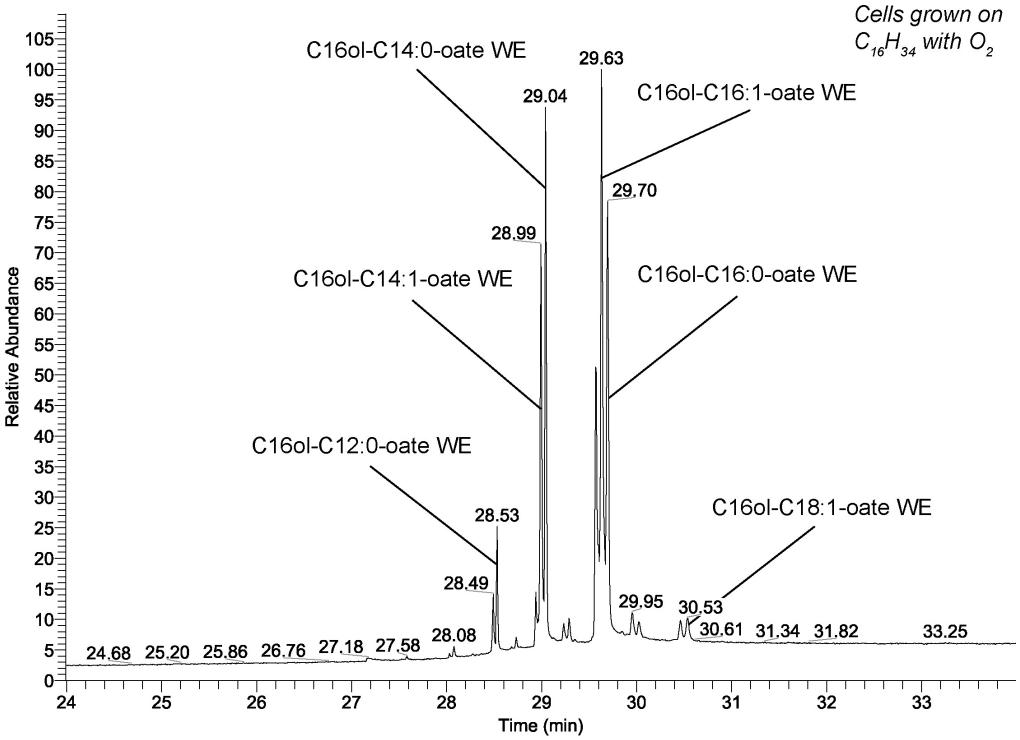

Fig. E5. Wax esters and FAMEs (grey caption) detected during analysis of ether extracts. Cells of strain HdN1 were grown with *n*-tetradecane ($C_{16}H_{34}$) under air (with O_2).

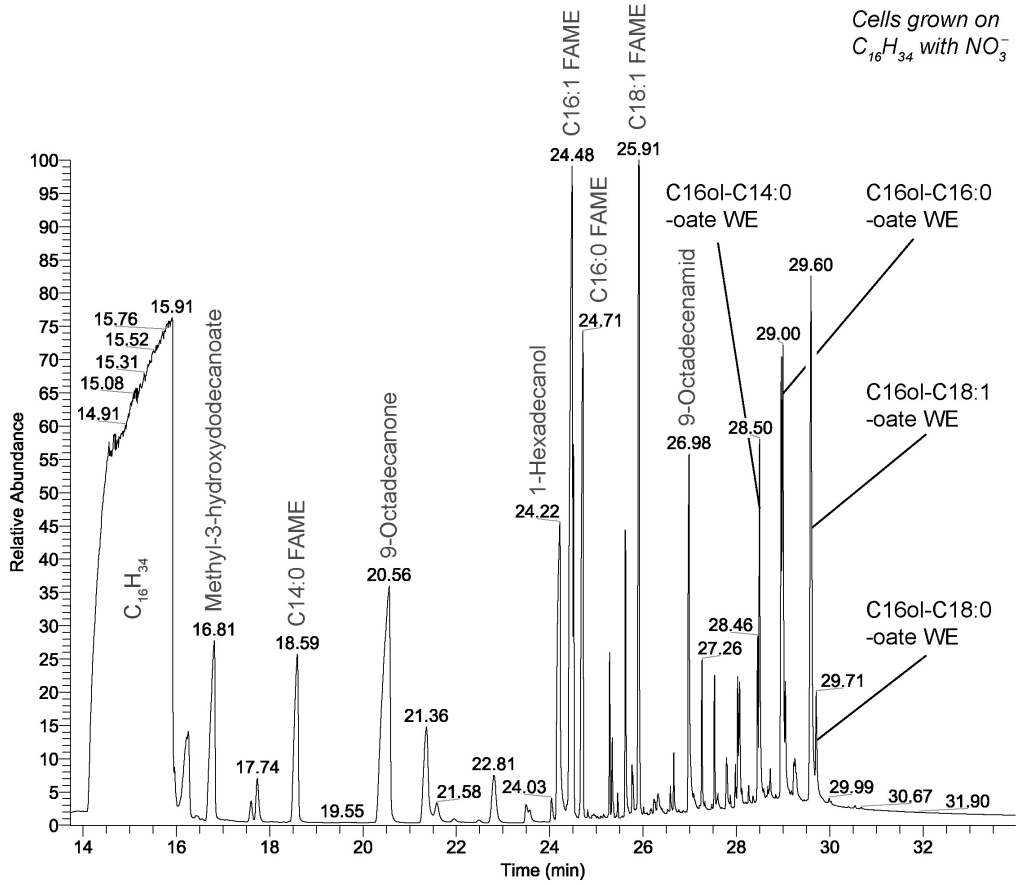

Fig. E6. Wax esters and FAMEs (grey caption) detected during FAME analysis. Cells of strain HdN1 were grown with *n*-hexadecane ($C_{16}H_{34}$) and nitrate (NO_3^-). Identification of other compounds (grey caption) was preliminary since authentic standards were not analyzed for comparison.

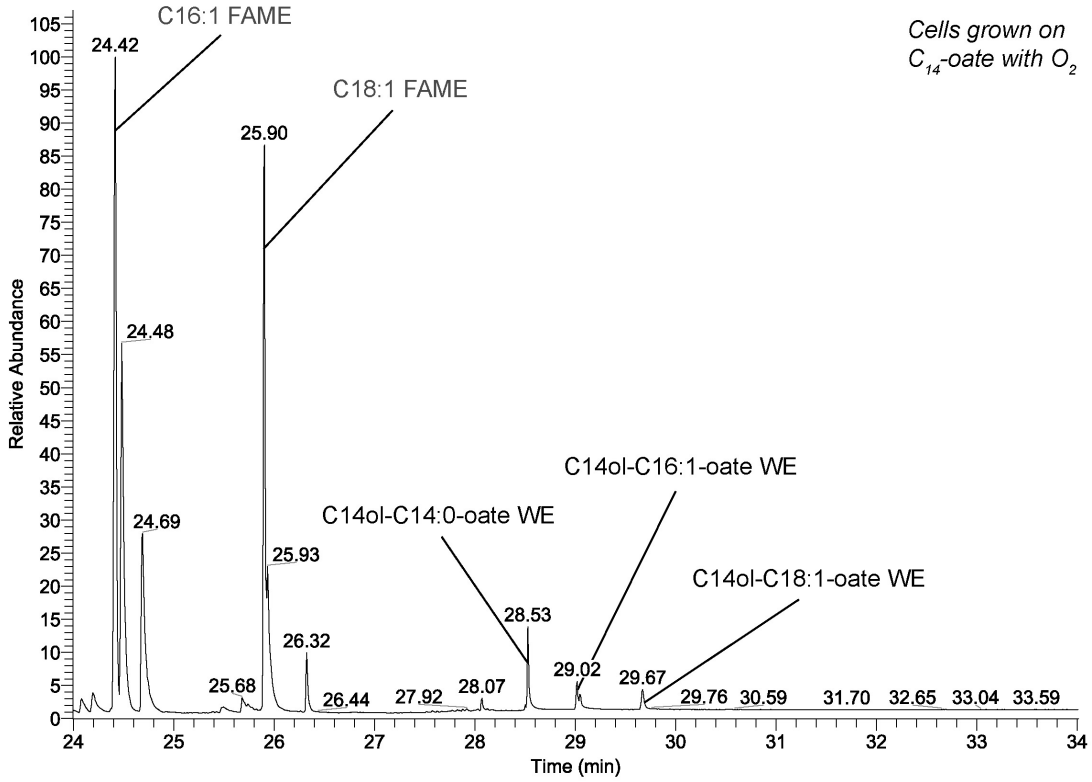

Fig. E7. Wax esters and FAMEs (grey caption) detected during FAME analysis. Cells of strain HdN1 were grown with tetradecanoate (C_{14}-oate) under air (with O_2).

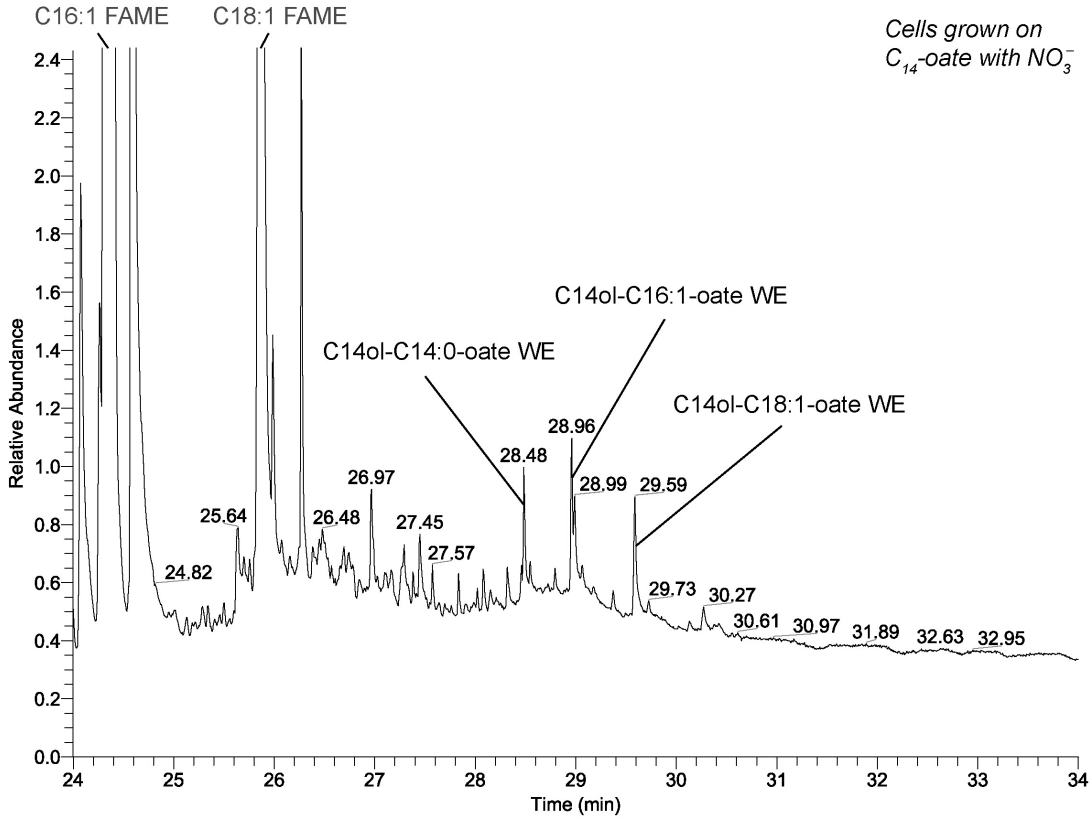

Fig. E8. Wax esters and FAMEs (grey caption) detected during FAME analysis. Cells of strain HdN1 were grown with tetradecanoate (C_{14}-oate) and nitrate (NO_3^-).

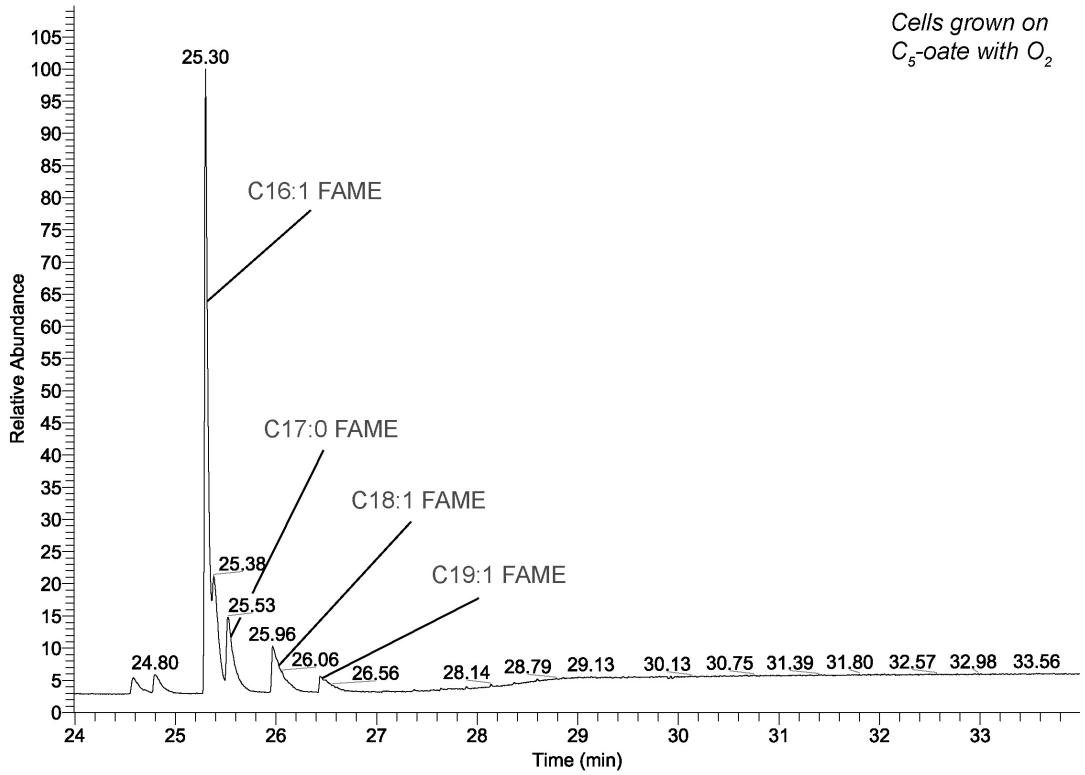

Fig. E9. FAMEs (grey caption), but no wax esters detected during FAME analysis. Cells of strain HdN1 were grown with pentanoate (C_5-oate) under air (with O_2).

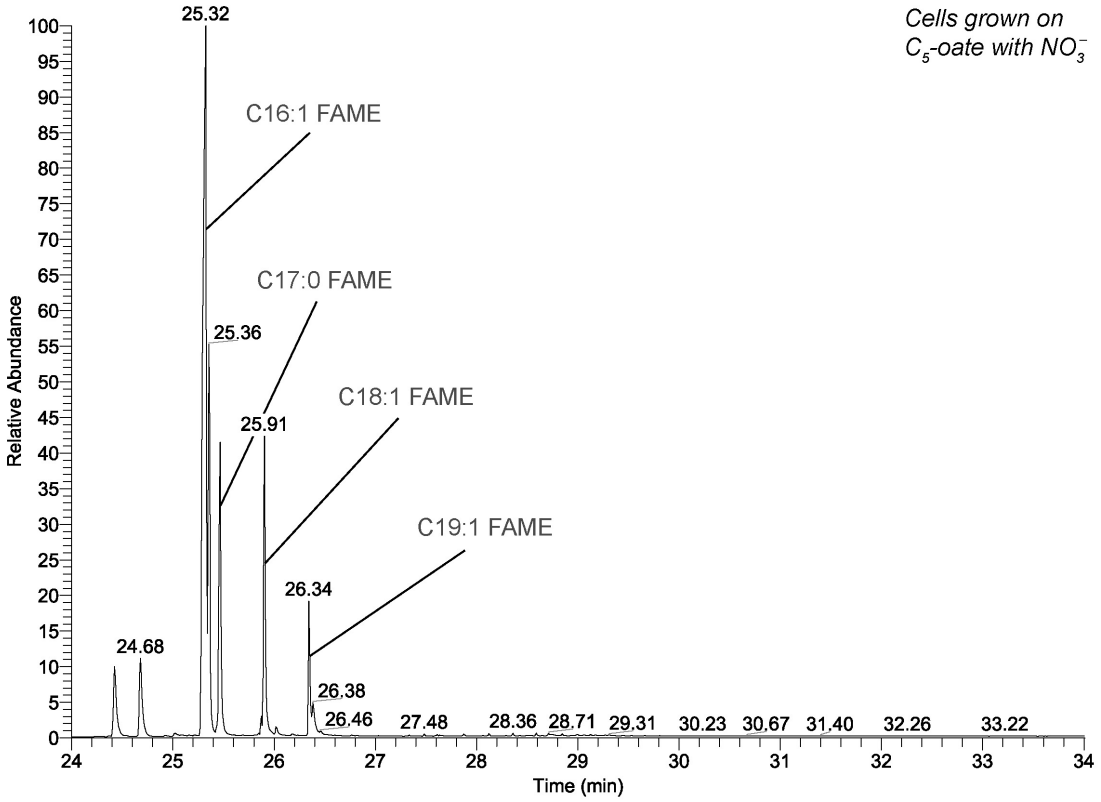

Fig. E10. FAMEs (grey caption), but no wax esters detected during FAME analysis. Cells of strain HdN1 were grown with pentanoate (C_5-oate) and nitrate (NO_3^-).

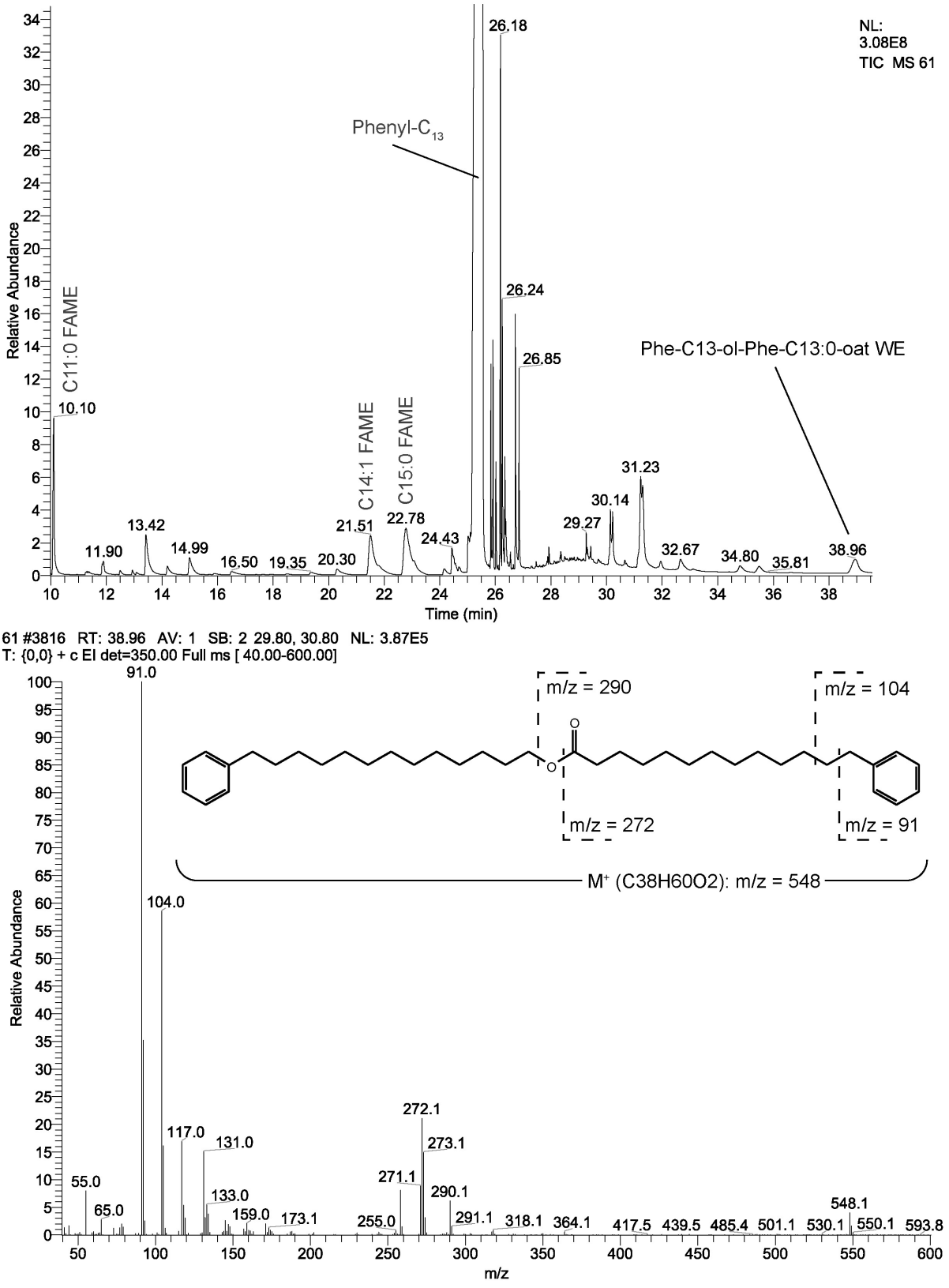

Fig. E11. Phenylalkyl wax esters produced during anaerobic growth of strain HdN1 with phenyl-tridecane. The Gas-chromatogram and mass fingerprint with indicative mass fragments and molecular ion (M^+) are depicted.

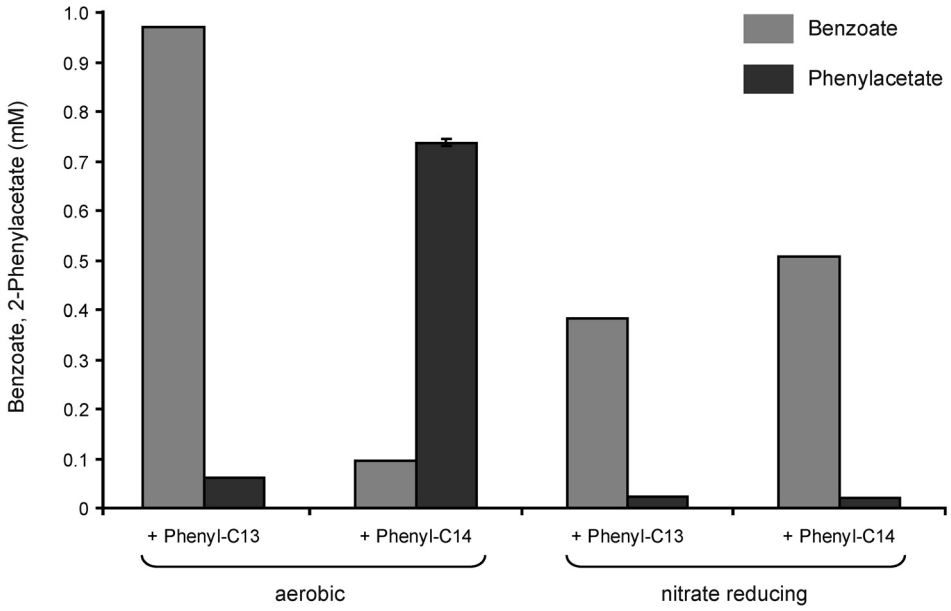

Fig. E12. Concentrations of benzoate (grey bars) and phenylacetate (black bars) in the aqueous phase of HdN1 cultures grown under aerobic or nitrate-reducing conditions with 1-phenyltridecane (+ Phenyl-C13) or 1-phenyltetradecane (+ Phenyl-C14).

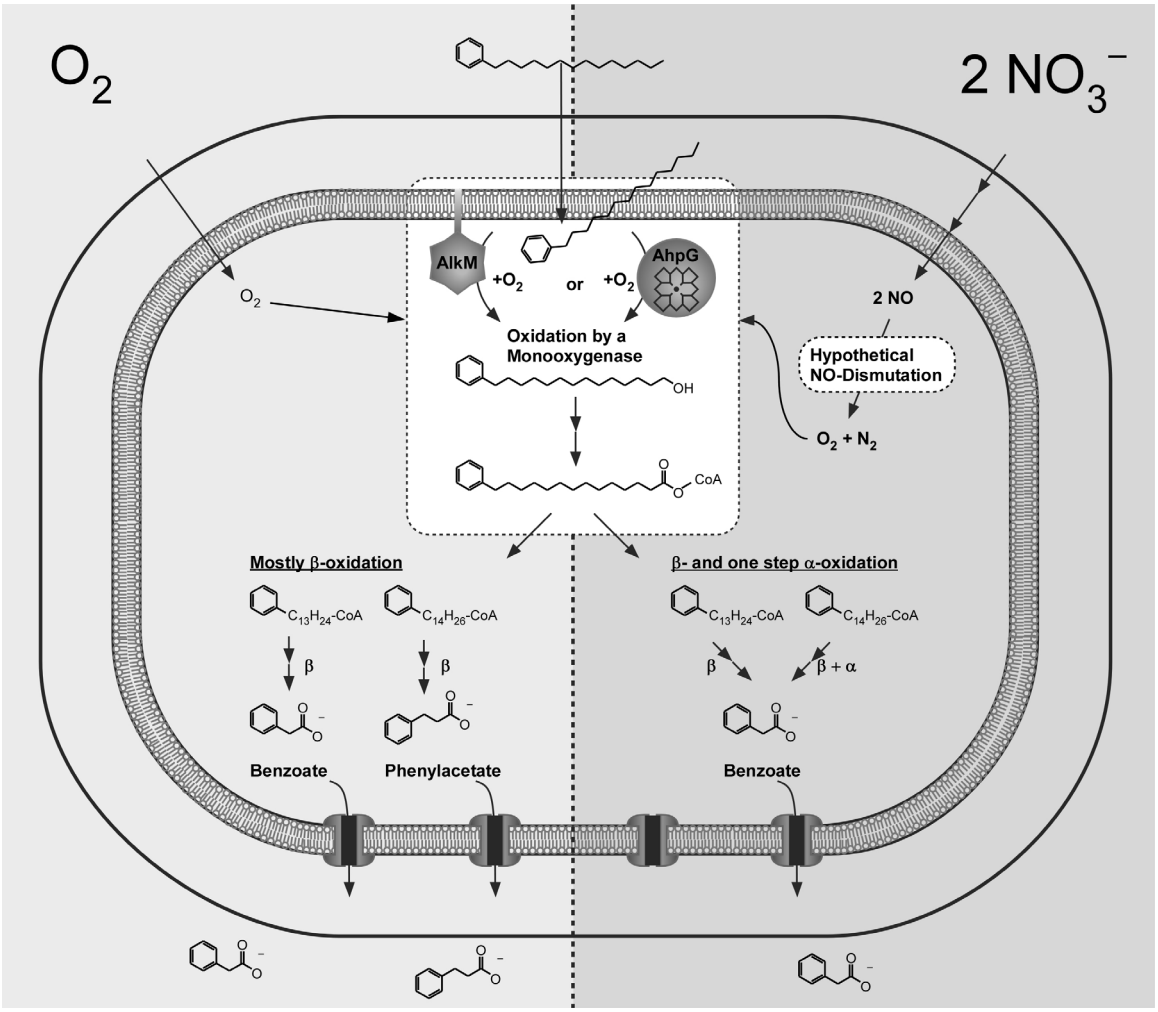

Fig. E13. Hypothetical pathways for the degradation of phenylalkanes under aerobic vs. nitrate-reducing conditions in strain HdN1. Phenylalkanes diffuse passively into the cell. The activation reaction (at least under aerobic conditions) should be similar to *n*-alkanes at a terminal C by a monooxygenases (in strain HdN1 e.g. the iron dependent AlkM or the P450 hydroxylase AhpG). Oxygen as a co-reactant is present under aerobic conditions and might be produced by NO-Dismutation under nitrate-reducing conditions enabling the same initial reactions. Since mostly benzoate is produced during growth with phenyltridecane and mostly phenylacetate is formed from phenyltetradecane, β-oxidation seems to be the main pathway employed under aerobic conditions. Under nitrate-reducing conditions growth with either phenyltridecane or phenyltetradecane leads to the formation of benzoate, suggesting that apart from β-oxidation with odd-numbered C-side chains, also β-oxidation of even numbered side chains followed by α-oxidation of phenylacetate might take place. Both carboxylic acids are deprotonated at the near-neutral pH present in the cultures so that either active transport or cell lysis would be necessary for their release.

E.1.4 Acetylene-inhibition of growth on alkanes and growth via N_2O-reduction

Table E7. Tests with strains HdN1 and OcN1 on acetylene-inhibition of growth on alkanes and on acetylene-inhibition of growth coupled to N_2O-reduction in strain HdN1. Acetylene is a potential monooxygenase inhibitor.

Electron acceptor	Growth substrate[a]	Additional substrate[b]	Additional (C_2H_2)[c]	Growth[d]	
				Short term[e]	Long term[f]
Acetylene-inhibition of growth with alkanes by with strain HdN1					
NO_3^-	no substrate		+	–	–
NO_3^-	n-tetradecane		+	–	+
NO_3^-	n-tetradecane	tetradecanoate	+	+	+
NO_3^-	tetradecanoate		+	+	+
O_2	no substrate		+	–	–
O_2	n-tetradecane		+	(+)	+
O_2	n-tetradecane	tetradecanoate	+	+	+
O_2	tetradecanoate		+	+	+
Tests with strain OcN1 for comparison					
NO_3^-	5% n-octane in HMN		+	–	n.d.
NO_3^-	5% n-octane in HMN	hexanoate	+	+	+
NO_3^-	5% n-octane in HMN		-	+	+
O_2	5% n-octane in HMN		+	+	+
O_2	5% n-octane in HMN	hexanoate	+	+	+
O_2	5% n-octane in HMN		-	+	+
N_2O-reductase inhibition by acetylene (strain HdN1)					
NO_3^-, N_2O	pentanoate		+	+	+
N_2O	pentanoate		+	–	n.d.
N_2O	pentanoate		-	+	+
NO_3^-, N_2O	tetradecanoate		+	+	+
N_2O	tetradecanoate		+	–	n.d.
N_2O	tetradecanoate		-	+	+

a If not indicated otherwise, the substrates were added in their pure form. Amounts were: Liquid hydrocarbons ~10 µl, tetradecanoate 1 mmol l^{-1}, pentanoate 3 mmol l^{-1}, hexanoate 3 mmol l^{-1}.
b The same amounts of additional substrate and growth substrate were typically added.
c Acetylene (C_2H_2) was added as gas saturated water to make up 10% of the final volume.
d Growth was assessed as obvious turbidity indicated as: + obvious growth, (+) little growth, – absence of growth, n.d. not determined.
e Short term was 4 to 7 days.
f Long term was more than 7 days.

E.2 Media additional to those described by Widdel and Bak (1992)

Table E8. Composition of phosphate buffered nitrate reducer medium (PNM).

	[in g l^{-1}]
KH_2PO_4 (for 30 mM)	1.5
K_2HPO_4 (for 30 mM)	3.36
NH_4CL	0.3
$NaNO_3$ (10 mM)	0.85
autoclave	
	[in ml l^{-1}]
$MgSO_4 \cdot 7\ H_2O$ (400 g l^{-1})[a]	1
$CaCl_2 \cdot\ 2\ H_2O$ (75 g l^{-1})[b]	1
Trace elements (chelated)	1
Se/Wo	1
5-Vitamine-Mix	1
Vitamine B_{12}	1
add 1 M HCl to	[in ml l^{-1}]
adjust pH to 6.8-7.2	3.25
1 M Ascorbate	4

a 20 g $MgSO_4 \cdot 7\ H_2O$ (400 g l^{-1}) for 50 ml stock.
b 3.75 g $CaCl_2 \cdot 2\ H_2O$ (75 g l^{-1}) for 50 ml stock.

Table E9. Composition of brackish medium.

	[in g l^{-1}]
NaCl	10.0
$MgSO_4 \cdot 7\ H_2O$	4.5
$CaCl_2 \cdot 2\ H_2O$	0.5
KH_2PO_4	0.5
H_2O (add to a final vol. of)	950 ml
autoclave	
	[in ml l^{-1}]
Trace elements (chelated)	1
Se/Wo	1
5-Vitamine-Mix	1
Vitamine B_{12}	1
adjust pH to 6.8-7.2	

Table E10. Composition of medium for agar plates for cultivation of strain HdN1.

	[in g l^{-1}]
NH_4Cl	0.3
$CaCl_2$	0.1
H_2O	929.9
autoclave	
	[in ml l^{-1}]
1 M HCl	8
$MgSO_4$ (7.5 g per 50 ml)	6.67
1 M KH_2PO_4	8.22
1 M K_2HPO_4	32.2
1 M $NaNO_3$	10
Trace elements	1
Se/Wo	1
5-Vitamine-Mix	1
Thiamine	1
Vitamine B_{12}	1
adjust pH to 6.8-7.2	
Substrates for purity-control plates:	
Yeast extract	2,5 g
0.5 M pentanoate	8 ml

Preparation: To prepare agar plates, autoclave in two different bottles: A) Agar (15.0 g) + H_2O (500 ml) B) Solution of NH_4Cl, $CaCl_2$ (see above) + H_2O (429,9 ml) Keep agar liquid at ~55°C and let salt solution cool to room temperature before addition of supplements (see above). After addition of all components, slowly and carefully pour salt solution into hot agar solution. Avoid bubble formation. Mix by gentle horizontal agitation. Pour plates.

E.3 Preparation of ^{15}N labeled nitric oxide

Labelled NO (water containing a mixture of ^{14}N- and ^{15}N-NO; 50:50, w/w) was prepared (from H_2SO_4, $FeSO_4$ and $NaNO_2$) with a setup different to the one used for ^{14}N-NO production to minimize the use of ^{15}N- NO_2^- for economic reasons: To an anoxic mixture of 195 mg $FeSO_4$ and 670 µl H_2SO_4 (25%) in a 4.5 ml glass tube, closed with a butyl rubber stopper, 500 µl of anoxic $NaNO_2$ (100 mg ml^{-1}) was added. About 6 ml of the NO gas liberated by gentle mixing was captured in a 10 ml syringe and injected into a 10 ml rubber stoppered glass-tube, completely filled with anoxic (helium saturated) water. A thin needle was also inserted in the septum, releasing liquid – establishing a slight overpressure in the tube, to gain an equal or slightly higher NO concentration than at NO-saturation under ambient pressure. The actual concentration has to be determined experimentally. The detailed preparation protocol was:

Material:

~195 mg $Fe^{II}SO_4$		≡ 0,7 mmol
670 µl H_2SO_4	(25% ≈ 3,0 M)	≡ 1 mmol
100 mg $NaNO_2$	(yielding at max. 17,1 ml NO)	≡ 0,7 mmol

4-5 ml Hungate-Tube (with septum & lid)
1 ml syringe
10 ml syringe
10 ml Hungate-Tube (headspace-free filled with anoxic water)
Reagent tube with 10 ml $KMnO_4$ (O,4 M), NaOH (0,12 M)
NaOH (Pellets) in syringe top piece to bind possibly produced NO_2 gas

Preparation:

Weigh 195 mg $Fe^{II}SO_4$ and transfer into 4-5 ml Hungate-Tube
Add 2140 µl H_2O_{mp}
Add 670 µl H_2SO_4 (the 25% H_2SO_4 has a concentration of roughly 3 M)
Close with septum and lid. Use long needle (reaching to the bottom of the vessel) and a short needle (attached to a tube leading into the $KMnO_4$-solution) to remove all oxygen. Flush (bubble) for at least 15 min with N_2 (or He).
Weigh 100 mg NaNO2 and transfer into a new 4 ml Hungate Tube
Add 900 µl H_2O_{mp}

Use long needle (reaching to the bottom of the vessel) and a short needle (as the outlet) to remove all oxygen. Flush (bubble) for at least 15 min with N_2 (or He or Ar). Take up 500 µl of the solution into a N_2-flushed 1 ml syringe and stick the needle into the septum of the $FeSO_4$, H_2SO_4 tube. Very slowly and with breaks (for gentle horizontal shaking) add the 500 µl $NaNO_2$.

After addition of about 250 µl $NaNO_2$ close the tube to the $KMnO_4$ and take up 2-3 ml of the produced NO (the produced gas pushes the plunger up with a little help over the initial resistance). Flush the syringe 3 times (2-3 ml) with the produced NO, so that the dead volume is completely filled with NO (open tube to $KMnO_4$ each time before pressing the plunger). Then withdraw 6 ml of NO (let the produced NO move the plunger up). Open the outlet tube to avoid overpressure and stick the needle as quickly as possible into the Hungate-Tube with the anoxic water. Use a small needle to release overpressure (let anoxic water flow out) during injection of NO gas and for a while afterwards. Draw out syringe with NO first and afterwards the outlet-needle to keep the pressure balanced with atmospheric pressure. For extensive NO-saturation of the anoxic water shake or vortex the tube vigorously. Possibly incubate over night for maximal dissolution of the NO. The actual concentration of NO has to be determined experimentally, e.g. with help of an NO microsensor.

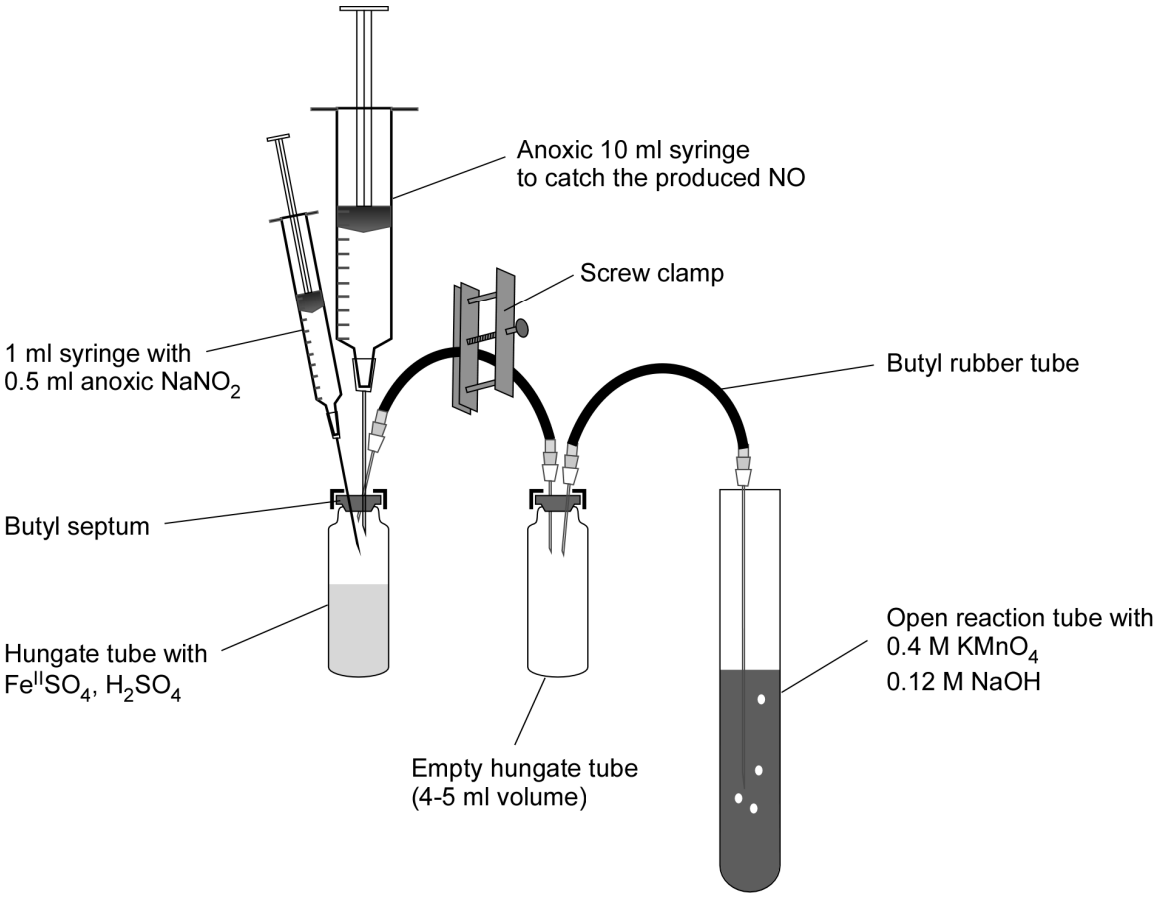

Fig. E14. Setup for ^{15}N-NO production in small volumes.

E.4 Further details on applied methods

E.4.1 The HdN1-specific oligonucleotide probe for whole cell hybridizations (FISH)

A 5' fluorescence (Cy3) labeled oligonucleotide probe specific for the HdN1 16S rRNA was designed using the ARB software package, which had a minimum number of four mismatches with all other species in the ARB database (SSU Ref NR 96, Oct 2008; Ludwig *et al.,* 2004; Pruesse *et al.,* 2007). The probe has the sequence 5'-TTC CTG CGC TAT CCT CAC-3' and binds at the *E. coli* position 112 to 16S rRNA of the ribosome. For whole cell hybridizations (also called fluorescence *in situ* hybridizations, FISH) 60% formamide concentrations were applied.

E.4.2 Comparative genomics

1493 completely sequenced bacterial genomes were downloaded from ftp://ftp.ncbi.nih.gov/genomes/Bacteria/all.gbk.tar.gz in September 2010. From a nonredundant set of these genome sequences (794, only a single genome per genus) a blast database was created with translations of all open reading frames encoding a protein of at least 50 aminoacids long. Protein sequences of all predicted open reading frames of Gammaproteobacterium strain HdN1 were blasted into this database with an evalue cutoff of 1e-10. Only the best 20 hits were kept. Open reading frames with a protein of *Candidatus* Methylomirabilis among the eight best blast hits were further inspected manually.

E.4.3 Gene analysis.

1962 full length aminoacid sequences of heme-copper oxidases (CCD206949) from sequenced genomes were obtained with text and homology searches from genbank in April 2012. The sequences were clustered with uclust (Edgar, 2010) at 70% aminoacid identity and from each cluster a single representative sequence was used for further analysis (536 sequences total). Representative sequences were aligned with MAFFT (Katoh *et al*., 2002) and a phylogenetic tree based on an approximate maximum likelyhood algorithm was created with FastTree2 (Price *et al.,* 2010). All sequences (112) belonging to the phylogenetic clade that contained the canonical nitric oxide reductases (encoded by *norB* and *norZ*) were extracted from the tree, realigned more precisely (MAFFT, --maxiterate 1000 option), and the alignment was inspected manually with JalView (Waterhouse *et al*., 2009). Before treeing a 10%

conservation filter was applied to the alignment, reducing the alignment from 1473 to 755 columns (the most conserved ones). Again, a phylogenetic tree was created with FastTree2 and gamma20 likelihoods were used to estimate the robustness of bifurcations (instead of "bootstrap" values, Price *et al*., 2010).

E.4.4 Membrane inlet mass spectrometry (MIMS)

The MIMS-setup consists of a gas-tight glass container connected to a membrane-inlet for mass spectrometrical analysis. It had been used before to study anaerobic methane oxidation coupled to NO_2^- reduction (Ettwig et al., 2010). A liquid sample is pumped constantly from the lower part (the "reactor") to the membrane-inlet via gas tight tubing by a peristaltic pump at ~0.7 ml/min. When the pumped liquid reaches the silicone membrane, volatile non-ionic compounds are degassed and transported to the quadrupole mass spectrometer (GAM 200, InProcess Instruments, Bremen, Germany) for analysis, passing a cold-trap (~ −19°C) for water vapor. The reaction chamber (perpetually mixed by a glass-coated stir bar) is connected to a liquid reservoir above, coupled to a constant flow of helium ("helium-line") ensuring that volume-loss to the pump is always balanced and no air is drawn into the setup. Since the connection to this upper part is a thin tube (3-5 mm × 115 mm), which impedes mixing, the volume in this chamber (370-380 ml, dependent on applied stoppers) is assumed to be constant for calculation of concentrations. Butyl-stopper closed openings on the sides allow addition of solutes using syringes flushed with an inert gas and insertion of microsensors via holes with matching diameters for gas-tight sealing. While such sensors measure directly in the reactor, the MIMS detects changes in the liquid volume only after a short transportation delay.

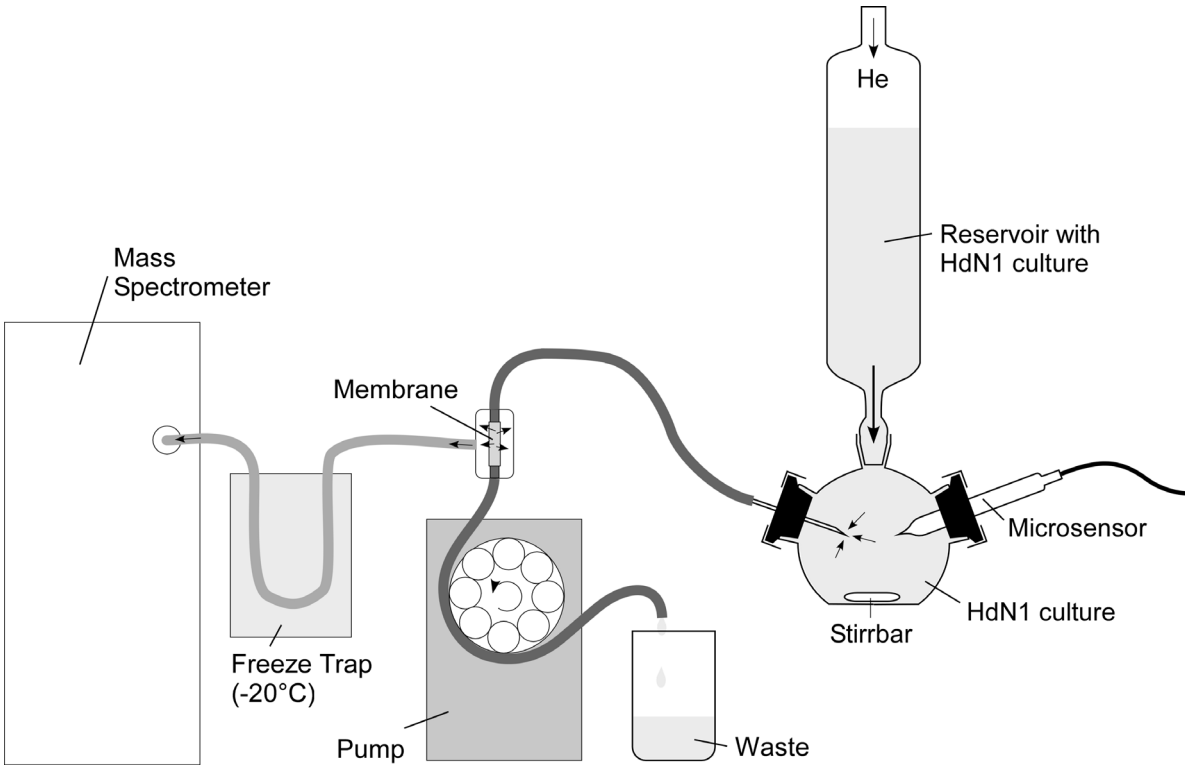

Fig. E15. MIMS setup for real-time analyses of volatile compounds dissolved in the culture liquid.

Table E11. Identities of some relative molecular masses (M_r) potentially detected in biological MIMS samples.

M_r	Possible identity	M_r	Possible identity
4	Helium	40	^{40}Argon
16	Methane (CH_4)	41	
18	$H_2{}^{16}O$	42	Propylene (C_3H_6)
20	$H_2{}^{18}O$, $D_2{}^{16}O$	43	
21		44	$^{14,14}N_2{}^{16}O$, $^{12}C^{16,16}O_2$, Propane (C_3H_8)
22		45	$^{14,15}N_2{}^{16}O$, $^{13}C^{16,16}O_2$
23			$^{15,15}N_2{}^{16}O$, $^{14,14}N_2{}^{18}O$, $^{14}N^{16,16}O_2$, $^{12}C^{18,16}O_2$
24		46	EtOH (C_2H_6O)
25		47	
26	Acetylene (C_2H_2)	48	$^{15,15}N_2{}^{18}O$, $^{14}N^{16,18}O_2$, $^{12}C^{18,18}O_2$
27	Cyanide (HCN)	49	$^{13}C^{18,18}O_2$
28	$^{14,14}N_2$, Ethylene (C_2H_4)	50	$^{14}N^{18,18}O_2$
29	$^{14,15}N_2$	51	$^{15}N^{18,18}O_2$
30	$^{15,15}N_2$, $^{14}N^{16}O$, Ethane (C_2H_6)	52	
31	$^{15}N^{16}O$	53	
32	$^{16,16}O_2$, $^{14}N^{18}O$, H_2S, Hydrazine, ($^{14,14}N_2H_4$), Methanol (CH_3OH)	54	
33	$^{15}N^{18}O$, Hydrazine ($^{14,15}N_2H_4$)	55	
34	$^{16,18}O_2$, Hydrazine ($^{15,15}N_2H_4$), Hydroxylamine ($H_3{}^{14}NO$)	56	
35	Hydroxylamine ($H_3{}^{15}NO$)	57	
36	$^{18,18}O_2$, ^{36}Ar, Hydroxylamine ($H_3{}^{14}N^{18}O$)	58	Propylene-oxide ($C_3H_6{}^{16}O$), Butane (C_4H_{10})
37		59	
38		60	Propylene-oxide ($C_3H_6{}^{18}O$)
39		61	
		62	

E.4.5 Epoxide assay

Two ml of phosphate buffered medium with only 2 µl of *n*-tetradecane as substrate were filled into reagent tubes (or 15 ml Hungate tubes for anaerobic cultivation) and inoculated with 0.02 ml inoculum from alkane grown HdN1 cultures. Approximately after 2 days (5 days during anaerobic cultivation) of incubation at 28°C in the dark, when the cultures had grown to a high density, 1 µl of 1-tetradecene was added and mixed with the aqueous phase by horizontal agitation. After one hour (four hours under anaerobic conditions), the cultures were extracted three times with 1.5 ml diethyl ether. The ether fractions were pooled in fresh glass vials equipped with teflon screw cap and evaporated to dryness in a rotary vacuum evaporator (Eppendorf, Hamburg, Germany). Extracts were re-dissolved in ~100 µl diethyl ether and analyzed on a TRACE GCMS (ThermoFisher, Waltham, USA).

E.5 Literature of the appendix

Edgar, R.C. (2010) Search and clustering orders of magnitude faster than BLAST. *Bioinformatics* **26:**19, 2460–2461.

Ehrenreich P. (1996) Anaerobes Wachstum neuartiger sulfatreduzierender und nitratreduzierender Bakterien auf *n*-Alkanen und Erdöl. *Ph.D.-thesis*, University Bremen

Katoh, K., Kazuharu, M., Kuma, K., Miyata, T. (2002) MAFFT: a novel method for rapid multiple sequence alignment based on fast fourier transform. *Nucleic Acids Res* **30:** (14) 3059–3066.

Ludwig, W., Strunk, O., Westram, R., Richter, L., Meier, H., Yadhukumar *et al*. (2004) ARB: a software environment for sequence data. *Nucleic Acids Res* **32**: 1363–1371.

Pruesse, E., Quast, C., Knittel, K., Fuchs, B.M., Ludwig, W.G., Peplies, J., and Glockner, F.O. (2007) SILVA: a comprehensive online resource for quality checked and aligned ribosomal RNA sequence data compatible with ARB. *Nucleic Acids Res* **35**: 7188–7196.

Price, M.N., Dehal, P.S., Arkin, A.P. (2010) FastTree 2 – approximately maximum likelihood trees for large alignments. *Plos One* 5(3)e9490.

Waterhouse, A.M., Procter, J.B., Martin, D.M., Clamp, M, Barton, G.J. (2009) Jalview Version 2 – a multiple sequence alignment editor and anaylsis workbench. *Bioinformatics* **25:** (9) 1189–1191.

Widdel, F., and Bak, F. (1992) Gram-negative mesophilic sulfate-reducing bacteria. In *The prokaryotes*. Balows, A., Trüper, H.G., Dworkin, M., Harder, W., and Schleifer, K.-H. (eds). New York: Springer, pp. 3352–3378.

E.6 Acknowledgements

Prof. Dr. Friedrich Widdel, I want to thank you for giving me the chance to work on this exciting, multifarious and challenging topic, that you always had time for me, even when your schedule was tight and your desk full and for all these countless hours you spend discussing with me the intriguing questions connected to my study. I highly appreciated your determination during the night-shifts when we submitted the papers. I can not thank you enough for everything I have learned from you.

Prof. Dr. Ralf Rabus, thank you for all your support and patience and help with proteomics and genomics and your enthusiasm for the HdN1 project. You have often been like a second supervisor for me.

Prof. Ir. Dr. Marc Strous, thank you for enthusiastic discussions, not only about work-related topics but also about philosophical questions, theatre and more. And thank you, that you had so much time for me and were so interested in the unsolved questions surrounding strain HdN1.

Prof. Dr. Marcel Kuypers, thank you for letting me use some of your expensive machines and thanks for lots of advices on many MIMS-related questions and your supportive nature.

Dr. Frank Schreiber, thank you for help with the MIMS-measurement and for introducing me into the world of microsensor and for all the exciting and inspiring discussions on NO and the special physiology of HdN1 and '*Ca*. M. oxyfera'.

Prof. Dr. Ulrich Fischer, thank your for your contributions during my thesis committee meetings and for being part of my board of examiners. Having you in my thesis committee is especially adequate since you have already been a reviewer of Petra Ehrenreichs thesis – who was my predecessor with work on strain HdN1.

Dr. Florin Musat, thank you for helping me with so many experimental and conceptual scientific questions, even though I was not working on your project any more. I highly appreciate your expertise and friendly nature and wish you all the best for your scientific future.

Prof. Dr. Jens Harder, thank you for being always present to help with biochemical and technical problems and for keeping so many things in the Microbio department running. And for giving P. Ehrenreich your failed negative controls that just kept growing anaerobically with paraffin and that carried an enrichment including strain HdN1.

Gabi Klockgether, thank you for support with the MIMS measurements and GCMS measurements and your patience and steady aid when repairs were necessary and urgent.

Ulrike Jaekel, thank you for the pleasant, reassuring company in the lab and in our small "hydrocarbon-degrader" discussion-group. And thanks for that nice balcony.

Sven Lahme, thanks for help with the HPLCs and other lab work and for being such a nice climbing partner and friend.

Stefano Romano, thank you for being such a supportive, bright, honest and humorous colleague in the office.

Jan Petasch, thank you for all the discussions on work, politics, and life-related questions in the lab and even more so in our office. And for climbing the Zugspitze with me.

Kathleen Trautwein, thank you for many illuminative and informative conversations, in our small “hydrocarbon-degrader” discussion-group and beyond.

Frauke Lüddeke, Kirsten Webner, Nadine Winkelman, Insa Werner for being such nice lab colleagues and help with all these small things.

Vladimir Bondarev, thank your for being such a good company in Bremen, Seattle and wherever. And thanks for game sessions and for reading my manuscript.

Dennis Enning, thank you for insightful and intelligent conversations in the lab about life and other negligibilities.

Verena Salman, thank you for discussions and unique salsa lessons at the MPI

Thomas, thank you for scientific support and for adding some entertainment to the microbiology department – it is not the same without you.

Gao, thank you for help with the UPLC and for precious conversations about science and life.

Richard, thank you for interesting discussions and for your helpful and supportive nature.

Danny Brodkorb, thank you for help with GC measurements and biochemical analysis.

I want to thank Ramona Appel, for being patient and supportive and for teaching me some important microbiological skills – and for your heartily honest nature. Thanks to Daniela Lange, for help with the preparations for mass cultivations, for a sample of strain HdN1 and to teach me some preparative techniques. Thanks to Christina Probian for help with HPLC-related questions and for exhilarant conversations at the GCPC. Thanks to Ingrid Kunze for being yourself.

I also want to thank the electronic workshop team for their helpful and uncomplicated nature.

I want to thank the whole Department of Microbiology which was my second home during the last five years.

I want to thank the whole Ecophysiology group for collaborations and good company.

I also want to thank Katharina Ettwig and all the other nice people I was was honored to get to know in the Nijmegen group. I really enjoyed spending time and working with you and I hope we stay in contact.

Also I want to thank my theater group and associated friends for offering me relief and diversion from the science world, for not blaming me much for my PhD-related delays and for the chance to try out a gamut of emotions on stage.

I want to thank my family for all their support, understanding and encouragement during the whole time of my PhD. Especially to my brother Andreas in Bremen who always had an open ear and helped me with countless challenges – and often with good food. I could not have done it without you all. Really.

And last but not least I want to thank my dear girlfriend Lena for all the strength and confidence she gave me and the understanding of my particular science life style which often robbed me from her due to PhD-related tasks.